# THE GEOLOGY AND GEOCHEMISTRY OF THE HOHONU BATHOLITH AND ADJACENT ROCKS, NORTH WESTLAND, NEW ZEALAND.

---

A thesis

submitted in fulfilment

of the requirements for the Degree

of

Doctor of Philosophy in Geology

at the

University of Canterbury

by

Tod Earle Waight.

---

University of Canterbury

March 1995.

Volume One: Text and map.

THESIS
QE
348.2
W5
W138
1995
v.1.
copy 2

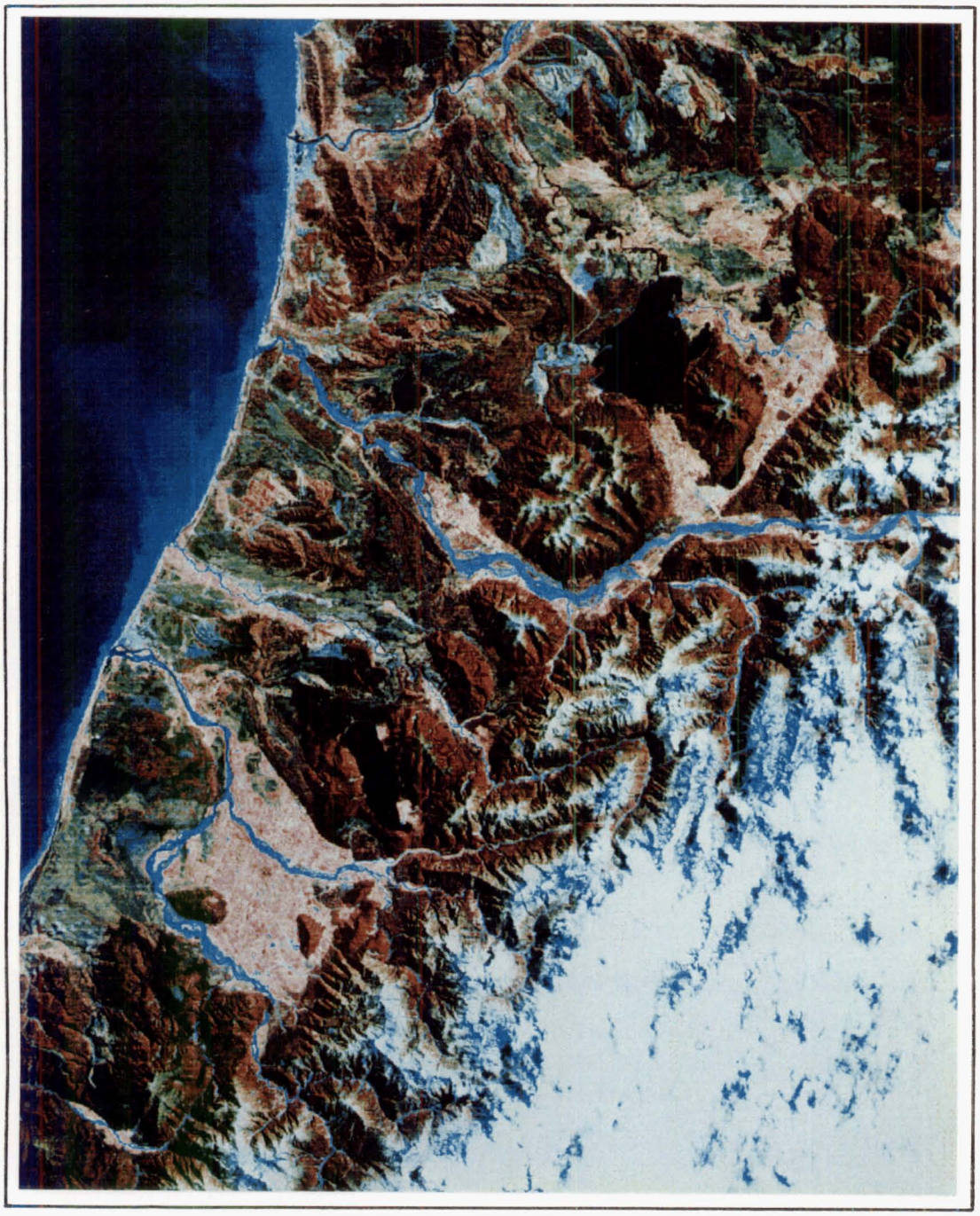

Landsat 1 image of the Hohonu Batholith (taken 8 December 1973). Black areas represent Lake Brunner and Lake Kaniere. Note the topographic expression of the Alpine Fault.
Image processed by Image Processing Group, Landcare Research.

## Abstract

The Hohonu Batholith lies within the Buller terrane, immediately adjacent to the Alpine Fault and inland from Hokitika and Greymouth on the West Coast of the South Island of New Zealand. Detailed mapping has identified ten distinct granitoids intruded into Greenland Group metasediments. Four geochemical suites are recognized within the Hohonu Batholith.

Palaeozoic magmatism in the batholith is represented by the Summit Granite, which yields a Palaeozoic (381.2 Ma) age and displays affinites with granitoids of the Karamea Suite of Tulloch (1988a). The informal name Summit Granite suite is used to describe this pluton. The Summit Granite has acted as country rock and is intruded by two Cretaceous plutons. The poorly constrained Mount Graham Granite may also belong within the Summit Granite suite.

The Hohonu Batholith is dominated by the mid-Cretaceous (114-109 Ma) I-type Hohonu Super-suite, which is considered to encompass the previously defined Rahu Suite of Tulloch (1988a). The Hohonu Super-suite is characterized by relatively restricted radiogenic isotopic compositions with $Sr_{(110)}$ = 0.7062 to 0.7085 and $\epsilon Nd_{(110)}$ = -4.4 to -6.1, and represents melting of a complex source combining depleted mantle-derived material, similar in composition to the source of the Early Cretaceous Separation Point Suite, and a complex, heterogeneous and largely unconstrained lower continental crustal component. A model is proposed whereby the Hohonu Super-suite was generated following the collapse and thinning of Western Province crust previously overthickened by the generation of the Median Tectonic Zone volcanic arc and its subsequent collision with the Western Province. Collapse of the overthickened crust is believed to be a consequence of the cessation of subduction along the Pacific Margin of the New Zealand portion of Gondwana and the subsequent removal of compressional forces maintaining crustal thickening. Rapid isothermal uplift of the thickened crustal root resulted in partial melting of the lower crust. Ambient temperatures in the lower crust were also raised by mafic underplating associated with isothermal uplift and adiabatic melting of the underlying mantle. Emplacement of the Hohonu Super-suite in an extensional environment is indicated by the intimate relationship between the Rahu Suite Buckland Granite and the Paparoa Metamorphic Core Complex, and the development of the extensional sedimentary basins of the Pororari Group. This extensional event is considered to predate and be unrelated to the separation of Australia and New Zealand and opening of the Tasman Sea.

Two suites are recognized within the Hohonu Super-suite in the Hohonu Batholith; the Te Kinga Suite and the Deutgam Suite. Geochemical contrasts between these two suites are attributed to melting at differing crustal depths, at varying water activities, and in equilibrium with different residual assemblages. The relatively mafic, metaluminous, I-type compositions of the Deutgam Suite are ascribed to dehydration melting in equilibrium with an amphibolitic (plagioclase + amphibole) residue. Residual plagioclase retains Sr, $Al_2O_3$, $Na_2O$ and Eu and results in the low concentrations of these elements which characterize this suite. In contrast, the peraluminous high silica compositions of the Te Kinga Suite are attributed to water-saturated to undersaturated melting in equilibrium with an eclogitic (garnet +

amphibole residue) at greater depths in the crust. Residual garnet produces the HREE-depleted nature of the suite, and a lack of residual plagioclase contributes to the characteristically higher Sr, $Al_2O_3$, $Na_2O$ and Eu contents of the Te Kinga Suite.

Late Cretaceous magmatism in the Hohonu Batholith is represented by the French Creek Suite. This suite comprises the composite French Creek Granite, which displays geochemical and petrographic features typical of A-type granitoids, and associated hypabyssal rhyolite dikes. The alkaline magmatism of the French Creek Suite and the closely associated Hohonu Dike Swarm are intimately linked to extension during the opening of the Tasman Sea. The Hohonu Dike Swarm consists of predominately doleritic dikes, with subordinate camptonites and rare phonolites, concentrated on the Hohonu Ranges and Mount Te Kinga. Field evidence indicates that the Hohonu Dike Swarm and French Creek Granite are, at least partially, contemporaneous. The age of this activity is constrained by an 81.7 Ma SHRIMP age for French Creek Granite and is contemporaneous with the generation of the first oceanic crust in the Tasman Sea. A strong WNW-ESE trend within the Hohonu Dike Swarm parallels the line of Australia-New Zealand break-up, and the alkaline compositions of both the dikes and the French Creek Granite are characteristic of emplacement into an anorogenic extensional environment. Consequently strong links are indicated between the opening of the Tasman Sea and genesis of the Hohonu Dike Swarm and French Creek Granite. Geochemical data are consistent with generation of French Creek Granite by prolonged fractionation of plagioclase and mafic phases from saturated and oversaturated members of the Hohonu Dike Swarm. Approximately 20% crustal contamination is also required to produce the isotopic compositions of French Creek Granite from the relatively depleted compositions of the Hohonu Dike Swarm.

Amphibolite-facies paragneisses, orthogneisses and metabasites of the Granite Hill Complex can be confidently correlated with similar rocks of the Fraser Complex. The dominance of metabasaltic rocks, distinct isotopic compositions and preliminary zircon inheritance studies, indicate these gneisses are unlikely to represent metamorphic equivalents of the Greenland Group and intrusive granitoids, as proposed for the Charleston Metamorphic Complex. Possible correlatives of the Fraser and Granite Hill Complexes may occur in Fiordland.

Poorly exposed Tertiary rocks along the north-west margin of the Hohonu Ranges are briefly described. These rocks are considered to represent material incorporated in a major fault zone along which the batholith has been uplifted and exposed during recent compression across the Alpine Fault.

## Table of Contents:

### Volume One.

## List of Figures.

### Volume One:



### Volume Two:

## List of Tables.

## Volume Two:

## List of Appendices.

### Volume Two:

# Chapter 1

# Introduction.

## 1.1: Location and confines of the study area.

The Hohonu Batholith (Tulloch 1988a) comprises the granitoid rocks outcropping between the Greenland Group massifs of Bell Hill in the north, and Mount Graham to the south. The area of this study is located to the east of the townships of Hokitika and Greymouth, between Lake Haupiri and the Kokatahi River, on the West Coast of the South Island of New Zealand. To the east and west the study area is bounded by the Alpine Fault and the Hohonu Fault respectively. The area investigated comprises eight basement massifs, the highest point being the summit of Mount Turiwhate (1368m). DOSLI Infomap 260 series sheets J32, J33, K32 and K33 give complete topographical coverage of the area (Fig.1.1).

## 1.2: Physiography.

The study region covers approximately 450 $km^2$ and consists of a series of basement massifs separated by low-lying valleys orientated approximately NW-SE and filled with Quaternary gravels. These valleys may represent glacial erosion along major structural weaknesses developed along NW-SE Riedel shears associated with dextral movement on the Alpine Fault (Koons 1978). The study area owes much of its present day morphology to glacial activity which has carved the steep sides of the mountains and deposited a veneer of glacial debris over the mountain slopes and lowlands. Terminal moraines and lateral moraines can be observed in many locations within, and to the west of, the study area. Several typical U-shaped valleys, hanging valleys and cirque head walls are visible on the Hohonu Ranges from State Highway 73. Two large, terminal moraine-bounded lakes, Brunner (Moana Kotuku) and Kaniere, occur in the field area, which is also traversed by two major braided rivers, the Taramakau and the Arahura, having their headwaters in the Southern Alps. Recent alluvial gravels make up a large proportion of the low-lying parts of the area and are currently being grazed primarily for dairy farming purposes. The area has a long history of timber milling and alluvial gold mining, the Greenstone River occurrence being one of the first discoveries of alluvial gold on the West Coast. The mountains of the area are covered by dense Rimu forest, and are either State Forest or Scenic Reserve under the control

of the Department of Conservation. Prevailing westerly winds and the topographical barrier of the Southern Alps have given Westland a somewhat damp reputation, hence Bell and Fraser (1906, page 16) wrote "While camped at Kawhaka Pass, between Mount Turiwhate and Island Hill, during the month of September, we had almost continuous wet weather". Rainfall is abundant and relatively constant throughout the year. The region receives upwards of 3000-4500 mm of rain per annum, increasing to over 5000 mm/yr on the Main Divide (N.Z.Met.Service 1980), heavy rain regularly causing flooding of waterways in the study area. State Highway 73, one of the major routes across the Southern Alps, and the Midland Railway, the only rail link between the West and East Coasts of the South Island, also pass through the area. The largest settlement of the study area is Moana, a small town primarily serving the recreational users of Lake Brunner.

**1.3: Regional geological setting and overview.**

The South Island of New Zealand is divided into the Eastern and Western Provinces (Landis and Coombs 1967) separated by the Median Tectonic Line. Recent work (Bradshaw 1993, Kimbrough *et al* 1993) has redefined the boundary between the two provinces as a complex belt of dismembered arcs known as the Median Tectonic Zone. The Western Province consists of the Buller and Takaka terranes, early to mid-Palaeozoic rocks occurring in the western part of the South Island and in Fiordland (R.Cooper 1979, 1989) (Fig.1.2). The Buller Terrane comprises a relatively uniform suite of quartz-rich turbidites (Greenland Group) cut by Palaeozoic and Cretaceous granitic plutons (Tulloch 1983, 1988a, Cooper and Tulloch 1992). Paragneisses and orthogneisses of the Charleston Metamorphic Group were previously considered to be Precambrian basement to the Greenland Group (Mason and Taylor 1987) due to their high degree of deformation and metamorphism and a 680 Ma Rb-Sr isochron (Adams 1975). Recent U-Pb dating has yielded typical Greenland Group and Western Province granitoid signatures and these gneisses are now considered to represent highly metamorphosed equivalents of these rocks (Kimbrough and Tulloch 1989, Tulloch and Kimbrough 1989a, Ireland 1992).

Expanding on earlier studies by Reed (1958) and Grindley (1961, 1971), Tulloch (1988a) separated the granitoids of the West Coast into a number of batholiths, dominated by the voluminous Karamea and Separation Point Batholiths (Fig.1.3). In addition, a number of smaller batholiths were identified, including the Hohonu Batholith as defined in this study (Fig.1.3). Tulloch (1988a) divided the granitoids of the Western Province into three suites on the basis of geochemistry, mineralogy, age and granite type (*sensu* Chappell and White 1974). The three suites proposed by Tulloch (1988a) are the S-type Palaeozoic Karamea Suite, and the Mesozoic I-type Separation Point Suite and intermediate I/S-type Rahu Suite. Tulloch (1988a) considered the Hohonu Batholith to consist entirely of Rahu Suite plutons, although he proposed a possible fourth suite, the Brunner Suite, to encompass granitoids with A-type affinities occurring on the Hohonu Ranges. The discovery of Palaeozoic A-types (Torupuihi Granite) and I-types (Paringa Granite) (Cooper and Tulloch 1992) has further complicated this suite subdivision.

Recent geochronological studies (Muir *et al* 1994a, 1994c) have identified two periods of plutonism in the Palaeozoic, the bulk of the Karamea Suite being intruded around 375 Ma, with the Cape Foulwind and Windy Point Granites representing a younger event at around 327 Ma. At least two periods of plutonism are also identified in the Mesozoic, with most Separation Point Suite granitoids intruding around 118 Ma, and indications that the Rahu Suite may be slightly younger at around 110 Ma (Graham and White 1990, Muir *et al* 1994a). The Separation Point Suite is considered to represent granitoid magmas derived by melting of recently underplated basaltic protoliths beneath a thickened continental arc (Muir *et al* 1995). In contrast, the Rahu Suite is generally considered to represent more typical calc-alkaline, subduction-related rocks, emplaced above a westerly dipping subduction zone (Tulloch 1988a, Muir *et al* 1995). A slightly older Jurassic magmatic event is recorded in the Median Tectonic Zone (Kimbrough *et al* 1993, Muir *et al* 1994d). Correlatives of the Separation Point Suite, Median Tectonic Zone and Karamea Suite are identified in the Fiordland region and Stewart Island (Tulloch 1983, Allibone 1993, Muir *et al* 1994d). No definitive correlatives of the Rahu Suite have been observed in Fiordland.

The Hohonu Batholith is bounded by, and uplifted along, two major fault systems. The Alpine Fault, the major plate boundary between the Indian-Australian and Pacific plates, dissects the South Island and acts as the eastern margin of the study area. The eastern extent of the batholith prior to Alpine Fault inception is unknown. A recent trace of the Alpine Fault occurs at Inchbonnie between the Taramakau River and Lake Poerua (Warren 1967, Tulloch and Brathwaite 1987). The trace offsets post-glacial river terraces 3 metres vertically and 7 metres dextrally (Angus 1984). The Hohonu Fault (Nathan *et al* 1986) consititutes the western boundary of the study area and has been the locus of uplift caused by convergence of the Australian and Pacific plates.

The north-eastern and south-eastern regions of the study area are dominated by the mylonites and amphibolite-grade gneisses of the Fraser Complex (Rattenbury 1987a, 1991) and the Granite Hill Complex (Mason 1990). The rocks of the Granite Hill Complex have been considered to be a northerly extension of the Fraser Complex and both suites of rocks have been correlated with the metamorphic rocks of the Charleston Metamorphic Complex in the Paparoa Ranges (Mason 1990, Mason and Taylor 1987) .

All basement units within the study area are intruded by the Hohonu Dike Swarm, a group of predominantly mafic dikes with lamprophyric affinities. The swarm is concentrated primarily on the Hohonu Ranges and Mount Te Kinga, although members of the swarm occur throughout the thesis area. The Hohonu Dike Swarm is considered to be Late Cretaceous and associated with Gondwana breakup. Correlations have been made between the Hohonu Dike Swarm a similar swarm in the Buller Gorge (Wellman and Cooper 1971, Nathan 1978, Bishop 1992).

During the separation of New Zealand and Australia, and the opening of the Tasman Sea in the Late Cretaceous, a marine transgression occured, commencing with the deposition of conglomerates, breccias and coal measures in extensional, fault-bounded basins (Pororari Group, Paparoa Coal Measures). This was followed by a succession of Eocene coal measures (Brunner Coal Measures), Oligocene mudstones (Kaiata Mudstone) and limestones (Nile Group Limestones) and Miocene mudstones

and sandstones (Blue Bottom Group). This sequence is overlain by conglomerates associated with the inception of uplift on the Alpine Fault around 10 Ma (Nathan *et al* 1986, Laird 1994). Pororari Group conglomerates and Brunner Coal Measures are poorly exposed around Mount Graham, and a thin sliver of Tertiary Blue Bottom mudstone and Cobden Limestone is infaulted along the western margin of the Hohonu Ranges. A more complete succession of Tertiary sediments is recognized in oil exploration drillholes to the west of the study area in the Grey Valley trough (Nathan *et al* 1986, Spanninga 1993).

Fission track studies (e.g. Kamp *et al* 1992) indicate that uplift of these basement massifs to their present level has occurred relatively recently, in association with the change to a compressional regime across the Alpine Fault.

Glaciation has played a major role in shaping the present day morphology of the area, with cirque valleys and various moraine structures being abundant. The late Pleistocene Taramakau glacier flowed down the Taramakau Valley and split into three lobes at Inchbonnie, one down the present path of the Taramakau River, another towards Lake Brunner and the third along the Alpine Fault. The glacial geology of the region has been described by Suggate (1985).

## 1.4: Previous geological accounts.

For clarity this section is separated into several parts describing previous geological accounts on the various rock units of interest.

### 1.4.1: Granitoids and geological mapping.

The first major geological publications on the Hohonu area were carried out by Bell and Fraser (1906) and Morgan (1911). Geological maps (1 inch to 80 chain) were presented indicating relationships between the granitoids, Greenland Group, Tertiary and Quaternary rocks. No detailed subdivision of granitoid units was undertaken. The most recent geological maps of the region are those of Warren (1967) and Gregg (1964), utilizing much of the earlier work of Bell and Fraser and Morgan. No subdivision of granitoid units is attempted in these maps, the granitoids deemed to

belong to the Palaeozoic Tuhua Group comprising "acid plutonic rocks...probably of different age and origins". The term Tuhua Group has since been abandoned.

General accounts of the granitoids of the West-Nelson and Westland area have been published by Tulloch (1983, 1988a, see Fig.1.3). Regional basement syntheses have been published by Tulloch and Brathwaite (1986) and Mason and Taylor (1987), both including brief mentions of granitoids from the Hohonu region. Fluorine analyses of several Hohonu Batholith granitoids are presented by Tulloch and Robertson (1987) and magnetic susceptibilities of Western Province granitoids are discussed by Tulloch (1989). On a more detailed scale, Tulloch (1979a) described and mapped the northern Victoria Range portion of the Karamea Batholith, White (1987) studied the Paparoa Batholith and Jury (1981) investigated the Rangitoto Batholith (see Fig.1.2). Muir *et al* (1995) have recently published a detailed geochemical study of the Separation Point Batholith. These authors are also currently involved in detailed geochronological and geochemical studies of the Karamea Batholith and the Eastern Fiordland region, initial results are presented in Muir *et al* (1994c, 1994d).

Hamill (1972) named and mapped the two granitoid units outcropping on the Western Hohonu Ranges. However, his thesis concentrated primarily on the Hohonu Dike Swarm and the infaulted Tertiary section at Taramakau, with the granitoids representing only a minor part of the study. Mason (1990) mapped the geological units of the Rotomanu area, including Mount Te Kinga and Granite Hill. Most of the mapping and geochemistry was of a reconnaissance nature and has been extended in this thesis. The works of both Hamill (1972) and Mason (1990) proved invaluable during field mapping for this study, and this thesis is considered to be an expansion of the investigations of these earlier workers. I began working in this area for my B.Sc. Honours thesis, completed in 1990. Some data from Mount Turiwhate, Island Hill and Mount Tuhua presented here come from this work (Waight 1990), and the results and interpretations of this thesis are revised and extended in the light of new, more detailed data.

### 1.4.2: The Hohonu Dike Swarm.

The Hohonu Dike Swarm was once considered consanguineous with a similar swarm in Haast and was used as measure of the Cretaceous offset on the Alpine Fault by Suggate (1963) and Hamill (1972). This correlation has since been discounted by Cooper *et al* (1987), due to distinct differences in age and chemistry between the Hohonu and Haast swarms. The only detailed study on the Hohonu Dike Swarm is that of Hamill (1972), who introduced the name Pakawera Formation for these dikes. Only limited geochemical data were available to Hamill, and his thesis concentrates primarily on the mineralogical features of the swarm. K/Ar dates for several dikes of the swarm are presented by Wellman and Cooper (1971), and ages for similar dikes in the Buller Gorge are presented by Adams and Nathan (1978). The occurrence of spinel harzburgite xenoliths in a mafic dike from Mount Te Kinga is discussed by Tulloch and Nathan (1990).

### 1.4.3: The Fraser and Granite Hill Complexes.

High grade metamorphic rocks west of the Alpine Fault were initially described by Morgan (1908), and later by Reed (1964), although it was not until 1968 that Young coined the term Fraser Formation. Young (1968) was also the first to give the name Fraser Fault to the structure that separates the Fraser Formation from the undeformed basement rocks to the west. The Fraser Formation has since been revised to Fraser Complex by Rattenbury (1987a and 1991).

Most of the work on the Fraser Complex has concentrated on the type area around Fraser Peak and Mount Misery between the Mikonui and Hokitika Rivers. Young (1968), Warren (1967) and Rattenbury (1991) show the Fraser Complex and Fault to extend as far north as east of Island Hill. Mason (1990) considered the fault that separates the gneisses of the Granite Hill Complex from the Greenland Group of Bell Hill to be an extension of the Fraser Fault, and the Granite Hill Complex to be a northerly extension of the Fraser Complex. Correlations have also been made between the gneisses of the Fraser and Granite Hill Complexes and similar rocks in the Southern Victoria Range (Mason and Taylor 1987). Kimbrough *et al* (1994a) have recently published a late Jurassic U-Pb age from the Fraser Complex.

### 1.4.4: Sedimentary cover.

Poorly exposed sediments at the northwestern end of Mount Graham were mapped by Warren (1967) as possible Eocene Omotumotu Formation (≈Brunner Coal Measures), and Bell and Fraser (1906) gave a description of a coal mine operating within these deposits at the turn of the century. The infaulted Tertiary sequence outcropping along the northwestern margin of the Hohonu Ranges from near the Taramakau township to Knoll Point was mapped by Morgan (1911) and Hamill (1972) and discussed at some length by Wellman (1950b) and Wellman and Suggate (1950). The occurrence of an oil seep near Kotuku (K32 837510), just to the west of the study area, has prompted significant oil exploration and a number of exploration wells have been drilled to the west in the Grey Valley Trough, although economic resources have not yet been identified. Much of the pre-1986 data is collated in Nathan *et al* (1986), with more recent data, including seismic sections, summarised in Spanninga (1993).

## 1.5: Methods.

A total of approximately 8 months was spent in the field during this study, mostly during the summers of 1991-1992 and 1992-1993 with additional work carried out during the intervening winters and the late summer of 1994. Accommodation was generally in a tent at Moana, Lake Kaniere or Hokitika. Tent camps were also used on the Hohonu Tops at Lake Ruby, and on the Turiwhate Tops. Road access to the study area is good, with major public roads providing access to most areas. Forestry roads and farm tracks also proved useful for access to some areas. The tops can be reached via well maintained tracks to Mount French and Mount Tuhua, and rather poorly maintained tracks onto Mount Te Kinga and Mount Turiwhate. Helicopter assistance was used where possible. Due to thick forest cover most mapping was restricted to stream beds and the exposed mountain tops, as outcrops in the bush proved elusive and invariably weathered. Location in the field is considered to be reasonably accurate and was established with the aid of ≈1:15,000 Forestry Department air photos, run in the early 1940s, 1:50,000 topographic maps, a hand held altimeter, triangulation and occasional guess work.

Geochemical and petrological samples were taken preferably from outcrop, although float samples were taken rarely if they were fresher than, and could be confidently linked to, nearby outcrop. Float samples were also rarely collected if a particular rock type was common in a stream, but no outcrop was found. Field numbers refered to in the text, University of Canterbury collection numbers, a brief sample description and grid references are presented in Appendix A. Samples prefixed TW were collected as part of my honours thesis (Waight 1990). Samples collected for isotopic analysis tended to be larger, weighing approximately 20 kg, and were thus taken from easily accessible sites. Grid references in the text and Appendix A are taken from NZMS260 1:50,000 topographic sheets K32, K33, J32 and J33. Grid references in the text prefixed "S" are taken directly from literature and refer to the older NZMS1 1:63,360 topographic sheets.

Petrographic work was undertaken utilizing a standard Zeiss transmitted light microscope and the mineralogy and petrology texts of Shelley (1985 and 1993) and Deer *et al* (1966). All mineralogical size data are given for the long axis of the mineral concerned and all igneous classifications are according to Le Maitre *et al* (1989). The term "granite" is used loosely when naming plutons which fall into several granitoid fields on the QAP plot of Le Maitre *et al* (1989).

XRF major and trace element analyses were carried out in the Geology Department of the University of Canterbury and are presented in Appendix C. Microprobe analyses were carried out at the Geology Department, University of Otago in Dunedin and are presented in Appendix D. INAA analyses were carried out by Professor G.Nelson Eby at the Department of Earth Sciences, University of Lowell, Massachusetts and are presented in Appendix E. Oxygen isotope analyses (Table 6.5) were run on whole rock powders by Dr Tony Fallick at the Scottish Universities Research and Reactor Centre, Glasgow. Nd and Sr isotope ratios of this study were the first to be processed and measured at the new TIMS laboratory in the Geology Department, La Trobe University, Melbourne and are presented in Tables 6.4, 6.8, 6.9, 7.2 and 8.1. Biotite and muscovite separates from representative samples of most plutons were also analyzed in an attempt to produce whole rock/mineral isochrons for

the batholith. Detailed descriptions of XRF, INAA, microprobe and isotopic analysis methods are given in Appendix B.

# Chapter 2

# The Greenland Group.

## 2.1: Introduction.

Greenland Group sediments were first described as the Kanieri Series by Bell and Fraser (1906). They represent the oldest known components of the Buller Terrane and rocks extend from Karamea in the north to as far south as Milford Sound. Sedimentation of the Greenland Group is considered to be in part Early Ordovician based on the discovery of rare graptolite fossils near Reefton (Cooper 1974). Recent U/Pb SHRIMP dating has shown that Greenland Group sediments contain zircons as young as 500 Ma, giving a maximum age of deposition (Ireland 1992). A Rb/Sr isochron of 495 $\pm$ 11 Ma (Adams 1975) is believed to date the greenschist facies metamorphism of the unit and thus gives a minimum age for the unit. These two observations indicate that the stratigraphic age of the Greenland Group and its metamorphism are reasonably constrained. The Greenland Group has been correlated with the Swanson Formation in Marie Byrd Land (Adams and Weaver 1990, Adams *et al* 1995), the Robertson Bay Group of Northern Victoria Land (Nathan 1976) and the Ballarat-Bendigo Belt of Victoria, South-east Australia (Cooper and Tulloch 1992).

The Greenland Group is a uniform series of green to grey, turbidite deposits, consisting almost entirely of sandstone and mudstone beds, metamorphosed to lower greenschist facies. Near intrusive contacts the Greenland Group loses it characteristic green colour and becomes brown to black, associated with the contact metamorphic growth of biotite. Most sediments classify as sub-feldsarenites or sub-litharenites and consist of detrital quartz and minor sodic plagioclase in a matrix of chlorite and sericite. The Greenland Group was considered by Laird (1972) to have a gneissic and/or granitic provenance, whereas Nathan (1976) preferred a polycyclic derivation from a pre-existing sedimentary terrain to explain the absence of kaolinite and alkali feldspar. The complex inheritance patterns revealed by SHRIMP studies indicate a complicated source region for the Greenland Group and a combination of the thoughts of Laird (1972) and Nathan (1976) seems likely. Gage (1948) estimated a minimum thickness of 5200 m for the Greenland Group in the Reefton District, although neither top nor base of the sequence are exposed. Sedimentalogical studies of the Greenland

Group (Laird 1972, Laird and Shelley 1974) indicate the sandstones are quartz-rich with minor plagioclase and rock fragments and generally no alkali feldspar. A geochemical summary of the Greenland Group has been published by Nathan (1976). Greenland Group commonly displays a well-developed axial planar cleavage, and evidence for two phases of folding is apparent on the coastal section between Greymouth and Barrytown. Many of the paragneisses of the Charleston Metamorphic Complex are considered to represent highly metamorphosed Greenland Group (Shelley 1970, Tulloch and Kimbrough 1989, Ireland 1992). A detailed study of the Greenland Group is beyond the scope of this thesis and no attempt is made to further clarify the geological setting or age of the Greenland Group sediments.

## 2.2: Greenland Group of the Hohonu region.

### 2.2.1: Introduction.

Greenland Group metasediments outcrop on Bell Hill, along the western margin of Granite Hill (in fault contact with Granite Hill Complex gneisses), on an unnamed hill (321m) near Kangaroo Lake[1], along the northern margin of the Hohonu Ranges (Fig.2.1), the western margin of Mount Tuhua and on much of Mount Graham (see map pocket). A small (10 m) outcrop of well bedded, fine grained metasediment was also located in Howitt Bay, Lake Brunner (K32 851431), although due to its limited size it is uncertain if this material is *in situ*. Most drillholes to the west of the study area intercept Greenland Group at their bases (Nathan *et al* 1986, Spanninga 1993). Metasedimentary and paragneissic inclusions within many granitoids of the batholith contain occasional sillimanite and probably represent Greenland Group country rock incorporated during the intrusion of these plutons.

### 2.2.2: Petrography.

Greenland Group rocks in the study area are typical, well-bedded to massive, well-indurated, poorly sorted, angular, fine grained subfeldsarenites with abundant chlorite and fine grained muscovite in a fine grained matrix. Petrographically, samples collected away from igneous contacts are typical Greenland Group; much of the quartz shows weak undulous extinction, no alkali feldspar is observed and igneous rock fragments indicate a granitic provenance. Sandstones appear to dominate the sequence,

1: This hill is mapped as Tuhua Granite by Warren [1967].

the few mudstone beds present have often acted as loci for deformation and/or folding (Fig.2.1). Much of the Greenland Group within the area occurs in close proximity to granitoid intrusives and has undergone contact metamorphism to brown-black biotite hornfels. These hornfelses are made up of a fine grained mosaic of quartz and minor feldspar with abundant plates of biotite and minor muscovite (Fig.2.2). No $Al_2SiO_5$ polymorphs or cordierite are observed (*cf* Tulloch 1979a). There is generally a strong preferred orientation of the micas in the hornfelsic rocks, presumably parallel to the margin of the pluton, and crenulation cleavages may be developed. A hornfelsic sample from near the contact between Greenland Group and Turiwhate Granodiorite on the south shore of Lake Kaniere (GMU3) contains large "spots" of quartz, which may represent original quartz layers or pebbles within the sandstone. A cave, marked on some maps as containing scheelite, is located near this contact. This mineralization may be similar to that associated with the Barrytown pluton as described by Tulloch (1986).

### 2.2.3: Geochemistry.

Two samples of Greenland Group (URC2 and GBC1) were collected for major, minor, rare earth element and isotopic analysis to ascertain the suitability of the Greenland Group as a source or contaminant for the granitoids of the batholith. Both samples have $K_2O/Na_2O > 1$, characteristic of Greenland Group sediments, and are chemically similar to the average argillite, greywacke and bulk Greenland Group analyses of Nathan (1976) (Fig.2.3). Sample URC2 shows some differences, notably higher Sr contents, coupled with elevated Sr/Rb and CaO greater than the 1.5 wt% limit defined by Nathan (1976)[2], possibly representing a greater proportion of plagioclase present within the sample. URC2 also has elevated Pb contents in comparison to the average analyses of Nathan (1976). The Greenland Group analyses presented here exhibit distinct negative Nb-Ta anomalies typical of many continental sediments.

REE plots of a single Greenland Group sample (GBC1) are compared with average Greenland Group analyses (Nathan 1976) and PAAS (Post Archean average Australian Shale (Taylor and M°Clennan 1985) in Fig.2.4. Average Greenland Group is

---

2: Mason (1977) has shown that geochemical variation beyond the limits set by Nathan (1976) occurs within the Greenland Group.

indistinguishable from PAAS, although the single sample analyzed for REE in this study has a distinctly higher proportion of HREE Gd to Yb, and a larger negative Eu anomaly (Eu/Eu* = 0.61). GBC1 has a REE pattern similar to P37731 of Nathan (1976), a greywacke from Mount William, and lies within the upper limits of REE analyses presented by Nathan (1976).

**2.2.4: Sr and Nd isotopes.**

Isotopic analyses of Greenland Group from the Hohonu Batholith area are summarised in Table 2.1 (see also Table 6.4). Variable measured $^{87}Sr/^{86}Sr$ for the samples, reflect differing Rb-Sr contents of individual samples. Most samples have similar initial ratios at 500 Ma, except TFQ10 which is likely to have undergone equilibration within its host granitoid (see below). Sr isotope analysis of a sample of Greenland Group from near Kangaroo Lake (33RO of Pickett and Wasserburg 1989) also gives similar values to those presented here. Initial ratios for the Greenland Group analyses from the Hohonu Batholith are higher than the 0.709 value calculated from an isochron by Adams (1975). It is likely that the initial ratio of Adams (1975) reflects greenschist facies metamorphism rather than the age of deposition.

Nd isotopic data on the Greenland Group are sparse in the literature. $\epsilon$Nd values for the two samples of this study are broadly similar and correlate well with the values of 33RO of Pickett and Wasserburg (1989). The initial Nd and Sr isotopic signatures and depleted mantle model ages ranging between 1.7 Ga to 2.5 Ga indicate a distinctly old, continental cratonic source for the Greenland Group (Pickett and Wasserburg 1989).

A large metasedimentary sheet included within granitoid on State Highway 73 (TFQ10) was also collected and analyzed for comparison to Greenland Group and to ascertain its affect upon assimilation into the host granitoid. This sample has isotopic compositions similar to those for analyzed Greenland Group. The low $Sr_{500}$ indicates some resetting by inclusion within the granitoid magma.

# Chapter 3

# Granitoid field relationships and petrography.

## 3.1: Introduction.

Ten plutons, recognized on the basis of their characteristic textural and mineralogical features, are identified in this study (see map). The plutons range in area from a few square kilometres to $\approx 120$ km$^2$ and are either intrusive into, or faulted against, Greenland Group metasediments and other plutonic rocks. This, coupled with ubiquitous intrusions of the Hohonu Dike Swarm ( $\approx 82$ Ma, Ch.7), constrains the batholith to between Ordovician and Late Cretaceous in age. The plutons are not restricted to individual topographical massifs, and show a crude NE-SW elongation, oblique to the present day outcrop of the batholith. The plutons display a wide range of petrographic types, ranging from quartz diorite to alkali feldspar granite (Fig.3.1). This chapter describes the field relationships, petrography and mineralogy of individual plutons, in order of occurrence from north to south. Mineral chemistry is described in more detail in Ch.4.

## 3.2: Jays Creek Granite.

### 3.2.1: Introduction and field relationships.

Outcrop of Jays Creek Granite (new name) is limited to a stream section at the base of Jays Creek (K32 882412) and an unnamed outlier (K32 895429) known locally as "Tuck's Hill". A typical exposure of Jays Creek Granite occurs where the Midland Railway crosses Jays Creek (Fig.3.2). The unit outcrops over an area of $\approx 3$ km$^2$, although its extent beneath the gravel cover is unknown. Jays Creek Granite is not observed in contact with other units, therefore its relationship to other plutons is unknown. It is assumed to intrude Greenland Group, which outcrops two kilometres to the east near Kangaroo Lake, and small biotite-rich xenoliths present on Tuck's Hill probably represent inclusions of Greenland Group.

### 3.2.2: Field description.

Jays Creek Granite is a massive, mesocratic, medium grained, biotite granitoid, containing sparse white phenocrysts of feldspar up to 2 cm long and rare muscovite

(Fig.3.3). The pluton is homogeneous over the limited outcrop available, and falls into both granodiorite and monzogranite fields on a QAP plot (Fig.3.1).

### 3.2.3: Petrographic description.

Quartz occurs as anhedral to subhedral crystals up to 6 mm across, making up between 17-39 modal percent of the rock. Ubiquitous undulose extinction is the only evidence for strain in samples examined (Fig.3.4).

Alkali feldspar makes up between 14-25% of Jays Creek Granite as occasional white, subhedral, Carlsbad-twinned, megacrysts up to 2 cm long. Alkali feldspar grew rapidly at a relatively late stage in the crystallization history and encloses most other phases. Transformation twinning and perthitic intergrowths are common, and myrmekite is often present at the junction of alkali feldspar and plagioclase feldspar. Microprobe analyses indicate that alkali feldspar is restricted in composition to 89-94% Or.

Plagioclase constitutes 34-46% of Jays Creek Granite as subhedral to euhedral crystals up to 6 mm long, exhibiting abundant albite and occasional Carlsbad twinning. Many crystals have strong normal zoning and microprobe studies determine plagioclase compositions of between An15-50%, mostly clustering around calcic oligoclase ($\approx$An28%). Sericitic alteration of plagioclase cores is common.

Biotite is the principal mafic constituent and makes up 6 to 14% of the rock. Biotite crystals (up to 4 mm) are subhedral to anhedral and exhibit strong yellow-brown pleochroism. Biotite is closely associated with opaques and contains numerous apatite inclusions. Biotite from specimens collected in Jays Creek have distinctive serrated or embayed margins, although this is not observed in specimens from Tucks Hill. Microprobe data on biotite of Jays Creek Granite indicate moderate Ti, Al(tot) and Fe/(Fe+Mg) contents.

Muscovite is a minor phase occurring as anhedral crystals up to 1 mm long in the groundmass or in the cores of altering plagioclase, rarely exceeding 1 modal percent. Microprobe analyses have low Ti and are indicative of a secondary origin.

Allanite is present in most specimens as ragged, resorbed crystals or euhedral, commonly zoned, brown pleochroic crystals up to 0.6 mm.

Accessory opaque minerals occur as subhedral to euhedral crystals (most likely magnetite) up to about 1 mm across, making up to 2 modal percent. Also present are numerous euhedral crystals of apatite up to 0.2 mm across, generally occurring in biotite, and a few small euhedral zircon crystals. Pleochroic haloes surrounding zircon in biotite are absent in Jays Creek Granite and rare in all other granitoid units of the Hohonu Batholith.

## 3.3: Pah Point Granite.

### 3.3.1: Introduction and field relationships.

Pah Point Granite was originally named the Pah Point Granodiorite by Mason (1990) who described a reddish-brown, megacrystic rock outcropping on the shores of Pah Point and the Refuge Islands in Lake Brunner. Modal classifications of Pah Point Granite indicate sub-equal alkali feldspar and plagioclase, resulting in a more accurate classification as monzogranite (Fig.3.1). Additional outcrops of Pah Point Granite occur on Mount Te Kinga in Rocky Creek, in a few small creeks draining into Lake Brunner north of Rocky Creek and in Jays Creek. Pah Point Granite outcrops over $\approx 4$ $km^2$, although its extent to the north is obscured by recent alluvium. To the north of Pah Point, in Howitt Bay, a small (1 $m^3$) outcrop(?) of fine grained Greenland Group occurs, and may indicate a northerly limit of Pah Point Granite. Typical exposures of Pah Point Granite can be found on Pah Point itself (Fig.3.5).

In Rocky Creek, brecciated Pah Point Granite is in fault contact with Uncle Bay Tonalite along a 50-100 metre wide zone of green, clay rich cataclasite, containing abundant tectonic pods of Uncle Bay Tonalite, Pah Point Granite, metasediment, pegmatites and mafic dike material, and gradually grading into intact Uncle Bay Tonalite upstream of the fault contact. The fault plane proper is well exposed and strikes E-W, dips to the south east at between 37-47° with slickensides plunging 15-37° towards the SSW. A number of thin (>2 cm) bands of dark brown to black, fine grained flinty material parallel the fault plane and are interpreted as pseudotachylite veins. The Rocky Creek fault is interpreted to be a reverse fault along which Mount Te

Kinga is being uplifted in response to recent compression across the Alpine Fault. This fault may extend to brecciated outcrops of Uncle Bay Tonalite near Lake Whitestone. In the middle reaches of Jays Creek, an isolated outcrop of Pah Point Granite occurs between outcrops of Jays Creek Granite and Uncle Bay Tonalite (A.J. Tulloch, *pers.comm.* 1992). The contact is not exposed and geological relationships between Jays Creek Granite and Pah Point Granite are unknown. It is assumed that the contact between Pah Point Granite and Uncle Bay Tonalite in the upper reaches of Jays Creek is an extension of the Rocky Creek fault.

### 3.3.2: Field description.

Pah Point Granite is a distinctive orange-brown, massive, mesocratic, coarse grained (2-5 mm) biotite granite, containing approximately 10% mafics and numerous, pink, Carlsbad twinned, euhedral alkali feldspar megacrysts up to 3 cm long (Fig.3.6). Outcrops on Pah Point and the Refuge Islands are highly jointed and cut by rare pink aplite dikes.

### 3.3.3: Petrographic description.

Quartz occurs as anhedral to subhedral crystals up to 1 cm across, although generally crystals are no larger than 5 mm. A second population of quartz exists as finer grained anhedral crystals about 0.3 mm across. In several samples large (up to 15 mm) subhedral patches of quartz are present, recrystallized to polycrystalline aggregates of finer grained, anhedral quartz. Undulose extinction occurs, but is the only evidence for deformation in the pluton. Quartz makes up between 17-37 modal percent (Fig.3.7).

Alkali feldspar is present as large ($\approx$3 cm) subhedral to euhedral megacrysts, and also as anhedral to subhedral crystals (up to 2 cm) within the groundmass. Alkali feldspar makes up 15-38% of this unit and is commonly perthitic and Carlsbad twinned. Inclusions of all other mineral phases present are incorporated within alkali feldspar, which occasionally develops a poikilitic-type texture as a consequence of rapid growth. Microprobe analyses indicate a range in alkali feldspar compositions between 76-89 wt% Or.

Plagioclase is present as subhedral to euhedral crystals (up to 6 mm), constituting 32-50% of Pah Point Granite. Crystals are commonly albite twinned, with few Carlsbad twins observed. Strong normal zoning is very common, and many crystals have a thin outer rim of feldspar with distinctly lower refractive index, probably albite. Microprobe data indicate the plagioclase is mostly calcic oligoclase to andesine ($\approx$An30%), ranging in composition from An18-46%.

Biotite is the dominant mafic phase, present as anhedral to euhedral crystals up to 5 mm across and constituting between 2-10% of the rock. Distinct straw-yellow to brown pleochroism is characteristic. Biotite crystals are often associated with opaque phases and contain many apatite crystals. Mason (1990) characterized biotite of this pluton on the basis of low Fe/(Fe + Mg) ratios and low $Al_2O_3$ contents. New microprobe data indicates relatively high Ti and relatively low Al(tot) and Fe/(Fe+Mg), consistent with the observations of Mason (1990), although biotite of Pah Point Granite is also similar in composition to that of Turiwhate Granodiorite.

Titanite is present in two specimens (KRC1 and PRI1) as euhedral crystals up to 2 mm across, often associated with biotite. Although abundant in the two sections mentioned, it was not observed in other specimens.

Sparsely distributed euhedral to subhedral zoned crystals of allanite, up to about 1.6 mm long, occur within most Pah Point specimens.

Opaques are abundant and contribute to the high magnetic susceptibility of the unit (Tulloch 1989). The opaque mineral is most likely magnetite, occurring as subhedral to euhedral crystals up to 1.5 mm across.

Apatite is ubiquitous, generally as euhedral, acicular crystals up to 0.4 mm across, enclosed within biotite. Relatively rare, small (0.1 mm) crystals of zircon are also present.

A 50 cm wide zone of medium grained, equigranular granodiorite occurs within typical megacrystic Pah Point Granite on the southernmost Refuge Island. In thin section (PRI2) this sample is similar to typical Pah Point Granite, containing allanite, titanite and abundant apatite as accessory phases. The granite differs in its finer grain size, dominance of plagioclase over alkali feldspar, and the absence of alkali feldspar megacrysts. An aplite dike from the northernmost Refuge Island (PRI3) consists of a very fine grained (0.05 mm average grain size) intergrown mixture of quartz, feldspar and minor biotite and muscovite. Also present within the aplite are a few larger anhedral crystals of quartz and alkali feldspar up to 0.4 mm across. The aplite has a 6 mm chilled margin immediately adjacent to the intrusive contact.

## 3.4: Uncle Bay Tonalite.

### 3.4.1: Introduction and field relationships.

Uncle Bay Tonalite was first identified by Mason (1990), who described it as an "equigranular quartz-plagioclase (An37%) biotite rock, with accessory titanite, epidote, allanite, apatite, magnetite and pyrite". Mason (1990) considered the mylonites along the south-eastern margin of Mount Te Kinga to have been derived ultimately from Uncle Bay Tonalite. These mylonites are now considered to consist primarily of Te Kinga Monzogranite, as discussed below in Ch.3.5.1. Mason (1990) also included the outcrops at the base of Jays Creek within Uncle Bay Tonalite. These are now distinguished as a separate intrusive phase, the Jays Creek Granite (Ch. 3.2).

A small exposure of brecciated Uncle Bay Tonalite at the base of Wallace Creek (K32 885399) is in fault contact with Greenland Group, which continues to outcrop for over a kilometre up the creek. An intrusive contact between Te Kinga Monzogranite and Greenland Group is exposed at the base of a waterfall (K32 876400) and several intrusive sheets of Te Kinga Monzogranite cut the Greenland Group immediately downstream of this contact. The Wallace Creek section is cut by a number of faults and shear zones running approximately sub-parallel to the Rocky Creek fault and are inferred to be the related to this fault. The Wallace Creek section is interpreted to represent a contact zone between Te Kinga Monzogranite and Uncle Bay Tonalite separated by a sheet of Greenland Group (see cross section A-A', map pocket). A similar sheet of hornfelsic Greenland Group outcrops between these two units on the

ridge below Te Kinga (K32 860386). Uncle Bay Tonalite and Te Kinga Monzogranite are found within close proximity on the south-western edge of Mount Te Kinga and the trace of the contact between the two units across Mount Te Kinga is indicative of a vertical contact. Mason (1990) describes a "knife sharp" intrusive contact between Uncle Bay Tonalite and Te Kinga Monzogranite at a quarry on an unnamed 149 m hill (K32 913394). This contact could not be located by the author and may have been removed during quarrying. A sharp bend in the intrusive contact, or a NW-SE dextral strike-slip fault between Lake Whitestone Hill and Rotomanu Railway Station, is required to join the quarry contact and contacts exposed in Wallace Creek. Uncle Bay Tonalite is faulted against Pah Point Granite in Rocky Creek and any contact relations between the Uncle Bay Tonalite and Jays Creek Granite are obscured by recent gravels.

A pegmatite of possible Te Kinga Monzogranite origin cuts Uncle Bay Tonalite at the base of Wallace Creek. Additionally, about 100 m below the Te Kinga Monzogranite-Greenland Group contact in Wallace Creek, a sheet of mafic biotite-hornblende-microtonalite (KWC9), probably related to Uncle Bay Tonalite, intrudes Greenland Group and is in turn cut by sheets of Te Kinga Monzogranite. It is therefore concluded that Uncle Bay Tonalite is intrusive into Greenland Group and in turn cut by the Te Kinga Monzogranite. Although this latter conclusion is based on somewhat tentative field relationships, it is confirmed by geochronological data (Ch.5). A small outcrop of megacrystic biotite granodiorite (KST3, KST6) strongly resembling Deutgam Granite occurs in Strauchon Creek (K32 849393) with apparent sharp contacts against typical Uncle Bay Tonalite. This outcrop may indicate Deutgam Granite intrusive into Uncle Bay Tonalite, also consistent with geochronological data.

### 3.4.2: Field description.

Uncle Bay Tonalite is a grey, massive, medium to coarse grained (2-10 mm), generally equigranular, mafic-rich, biotite tonalite (Fig.3.8, Fig.3.9). Titanite crystals are obvious in hand specimen and plagioclase megacrysts occur sparsely. The generally equigranular and more biotite-rich nature of Uncle Bay Tonalite distinguishes it from the otherwise similar Jays Creek Granite. The pluton outcrops over $\approx$35 km$^2$ as a NE-SW wedge along the northern face of Mount Te Kinga and on the low lying outliers around Lake Whitestone. Uncle Bay Tonalite is often heterogeneous and contains

numerous large metasedimentary sheets and inclusions (Greenland Group) in various stages of disaggregation. Uncle Bay Tonalite is also intruded by many mafic dikes of the Hohonu Dike Swarm (Fig.3.8), and cut by a number of small faults (see map), along which several streams drain into Lake Brunner. Modal classifications confirm a tonalitic designation (Fig.3.1). Typical outcrops of Uncle Bay Tonalite occur in an unnamed creek south of Strauchon Creek (K32 845386).

### 3.4.3: Petrographic description.

Quartz makes up between 14-40% of Uncle Bay Tonalite, as anhedral crystals up to 10 mm across (Fig.3.10). Quartz commonly indicates evidence for minor deformation with irregular grain boundaries, undulose extinction and deformation banding. Some fracturing and recrystallization of the quartz is also evident in deformed samples from near the Rocky Creek fault.

Alkali feldspar is minor or absent and comprises up to 6 modal percent as anhedral, microcline twinned, interstitial crystals up to 3 mm across. Three microprobe analyses of alkali feldspar from KNB8 indicate compositions between 86-94wt%Or.

Plagioclase occurs as subhedral to euhedral crystals up to 7 mm across, and as occasional megacrysts up to 15 mm in hand specimen. Microprobe data indicates the plagioclase is mostly $\approx$An36%, ranging from An30-50%. Plagioclase crystals are highly albite twinned with occasional Carlsbad twins. Normal zoning is common, and is sometimes strongly developed. Some oscillatory zoning is also present, particularly in the larger plagioclase crystals. Plagioclase constitutes up to 55% of Uncle Bay Tonalite.

Biotite is the most abundant mafic phase, making up to 28 percent of the mode. It is present as subhedral to euhedral, platy crystals up to 4 mm across, with yellow-brown to green-brown or brown pleochroism and abundant apatite inclusions. Microprobe analyses indicate moderate Ti, Al(tot) and Fe/(Fe+Mg). Rare deuteric alteration of biotite to chlorite and a fine grained, amorphous mixture of garnet, prehnite, epidote and titanite (as described by Tulloch 1979b) occurs along alteration planes parallel to cleavage in altered specimens.

Amphibole makes up to 7% of the more mafic varieties but is generally absent in more typical Uncle Bay Tonalite. The amphibole is present as anhedral to subhedral crystals up to 2 mm long, exhibiting strong brown to green pleochroism. Amphibole often occurs in glomeroporphyritic clots with other mafic phases, particularly biotite and magnetite. Microprobe analyses of amphibole from KST7 indicate classification as magnesio-hornblende according to the classification system of Leake (1978).

Titanite makes up to 1% of the rock in a variety of forms. Titanite occurs as euhedral to subhedral crystals up to 3 mm long; as smaller, resorbed anhedral crystals commonly associated with biotite; or rimming opaque phases. Titanite also occurs as a secondary alteration product of biotite and both varieties may be present within a single specimen. Titanite is more common in amphibole-bearing samples of Uncle Bay Tonalite.

Allanite is a common accessory phase as subhedral to euhedral, red to red-brown pleochroic, commonly zoned crystals up to 1.5 mm long, occasionally rimmed by epidote. Epidote is also relatively common within Uncle Bay Tonalite, particularly as a secondary alteration product of feldspar. Large subhedral patches of epidote, and epidote rimming allanite is likely to be of a primary igneous origin.

Opaque phases are surprisingly scarce considering the mafic nature of the granitoid, constituting no more than 0.4% of the rock as subhedral to euhedral crystals up to 1 mm across.

Tourmaline occurs in an aplite sample collected from Little Uncles Creek (KUC3) and also occurs very sparsely in the typical granitoid (KNB8, KNB9 and KST7) as subhedral to anhedral crystals up to 1.5 mm long. The tourmaline exhibits brown to strong blue pleochroism, indicative of schorl.

Accessory phases include ubiquitous, euhedral apatite crystals up to 1 mm across. Zircon is less common than apatite, occurring as euhedral crystals up to 0.5 mm long. Some muscovite was also observed in specimens from Wallace Creek and is probably secondary in origin.

Mafic inclusions within the Uncle Bay Tonalite are relatively common, and one collected from Little Uncles Creek (KUC5) contains only minor quartz and is a hornblende-biotite-tonalite/diorite. Mafic phases, including yellow-brown to green-brown biotite, green amphibole and titanite, are abundant and make up 33% of the inclusion.

## 3.5: Te Kinga Monzogranite.

### 3.5.1: Introduction and field relationships.

Te Kinga Monzogranite was described originally by Mason and Taylor (1987), but not named officially until Mason (1990) coined the name "Te Kinga Adamellite". The name is converted to Te Kinga Monzogranite here to confer with the classification system of Le Maitre *et al* (1989). Te Kinga Monzogranite outcrops over $\approx$45 km$^2$ as a fine or coarse grained, occasionally megacrystic, muscovite biotite monzogranite. The pluton occurs on the central and eastern parts of Mount Te Kinga, with outcrops also occurring in a quarry on a small unnamed hill (K32 913394) to the north of Mount Te Kinga, and on the Hohonu Ranges near Inchbonnie. Typical exposures of Te Kinga Monzogranite occur in the remains of a small quarry on Hodgkinson Road (K32 899380), about 1 km south of Rotomanu Railway Station and nearby in the banks of the Poerua River.

Exposures on the south-eastern margin of Mount Te Kinga were originally mapped by Mason (1990) as mylonitized Uncle Bay Tonalite. Mapping along this margin during this study indicates that the mylonites are largely derived from the Te Kinga Monzogranite, particularly on the shores of Lake Poerua, although tectonic inclusions of Uncle Bay Tonalite, sheared Greenland Group and Granite Hill Complex gneiss are also present (e.g. Brums Creek, cross section A-A', map pocket). Deformation decreases rapidly to the north-west, and is largely absent in Fred's Creek and the middle reaches of Fleming Creek. Mason (1990) attributed mylonitization of this margin to the proximity of the Fraser Fault. Only cataclasis has been observed in the footwall of the Fraser Fault (Rattenbury 1987a, 1991, Ch.8) and the mylonitization is here considered to result from the presence of the Alpine Fault within 1 km of many of these outcrops.

Te Kinga Monzogranite intrudes Greenland Group in Wallace Creek. At Fleming Creek (K32 896366) many sheets of hornfelsic metasediment closely resembling Greenland Group, occur within the granitoid. In places these sheets make up over 50% of the outcrop, and the exposures are interpreted as a diffuse, sheeted, intrusive contact between Greenland Group and Te Kinga Monzogranite, or a large inclusion of Greenland Group metasediment within the pluton.

Relationships between Te Kinga Monzogranite and Uncle Bay Tonalite are described more fully in Ch.3.4.1. Exposures of Te Kinga Monzogranite occur on the south-eastern corner of the Hohonu Ranges, although no contact was observed between Te Kinga Monzogranite and Deutgam Granite.

### 3.5.2: Field description.

Te Kinga Monzogranite is a white, generally equigranular, leucocratic to mesocratic, fine or coarse grained biotite muscovite granitoid (Fig.3.11, Fig.3.12) which exhibits a mylonitic fabric along the south-eastern margin of Mount Te Kinga. Porphyritic varieties of Te Kinga Monzogranite, containing megacrysts of alkali feldspar up to 3 cm long, are exposed sporadically above the bush line on Mount Te Kinga. Distinct coarse and fine grained variants of Te Kinga Monzogranite occur and were observed in sharp contact in Fred's Creek, and similar relationships are described by Mason (1990) from Hodgkinson Road. No chilled margins are observed at these contacts. The two varieties are similar in terms of mineralogy and geochemistry and are considered to be consanguineous and contemporaneous. Coarse grained varieties of Te Kinga Monzogranite are well exposed at Rotomanu Railway Station, whereas the quarry at the unnamed 149 m hill is a good example of fine grained Te Kinga Monzogranite. Exposures at the latter quarry display a strong magmatic foliation and are cut by several tourmaline and garnet-bearing pegmatites. Pegmatites are rare in the remainder of the pluton and as hornfelsic Greenland Group outcrops less than a kilometre from this quarry at "Bobs Knob" (K32 918416), the abundance of pegmatites at this quarry may be due to the concentrated activity of magmatic water near an igneous contact. The pegmatites contain blue pleochroic tourmaline (var. schorl) crystals up to 5 cm long and numerous small (0.2 mm) euhedral garnet crystals.

Several zones of hydrothermal alteration were located along the north-eastern side of Mount Te Kinga.

### 3.5.3: Petrographic description.

Quartz occurs in Te Kinga Monzogranite as anhedral crystals, up to 6 mm across, with irregular, serrated, dynamically recrystallizing margins and fine, interstitial sub-grains (Fig.3.13). Most crystals show some degree of undulose extinction and in the more deformed examples, quartz ribbons have developed. Exposures on the tops of Mount Te Kinga, at higher levels within the pluton, contain hexagonal areas of polycrystalline quartz up to 7 mm across indicative of high level intrusion and rapid quartz growth, and give the granitoid a porphyry appearance. Quartz makes up 26-47% of Te Kinga Monzogranite.

Plagioclase constitutes 20-35% of the rock as anhedral to subhedral crystals up to 4 mm long. Albite twinning is common and crystals show occasional weak normal zoning. In the protomylonitic-mylonitic samples feldspar crystals resist deformation and become augen. Microprobe data indicates the plagioclase is mostly sodic oligoclase ($\approx$An24%) with analyses ranging from An13-28%.

Alkali feldspar makes up 18-31% of the mode as anhedral crystals (up to 4 mm) within the groundmass of the rock. Occasional euhedral to subhedral megacrysts up to 3 cm long occur towards higher levels of the pluton. Groundmass alkali feldspar is generally perthitic and may exhibit transformation twinning. Microprobe analyses of groundmass alkali feldspar indicate compositions of between Or87-95%. Megacrystic alkali feldspar commonly contains small euhedral inclusions of plagioclase with subordinate biotite and quartz, oriented parallel to the crystal margins, representing crystals attached to the side of the megacrysts during growth.

Biotite occurs as yellow-brown to brown or slightly red-brown pleochroic platy crystals up to 3 mm long. In deformed specimens biotite is often sheared around resistant feldspars. Biotite makes up to 12 modal percent of some specimens, but is generally much lower at around 5%. Microprobe data indicates moderate Ti contents and relatively high Al(tot) and Fe/(Fe+Mg).

Muscovite is present as subhedral to euhedral crystals up to 7 mm long. Muscovite is sheared parallel to foliation in deformed specimens of Te Kinga Monzogranite, although it is less affected by the deformation than coexisting biotite. Microprobe analyses of muscovite from several specimens indicate relatively restricted compositions with Mg/(Mg+Fe) less than muscovite of the Summit Granite and relatively high Ti. Muscovite makes up to 8% of Te Kinga Monzogranite.

Te Kinga Monzogranite contains rare, small, euhedral opaque crystals up to 0.2 mm across. Apatite and minor zircon are also present as small, acicular crystals up to 0.2 mm long. A single specimen (KWC7) collected from a thin sheet of Te Kinga Monzogranite cutting Greenland Group in Wallace Creek contains several anhedral crystals of blue-brown pleochroic tourmaline, and may be pegmatitic in origin.

Along the shores of Lake Poerua, Te Kinga Monzogranite has been transformed into a leucocratic, fine grained, equigranular muscovite biotite monzogranitic mylonite. Mineralogically these rocks are identical to less deformed examples at Rotomanu. Quartz is generally highly recrystallized, forming large areas of fine grained (0.01 mm) crystals in areas of high strain, although larger crystals of quartz are still present, generally exhibiting strong undulose extinction. In KLP2, the quartz has formed quartz ribbons and has recrystallized in cracked feldspar augen. Feldspars have acted in typical mylonitic fashion and have acted brittly to form augen surrounded by quartz shadows. Myrmekite is common in the mylonitic varieties of Te Kinga Monzogranite. Micas have been strongly sheared by deformation.

## 3.6: Deutgam Granite.

### 3.6.1: Introduction and field relationships.

Deutgam Granite, previously called the Deutgam Adamellite by Hamill (1972), is the largest and most complex of the granitoids of the Hohonu Batholith, outcropping over an area of $\approx 120$ km$^2$. Deutgam Granite makes up the bulk of the Hohonu Ranges, and also includes deformed granitoids outcropping on the south-eastern end of Mount Turiwhate, formerly termed Fitzgerald Granodiorite (Waight 1990).

Deutgam Granite displays sharp, intrusive contacts with the Greenland Group (Fig.3.14) along its northern margin (e.g. K32 769384), and is in turn cut by numerous members of the Hohonu Dike Swarm. In Clear Creek (≈K32 702330) Deutgam Granite exhibits a strong, mainly magmatic, foliation parallel to an obscured, presumably intrusive, contact with Greenland Group.

Relationships between Deutgam Granite and Te Kinga Monzogranite and Uncle Bay Tonalite have been discussed previously. Relationships between Deutgam Granite and the neighbouring French Creek Granite clearly indicate French Creek Granite is intrusive into Deutgam Granite, consistent with geochronological data (Ch.5). In the Eel Creek region, French Creek Granite intrudes Deutgam Granite (Fig.3.15), although this contact has since been reactivated into a steep reverse fault. In the Eastern Hohonu River numerous aplites derived from French Creek Granite cut Deutgam Granite near an obscured contact between the two units (K32 756378) (see Fig.3.25). Deutgam Granite is also intruded by numerous, glassy, rhyolite dikes related to French Creek Granite (Ch.3.12.2).

Deutgam Granite and Summit Granite occur in close proximity on Mount Turiwhate (≈K33 704252), although the actual contact is not seen to outcrop. A possible sheet of Deutgam Granite cutting the Summit Granite also occurs nearby (K32 700257).

Outcrops in Grahams Creek (J33 700273) are interpreted as a wedge of Greenland Group, cut by numerous aplites, separating Turiwhate Granodiorite and Deutgam Granite (Fig.3.16). A south-dipping reverse fault runs up Grahams Creek and separates Greenland Group and Turiwhate Granodiorite. In contrast, the contact between the Greenland Group wedge and Deutgam Granite is diffuse and marked by a wide zone of assimilation of metasedimentary xenoliths into the granitoid and is interpreted as either Greenland Group incorporated within Deutgam Granite as a large xenolith, or a diffuse intrusive contact between Deutgam Granite and Greenland Group. Similar xenoliths were observed near a Greenland Group-Deutgam intrusive contact on the Hohonu Ranges (K32 788387). A schematic interpretation of this contact is presented in Fig.3.16. Megacrystic Deutgam Granite is brecciated and cut by

epidotized shear zones at Carew Creek Falls, due to the proximity of the Hohonu Fault which runs between this outcrop and Tertiary limestone exposed at Knoll Point.

### 3.6.2: Field description.

#### 3.6.2.1: Introduction.

*"Intensely corrugated gneiss .... apparently intruded by fairly acid faintly gneissose granites, with which are associated basic porphyritic gneissoid granites.....giving a most complex though interesting section"*
Bell and Fraser (1906, p65) describing the State Highway 73 section along Mount Turiwhate.

Mineralogically, texturally, and geochemically the Deutgam Granite is an extremely variable unit, ranging from relatively mafic, coarse grained megacrystic hornblende biotite tonalite to equigranular biotite granite and leucocratic muscovite biotite syenogranite aplite. Foliations are variably developed, with most outcrops being massive and unfoliated whereas others are deformed, most probably due to deformation in association with the Alpine Fault (e.g. Fig.3.19). However, some outcrops also display a magmatic foliation identified by aligned, euhedral, undeformed alkali feldspar megacrysts. Abundant metasedimentary inclusions and sheets are also present within Deutgam Granite, being especially prevalent along the south-eastern margin from Inchbonnie to the Big Wainihinihi River.

The dominant variety of Deutgam Granite is a megacrystic biotite granodiorite outcropping over most of the Hohonu Ranges and in the Big Wainihinihi River, Mount Turiwhate. Equigranular variants of the Deutgam Granite occur sporadically above the bush line, particularly around Mount French, and appear to be more dominant along the eastern edge of the Hohonu Ranges. Sparse outcrops of leucocratic aplitic Deutgam Granite also occur on the tops of the Hohonu Ranges. It proved difficult to distinguish these varieties as distinct mappable bodies and all are considered to belong to the same episode of plutonic activity. Also included in this discussion are the equigranular tonalites exposed at Inchbonnie Quarry, tentatively included within the Deutgam Granite. All varieties are described in an attempt to portray the heterogeneity of the pluton.

**3.6.2.2: Megacrystic Deutgam Granite: Field description.**

The dominant variety of Deutgam Granite is a massive, mesocratic, coarse grained, biotite granodiorite containing abundant, euhedral, salmon pink alkali feldspar megacrysts up to about 7 cm long (Fig.3.17, Fig.3.18). Typical outcrops of this granitoid occur in road cuts at Camp Point and Granite Point on the southern shores of Lake Brunner (K32 815383). Typical megacrystic Deutgam Granite also outcrops over most of the exposed tops of the Hohonu Ranges, being especially well exposed in the Mount Treacey and Mount Bruce Murray areas. Outcrops along the Taramakau River, State Highway 73, Big Wainihinihi River and in Clear Creek show a strong foliation, excellent exposures occurring in Fitzgerald's Quarry (K33 726262) (Fig.3.19). The foliated rocks may contain abundant metasedimentary and paragneissic material and form most of the southernmost portion of the pluton. Along the Taramakau and Big Wainihinihi Rivers the foliation largely parallels the Alpine Fault, and is probably associated with movement on this structure. Shear sense indicators in the Taramakau River indicate a dextral motion, consistent with movement on the Alpine Fault. However, evidence for a pre-existing magmatic/syn-tectonic foliation is also present along much of State Highway 73 and Clear Creek, recognized by the presence of largely undeformed, orientated, euhedral alkali feldspar megacrysts, and numerous orientated sheets of metasediment. Brittle rotation of feldspar megacrysts to their current alignment would result in the formation of augen, bookshelf structures and other such indicators of brittle deformation. Although such features are present, they are not sufficiently abundant to explain rotation from an originally randomly orientated precursor and a pre-existing flow orientation is required. Similar overprinting of a pre-existing magmatic foliation by a later tectonic foliation occurs in the Cape Foulwind Granite near Westport. At Fitzgerald's quarry, and along the Big Wainihinihi River this foliation is complicated by overprinting by the Alpine Fault. Foliations observed in Clear Creek cannot have been caused by movement along the Alpine Fault as they are separated from the Alpine Fault by undeformed granitoids in the Mount Bruce Murray and Mount Treacey areas, although movement on the Hohonu Fault may have contributed to the observed foliation. The foliated varieties of the Deutgam Granite are restricted to the south-western margin of the pluton, and are possibly indicative of intrusion into a tectonically active environment. Gabbroic blocks incorporated within megacrystic Deutgam Granite are described in Ch.3.12.1.

**3.6.2.3: Megacrystic Deutgam Granite: Petrographic description.**

Quartz is present in the megacrystic Deutgam Granite as anhedral crystals up to 10 mm across, often in polycrystalline clumps, and makes up between 11-32% of the rock (Fig.3.20). Undulose extinction is virtually ubiquitous and becomes more intense in those samples foliated in outcrop. More extremely foliated samples contain dynamically recrystallized quartz with a strong lattice preferred orientation. Symplectites are common, particularly in the more deformed samples.

Plagioclase makes up between 21-49% of the mode and is present as subhedral to euhedral, albite twinned crystals up to 7 mm long. Plagioclase composition in the entire Deutgam Granite is variable, ranging between An2-43% (mostly An23-40%). In contrast, the megacrystic variety has plagioclase compositions restricted to between An32-43%. In general anorthite content of plagioclase decreases with increasing evolution and silica content in Deutgam Granite. Normal zoning is common, and occasional oscillatory zoning is also observed. Several plagioclase crystals were observed with high relief, unzoned, high An%, cracked cores, enclosed by an outer rim of andesine and lower An% feldspar separated by a sharply normal and oscillatory zoned transition. These cores may represent restitic plagioclase cores as proposed by Chappell *et al* (1987). Such cores are rare in the Deutgam Granite, and in other plutons in the batholith, and along with geochemical evidence, indicate that restite unmixing is an unimportant process in the petrogenesis of these plutons.

Alkali feldspar occurs as both a groundmass and megacryst phase and constitutes $\approx 15\%$ of the granitoid. Alkali feldspar megacrysts generally have a distinct salmon pink colour and occur as euhedral to subhedral crystals up to 7 cm long. The megacrysts commonly exhibit both Carlsbad twinning, often obvious in outcrop, and transformation twinning and are generally perthitic. Microprobe analyses indicate relatively restricted Or contents (Or88-94%), and the presence of transformation twinning and a large $2V_x$ suggest a microcline structural state. Many megacrysts contain abundant inclusions of most other mineral phases present in the granitoid. Alkali feldspar also occurs in the groundmass of not only the megacrystic variety but also in more felsic equigranular varieties. It generally occurs as interstitial, anhedral

crystals up to 10 mm long, and may be featureless, perthitic or show abundant transformation twinning.

Clusters of alkali feldspar, up to 1 m in diameter, are relatively common and are closely linked to the presence of biotite-rich mafic enclaves. Dehydration of biotite in these enclaves may have enhanced the crystallization and growth of alkali feldspar megacrysts. Similar clusters of alkali feldspar megacrysts in the Macey Granite in the Victoria Range were attributed by Tulloch (1979a) to an early formed cumulate phase and no association with mafic enclaves was noted by Tulloch (1979a).

Biotite is the dominant mafic mineral in the megacrystic granodiorite, comprising between 10-28 modal percent as anhedral to subhedral yellow-brown to green-brown or brown pleochroic crystals up to 4 mm across. In foliated samples, biotite is sheared and orientated sub-parallel to the foliation. Serrated margins, indicating reaction with felsic melt phases, are common in some samples and most biotite includes abundant apatite and occasional zircon crystals. Pleochroic haloes around zircon crystals are uncommon. Biotite often occurs in clots associated with other mafic minerals, in particular Fe-Ti oxides, amphibole and titanite. Microprobe analyses of biotite from Deutgam Granite reveal highly variable compositions, generally with relatively low Ti contents and moderate Al(tot) and Fe/(Fe+Mg). Little consistent variation in biotite composition is evident between textural or chemical varieties of Deutgam Granite, apart from a crude increase in Ti and Al with increasing bulk rock $SiO_2$.

Titanite is common, particularly in the more mafic varieties, as subhedral to euhedral sugary brown crystals up to 4 mm in size. Crystals encased in biotite retain their euhedral nature whereas anhedral titanite remnants surrounded by feldspar and quartz indicate reaction between titanite and felsic melts. Twinning in titanite is rarely present. Several titanite crystals were observed to be partially rimmed by epidote or opaques.

Amphibole is abundant in the more mafic samples of megacrystic granodiorite but becomes rare to absent in samples containing over $\approx 65\%$ $SiO_2$. Amphibole is most abundant in the granitoids outcropping in the centre of the pluton around Deutgam Peak, Mount Bruce Murray and Mount Treacey, suggesting a crude zonation of the pluton. Amphibole occurs as anhedral to subhedral crystals up to 5 mm in size, commonly in mafic clumps with biotite, titanite and Fe-Ti oxides. No relict pyroxene cores were observed (*cf* Turiwhate Granodiorite). Pleochroism in amphibole is variable with the majority of crystals exhibit green to light brown pleochroism, although occasionally blue-green colours also occur. Microprobe analyses of amphiboles indicate classification as magnesio-hornblende (Leake 1978).

Allanite is a relatively common accessory phase, occurring as euhedral, zoned crystals with intense red-brown pleochroism. Allanite crystals are up to 1.5 mm in size, and many are rimmed by epidote with a similar lattice orientation.

Epidote is common in the more mafic, amphibole bearing varieties. Much of the epidote is undoubtedly secondary, reflecting greenschist facies deformation and deuteric alteration. Secondary epidote occurs as yellow-green veins cutting deformed outcrops, and bright yellow-green material in the cores of altered feldspar and mica crystals. However, many epidote crystals, up to 2.5 mm in size, display primary igneous features, notably oscillatory concentric zoning, twinning and euhedral crystal shapes. Crystals identified as primary magmatic epidote also lack the strong yellow-green colour which characterizes secondary epidote (Tulloch 1986). Primary igneous features are well preserved in crystals which are protected from the felsic melt by encapsulation in biotite. Other crystals in contact with quartz and feldspar retain their euhedral shapes but have been resorbed, indicating instability in the magma. The presence of igneous epidote has been the subject of much controversy, firstly as to whether it can actually exist and secondly what, if any, magmatic and pressure-temperature conditions it represents. Tulloch (1979a+b and 1986) has identified magmatic epidote in several Rahu Suite and Separation Point Suite plutons, and has questioned its use as an indicator of emplacement depths.

Accessory phases include ubiquitous euhedral apatite crystals up to 0.5 mm in size, and relatively sparse smaller zircon crystals. A single crystal of blue pleochroic tourmaline occurs in a specimen from the Deutgam Peak Region (HDP10). Opaque phases generally occur as euhedral magnetite crystals up to 2 mm in size.

### 3.6.2.4: Equigranular Deutgam Granite: Field description.

Locally within the Deutgam pluton are outcrops of a medium to coarse grained, mesocratic to leucocratic, equigranular, biotite monzogranite. This variety is particularly common in the Mount French area and along the eastern margin of the Hohonu Ranges, from Waterfall Creek to Inchbonnie Quarry. Foliated varieties also occur, interleaved with foliated megacrystic granodiorite (e.g. TFQ4). Sharp, non-chilled, vertical igneous contacts between megacrystic biotite rich granodiorite (TFQ1) and the more felsic equigranular monzogranite (TFQ4) exposed in a recent road cut on State Highway 73 (K33 723267) indicate the two magmas were consanguineous. A leucocratic, medium grained, equigranular, biotite syenogranite (TFQ5) also intrudes TFQ4 at this locality, and is interpreted as an aplite dike. Pegmatites also occur at this road cut and all rocks display a strong foliation, most obvious in the biotite-rich megacrystic phase. The complexities of this exposure indicate the difficulties encountered when attempting to interpret small isolated outcrops.

### 3.6.2.5: Equigranular Deutgam Granite: Petrographic description.

Quartz occurs as anhedral crystals up to 3 mm across and is commonly recrystallized and exhibits undulose extinction, particularly in those specimens with a strong foliation. Quartz makes up 22-30% of the mode (Fig.3.21).

Plagioclase constitutes 16-38% of the rock as subhedral, poorly albite twinned crystals of sodic oligoclase to andesine (An 11-31%) up to 4 mm long. Zoning of plagioclase is rare but when present is generally normal or occasionally oscillatory.

Alkali feldspar is present as white, anhedral to subhedral, commonly perthitic crystals up to 7 mm in size, displaying occasional transformation twinning. Microprobe analyses indicate compositions between 86-96wt% Or. Some specimens (e.g. HMF7)

contain relatively large, pink, Carlsbad twinned, alkali feldspar crystals, and may be transitional to the megacrystic granitoids.

Biotite is the most abundant mafic phase, making up between 5-10 modal percent, as anhedral, yellow-brown to green-brown pleochroic crystals up to 2 mm across and commonly displaying serrated crystal margins. Biotite often contains abundant inclusions of apatite and, less commonly, zircon.

Titanite occurs occasionally as anhedral to subhedral, commonly resorbed, crystals. Euhedral titanite crystals up to 0.5 mm occur only when the crystals are mantled by biotite and have been protected from the melt.

Allanite occurs rarely as euhedral, red-brown pleochroic, zoned crystals up to 1 mm across. HWC4 is an exception and contains abundant allanite, approximately 10 crystals within a single thin section.

Muscovite occurs sporadically and is mostly secondary and associated with sericitization of feldspars.

Accessory minerals include subhedral opaques up to 1.2 mm across, abundant euhedral apatite up to 0.5 mm long and less abundant euhedral zircon up to 0.1 mm long.

**3.6.2.6: Aplitic Deutgam Granite: Field description.**

Infrequently outcropping within Deutgam Granite is an equigranular, fine to medium grained, leucocratic aplitic monzogranite to syenogranite. On the exposed tops these rocks tend to occur as areas $\approx 20$ m$^2$ in size (Fig.3.22) and may represent pools of evolved felsic magma trapped at the top of the pluton, fed by aplitic dikes such as those observed at lower levels, e.g. Camp Point (HRS17) and below the Carew Creek Falls (HCC1).

**3.6.2.7: Aplitic Deutgam Granite: Petrographic description.**

Quartz is abundant, making up between 26-44% of the specimens examined. Quartz occurs as anhedral to subhedral crystals up to 2 mm across.

Plagioclase is generally subordinate to alkali feldspar, making up between 19-35% of the rock and occurring as anhedral to subhedral poorly twinned crystals of albite to sodic oligoclase (An6-17%). Specimen HRS8, an aplite dike, contains plagioclase between An2-7% (albite). Occasional normal zoning occurs, these crystals commonly exhibiting sericitized cores.

Alkali feldspar makes up between 31-37% of the aplitic varieties as anhedral to subhedral perthitic crystals up to 2.5 mm across. Occasional transformation twinning is also present. Microprobe analyses indicate compositions between 83-97wt% Or.

Biotite is present as occasional yellow-brown to green-brown and rarely reduced red-brown anhedral crystals up to 0.75 mm across. Biotite is commonly altered to chlorite and makes up only 1-3% of the aplites, reflecting their extreme leucocratic nature.

Allanite occurs in specimen HRS17 as small (0.1 mm) dark red euhedral crystals, but is absent from all other aplitic specimens examined.

Titanite occurs in HBC5 as a few skeletal, resorbed euhedral crystals up to 1.5 mm long. A few small (0.15 mm) subhedral crystals of blue pleochroic tourmaline also occur within this specimen.

Muscovite occurs within the aplitic varieties and is mostly of secondary origin as a consequence of feldspar sericitization, although the presence of primary muscovite in rocks of these evolved compositions is feasible. Microprobe analyses of muscovite indicate generally low Ti, characteristic of a secondary origin (Miller *et al* 1981).

Other accessory minerals include small magnetite crystals and euhedral apatite and zircon crystals up to 0.25 mm long.

### 3.6.2.8: Inchbonnie Tonalite: Field description.

An excellent exposure of foliated, medium grained, equigranular, mesocratic to melanocratic titanite-biotite tonalite occurs at a large quarry (K32 825305) at Inchbonnie, about 500 m from the main body of the Hohonu Ranges. No other outcrops of this rock are known and no contacts with other granitoids are exposed, the nearest outcrops being of typical equigranular Deutgam Granite on the nearby ranges, and highly foliated megacrystic Deutgam Granite at Inchbonnie Bluff on the Taramakau River. Combined field, geochemical and isotopic data suggest correlation with the Deutgam Granite, although it is petrographically distinct and may represent a separate intrusive event. The tonalite is foliated, probably due to the proximity of the Alpine Fault, and is characterized by numerous oriented mafic inclusions and abundant thin aplitic dikes.

### 3.6.2.9: Inchbonnie Tonalite: Petrographic description.

Quartz occurs as crystals up to 5 mm, but mostly about 0.5 mm, across and makes up around 30% of the rock. The quartz is mostly recrystallized and strained, exhibiting near ubiquitous undulose extinction (Fig.3.23).

Plagioclase makes up 37-45% of the tonalite as albite twinned subhedral crystals of calcic oligoclase ($\approx$An 30%) up to 6 mm long.

Alkali feldspar is rare and makes up only 6% of one specimen (IQ1) and is absent within the other (IQ6), confirming designation as a tonalite. Alkali feldspar occurs as anhedral crystals up to 3 mm across.

Biotite is the dominant mafic phase, making up 22-24% of the rock as sheared green-brown pleochroic crystals up to 3 mm across. The mica contains abundant inclusions of apatite, zircon and opaques.

Hornblende occurs in one specimen examined (IQ1) as distinctly blue-green to green-brown pleochroic, subhedral to anhedral crystals up to 2 mm long.

Titanite is abundant and characteristic of the tonalite, comprising around 1% of the rock, as subhedral, occasionally twinned, crystals up to 1 mm across. Titanite is closely associated with biotite and is often observed enclosed within it.

Accessory phases include abundant euhedral apatite and zircon crystals up to 0.25 mm across and rare allanite up to 2 mm across, often rimmed by epidote. Opaque phases make up approximately 1% of the rock as subhedral magnetite crystals up to 0.5 mm across.

**3.6.2.10: Enclaves.**

Dioritic enclaves within Deutgam Granite are not particularly common, and difficult to sample. Enclaves examined from State Highway 73, Camp Point and Lake Ruby are generally no larger than a few decimetres across and are composed of fine grained, equigranular quartz diorite or diorite. The four enclaves examined (TFQ3, HRS1, HRS15, HLR1) are similar and consist of minor quartz, abundant plagioclase, amphibole, titanite, opaques, occasional allanite and accessory apatite, opaques and zircon. Plagioclase occurs as subhedral to euhedral laths of albite twinned calcic oligoclase (An 27-30%) up to 1 mm long, often normally zoned. Amphibole is abundant (HRS1 being an exception) making up around 30% of the enclaves, as subhedral, blue-green to brown pleochroic crystals up to about 0.25 mm across. Biotite is the other abundant mafic phase, present as small, subhedral to anhedral, yellow-brown to green-brown crystals up to 0.5 mm across. Titanite occurs as euhedral, resorbed crystals up to 0.25 mm long. In HLR1, titanite is generally surrounded by $\approx 1$ mm of plagioclase and quartz, free of mafics, giving the rock a spotted appearance.

Paragneissic and metasedimentary inclusions are common within the south-western portion of the Deutgam Granite. These inclusions may reach quite large dimensions, such as the 20+ m wide inclusion exposed on State Highway 73 (TFQ10, K33 720270). Varying degrees of assimilation are evident, with many inclusions bearing a striking resemblance to Greenland Group metasediments, whereas others are much more paragneissic in appearance. Some of the more intact inclusions contain felsic-rich sheets indicative of partial melting. TFQ10 is a sample of a micaceous quartzofeldspathic paragneiss sheet which, in thin section, consists of abundant fine

grained (0.75 mm) red-brown pleochroic biotite and larger (5 mm) crystals of muscovite, both displaying a strong lattice and shape preferred orientation. Abundant fibrous sillimanite occurs as fine grained needles throughout the section. Sillimanite also occurs in similar inclusions on Mount Turiwhate (D.Shelley, *pers.comm.* 1993) and in Mays Creek (A.F.Cooper, *pers.comm.* 1993). Geochemical and isotopic data indicate affinities of this paragneissic inclusion to the Greenland Group (Ch.2).

## 3.7: French Creek Granite.

### 3.7.1: Introduction and field relationships.

The name Brunner Granite was introduced by Hamill (1972) to describe the red granites on the western edge of the Hohonu Ranges, and this name was subsequently used by Tulloch (1988a) to propose the Brunner Suite. The granitoid has since been renamed the French Creek Granite by Tulloch *et al* (1994).

French Creek Granite is a distinctive red, equigranular granitoid that outcrops over $\approx 10$ km$^2$ along the north-western margin of the Hohonu Ranges, extending from a tributary of Eel Creek on the northern Hohonu Ranges to the headwaters of Deep Creek in the west. Most varieties of French Creek Granite are well exposed in the lower reaches of the Eastern Hohonu River.

The north-west margin of the pluton is reverse faulted against recent gravels in the Little Hohonu River (K32 724375) and against Greenland Group in Deep Creek (K32 700341). French Creek Granite also outcrops within 100 m of Tertiary sandstone in the Eastern and Little Hohonu Rivers and is described by Hamill (1972) and Morgan (1911) as being faulted against Blue Bottom sediments in the Greenstone River. This exposure was not observed during the present study. French Creek Granite intrudes the neighbouring Deutgam Granite in the headwaters of Eel Creek (K32 764383), along an intrusive contact reactivated by recent faulting. A dike of French Creek Granite can be seen to cross cut Deutgam Granite at this outcrop (see Fig.3.15). In the Eastern Hohonu River a concealed contact between Deutgam Granite and French Creek Granite can be located to within a few tens of metres (K32 757377). Several aplitic dikes derived from French Creek Granite cut the Deutgam Granite immediately upstream of this contact (see Fig.3.25). Over much of the Hohonu massif, felsic rhyolite dikes,

believed to be related to French Creek Granite (see Ch.3.12.2), also intrude Deutgam Granite.

Intrusive relationships between French Creek Granite and the Hohonu Dike Swarm are complex and are indicative of broadly contemporaneous magmatic activity (Ch.7). Members of the Hohonu Dike Swarm intrude French Creek Granite (Fig.3.24), whereas aplites near the contact between French Creek Granite and Deutgam Granite are observed cutting mafic dikes (Fig.3.25). Cross cutting relationships between the mafic dikes and the hypabyssal rhyolitic dikes are similarly ambiguous. Composite dikes described in Ch.7 also suggest contemporaneous activity in the French Creek Granite and Hohonu Dike Swarm. Of particular note is the scarcity of mafic dikes intruding French Creek Granite, compared to their much greater abundance in the neighbouring Deutgam Granite.

A 30 metre zone of intense hydrothermal calcitic alteration is exposed in the Eastern Hohonu River (K32 755380). The French Creek Granite is altered to an orange colour and cut by a number of calcite veins up to 1 metre wide. An altered mafic dike within the zone of alteration indicates alteration post-dates mafic dike emplacement. Alteration appears most intense around the dike which suggest it may have acted as a fluid conduit. Similar zones of alteration occur in Greenland Group in Deep Creek, and in Turiwhate Granodiorite in Fred's Creek and Grahams Creek. Numerous calcitic float blocks also occur in Rose Creek, Mount Tuhua (Waight 1990). Their origin is unknown, but the alteration appears to occur within close proximity of contacts along the north-western margin of the batholith and may be related to the movement of fluids along this lineament.

French Creek Granite is immediately distinguishable from the other granitoids of the batholith by its distinctive orange-red colouration, enabling recognition of the unit from a distant. The granitoid is often weathered and soft, and forms relatively low lying gentle slopes incised by deep gorges along the margin of the Hohonu Ranges. The unusual chemistry of the unit results in the growth of a distinct forest cover recognizable on air photos, dominated by Yellow Pine (Fig.3.26).

The French Creek Granite is a complex unit and comprises subsolvus syenogranite, hypersolvus monzogranite and quartz alkali feldspar syenite, suggesting intrusion and crystallization of several magma pulses. These varieties, and other associated rocks, are described below in order of abundance. The subsolvus syenogranite dominates the pluton, the remaining phases were only found to outcrop in the Eastern Hohonu River and may represent marginal phases. Hypabyssal rhyolitic dikes, chemically similar to the French Creek Granite are described in Ch.3.12.2.

### 3.7.2: Subsolvus biotite syenogranite: Field description.

The dominant variety of French Creek Granite is a massive, homogeneous, distinctively brick-red, medium to coarse grained, equigranular biotite syenogranite consisting of clear quartz, pink alkali feldspar, white (commonly altered) plagioclase and less than 10% mafics (Fig.3.27, Fig.3.28). This variety occurs throughout most of the pluton and is well exposed in the Greenstone, Little and Eastern Hohonu Rivers. In the Greenstone River, the biotite syenogranite contains numerous miarolitic cavities including secondary, euhedral quartz crystals (up to 5 mm) and micas altering to powdery iron oxides. The granitoid is commonly highly weathered, probably a result of late stage deuteric alteration. No enclaves or pegmatites were observed within the French Creek Granite although rare aplite dikes occur within French Creek Granite and cutting Deutgam Granite.

### 3.7.3: Subsolvus biotite syenogranite: Petrographic description.

The biotite syenogranite consists primarily of quartz and perthitic alkali feldspar in a distinctive granophyric texture, plagioclase and biotite (Fig.3.29).

Quartz constitutes between 23-39% of the mode as unstrained, often near euhedral, crystals up to 7 mm in size. Quartz forms granophyric intergrowths with alkali feldspar, exhibiting the same optical orientation over relatively large areas. In some instances it appears that granophyric intergrowths have grown by rapid undercooling of a melt containing pre-existing subhedral alkali feldspar crystals, as intergrowths may occur with sharp geometric boundaries on the outer rim of homogeneous alkali feldspar crystals.

Alkali feldspar occurs as euhedral to subhedral perthite crystals up to 10 mm long, making up 48-66% of the rock. In hand specimen the alkali feldspar is distinctively pink. Perthite crystals display high relief and are dusty brown, the brown colouration being distributed throughout entire crystals, rather than just the potassium-rich host (*cf* Hamill 1972). Concentration of this staining along cleavages was apparent in some crystals and may be attributable to very fine iron oxides produced during feldspar unmixing and/or deuteric alteration as proposed by Smith and Brown (1988). Perthite generally displays interlocking type intergrowths as described by Deer *et al* (1966). The perthitic crystals are commonly Carlsbad twinned, although a few transformation twins are also observed. Microprobe analyses indicate a wide range of compositions ($\approx$Or60-88%), with significant quantities of the albite molecule. Given the highly unmixed nature of the alkali feldspar, microprobe analyses will only give a minimum indication of original ternary feldspar composition.

Plagioclase crystals are subhedral to euhedral, up to 8 mm in length, and commonly albite twinned. Refractive index determinations and microprobe studies, indicate predominantly albitic compositions, with some scatter towards sodic oligoclase (An0-20%, mostly $\approx$An9%). The cloudy, high relief, iron staining evident in the alkali feldspar has also affected plagioclase but to a lesser degree. Normal zoning is evident, and the cloudy alteration of the plagioclase is often concentrated towards crystal cores, suggesting a compositional control.

The presence of two distinct feldspar phases indicates the French Creek Granite has undergone a subsolvus history (*cf* Hamill 1972). However, the perthitic, exsolved nature of the alkali feldspar and the abundance of granophyric intergrowths indicate that the final stages of crystallization may have occurred at hypersolvus conditions. Rapid crystallization of both quartz and alkali feldspar to produce the granophyric intergrowths is an anhydrous process and would generate residual aqueous fluids that may be responsible for the abundant deuteric alteration of the pluton and the pink colouration of the alkali feldspar.

Biotite is present as anhedral to subhedral crystals up to 3 mm across. When fresh, the mica exhibits distinctive yellow to yellow-brown pleochroism, indicative of an iron-rich composition. Microprobe analyses confirm this with Fe-rich annite compositions, high Ti and low Al(tot), distinctive from the biotite of other plutons (see Fig.4.1). More commonly biotite is altered to iron oxides and/or green chlorite (var. daphnite?).

Hornblende is rare within this unit and a few analyses of the single crystal observed indicate classification as ferroedenitic-hornblende.

Accessory phases include minor allanite, aenigmatite and interstitial calcite. Also present are ubiquitous euhedral apatite crystals, up to 0.5 mm long, and relatively abundant and large (0.2 mm), zircon crystals. Euhedral crystals of an opaque phase, probably magnetite, are also common.

### 3.7.4: Hypersolvus monzogranite: Field description.

The hypersolvus variety of French Creek Granite is exposed from a narrow gorge in the Eastern Hohonu River (≈K32 755380) to near the contact between the French Creek and Deutgam Granites. The hypersolvus monzogranite is a massive, medium to coarse grained, equigranular monzogranite varying from pink to more commonly brown or blue-green in colour (Fig.3.30). The monzogranite is invariably highly jointed and weathered. Miariolitic cavities were observed in a single, large angular float block in the Eastern Hohonu River.

### 3.7.5: Hypersolvus monzogranite: Petrographic description.

The hypersolvus monzogranite consists primarily of mesoperthitic feldspar and alkaline pyriboles. Following the recommendations of Le Maitre *et al* (1989), mesoperthite is assigned in equal proportions to alkali feldspar and plagioclase, hence designation as a monzogranite.

Feldspar comprises 63-68 modal percent of the rock as subhedral to anhedral, Carlsbad twinned, mesoperthitic crystals up to 8 mm long (Fig.3.31). The feldspar is invariably affected by the same high relief brown staining evident in the main

syenogranitic variety. The presence of a single feldspar indicates a hypersolvus crystallization history.

Quartz comprises 27-32% of the monzogranite as unstrained, subhedral to near euhedral crystals up to 4 mm in size. Embayed quartz is occasionally present, indicative of disequilibrium conditions. Granophyric intergrowths are present but are less pervasive than in the main syenogranitic phase.

The dominant mafic phase in the monzogranite is an alkali amphibole, identified as arfvedsonite on the basis of its yellow-brown to intense blue-green to dark green pleochroism, but more commonly altering to bright red-orange pseudomorphs. Amphibole occurs as euhedral to subhedral crystals up to 2 mm in size, often displaying good amphibole cleavage traces. Amphiboles from EHR14 classify as the sodic-calcic amphiboles katophorite or ferrobarroisite using the scheme of Leake (1978) (Fig.4.5). The analyses have very high iron contents, greater than 20%, accounting for their unusual pleochroic scheme. The presence of alkali amphiboles is consistent with the peralkaline chemistry of this rock.

Mafic accessory phases include anhedral crystals up to 1 mm across exhibiting very strong red-brown pleochroism identified as aenigmatite. They are commonly intimately related with, and enclosed by, alkali amphibole suggesting a replacement relationship. Also present are occasional anhedral crystals of brown to dark brown pleochroic biotite with strong orange-red interference colours, displaying minor alteration to green chlorite. In many samples examined all mafic minerals are altered to a complex mixture of fine grained opaques, calcite and quartz. Mafic phases make up to 7% of the granitoid.

Other accessory phases include relatively abundant, euhedral magnetite (up to 1 mm) and relatively abundant and large ($\approx$0.2-1.0 mm) zircon crystals.

### 3.7.6: Quartz alkali feldspar syenite.

The southernmost outcrops of French Creek Granite in the Eastern Hohonu River are of a altered grey-green to red-brown, equigranular, medium grained quartz alkali feldspar syenite.

Quartz makes up to 12% of the alkali feldspar syenite as anhedral crystals up to 2 mm in size, generally infilling spaces between alkali feldspar crystals. Some granophyric intergrowths are present (Fig.3.32).

Alkali feldspar is the most abundant mineral in this rock, making up around 80 modal percent as subhedral to anhedral crystals up to 4 mm in size. The rock is more affected by deuteric alteration than the other varieties of French Creek Granite, possibly a consequence of concentration of fluids near the pluton margin. Alkali feldspar is consequently very cloudy, although some remnant transformation twins are visible. Classification of the feldspar as perthite results in modal classification as a quartz alkali feldspar syenite. A few small (1.5 mm), albite twinned subhedral crystals of plagioclase were also observed in one specimen and indicate an at least partially subsolvus history.

Mafic phases in the alkali feldspar syenite are predominantly altered to a mixture of calcite and iron oxides. A few remnant anhedral to euhedral $\approx$2 mm crystals of amphibole display green pleochroism, distinct from that observed in the hypersolvus monzogranite. Also present are surprisingly fresh, subhedral crystals of biotite up to 2 mm long, exhibiting strong straw-yellow to yellow-brown or foxy-red pleochroism. Other accessory phases include euhedral to subhedral magnetite up 2 mm long and relatively large (0.2 mm) euhedral crystals of zircon and apatite. Secondary calcite and opaques are also present.

### 3.7.7: Aegirine arfvedsonite alkali feldspar syenite.

Although not found in outcrop, a distinctive grey-green, medium to coarse grained, equigranular mafic syenitic rock is relatively common in float in the northernmost branch of the Little Hohonu River (K32 731380). A single float sample (LHR10) classifies as alkali feldspar syenite.

Alkali feldspar makes up 77% of the rock as subhedral to euhedral, perthitic to occasionally mesoperthitic, Carlsbad twinned crystals up to 8 mm long. Notably, the high relief and brown colouration seen in the feldspars of all other varieties of the French Creek Granite is largely absent in this sample. The relatively unexsolved nature of the alkali feldspar of this rock, compared with typical French Creek Granite suggests a strong link between the exsolution process and clouding of the feldspars. No plagioclase is present in the specimen.

Quartz makes up 6% of the rock as subhedral crystals infilling crystal spaces between feldspar. Granophyric intergrowths between alkali feldspar and quartz are common.

Aegirine-augite, displaying high interference colours and yellow-green pleochroism, is abundant in this rock, distinguishing it from the other varieties of French Creek Granite. Pyroxene makes up 6% of the rock as euhedral crystals up to 4 mm across with abundant cleavage and some zoning from brown pleochroic, augite-rich material in the cores to green-pleochroic aegirine-rich material on the rims. The abundance of alkali feldspar and aegirine-augite, and the rarity of quartz, in this sample may indicate a cumulate origin.

Arfvedsonite is also present as euhedral to subhedral, occasionally twinned crystals up to 3 mm long. A few arfvedsonite crystals contain relict cores of pyroxene indicating a replacement relationship between the two phases. Also present are a number of euhedral six-sided crystals with strong red brown pleochroism and evidence of a single cleavage. These are tentatively identified as either aenigmatite or astrophyllite.

Accessory phases include euhedral magnetite crystals up to 1 mm across, large zircons and apatite.

### 3.7.8: Aplite dikes.

Aplite dikes are rare in the French Creek Granite. Petrographic observations on two samples (EHR16 and EHR22) indicate fine to medium grained, slightly porphyritic

textures. The dikes contain abundant quartz as subhedral to anhedral crystals and also as granophyric intergrowths with abundant, subhedral, high relief, cloudy perthitic alkali feldspar. Occasional Carlsbad twinned phenocrysts of alkali feldspar may occur. Plagioclase is present as euhedral to subhedral crystals of albite up to 1 mm across. The presence of two distinct feldspars indicate subsolvus crystallization conditions. Anhedral green-brown biotite crystals up to 1.5 mm across, large zircons (up to 0.2 mm) and euhedral magnetite up to 1 mm in size also occur. EHR16 also contains a population of small (0.4 mm) euhedral brown crystals of allanite.

**3.7.9: Discussion.**

The distinctive characteristics of French Creek Granite warrant further discussion. In terms of field geology, petrography, and also geochemistry (Ch.6.6), the French Creek Granite displays characteristics typical of A-type granitoids (Clemens *et al* 1986, Whalen *et al* 1987, Eby 1990). Several observations can be made about the emplacement and crystallization of French Creek Granite based on field and petrographic observations.

The presence of abundant granophyric intergrowths are generally interpreted as indicating crystallization at relatively low pressures ($\approx$ 1 kb) and hypersolvus conditions (Barker 1970). Miarolitic cavities are also suggestive of crystallization at relatively shallow depths. Despite these indications for sub-volcanic conditions, no sub-aerial volcanic equivalents of French Creek Granite are known. The lack of mafic and country rock xenoliths and the plutons' equigranular nature (i.e. lack of phenocrysts) also suggest emplacement of the pluton in a wholly molten state. Petrographic evidence for a hypersolvus history, in association with the rarity of aplites and pegmatites, indicates a relatively dry magma, typical of the anhydrous A-type granitoids. However, late stage water-saturation must have occurred to allow crystallization of interstitial mafic phases and the formation of miarolitic cavities. The brick-red colour, abundant deuteric alteration and a mineralogical assemblage dominated by alkali feldspar and quartz, with annite-rich biotite and alkali amphiboles, is typical of many A-type granitoids (e.g. Whalen *et al* 1987). Bimodal associations with alkaline mafic activity, such as observed between the French Creek Granite and the Hohonu Dike Swarm, also appears to be a common in many A-types.

## 3.8: Turiwhate Granodiorite.

### 3.8.1: Introduction and field relationships.

Turiwhate Granodiorite is a massive, medium grained, equigranular titanite hornblende biotite granodiorite outcropping over approximately 40 $km^2$ from the Styx River to the north-western end of Mount Turiwhate. This unit was originally named by Waight (1990) and the name is also used here to include the Kaniere Granodiorite of Waight (1990). Typical outcrops of the Turiwhate Granodiorite occur at the base of Dorothy Falls, Mount Tuhua (J33 604166) (Fig.3.33) and in a small quarry near Mount Upright on the Styx River (J33 123559). Occasional swarms of partially resorbed, rounded enclaves up to about 20 cm long occur and indicate magmatic flow within the pluton (Fig.3.33). Turiwhate Granodiorite is distinguished by its mafic, equigranular, medium grained nature and the abundance of hornblende and titanite. Turiwhate Granodiorite is a relatively soft unit, and a distinct morphological contrast is evident between it and the more resistant Summit and Deutgam Granites on Mount Turiwhate.

Intrusive contacts between Turiwhate Granodiorite and Greenland Group are exposed in several small creeks draining the south-west side of Mount Tuhua. Best exposures are seen in a small creek about 1.5 km north of Camp Creek (J33 601173) and in the south-eastern branch of Rose Creek (J33 605190). Contacts are sub-vertical and sharp, with Greenland Group metamorphosed to a foliated biotite hornfels. Diorite exposed at the Rose Creek contact is described in Ch.3.12.3 and may represent a marginal phase of Turiwhate Granodiorite.

Turiwhate Granodiorite and Summit Granite are in intrusive contact in a low saddle on the north-western end of the Turiwhate Ranges (J33 688271). A chilled margin of mafic, fine grained granitoid is present up to 70 cm away from the contact, grading into more typical Turiwhate Granodiorite. Enclaves of Summit Granite are present within Turiwhate Granodiorite and small sheets of Turiwhate Granodiorite can also be seen to intrude Summit Granite at this contact. These field relationships indicate Turiwhate Granodiorite is intrusive into Summit Granite, consistent with geochronological data (Ch.5). Turiwhate Granodiorite is in fault contact with Deutgam Granite in Grahams Creek (see Fig.3.16). Little displacement can have occurred on this fault as the intact intrusive contact between Turiwhate Granodiorite and Summit Granite

is exposed only ≈300 vertical metres above, and this fault may represent small amounts of movement on a pre-existing intrusive contact. Turiwhate Granodiorite is highly altered adjacent to the fault contact with Deutgam Granite in Grahams Creek (e.g. TGC3 and TGC4) and several calcitic veins and areas of hydrothermal alteration are present, possibly a consequence of deuteric alteration adjacent to an intrusive contact. Similar calcitic veining is also present in Fred's Creek, Mount Turiwhate, and is abundant in float in Rose Creek on Mount Tuhua (Waight 1990), both locations occurring adjacent to Greenland Group contacts. A small "cave" occurs in Greenland Group, within twenty metres of an intrusive contact with Turiwhate Granodiorite, on the southern shores of Lake Kaniere (J33 581142). This cave was once the site of a scheelite mine, although no written confirmation of grades or history has been located by the author, and no mineralization was obvious during a cursory examination. Field relationships also indicate Turiwhate Granodiorite is intruded by the Arahura Granite, consistent with geochronological data. Mafic dikes are relatively rare in Turiwhate Granodiorite, largely due to its distance from the locus of the Hohonu Dike Swarm.

### 3.8.2: Field description.

Turiwhate Granodiorite is a white to slightly green, holocrystalline, medium grained (≈3 mm), equigranular granodiorite with prominent hornblende, biotite and caramel-brown titanite. Plagioclase is white, or green if slightly weathered, and alkali feldspar is generally slightly pink in hand specimen (Fig.3.34). Modal classification indicates a granodioritic composition with some spread into the monzogranite field. Turiwhate Granodiorite is undeformed in outcrop, in sharp contrast to the neighbouring Summit Granite and Deutgam Granite, although oriented mafic enclaves indicate a primary magmatic foliation in places.

### 3.8.3: Petrographic description.

Quartz makes up between 21-39% of the mode as anhedral crystals up to 4.5 mm across, often displaying weak undulose extinction. Myrmekite is occasionally present (Fig.3.35).

Alkali feldspar comprises 10-25% of the rock as crystals up to 4 mm across. The alkali feldspar occurs as anhedral, generally featureless crystals, although some minor perthite and a few rare Carlsbad twins are present. Compositions range between 77-97wt% Or, averaging ≈Or85%.

Plagioclase occurs as subhedral to euhedral crystals up to 4 mm long, comprising 10-25% of the granodiorite. Plagioclase is generally highly twinned, with both albite and Carlsbad twins. Sericitization of the plagioclase is ubiquitous within the pluton, even in the freshest possible specimens. Microprobe analyses indicate plagioclase compositions ranging from An18-50%, mostly clustering around andesine (An30-40%). Normal zoning is common.

Biotite occurs as anhedral to platy crystals up to 2.5 mm long and constitutes up to 11% of Turiwhate Granodiorite. It exhibits a distinctive yellow-brown to dark brown pleochroism, although alteration to chlorite is common. Microprobe analyses indicate relatively high Ti and relatively low Al(tot) Fe/(Fe+Mg). Even when fresh the biotite often contains abundant secondary prehnite and epidote, minor titanite and alkali feldspar, developed parallel to cleavage as low grade deuteric alteration products as described in detail by Tulloch (1979b). Such alteration is common in granitoid biotite, but is particularly well developed in Turiwhate Granodiorite (A.J.Tulloch *pers.comm.* 1992).

Amphibole makes up to 8.4% of Turiwhate Granodiorite and is present as subhedral to euhedral, often embayed, crystals up to 4 mm long. The hornblende is brown-green to green pleochroic and is commonly twinned, and occasionally zoned. Occasional relict cores of clear pyroxene are preserved within amphiboles. Microprobe analyses of the hornblende indicate classification as magnesio-hornblende. Exceptions occur in TW93 which contains actinolitic hornblende and actinolite of probable secondary origin.

Titanite is obvious in hand specimen as a honey brown mineral and making up to 1% of the rock. Titanite is common in thin section as resorbed anhedral crystals, or euhedral crystals up to 3 mm long.

Opaque phases make up to 2% of the rock and are generally present as euhedral crystals up to 1 mm across. Limited microprobe analyses reveal little to no titanium, indicating magnetite.

Accessory phases include occasional, small (up to 0.2 mm) crystals of apatite and zircon and a few small (0.2 mm) subhedral crystals of allanite in one specimen (UDC1).

### 3.8.4: Mafic Enclaves.

Enclaves are only rarely abundant in Turiwhate Granodiorite, but appear to become more numerous towards the southern contact with the Greenland Group. The inclusions are generally small (<20 cm) and in various stages of assimilation. Flow orientation of mafic inclusions was seen in Dorothy Creek (Fig.3.33) and in the Styx River. Many enclaves represent Greenland Group xenoliths.

A quartz monzodiorite inclusion from Johnson Creek, Mount Tuhua (UJC1) contains abundant hornblende and titanite and may represent a cogenetic xenolith. Quartz displays a granophyric type texture with alkali feldspar and hornblende, plagioclase ($\approx$An37%) occurs as subhedral, highly twinned crystals up to 3 mm long and alkali feldspar occurs as large (7 mm), sub-ophitic, anhedral to subhedral areas containing numerous small (0.2 mm) inclusions of euhedral biotite, hornblende, quartz and abundant apatite. Biotite is yellow-brown to brown pleochroic and is present as subhedral to euhedral crystals up to 1 mm across, hornblende is very abundant as subhedral, embayed, green pleochroic crystals up to 1.5 mm long, containing rare pyroxene cores. A few anhedral resorbed crystals of titanite are present.

### 3.8.5: Contact variants of Turiwhate Granodiorite.

Outcrops of Turiwhate Granodiorite at or near intrusive contacts are commonly, although not always, somewhat more mafic than the bulk of the pluton and may be related to the Rose Creek Diorite (Ch.3.12.3). At Camp Creek, Mount Tuhua (J33 601173), a few metres of grey, equigranular, fine grained biotite-granodiorite (UCC7) outcrop close to an inferred contact with Greenland Group. This rock lacks the titanite and hornblende which characterize Turiwhate Granodiorite and displays a distinct

preferred flow orientation of plagioclase (≈An35%). Biotite is mostly altered to green chlorite and also distinctive from typical Turiwhate Granodiorite biotite by having slightly redder pleochroism, probably as a consequence of slightly more reducing conditions adjacent to the margin of the pluton. Also present within this rock are several patches of fine-grained biotite rich material which are interpreted as absorbed metasedimentary material. Dark green, mesocratic equigranular hornblende-biotite-granodiorite (UCC8) outcrops immediately upstream of this exposure. Although this sample is similar to the bulk of Turiwhate Granodiorite, it is distinguished in having a slightly higher percentage of mafics (≈22%), more abundant allanite (rare in the remainder of the pluton) and a distinct flow alignment of plagioclase. Similar biotite granodiorites and more mafic variants of Turiwhate Granodiorite (UCC3 and UCC4) are also found in a small creek about 1.5 km north of Camp Creek (J33 603179) where the contact between Turiwhate Granodiorite and Greenland Group is well exposed. Typical Turiwhate Granodiorite is exposed 50 m inboard of the contact.

## 3.9: Summit Granite.

### 3.9.1: Introduction and field relationships.

Summit Granite was originally termed the Summit Granodiorite by Waight (1990). Summit Granite is a foliated, leucocratic, generally equigranular, medium grained biotite muscovite granitoid outcropping above the bush line on the Turiwhate Ranges, with typical outcrops occurring on Mount Turiwhate proper (1368 m). Summit Granite is characterized by its leucocratic nature, the presence of abundant muscovite and a pervasive foliation which affects most outcrops. Metasedimentary inclusions are common and generally orientated parallel to foliation (Fig.3.36). Summit Granite appears to be a relatively resistant unit, possibly due to its felsic, quartz-rich nature, and has produced the ragged, bluffy tops of Mount Turiwhate, in marked contrast to the more subdued topography of the underlying Deutgam and Turiwhate granitoids.

Relationships along the western side of Mount Turiwhate are uncertain, a consequence of a lack of easily accessible exposure. Highly foliated, biotite-rich equigranular granitoid probably related to the Deutgam Granite (TCC1 and TCC2) occurs near the fork in Camp Site Creek (J33 688249), and Turiwhate Granodiorite (TCC4) was found to outcrop in a small creek south-east of here (J33 683242). Summit

Granite was not found to outcrop along the western edge of Mount Turiwhate, although it was common as float in several creeks draining these slopes. Summit Granite is intruded by Turiwhate Granodiorite to the north-west and Deutgam Granite to the south-east and field relationships indicate the Summit Granite occurs as an isolated cap on the tops of the Turiwhate Ranges, suggesting it represents older country rock into which the other granitoids have intruded (see cross section C-C', map pocket). A Palaeozoic age for the Summit Granite (Ch.5) confirms these field relationships and indicates the Summit Granite may be related to the Karamea Suite (Tulloch 1983, 1988a).

### 3.9.2: Field description.

Summit Granite is a leucocratic, fine to medium grained, generally equigranular, biotite muscovite granodiorite or monzogranite (Fig.3.36, Fig.3.37). Prominent vertical joint planes, oriented 070°, are conspicuous on aerial photos of Mount Turiwhate. Sheets of included metasediment/paragneiss are common (Fig.3.36) and the unit commonly displays a moderate to strong foliation. Summit Granite predominantly classifies as a monzogranite although some samples plot in the granodiorite field (Fig.3.1).

### 3.9.3: Petrographic description.

Quartz constitutes between 15-45% of the mode although it is generally consistent at around 38 modal percent. Quartz crystals are anhedral, up to 6 mm long and show varying degrees of undulose extinction (Fig.3.38). Although most outcrops of Summit Granite are foliated, only the most deformed samples contain quartz ribbons or any obvious preferred orientation of quartz. Any lattice preferred orientations of quartz are diffuse and indicate low temperature deformation by basal slip. In some specimens the quartz has developed a regular mosaic indicative of static recrystallization.

Alkali feldspar makes up between 8-35 modal percent and is generally sub-equal in proportion to plagioclase feldspar. Alkali feldspar is present as anhedral to subhedral crystals up to 10 mm long. Most alkali feldspar is perthitic and transformation twinned and a few Carlsbad twins are also rarely present. Crystals have become augen in the

more deformed samples. Microprobe analyses indicate compositions ranging between Or92-99%.

Plagioclase occurs as anhedral to subhedral rarely twinned crystals up to 7 mm long, constituting 16-35 modal percent of Summit Granite. Microprobe analyses indicate the plagioclase is mostly sodic oligoclase ($\approx$An15%) with analyses ranging between An7-20%. Deformation twins and bending of twin planes occurs occasionally.

Biotite is present as anhedral platy crystals up to 4 mm long. Biotite makes up to between 1-9% of the granitoid and is generally sub-equal or subordinate to muscovite. The biotite has a distinct and strong yellow-brown to red-brown pleochroic scheme, indicative of reduced compositions. Microprobe analyses of biotite indicate relatively low Ti and high Al(tot) and Fe/(Fe+Mg) compared with other plutons of the batholith. Biotite is often partially or completely replaced by chlorite.

Muscovite is ubiquitous, making up to 15% of the rock. Muscovite is obvious in hand specimen, occurring as subhedral platy crystals up to 5 mm long. The muscovite is always distinctly less altered and less deformed than biotite. Deformation is evident as kinking of cleavage and some "fish tailing" of muscovite crystals. Muscovite and biotite are commonly orientated sub-parallel to the foliation in the Summit Granite.

Garnet occurs in only two specimens (MT16 and MT23) as isolated, pink, euhedral crystals up to 1 mm across. Other accessory phases include abundant, large (up to 1 mm) euhedral apatite, and small zircons creating a small pleochroic halo in biotite, a feature absent in the other plutons of the batholith. Summit Granite is also characterized by an almost complete lack of opaque phases. The only opaque seen in the granitoid is ilmenite associated with the breakdown of biotite to chlorite.

Metasedimentary material is common within Summit Granite and shows varying degrees of assimilation. A relatively intact specimen (MT19) displays a strong preferred orientation of red-brown biotite crystals, up to 1 mm long, set in a mosaic of fine grained ($\approx$0.2 mm) equigranular quartz, plagioclase and alkali feldspar. Also present

are abundant, large, euhedral apatite crystals and numerous small zircons with pleochroic haloes in surrounding biotite.

On the summit of Mount Turiwhate is a limited outcrop of a green-white, very fine grained cataclastic rock (MT4), described more fully by Waight (1990). This outcrop is inferred to represent a major fault/shear zone cutting Summit Granite.

## 3.10: Arahura Granite.

### 3.10.1: Introduction and field relationships.

Arahura Granite (new name) is a large pluton, outcropping over nearly 100 $km^2$, making up the bulk of Mount Tuhua and all of Island Hill, as well as a small region of Mount Upright. The Arahura Granite encompasses the Milltown Granodiorite, Island Hill Monzogranite and Geologists Creek Monzogranite of Waight (1990). Typical outcrops occur in the Arahura Gorge (Fig.3.39) (J33 629235), the Kawhaka Creek Weir (J33 646264) and at a small disused quarry near Milltown (J33 639200). Modal point count studies designate the unit as a monzogranite. Arahura Granite is recognized in the field by its leucocratic nature, lack of foliation and presence of large, often pink, alkali feldspar megacrysts (Fig.3.40).

Arahura Granite and Turiwhate Granodiorite are found in close proximity in the Arahura Gorge, on Pyramid Hill, on the track to Mount Tuhua and near Lawyers Delight. A contact between Arahura Granite and Turiwhate Granodiorite is poorly exposed on the shores of Lake Kaniere to the east of Lawyers Delight Hut. The contact is sharp, strikes ENE and dips steeply to the south. A possible, thin chilled margin of Arahura Granite occurs adjacent to the contact. The contact extends along the western side of Mount Tuhua, running through a low saddle to the east of the 852 metre point on the Mount Tuhua track, northwards through Pyramid Hill and a large meander in the Arahura River. Highly altered orange Arahura Granite outcrops within 300 metres of Turiwhate Granodiorite in the Arahura River gorge (J33 626240). The alteration may possibly be consequence of fluid movement along the contact during intrusion of Arahura Granite, although it was not observed close to any other Turiwhate-Arahura contacts. Greenland Group does not occur in close proximity of Arahura Granite and the unit is inferred to be wholly intrusive into Turiwhate Granodiorite, consistent with

geochronological data (Ch.5). Exposures of Arahura Granite on the southern end of Island Hill, particularly near the junctions of Lebel Creek and Wainihinihi Creek (J33 663201) (described by Reed 1964 and Bell and Fraser 1906) and in Geologist's Creek are brecciated due to the proximity of the Fraser Fault. Cataclasis increases towards the Fraser Fault in a tributary of Geologists Creek (J32 614149), although Arahura Granite is still recognizable as such to within 20 m of the fault. Within 10 m of the fault Arahura Granite becomes a green, chloritized and epidotized, medium grained cataclasite cut by occasional clay pug zones.

### 3.10.2: Field description.

Arahura Granite is a homogeneous, white, medium to coarse grained, mesocratic to leucocratic, megacrystic biotite-monzogranite. It is characterized by euhedral megacrysts of alkali feldspar up to 5 cm long, and minor muscovite (Fig.3.40). Alkali feldspar megacrysts are commonly salmon pink and may have an outer rim of white feldspar. On the summit of Mount Tuhua (1125 m) the Arahura Granite becomes finer grained and has a porphyritic appearance caused by abundant large quartz phenocrysts and large euhedral alkali feldspar phenocrysts. The porphyritic, finer grained nature of Arahura Granite on the tops of Mount Tuhua is taken to indicate high level crystallization of the magma, presumably near the top of the pluton.

### 3.10.3: Petrographic description.

Quartz makes up between 19-44% of the rock as anhedral to subhedral crystals up to 7 mm across (Fig.3.41). The only indication of deformation within Arahura Granite, excluding the retrograde, brecciated granitoids adjacent to the Fraser Fault, is the presence of minor undulose extinction of quartz in several specimens. Samples from the summit of Mount Tuhua (e.g. MTU2) contain large (up to 8 mm) pentagonal to hexagonal, euhedral areas of quartz. In thin section these are aggregates of several crystals, probably resulting from recrystallization of large bipyramidal quartz phenocrysts (Fig.3.42).

Alkali feldspar is present in two forms. Most conspicuous are euhedral megacrysts up to 5 cm long, varying in colour from salmon pink to occasionally pure white. Megacrysts occasionally exhibit a thin white band of albite rimming the crystal. The megacrysts are euhedral, perthitic, commonly Carlsbad twinned and often exhibit weak oscillatory zoning. Minor transformation twinning is also present. Many of the megacrysts contain included crystals of euhedral albite (An3%), quartz and biotite, generally oriented parallel to the crystal faces. Alkali feldspar also occurs as anhedral, perthitic crystals up to 5 mm long in the groundmass of the rock. Microprobe analyses indicate a wide range of Or compositions (70-96wt%), reflecting exsolution of the feldspars. Backscatter electron microprobe images confirm that significant exsolution has occurred within the crystals. Alkali feldspar makes up between 14-45% of the Arahura Granite.

Plagioclase occurs within Arahura Granite as subhedral to euhedral, commonly highly zoned, crystals up to 7 mm long. Microprobe analyses indicate compositions mostly ranging between An13%-33%, although compositions reach as low as An4% in UMQ2 (Milltown Quarry), indicating some variation in plagioclase composition throughout the pluton. Albite twinning is common and many of the crystals are sericitized.

Biotite represents the dominant mafic phase in this unit. It occurs as subhedral platy crystals up to 2 mm long with yellow-brown to brown pleochroism. Inclusions of apatite are common. Much of the biotite present within Arahura Granite has been altered to green chlorite with distinctive purple interference colours, occasionally containing small rutile needles. Biotite and chlorite combined make up between 1.5 and 8.4% of Arahura Granite. Microprobe analyses of biotite are variable and suggest some heterogeneity within the pluton.

Muscovite is present in many, but not all, samples examined, making up to 3% of the rock. Muscovite seems to become more common towards the centre of the pluton, indicating possible zonation of the pluton. Muscovite occurs as anhedral to occasionally platy crystals up to 1.5 mm across. Microprobe analyses have variable Ti and indicate both primary and secondary muscovite. The presence of occasional

muscovite crystals which are slightly green in plain polarised light indicates significant amounts of $Fe^{2+}$ or Cr may also be present. Muscovite is also common as a secondary mineral in the cores of sericitized plagioclase.

Opaque phases make up to 1.4% of Arahura Granite as subhedral to anhedral crystals up to 2 mm in size, although generally the crystals are much smaller. Most opaques are identified as magnetite on the basis of crystal shape, although a few ilmenite crystals may be also present.

Titanite is present in only a single sample (AR5) as abundant, euhedral to anhedral crystals up to 1 mm across. This sample was located within 500 m of a contact with Turiwhate Granodiorite and may represent a marginal phase of Arahura Granite.

Allanite is also present in only a single sample (UJC2), also collected relatively close to an inferred Arahura Granite-Turiwhate Granodiorite contact. The allanite occurs as two, weakly brown pleochroic, crystals approximately 0.5 mm across and rimmed by epidote.

Other accessory phases present within Arahura Granite are apatite and zircon as euhedral crystals up to 0.3 mm long, commonly associated with biotite.

## 3.11: Mount Graham Granite.

### 3.11.1: Introduction and field relationships.

Mount Graham is a comparatively low (829 m) mountain on the western side of Lake Kaniere, composed primarily of Greenland Group intruded by a small pluton ($\approx 10$ km$^2$) named the Mount Graham Granite (new name). The mountain is bush clad, with no exposed tops, and exposure is poor as Mount Graham is flanked on both sides by glacial moraines to a height of at least 500 m. Lateral moraines make up most of the elevated plateau in the Blue Bottle Creek region.

Mount Graham Granite was first mapped by Bell and Fraser (1906) and outcrop patterns on the map accompanying this thesis are largely based on their work. Mount Graham Granite is, strictly speaking, not part of the Hohonu Batholith as it is separated from the granitoids to the east on Mount Tuhua by 4 horizontal kilometres of Greenland Group. Due to its proximity to the batholith, and lack of previous description, it is included as a minor part of this study. No intrusive contacts between Mount Graham Granite and any other phase were observed in this study, although it is assumed to be intrusive into Greenland Group.

### 3.11.2: Field description.

The best exposures of Mount Graham Granite were found in the headwaters of Kent Creek. It is a massive, leucocratic, equigranular, medium grained, biotite-muscovite granite (Fig.3.43). Outcrops occurring on the western side of Mount Graham in Sawpit Creek are brecciated and weathered intensely but are similar to fresher granitoids found in float. Brecciation at this outcrop may indicate the proximity of a large fault bounding the Kokatahi basin. All outcrops observed were considered too altered to sample directly for geochemical analysis, and consequently the samples described below are taken from float. All creeks visited draining the pluton contain large amounts of Mount Graham Granite float which appears to show little variation, so despite only collecting four samples of this granitoid they are thought to be representative of the pluton. Point count studies indicate classification as a biotite muscovite monzogranite. Petrographically, and in the field, Mount Graham Granite bears a distinct resemblance to the Summit Granite.

### 3.11.3: Petrographic description.

Quartz makes up between 37-41% of Mount Graham Granite. It occurs in anhedral to subhedral crystals up to 4 mm in size. Undulose extinction is ubiquitous (Fig.3.44).

Plagioclase feldspar makes up around 25-35% of Mount Graham Granite as subhedral to euhedral albite twinned crystals up to 5 mm long. Michel-Lévy methods indicate that the plagioclase lies on the boundary of albite and sodic oligoclase

(≈An10%). Sericitization of the cores of plagioclase is common and indicates some normal zoning.

Alkali feldspar occurs as anhedral crystals up to 3 mm across, generally lacking many internal features apart from occasional perthitic intergrowths, transformation twinning and rare Carlsbad twins. A $2V_x$ of around 80° indicates microcline, with near 100 Wt.% Or. Alkali feldspar makes up between 20-22% of this rock, and is sub-equal to plagioclase.

Biotite is largely altered to chlorite, with minor associated opaques (probably ilmenite), epidote and muscovite. The chlorite is green pleochroic and exhibits anomalous blue interference colours indicative of an Fe- and Si- rich variety. Crystals are anhedral and up to 2 mm in size. The few remnants of fresh biotite exhibit yellow-brown to red-brown pleochroism.

Muscovite is the most obvious accessory mineral, occurring as subhedral, platy crystals up to 3.5 mm long, obvious in hand specimen. Although occasionally buckled the crystals are otherwise very fresh, in sharp contrast to the accompanying biotite. Muscovite makes up between 2-10% of Mount Graham Granite. Secondary muscovite occurs in the cores of altered plagioclase.

Few accessory minerals are present within this rock. Opaques are absent except as the products of the alteration of biotite to chlorite. Apatite is also surprisingly rare with only a few small crystals being observed in the sections, and one large (1 mm) anhedral crystal found in specimen GKC2. No zircon was observed. Some allanite-epidote was also seen within the rocks, although limited to one or two crystals per section.

## 3.12: Miscellaneous units.

### 3.12.1: The Eastern Hohonu River Gabbro.

Float in the Eastern Hohonu River contains relatively abundant plutonic mafic rocks, traced to the third tributary on the true left side of the Eastern Hohonu River (≈K32 758368) where large blocks (up to 3 $m^2$) of mafic gabbroic material are

enclosed within Deutgam Granite. The contact between the gabbro and Deutgam Granite is diffuse and marked by numerous blocks of gabbro, in various states of disaggregation but commonly angular with sharp contacts (Fig.3.45). Outcrops above the second waterfall in the easternmost fork of the tributary show reaction rims ($<1$ cm) of radiating amphibole and leucogranite (possible chilled or reaction margins) surrounding large angular blocks of layered, fine to coarse grained, gabbroic material with no obvious chill margin against the granitoids (Fig.3.46). The lack of chilled margins and the angular nature of the gabbroic blocks suggest inclusion within the granitoid as solid crystalline material rather than by processes of magma mingling or mixing.

The gabbroic material, sampled from float (EHR8) and outcrop (EHR29), is characterized by subhedral to euhedral crystals of plagioclase ($\approx$An48%) up to 4 mm long and abundant amphibole, clinopyroxene and opaques. Amphibole is present as anhedral to subhedral, yellow-brown to red-brown pleochroic crystals up to 6 mm long and makes up $\approx$23% of the gabbro. Clinopyroxene occurs as prismatic, light green coloured, twinned crystals up to 7 mm long. Both the amphibole and clinopyroxene show extensive replacement by secondary actinolite, tremolite and chlorite. Magnetite occurs as subhedral crystals up to 3 mm long (Fig.3.47).

Both mafic and felsic material was examined from a zone of complex assimilation and/or intermixing at the base of the second large waterfall in the tributary (see Fig.3.45). The mafic material (EHR24) occurs as sub-rounded, partially disaggregated "blobs" within a relatively felsic equigranular granitoid. Petrographically, the mafic "blobs" contain minor ($\approx$1%), anhedral, interstitial quartz crystals up to 1 mm, and abundant, subhedral to euhedral crystals (2 mm) of strongly normal zoned plagioclase (An 40%). Alkali feldspar is subordinate to plagioclase and occurs as perthitic, interstitial, anhedral to subhedral crystals up to 2 mm across. Mafic minerals consist of; light blue-green to brown pleochroic amphibole, as anhedral to subhedral crystals up to 1 mm in size, commonly containing cores of relict clinopyroxene; minor light-green pleochroic clinopyroxene; and abundant yellow-brown to brown pleochroic biotite crystals up to 2 mm in size. Titanite is present as anhedral crystals up to 0.7 mm across, commonly enclosing opaques but in turn enclosed by amphibole. Also

present are abundant euhedral to subhedral magnetite crystals up to 0.5 mm across and relatively abundant, acicular apatite crystals up to 0.75 mm long.

The felsic granitoid (EHR25) contains more abundant modal quartz and alkali feldspar, and lower An% plagioclase, around An20%, when compared to the mafic inclusions. Similar mafic minerals occur, including 0.5 mm crystals of allanite, but in much lower abundances than in the mafic material. The margin between the two phases is sharp, with no evidence for marginal chilling, although the felsic phase appears to intrude the more mafic phase on a microscopic scale. The transition is marked largely by a decrease in modal mafics and increase in crystal size from mafic to felsic material.

A mafic-rich hornblende quartz monzodiorite (HMF2) occurs within the Deutgam Granite, exposed on a ridge heading due east below the transmitter aerial on Mount French No.1 (≈K32 750360). The rock consists of ≈5% anhedral quartz up to 3 mm in size, subhedral to euhedral zoned crystals of calcic andesine (An 20?-50%), and occasional, anhedral crystals of alkali feldspar up to 2 mm long. Mafic phases consist of sub-equal euhedral to subhedral crystals of green brown pleochroic amphibole up to 2 mm long, and subhedral crystals of brown pleochroic biotite up to 3 mm across. Titanite is relatively abundant as anhedral crystals up to 1.5 mm, as are opaque phases as euhedral to subhedral crystals up to 0.5 mm across. Accessory apatite and zircon are also present. The relationship between HMF2, the Eastern Hohonu River Gabbro and the Deutgam Granite is unknown, however it may represent a large mafic enclave, or a more mafic phase or cumulate of the Deutgam Granite.

### 3.12.2: Rhyolitic and trachytic dikes.

Blue to cream-grey dikes (up to 15 m wide) are widespread and intrude Deutgam Granite on the Hohonu Ranges. Originally considered to represent extreme differentiates of the Hohonu Dike Swarm (Hamill 1972), these dikes have many chemical similarities to French Creek Granite and are considered to represent hypabyssal equivalents of this pluton (Ch.6.6.7.3).

The dikes are characteristically blue when fresh, but are more commonly altered to a cream-brown colour (Fig.3.48). Many of the rhyolitic dikes are porphyritic and highly jointed. Most dikes are rhyolitic in composition, except for EHR21 and EHR6 which are trachytic and may be related to the quartz alkali feldspar granite variant of French Creek Granite (Ch.6.6.7.2).

The dikes are characterized texturally by a very fine grained ($\approx$0.3 mm average grain size) felsitic matrix of complexly intergrown quartz and alkali feldspar with irregular, anastomosing grain boundaries. The dikes may contain phenocrysts of quartz and alkali feldspar, or consist entirely of blue glass. Spherulites are abundant in some specimens, often rimming phenocrysts, and are occasionally evident in hand specimen (Fig.3.49). The fine grained, felsitic matrix of these dikes is typical of rhyolites which have undergone a very high degree of undercooling (Shelley 1993) and represent devitrification of an original glassy groundmass. Similar textures and mineralogy are also observed in the Triassic Sams Creek dike exposed near Takaka (Tulloch 1992).

Quartz occurs within the groundmass and as subhedral to euhedral, bipyramidal phenocrysts up to 1.5 mm across. Quartz phenocrysts may be embayed, indicative of corrosion and instability within the melt (Fig.3.50).

Alkali feldspar occurs in the groundmass and as subhedral to euhedral phenocrysts mostly up to 3 mm long, although phenocrysts up to 7 mm long occur in one sample (EHR6). The phenocrysts may show a flow orientation, and are generally perthitic with occasional Carlsbad twinning. A few crystals were observed to be rimmed by granophyric intergrowths with quartz, resembling "xenocrystic" material removed from French Creek Granite.

Alkali amphiboles are abundant within the dikes, generally as small ($\approx$0.2 mm) flow oriented subhedral to euhedral acicular crystals (Fig.3.51). Rare subhedral phenocrysts are also present. Most show a dark green to inky blue to near black pleochroic scheme indicative of riebeckite or arfvedsonite. The abundance of alkali amphiboles in these dikes is the cause of the distinctive blue colour of the fresh rock.

Biotite occurs only in the more mafic trachytic dikes as small as rare, corroded phenocrysts up to 1.5 mm across (EHR6).

Opaques are often abundant in the dikes as fine grained ($\approx$0.1 mm) euhedral magnetite crystals. Some opaques are likely to be secondary and associated with alteration.

Accessory minerals include spindly red to orange brown pleochroic, anhedral crystals up to 1.5 mm long provisionally identified as astrophyllite, and rare cloudy zircon crystals.

### 3.12.3: The Rose Creek quartz diorite.

In the south-eastern branch of Rose Creek, Mount Tuhua (J33 601189), a contact is exposed between Greenland Group and a melanocratic, equigranular, medium grained biotite hornblende quartz diorite (TW58 & URC3). The diorite contains $\approx$9% quartz as rare, anhedral, unstrained crystals up to 1 mm across. Plagioclase is andesine ($\approx$An40) and occurs as subhedral to euhedral, sericitized crystals up to 5 mm long. No alkali feldspar is evident. Hornblende is the dominant mafic phase, making up 22% of the rock as subhedral to anhedral, green-brown to green pleochroic crystals up to 3 mm long. Also present is abundant light-brown to brown pleochroic biotite, abundant opaques and rare titanite. The relationships between this quartz diorite and Turiwhate Granodiorite were not observed in the field. Typical Turiwhate Granodiorite is exposed near Greenland Group in the northern branch of Rose Creek, and to the south in Camp Creek, therefore this unit must be of limited areal extent. The Rose Creek quartz diorite may represent a related, mafic contact phase of Turiwhate Granodiorite.

## 3.13: Preliminary subdivision of the plutons of the Hohonu Batholith.

Using petrographic observations, and the granitoid classification scheme proposed by Chappell and White (1974 and 1992), it is possible to make several broad subdivisions of the Hohonu Batholith granitoids. The Jays Creek, Pah Point, Uncle Bay, Deutgam and Turiwhate plutons are all biotite ($\pm$ titanite $\pm$ hornblende) granodiorite and tonalites and have characteristics typical of I-type granitoids. The relatively evolved two-mica monzogranites of the Te Kinga and Arahura plutons do not

fit easily into either the I- or S-type categories of Chappell and White (1992), and from a petrographic view point are ambiguous in terms of I- and S-type criteria. As noted previously, the French Creek Granite has many characteristics typical of A-type granitoids (e.g. Whalen *et al* 1987, Eby 1990) and is obviously distinct from the other plutons of the batholith. Finally, the Summit Granite and the Mount Graham Granite are also somewhat ambiguous in terms of I- and S-type criteria, but the abundance of muscovite, coupled with the occurrence of garnet and abundant metasedimentary inclusions in the Summit Granite indicate an S-type (or S-like) classification may be appropriate. These four preliminary groupings of plutons are expanded upon in the geochemistry chapter (Ch.6).

# Chapter 4

# Hohonu Batholith granitoids:

# Comparative mineral chemistry and conditions of emplacement.

## 4.1: Introduction.

This chapter compares and contrasts microprobe analytical data for various key minerals of the granitoids of the Hohonu Batholith (except the Mount Graham Granite, for which no microprobe data were collected). Microprobe analyses are presented in Appendix D. Also included in this chapter is application of the Al-in-hornblende geobarometer of Schmidt (1992) and the two feldspar geothermometer of Fuhrman and Lindsley (1988) to Hohonu Batholith granitoids.

## 4.2: Biotite.

Biotite is the dominant mafic phase in all plutons studied, although in the Arahura Granite and Turiwhate Granodiorite much of the biotite is replaced by chlorite. The range of biotite compositions in the Hohonu Batholith granitoids are summarized in Table 4.1. Analyses were generally made from the core to the rim of crystals and no chemical zoning was obvious in any biotite analyzed. No consistent variations in biotite composition with whole rock $SiO_2$ content are observed, despite a 66-76% range in $SiO_2$ contents of probed samples.

Biotite analyses are plotted in the phlogopite-annite-siderophyllite-eastonite system in Fig.4.1. All analyses fall within the biotite field, with the division between biotite and phlogopite being arbitrarily set at Mg:Fe = 2:1 (Deer *et al* 1966). A general increase of Fe/(Fe+Mg) with Al(tot) is observable in this plot, suggesting a replacement relationship between Mg, Fe and Al. Most plutons can be distinguished by their characteristic biotite compositions. The Fe-rich biotite of French Creek Granite is distinctive, plotting close to the annite corner in Fig.4.1, annite being characteristic of many A-type plutons (Eby 1990, Whalen *et al* 1987), A maximum of 1.04% fluorine was present in the few biotites of the French Creek Granite analyzed for this element. Both Pah Point Granite and Turiwhate Granodiorite have biotite with relatively low Al(tot) and Fe/(Fe+Mg), a feature previously noted in Pah Point Granite

by Mason (1990). The remaining more mafic plutons, Uncle Bay Tonalite, Jays Creek Granite and Deutgam Granite, are characterized by similar biotite compositions with relatively intermediate Fe/(Fe+Mg) and Al(tot) compositions. Summit Granite and Te Kinga Monzogranite have relatively high Al(tot) and Fe/(Fe+Mg) compared with the other plutons (excluding French Creek Granite). Arahura Granite exhibits highly variable biotite compositions, with a wide spread of increasing Fe/(Fe+Mg) with increasing Al(tot). Despite the wide variation in composition within the pluton, biotites from individual samples of Arahura Granite plot in restricted groupings, indicating the variation represents diversity within the pluton, rather than within individual samples. Further work is required to establish if this variation represents zoning within the pluton as has been tentatively indicated by variable mineralogy (see Ch.3.10.3).

Many of the plutons also display distinctive biotite compositions in a plot of Fe against Mg (Fig.4.2). French Creek Granite is again distinctive with high Fe and low Mg. Both Turiwhate Granodiorite and Pah Point Granite have similarly high Mg and low Fe, whereas Summit Granite and Te Kinga Monzogranite have lower Mg coupled with higher Fe. Jays Creek Granite, Uncle Bay Tonalite and Deutgam Granite have biotite compositions intermediate between these two groupings. Again, as in Fig.4.1, biotite from the Arahura Granite is variable in composition.

Variation in biotite composition will reflect variation in the geochemistry and mineralogy of the host rocks. Both Te Kinga Monzogranite and Summit Granite contain abundant muscovite, and biotites from these plutons have higher Al and Fe/(Fe+Mg), reflecting the more aluminous nature of the host magmas. Arahura Granite is also muscovite-bearing, however modal quantities are variable and muscovite is subordinate to biotite. This may be reflected in the variability of biotite compositions in the Arahura Granite, and their contrasting compositions compared with biotites of the Te Kinga and Summit plutons. Biotite from the amphibole-bearing plutons (Turiwhate, Uncle Bay and Deutgam) has lower Fe/(Fe+Mg) and Al(tot) contents than the muscovite-bearing plutons, but have similar biotite compositions to other amphibole-free plutons (Jays Creek, Pah Point). Consequently, amphibole appears not to have played a large role in controlling biotite composition. Apart from slightly lower

abundances in Summit Granite, little variation in Ti is observed in biotite compositions throughout the Hohonu Batholith.

## 4.3: Muscovite.

Primary muscovite occurs in Arahura Granite, Te Kinga Monzogranite and Summit Granite. Muscovite is also present in Jays Creek Granite, evolved members of Deutgam Granite, and rarely in the Granite Hill paragneisses. Petrographic evidence (i.e. anhedral, fine grained crystals often enclosed by other phases, especially feldspar and biotite) suggests a secondary origin for muscovite in these latter rocks. Muscovite analyses are summarised in Table 4.2. Muscovite from Summit Granite and Arahura Granite is largely similar in composition, and can be distinguished from Te Kinga Monzogranite muscovite by lower Ti and higher Na contents.

Using petrographic features to discriminate between primary magmatic muscovite and secondary metamorphic muscovite, Miller *et al* (1981) concluded that primary muscovite is characterized by higher Ti, Na and Al, and lower Mg and Si, than secondary muscovite. Muscovite analyses from the Hohonu Batholith are plotted on a Mg-Ti-Na plot in Fig.4.3, with the fields of primary and secondary muscovite from Miller *et al* (1981) added for comparison. Muscovite from both Summit Granite and Arahura Granite fall within the primary muscovite field, the more Ti- and Mg-rich nature of muscovite from the Te Kinga Monzogranite, compared with that from the Summit Granite, being well illustrated in Fig.4.3. Muscovite analyses from Arahura Granite display a wide scatter from the primary field into the secondary field. Unlike biotite, this spread is evident within individual samples and, combined with petrographic evidence, indicates that both secondary and primary muscovite occur within Arahura Granite. Primary muscovite analyses from Arahura Granite have compositions similar to those from Summit Granite. Analyses of muscovite crystals from Jays Creek Granite plot within the secondary field, with distinctly low Ti and Na. Most muscovite in Jays Creek Granite occurs enclosed within feldspar crystals and is likely to be a secondary alteration product. Muscovite is rare in the Granite Hill Complex rocks, two analyses of muscovite from the summit of Granite Hill (GH2) also plot in the secondary field.

Experimental studies indicating that the intersection of the muscovite breakdown curve and the granite solidus of Tuttle and Bowen (1958) lies between 3-4 kb suggest that muscovite will be unstable at shallow, "epizonal" depths. Consequently, muscovite-bearing plutons are considered to be deep-seated and to represent crystallization at $>3$ kb ($\approx 11$ km). However, primary muscovite occurs in many plutons which, from independent geological evidence, appear have been intruded at depths shallower than 11 km (e.g. see references in Miller *et al* (1981) and discussion in Hewitt and Wones (1984)). Arahura Granite and Te Kinga Monzogranite display petrographic and field evidence for relatively shallow levels of emplacement, both plutons becoming finer grained and containing large euhedral phenocrysts of feldspar at higher levels of exposure. Arahura Granite, in particular, has a porphyry texture on the summit of Mount Tuhua, containing large, euhedral crystals of quartz (see Fig.3.42) and phenocrysts of alkali feldspar. Thus the presence of primary muscovite in both Arahura Granite and Te Kinga Monzogranite also appears to contradict experimental evidence that primary muscovite can only occur in relatively deep seated plutons.

## 4.4: Allanite and epidote.

Epidote, either as independent crystals or rimming allanite crystals, is a common phase in many of plutons of the Hohonu Batholith. Several analyses of allanite and epidote from several samples are presented in Appendix D. Totals are generally low (averaging 78%) and range from 66% to 100%, with epidote consistently giving higher totals than allanite. The low totals in allanite analyses represent unanalyzed REE (replacing Ca) and Th, indicating allanite is likely to be an important mineral in controlling REE content in the granitoids.

## 4.5: Amphibole.

Amphibole is present in the Uncle Bay Tonalite, Deutgam Granite, Turiwhate Granodiorite and the various phases of French Creek Granite. Microprobe analyses of amphiboles from these plutons are summarized in Table 4.3. All amphiboles are classified using the schemes of Leake (1978).

Amphibole analyses from Deutgam Granite, Uncle Bay Tonalite, Turiwhate Granodiorite and the dominant, subsolvus phase of French Creek Granite classify as calcic amphiboles (i.e. $(Ca+Na)_B \geq 1.34$, $Na_B < 0.67$) *sensu* Leake 1978). These amphiboles are plotted on a modified classification scheme in Fig.4.4. Amphiboles from Uncle Bay Tonalite and Deutgam Granite are very similar in composition and classify as magnesio-hornblende. Amphiboles from Turiwhate Granodiorite are more variable in composition. Amphiboles from the Styx River Quarry (GSR1) have compositions similar to those of the Uncle Bay Tonalite and Deutgam Granite whereas amphiboles from Mount Turiwhate (TTC1 and TW81) also classify as magnesio-hornblendes but have somewhat higher $Mg/(Mg+Fe^{2+})$ and Si values, coupled with lower Ti concentrations. In contrast, amphiboles from TW93 classify as actinolitic hornblende to actinolite and have Si contents (7.31-7.58 cations) greater than the 7.3 limit proposed for primary igneous amphiboles (Leake 1978). These actinolitic amphiboles are also characterized by low Ti contents (0.03-0.07 cations) yet are petrographically indistinguishable from other amphiboles within the Turiwhate Granodiorite.

Amphiboles from French Creek Granite have varied chemistry, reflecting the variable petrographic nature of this pluton. Analyses from a single crystal of red-brown amphibole in the subsolvus phase of the French Creek Granite indicate classification as the calcic amphibole ferroedenite (Fig.4.4). The dominant accessory phase in the hypersolvus monzogranitic phase is identified optically as arfvedsonite (Ch.3.7.5). Most analyses of this phase give totals less than the 98.5% (anhydrous) limits used in this study, a probable consequence of their small size and the effects of alteration. The amphiboles have high iron contents, greater than 20%, and discrepancies in the calculated $Fe^{2+}/Fe^{3+}$ ratios may also contribute to the anomalously low totals. The amphiboles classify as sodic-calcic amphiboles ($(Ca+Na)_B \geq 1.34$, $0.67 \leq Na_B \leq 1.34$), straddling the $(Na+K)_A = 0.50$ boundary between katophorite and ferrobarroisite (Fig.4.5). Si contents are high at between 7.2-7.41 cations, overlapping the limit of 7.3 for igneous amphiboles proposed by Leake (1978). Katophorites are "comparatively rare amphiboles which occur mainly in the more basic alkaline rocks" (Deer *et al* 1966, p186) making their occurrence in these monzogranites somewhat unusual.

Limited analyses of dark green, inky blue to near black pleochroic amphiboles in HMS5, a trachytic dike probably related to the Hohonu Dike Swarm (Ch.7.7.2) have $Na_B \geq 1.34$, indicative of alkali amphiboles. Values of $Fe^{3+}/(Fe^{3+}+Al^{vi})$ approaching 1 and very low $Mg/(Mg+Fe^{2+})$ indicate these amphiboles are near pure riebeckite.

**4.5.1: Amphibole geobarometry.**

Much has been written on the merits of Al-in-hornblende geobarometry. Hammarstrom and Zen (1986) and Hollister *et al* (1987) proposed the first empirical Al-in-hornblende geobarometers, based on pressures derived from contact aureole geobarometry. Both methods have large errors ($\pm 3$ kb and $\pm 1$ kb respectively) representing the scatter of their hornblende data and the empirical nature of their studies. Al-in-hornblende geobarometers were later refined experimentally by Johnson and Rutherford (1989) and Schmidt (1992) with a concomitant reduction in errors. Blundy and Holland (1990) refuted the applicability of these geobarometers and instead proposed an amphibole-plagioclase geothermometer. The calibration of Blundy and Holland (1990) uses data from a wide range of rock types and has been discussed at length by Hammarstrom and Zen, Rutherford and Johnson, and Poli and Schmidt (all 1992). All authors concerned, including replies by Blundy and Holland (1992 a+b), concur that Al-in-hornblende geobarometers are applicable for the restricted range of granitoid solidus temperatures ($\approx$600-700°C) that are considered appropriate for the final stages of granitoid crystallization and amphibole equilibration.

Al-in-hornblende geobarometers can only be used on granitoids containing an assemblage of hornblende + biotite + plagioclase + quartz + alkali feldspar + titanite + ilmenite or magnetite $\pm$ epidote. This assemblage occurs within three plutons of the Hohonu Batholith: Uncle Bay Tonalite, Deutgam Granite, and Turiwhate Granodiorite. Attempts at applying these geobarometers to other hornblende bearing rocks (i.e. French Creek Granite and associated dikes, and the Hohonu Dike Swarm) gave spurious, often negative results, indicating unsuitability of these rocks for Al-in-hornblende geobarometry.

The Al-in-hornblende geobarometers of Hammarstrom and Zen (1986), Hollister *et al* (1987), Johnson and Rutherford (1989), Thomas and Ernst (1990) and Schmidt (1992) were applied to the appropriate plutons of the Hohonu Batholith. The equations of Hammarstrom and Zen (1986), Hollister *et al* (1987) and Schmidt (1992) gave similar pressure estimates, generally within $\pm$ 1 kb of each other. The geobarometer of Johnson and Rutherford (1989) produced pressure estimates consistently lower than the others, a phenomena noted by Schmidt (1992) who attributed this to the use of a mixed $CO_2$-$H_2O$ fluid phase to buffer the geobarometer, and a consequent elevation in the solidus and phase stability fields. The geobarometer of Thomas and Ernst (1990) gave pressure estimates consistently 2.0-2.2 kb lower than the calibrations of Hammarstrom and Zen (1986), Hollister *et al* (1987) and Schmidt (1992). The calibration of Thomas and Ernst (1990) was rejected from this study as the defining experiments were conducted at between 6-12 kb and the authors note that results are consistently low when extrapolated to lower pressures. Following the comparison of these various methods, the most recent geobarometer of Schmidt (1992)[3] was chosen for use in this study as it is calibrated over the widest range of pressures (2.5-13 kb), provides results consistent with the empirical studies of Hammarstrom and Zen (1986) and Hollister *et al* (1987), and has the smallest errors. Pressures calculated for individual analyses are included in Appendix D.

Although amphibole analyses are limited from both Uncle Bay Tonalite and Deutgam Granite both give similar average estimates of pressure of crystallization of 4.2 and 4.0 kb respectively, both within the 0.6 kb error estimated by Schmidt (1992), and a total range of calculated pressure estimates of 3.9-4.4 kb. Application of Al-in-hornblende geobarometry to analyses from four samples from Turiwhate Granodiorite gives varying results. Amphiboles from TW93 classify as actinolite or actinolitic hornblende and are indicative of post-magmatic equilibration, and are considered unsuitable for geobarometric studies. Of the remaining three samples, two give similar results and the last provides somewhat higher pressure estimates. Limited amphibole analyses from TW81 (north-western Turiwhate) give pressure estimates between 1.4-2.2 kb, averaging to 1.8 $\pm$ 0.6 kb. A larger data set from TTC1 (Turiwhate Creek) provides similar pressure estimates of 1.9-2.5 kb, averaging to 2.2 $\pm$ 0.6 kb.

---

3: P ($\pm$ 0.6 kb) = -3.01 + 4.76 $Al_{(Total)}$ ($r^2$ = 0.99).

Amphiboles from a single sample from the southern end of the pluton (GSR1 from Styx River Quarry) provide pressure estimates of between 3.3-3.5 kb averaging to 3.4 kb ± 0.6 kb. The apparent increase in pressure of crystallization from 2.2 to 3.5 kb from north to south within the Turiwhate Granodiorite, although based on only limited data, implies deeper levels of the pluton are exposed to the south of the field area. A difference in exposure level of ≈4 vertical kilometres over a lateral distance of ≈15 km is indicated. The higher pressure sample is approximately 1 km from the Alpine Fault, whereas the lower pressure samples are about 7 km from the Alpine Fault, indicating that deeper levels of exposure may be a consequence of preferential uplift, and tilting of the pluton, adjacent to the Alpine Fault.

## 4.6: Feldspar.

Feldspar compositions from all plutons (except Mount Graham Granite) are summarized in Table 4.4. Figure 4.6 summarizes all microprobe analyses of alkali and plagioclase feldspar for plutons of the batholith.

### 4.6.1: Alkali feldspar.

Alkali feldspar analyses from the Hohonu Batholith are plotted in Fig.4.6A. Most plutons show fairly consistent alkali feldspar compositions of between 85-95 weight % orthoclase, although Pah Point Granite shows somewhat lower than average orthoclase compositions. The high degree of unmixing and the perthitic nature of alkali feldspar within French Creek Granite is well illustrated in Fig.4.6A, with a wide range in compositions and no clear clustering of data points. Unmixing is also evident, to a lesser extent, in Turiwhate Granodiorite.

### 4.6.2: Plagioclase feldspar.

Plagioclase compositions throughout the batholith show abundant variation, ranging from albite to calcic andesine (An1-50%) (Fig.4.6B). The greatest variation in plagioclase composition occurs in the Deutgam Granite, reflecting its wide variation in mineralogy and $SiO_2$ contents. Within the Deutgam Granite, anorthite content of plagioclase broadly decreases with increasing whole rock silica contents. A similar trend of increasing $SiO_2$ content and decreasing plagioclase composition in the entire

batholith is evident in Fig.4.6B where plutons are ordered from left to right relative to their average $SiO_2$ content.

**4.6.3: Two feldspar geothermometry.**

The ternary feldspar system Ab-Or-An ($NaAlSi_3O_8$-$KAlSi_3O_8$-$CaAl_2Si_2O_8$) has received much attention in the literature as a potential geothermometer based on the complete solid solution of Ab-Or and Ab-An and the limited solid solution of An-Or. The two feldspar thermometer of Fuhrman and Lindsley (1988) was used in an attempt to establish temperatures of crystallization for plutons in this study. The formulation of Fuhrman and Lindsley (1988) takes into account ternary solid solution and uses experimental data and volume data to calculate equilibrium temperatures for Anorthite ($T_{An}$), albite ($T_{Ab}$) and orthoclase ($T_{Or}$). The programme also has the advantage that it accounts for analytical errors by systematically adjusting the measured compositions (to a maximum of $\pm 2$ mol%) in an attempt to minimize the sum of differences between the calculated temperatures. Three possible variations of calculated $T_{An}$, $T_{Ab}$ and $T_{Or}$ may occur.

1. Equilibrium Pair: If the sum of differences between the three temperatures is less than 80°C (i.e. all temperatures are within $\approx$40°C of each other) then the feldspar pair is considered to be in equilibrium. The temperature is taken to be the average of $T_{An}+T_{Ab}+T_{Or}$ ($\pm$30-50°C).

2. Close to Equilibrium pair: Two temperatures are similar and the third is higher or lower by $\approx$100°C. This situation is considered by Fuhrman and Lindsley (1988) to represent an error in the determination of the minor ternary component of the feldspar. The temperature is considered to be the average of the two concordant temperatures.

3. Non-equilibrium pair: The sum of differences between the three temperatures is greater than 200°C. Fuhrman and Lindsley (1988) note that in special circumstances a non-equilibrium pair can give crystallization temperatures, but should be treated with suspicion. Only equilibrium and close to equilibrium pairs were considered appropriate for use in this study.

The geothermometer of Fuhrman and Lindsley (1988) was applied to all probed samples containing co-existing feldspars. Feldspar pairs used were generally adjacent or in close proximity, and both core and rim compositions were used. The

geothermometer is pressure dependant, consequently feldspar pairs from French Creek Granite were calculated at 1 kb as the presence of miarolitic cavities indicate intrusion at relatively shallow depths. Feldspar pairs from Turiwhate Granodiorite samples collected from Mount Turiwhate were calculated at 2 kb whereas those from the Styx River Quarry were calculated at 4 kb, in accordance with Al-in-hornblende geobarometry. Feldspar pairs from Deutgam Granite and Uncle Bay Tonalite were calculated at 4 kb following Al-in-hornblende geobarometry and all other plutons are calculated at 4 kb in the absence of geobarometric indicators. Variation by up to 2 kb of the pressure used in the geothermometer resulted in only small variations in calculated temperatures for equilibrium feldspar pairs. A maximum change of 40°C was noted, with an average change of only around 10°C, well within the errors stipulated by Fuhrman and Lindsley (1988). Several close to equilibrium pairs exhibited changes of up to 100°C, but most also only changed by $\approx$40°C. Feldspar compositions for two samples, previously adjusted using the programme of Fuhrman and Lindsley (1988), were used in the two feldspar thermometer of Haselton *et al* (1983) in order to compare the two methods (Fig.4.7). Most temperatures calculated by both methods lie within $\pm$30°C of each other, however, the temperature estimates of Haselton *et al* (1983) appear to produce slightly higher temperatures, a phenomenon also noted by Fuhrman and Lindsley (1988).

Results from the Fuhrman and Lindsley (1988) geothermometer for 265 plagioclase and alkali feldspar pairs are presented in Fig.4.8. All plutons give results which are anomalously low for typical conditions of granitoid crystallization, clustering around 400°C, with some spread up to around 700°C. The Fuhrman and Lindsley (1988) thermometer is primarily intended for use on ternary feldspar pairs. None of the feldspars analyzed are true ternary feldspars, even in the hypersolvus French Creek Granite, with very few feldspars containing more than 2% of the ternary component (i.e. An in alkali feldspar and Or in plagioclase). Consequently, the lower temperatures calculated represent post-crystallization equilibration of the feldspars and unmixing along the feldspar solvus during slow cooling of the rock. As noted by Fuhrman *et al* (1988) most geothermometers in plutonic rocks are reset during slow cooling, firstly by intergrain processes, then by intragrain processes. Despite this it is interesting to note that many of the feldspar pairs of the Hohonu Batholith produced equilibrium

temperatures with low sums of differences, indicating that the post-crystallization re-equilibration process has left the feldspars in a state of equilibrium. The relatively sharp lower limit of about 400°C is also interesting and may represent the closure temperature of feldspar re-equilibration during cooling, below which no further unmixing occurs. Fuhrman *et al* (1988) and Kolker and Lindsley (1989) interpret two feldspar thermometer temperatures of 600-700°C from exsolved feldspars to represent the blocking temperature for intergrain equilibration. However lower temperatures, in accordance with those seen in the Hohonu Batholith, have been observed by Barth (1969) who describes exsolution in alkali feldspar occurring at temperatures as low as 400°C. Below this temperature exsolution ceases due to the energy barrier preventing further diffusion. More recently Brown and Parsons (1989) identified ordering in alkali feldspar down to as low as ≈200°C in potassium feldspar and 500°C in albite, and Evanelakakis *et al* (1993) have identified exsolution of alkali feldspar in amphibolite and granulite facies rocks to as low as 300-350°C. Consequently, closure temperatures of ≈400°C for the granitoids of the Hohonu Batholith are conceivable.

The scattering of higher calculated temperatures in the Arahura Granite, Pah Point Granite and Turiwhate Granodiorite probably represent closure of feldspar equilibration at higher temperatures, or remnants of actual crystallization temperatures. Higher temperatures from the Turiwhate Granodiorite are from samples calculated at 2 kb in accordance with Al-in-hornblende geobarometry, although as noted above, changing pressure within the Fuhrman and Lindsley geothermometer does not appear to drastically affect the calculated temperature. The higher temperatures of French Creek Granite may reflect the lower pressures (1 kb) used in temperature calculation, the generally higher crystallization temperatures characteristic of A-type granitoids, or the more ternary nature of the feldspars. Experiments by Tuttle and Bowen (1958) indicate that unmixing of once homogeneous feldspars is greatly facilitated below about 660°C by the presence of volatile phases. A-type granites such as the French Creek pluton are typically anhydrous and the absence of volatiles could have restricted the unmixing of the feldspars. However, most feldspars in the French Creek Granite are perthitic and have obviously undergone significant exsolution. Additionally, the presence of miarolitic cavities and abundant deuteric alteration indicate the presence of volatiles within the French Creek magma. Temperatures recorded in the French Creek Granite

($\approx$650°C) are similar to temperatures recorded in exsolved feldspars from the Sybille Monzosyenite, which are interpreted as representing the closure temperature of feldspar unmixing (Fuhrman *et al* 1988). True crystallization temperatures for the French Creek Granite are most certainly much higher, as indicated by petrographic evidence for a significant hypersolvus history.

Temperatures of 400°C and pressures of 4 kb, as recorded over much of the Hohonu Batholith, are indicative of greenschist facies metamorphism. Many of the plutons show evidence of greenschist facies alteration in saussuritization of feldspars, growth of chlorite and the alteration of biotite to epidote and titanite and chlorite. Most of the mafic dikes also contain a greenschist facies deuteric alteration assemblage (Ch.7). It is therefore probable that the conditions recorded by geothermobarometry and the greenschist facies alteration observed petrographically are both representative of the uplift and slow cooling of the plutons along the geothermal gradient. Alternatively, and somewhat tentatively, the close proximity of the Alpine Fault, and the mylonitization of proximal rocks, may suggest a greenschist facies overprint of the batholith in association with the inception of compression across the Alpine Fault.

In summary it is concluded that:

(1) Two feldspar geothermometry is inappropriate for estimating crystallization temperatures of granitoids such as those from the Hohonu Batholith.

(2) The exsolution of feldspars at sub-solidus conditions will result in two feldspar thermometry recording the sub-solidus history of the plutons and giving no indication of true crystallization conditions.

(3) A closure temperature for feldspar exsolution of $\approx$400°C appears to be recorded.

# Chapter 5

# Geochronology and uplift history of the Hohonu Batholith.

## 5.1: Introduction and methods.

In this chapter, U-Pb zircon, Rb-Sr and fission track geochronological data for the Hohonu Batholith granitoids are presented, and correlations within the Western Province are made.

Available geochronological data for the granitoids of the Hohonu Batholith are summarized in Table 5.1 and new SHRIMP (Sensitive High Resolution Ion Microprobe) and Rb-Sr whole rock data are presented in Fig.5.1 to Fig.5.3. Mineral separate Rb-Sr data are presented in Table 5.2 with corresponding whole rock isotope data and analyses used in Rb-Sr errorchrons also presented in Tables 6.4, 6.8 and 6.9.

Ion microprobe U-Pb zircon (SHRIMP) ages were determined by Trevor Ireland at Australian National University, Canberra, using methods described by Muir *et al* (1994a). Rb-Sr whole rock (WR) ages, errors, initial ratios and MSWD's were calculated using the two error regression analysis of the PETMIN program; a detailed discussion on Rb-Sr isotope methods is given in Appendix B.

For those units which are dated by both the SHRIMP and conventional U-Pb zircon methods, SHRIMP ages are taken as the better estimate of crystallization age, as they are considered to be more reliable due to the ability to distinguish between igneous and inherited zircons. For those plutons lacking SHRIMP data, conventional U-Pb data and Rb-Sr mineral ages give an indication of crystallization age. The only unit with no age control is the Mount Graham Monzogranite.

Geochronological data (Table 5.1) indicate that three discrete phases of granitoid plutonism are represented in the Hohonu Batholith, confirming field relationships and the recognition of two suites and one super-suite, as discussed in Ch.6.

Palaeozoic plutonism, more extensive to the north in the Karamea Batholith (Tulloch 1988a, Muir *et al* 1994c), is represented in the Hohonu Batholith by the Summit Granite. This pluton has subsequently acted as country rock and been intruded by the Cretaceous Deutgam and Turiwhate granitoids, and is preserved as a cap to these plutons.

Late Cretaceous alkaline magmatism is recorded in the A-type French Creek Granite, a SHRIMP age of 81.7 ± 1.8 Ma confirming the conventional U-Pb zircon age of Tulloch *et al* (1994) and in agreement with Rb-Sr whole rock data and K-Ar (hornblende) data.

The remainder of the Hohonu Batholith constitutes the Hohonu Super-suite (Ch.6.1.1) and was emplaced between 113.5 Ma (Uncle Bay Tonalite) and 108.7 Ma (Te Kinga Monzogranite). These ages just overlap at the two sigma confidence limit, but the suggestion that the intermediate plutons of the Deutgam Suite may slightly predate the more evolved Te Kinga Suite is broadly in accord with field evidence.

## 5.2: Regional correlations.

### 5.2.1: Summit Granite.

The Devonian age of Summit Granite suggests correlation with the Palaeozoic Karamea Suite of Tulloch (1988a), as do geochemical data (Ch.6.7). The age of Summit Granite is also within error of the restricted 375 ± 4 Ma range of ages derived from the Karamea Batholith and related rocks (Muir *et al* 1994c).

Although Palaeozoic granitoids are common in the Buller Terrane, the Summit Granite is somewhat isolated. The nearest Devono-Carboniferous plutons are the Rangitoto Granite ≈55 km to the south (minimum biotite and feldspar K-Ar ages of 295 ± 2 and 314 ± 2 Ma, Jury 1981, 359 ± 10 Ma mineral + WR Rb-Sr isochron, Aronson 1968), the Tarn Summit Suite 90 km to the north east in the Victoria Range (360-370 Ma, Cooper and Tulloch 1992, ≈ 380 Ma Rb-Sr WR isochron, Tulloch 1979a) and the Barrytown Pluton 70 km to the north (372 ± 5 Ma, Muir *et al* unpublished SHRIMP data 1994). As discussed further in Ch.6.7.6, despite petrographic similarities, unrealistically low calculated $Sr_{(381)}$ in the Mount Graham

Granite indicates that it may not be Palaeozoic and therefore be unrelated to the Summit Granite or Karamea Suite. The pulse of Mid-Late Devonian activity represented by the Karamea Batholith and the Summit Granite can also be recognized in Antarctica (Admiralty Intrusives of Northern Victoria Land and Ford Granodiorite of Marie Byrd Land), northeast Tasmania, and in the central Lachlan Fold Belt (Muir *et al* 1994c). A Devonian subduction zone along the margin of Gondwana is typically invoked to account for these granitoids (Weaver *et al* 1991).

**5.2.2: The Hohonu Super-suite.**

Based on their geochemical similarities, the Jays Creek, Pah Point, Te Kinga, Uncle Bay, Deutgam, Turiwhate and Arahura plutons constitute the Hohonu Super-suite (see Ch.6.1.2). Geochronological data indicate that the Hohonu Super-suite represents a relatively short pulse of magmatism, concentrated at about 110 Ma. Similar ages have been determined for plutons belonging to the Rahu Suite of Tulloch (1988a), a correlative of the Hohonu Super-suite, namely Buckland Granite (109.6 $\pm$ 1.7 Ma, Muir *et al* 1994a), several plutons in the Victoria Range (106 to 96 Ma K-Ar ages, Tulloch 1979a) and the Berlins Quartz Porphyry (111.0 $\pm$ 2.0 Ma, Muir *et al* unpublished data 1994). Although the Hohonu Super-suite postdates the emplacement of the bulk of the Separation Point Batholith (125-118 Ma, Muir *et al* 1994a, 1994d, 1995), the Olympus Granite (111.4 $\pm$ 2.0 Ma Muir *et al* 1994a) indicates limited Separation Point Suite composition magmatism continued contemporaneously with the intrusion of the Hohonu Super-suite. The age of the Hohonu Super-suite is broadly contemporaneous with the cessation of subduction along the continental margin of Gondwana at 105 $\pm$ 5 Ma (J.D.Bradshaw 1989) and the onset of crustal extension as discussed further in Ch.6.5.4.

Despite the recognition of Separation Point composition magmatism in Fiordland (Muir *et al* 1994d, 1995), no 110 Ma Hohonu-type plutonic event has yet been recognized south of the Hohonu Batholith or in the Fiordland region (except see Gibson and Ireland 1994). This may reflect their absence, or simply be a consequence of the restricted and poorly known Buller Terrane equivalents located in the remote southwest corner of Fiordland.

**5.2.3: The French Creek Granite.**

French Creek Granite represents the only known Late Cretaceous felsic plutonism in the Western Province. Slightly older to contemporaneous alkaline, felsic, extensional magmatism is relatively widespread in the Eastern Province and probably related to extension during New Zealand-Antarctica break-up (e.g. Weaver and Pankhurst 1991). The 81.7 Ma age for French Creek Granite has very important tectonic implications, as discussed by Tulloch *et al* (1994) and further in Ch.6.6.10. Geological evidence indicates the French Creek Granite is contemporaneous with late members of the Hohonu Dike Swarm which indicate intrusion into a strongly NNE-SSW extensional environment (Ch.7). The Late Cretaceous age of French Creek Granite coincides remarkably well with crustal extension in the Western Province and the appearance of the first oceanic crust in the Tasman Sea. Thus a strongly extensional, anorogenic environment is indicated during emplacement of French Creek Granite, consistent with its characteristic A-type chemistry (see Ch.6.6.10).

**5.3: Comparison of methods.**

**5.3.1: SHRIMP versus conventional U-Pb.**

Although SHRIMP and conventional U-Pb ages from the Hohonu Batholith are broadly similar, they often differ significantly at the 2 sigma level of calculated error. Moreover, the conventional method fails to identify the discrete pulse of magmatism at $\approx$110 Ma indicated by SHRIMP data. SHRIMP ages have also greatly reduced calculated errors on some of the units previously dated by the conventional method, for example Deutgam Granite (Table 5.1). Ion microprobe dating is advantageous in that igneous and inherited zircons can be distinguished. Conversely, conventional methods tend to average the true crystallization age and any inherited component and may thus produce slightly older ages. This is the case in the Te Kinga Monzogranite which yields a SHRIMP age of 108.7 $\pm$ 3.0 Ma, in contrast to the 119 $\pm$ 2 Ma conventional age, the older conventional U-Pb age reflecting the large amount of older, inherited zircons in this granitoid (T.Ireland *pers.comm.* 1994). The only major unit on which a SHRIMP age has not been determined is the Turiwhate Granodiorite. Inheritance in the intermediate, I-type Deutgam Suite plutons is minor (T.Ireland *pers.comm.* 1994), by inference the strong I-type nature of Deutgam Suite Turiwhate Granodiorite indicates

any inherited component will be minor and the conventional U-Pb age is likely to be an accurate indication of age of crystallization.

**5.3.2: Whole rock Rb-Sr geochronology.**

Several whole-rock and mineral samples from the French Creek and Deutgam Granites were analyzed in an attempt to construct Rb-Sr whole rock isochrons. Large MSWD's (mean squared weighted deviates, a measure of scatter of the data) result in neither data set forming a true isochron. An MSWD of greater than 2.5 is generally considered to indicate the presence of geological scatter in the data, i.e. the magma was not initially homogeneous in Sr isotopic composition or underwent varying amounts of heterogeneous contamination during crystallization (Rollinson 1993).

The Rb-Sr WR errorchron for the Deutgam Granite (Fig.5.2) gives an age of 110.8 $\pm$ 1.4 Ma, coinciding remarkably well with the SHRIMP age of 110.4 $\pm$ 2.2 Ma. Little variation in measured whole rock $^{87}Rb/^{86}Sr$ and $^{87}Sr/^{86}Sr$ make the errorchron far from ideal, being largely defined by a single aplitic sample (HRS17). Furthermore, the MSWD of 13.2 is beyond acceptable standards for an ideal isochron, and the coincidence with the SHRIMP age may be purely coincidental. The biotite separate from HRS12 does not fall on the whole rock isochron (Fig.5.2, inset) and was not used in the age calculation.

Whole rock Rb-Sr errorchrons for French Creek Granite (Fig.5.3) have very high MSWD's and do not constitute true isochrons, although calculated ages are similar to the 81.7 $\pm$ 1.8 Ma SHRIMP age presented in this study. Calculated errors on the Rb-Sr errorchron are large and vary considerably depending on which samples are used in the calculations, consequently, the Rb-Sr ages are treated with caution. Given the low Sr contents of French Creek Granite, and isotopic evidence for open system behaviour (Ch.6.6.6), the failure to yield an acceptable isochron is not surprising. As shown in the inset of Fig.5.3, the single rhyolitic dike analyzed (HDP8) falls considerably below the errorchron and this sample was not used in the age calculations.

**5.3.3: Two point mineral-whole rock (WR) isochrons.**

Mica-WR ages were calculated for single samples of all units of the Hohonu Batholith (except Mount Graham Granite) and are presented in Table 5.2. In the absence of geological control and other geochronological data, the biotite-WR isochrons for Jays Creek Granite and Pah Point Granite are taken to represent their crystallization ages. The calculated ages are within error of the 113.5 to 108.7 Ma range of SHRIMP ages observed in the remaining Hohonu Super-suite plutons. However, throughout the Hohonu Batholith, biotite-WR ages are consistently younger than muscovite-WR ages which are in turn younger than SHRIMP and conventional U-Pb zircon ages. This relationship is also observed in the Buckland Granite, with a SHRIMP age of 109.4 $\pm$ 1.4 Ma (Muir *et al* 1994a) and muscovite-WR ages of mostly 106.8 to 103.4 Ma and biotite-WR ages of 94.1 to 98.5 Ma (Graham and White 1990). As a consequence, the calculated biotite-WR ages for Jays Creek and Pah Point Granites must be considered as only minimum estimates of their crystallization ages.

Considerably younger Cretaceous biotite-WR and muscovite-WR ages for the Palaeozoic Summit Granite must be a consequence of resetting during intrusion of the Deutgam Granite and Turiwhate Granodiorite. Similarly, the young biotite-WR age from a mylonitized sample of Te Kinga Monzogranite indicates partial resetting, but probably as a consequence of protomylonitic deformation during movement on the Alpine Fault. Temperatures reached during mylonitic deformation were obviously not high enough to reset the muscovite Rb-Sr system, as this yields an age similar to the SHRIMP age. A 70 $\pm$ 4 Ma K-Ar biotite age for a sample of Te Kinga Monzogranite from the same locality (Hurley *et al* 1962) is also likely to reflect argon loss and partial resetting associated with this deformation.

The discrepancies between results obtained by U-Pb and Rb-Sr mineral-WR dating reflect reducing blocking temperatures for each of the three different methods, from >800°C for U-Th-Pb in zircon to >500°C for Rb-Sr in muscovite down to 320°C for Rb-Sr in biotite (Harland *et al* 1990). As such, these can then be used to calculate average cooling or uplift rates. Using the closure temperatures of Rb-Sr in biotite and U-Pb in zircon of Harland *et al* (1990) above, cooling rates range between 27°C/Ma to 104°C/Ma, apparently increasing to the south. In a similar manner,

assuming a geothermal gradient of 35°C/km, calculated uplift rates are geologically reasonable and range between 0.4 to 2.8 mm/year, also apparently increasing towards the southern end of the batholith. The presence of miarolitic cavities and hypersolvus textures in the French Creek Granite indicate emplacement and crystallization at relatively shallow depths ($\approx$3 km $\approx$1 kb) at 82 Ma. Preliminary geobarometric data from the Deutgam Granite (Ch.4.5.1), which has acted as country rock to the French Creek Granite, indicates emplacement at $\approx$4 kb ($\approx$12 km). Consequently, the Deutgam Granite, and presumably the remainder of the Hohonu Batholith, must have been uplifted from $\approx$12 km to $\approx$3 km between 110 Ma and 82 Ma, easily accomplishable at the calculated uplift rates.

**5.4: Fission track data and uplift history.**

Fission track ages from the study area are numerous and are compiled in Fig.5.4; a detailed analysis of the data is considered beyond the scope of this study. Apatite ages range from 10.8 $\pm$ 1.1 Ma to 1.6 $\pm$ 0.9 Ma (excluding a single Greenland Group sample of 17.8 $\pm$ 4.5 Ma). As has been shown in the Western Province in general, ages decrease towards the Alpine Fault, and are consistent with recent uplift through the apatite annealing zone ($\approx$120°C) in association with Late Cenozoic compression across the Alpine Fault (Kamp *et al* 1992).

Sparse zircon data yield variable ages, ranging from 80.2 $\pm$ 9.4 Ma to 9.3 $\pm$ 1.5 Ma. The single Cretaceous zircon age (Dorothy Creek, Mount Tuhua) overlaps a 90-80 Ma period when apatite was widely reset in North Westland (White and Green 1986), possibly in association with uplift and crustal extension during Antarctica-New Zealand-Australia separation (see also Laird 1993). A single titanite age from Styx River quarry probably also reflects this event as titanite has a somewhat higher annealing temperature ($\approx$290 $\pm$ 40°C) than zircon, which has partially annealed at this locality (White and Green 1986). Apatites in the Hohonu Batholith do not retain this event and have been overprinted by the Alpine Fault. Titanite ages from the Hohonu Ranges also appear to have been completely reset. A Late Cretaceous uplift event is consistent with Rb-Sr biotite-WR ages from the Hohonu Batholith, which indicate uplift to relatively shallow crustal levels prior to emplacement of the French Creek Granite. The remaining zircon fission track ages from the Hohonu Batholith range from 57.3 $\pm$

5.8 Ma to 9.3 ± 1.5 Ma and are interpreted to represent partial to complete annealing in the middle to lower parts of the zircon annealing zone (≈200°C) prior to Late Cenozoic uplift (Kamp *et al* 1992). A single zircon age from the Fraser Complex is much younger (7.3 ± 0.8 Ma) than zircon ages to the west of the Fraser Fault, and indicates rapid uplift through the zircon closure temperature, consistent with other zircon data from further south in the Fraser Complex (Kamp *et al* 1992). However, a zircon sample from the Granite Hill Complex (Seward 1989) retains an older age, consistent with partial annealing, and indicating that uplift to the north may not have been as rapid (see Ch.8).

Biotite K-Ar ages of 70 ± 4 Ma from Rotomanu Railway Station (Hurley *et al* 1962), 51.57 ± 1.16 Ma from Smart Creek, Hohonu Ranges, and 47.53 ± 1.16 Ma from Inchbonnie Quarry (Seward 1989) indicate continued cooling of the granitoids through to Eocene times. The K-Ar ages of Seward (1989) are also similar to those determined by Rattenbury (1987a) from the Fraser Complex. These variable, young K-Ar ages indicate the extreme difficulties of the K-Ar method to determine crystallization ages in this region (e.g. Wellman and Cooper 1971), largely a consequence of the proximity of the Alpine Fault.

Combining fission track and Rb-Sr and U-Pb zircon data a schematic cooling/uplift curve can be generated for the Hohonu Batholith (Fig.5.5). Following crystallization a period of rapid uplift and cooling is indicated in the Late Cretaceous, probably associatted with Gondwana break-up. This is followed by a period of relative hiatus, resulting in partial annealment of many zircon and titanite samples. Rapid Cenozoic uplift of the batholith associated with compression across the Alpine Fault is reflected in young apatite ages, generally less than 10 Ma.

Kamp *et al* (1992) interpret regional fission track data to represent uplift of the Westland-South Westland region in two blocks, termed the Greenland Block (including the Hohonu Batholith) and the Fraser Block (Fig.5.6). The Fraser Block has been uplifted a minimum of 10.6 km (assuming a geothermal gradient of 25°C/km) since about 10 Ma as a wedge adjacent to the Alpine Fault. The Greenland Block has undergone less uplift than the Fraser Block, around 8 km around the Hohonu Batholith

with uplift decreasing to the south. The differential uplift is supported by the absence of Late Cretaceous - Tertiary outliers in the north of the Greenland Block (Kamp *et al* 1992). Uplift is assumed to have occurred along the Hohonu and Fraser-Granite Hill Faults (see Fig.5.6). To the east the Alpine schists have been uplifted a minimum of 12-13 km along the Alpine Fault (Kamp *et al* 1989).

# Chapter 6

# Geochemistry and petrogenesis of the Hohonu Batholith granitoids.

## 6.1: Introduction.

The granitoids of the Hohonu Batholith encompass a wide spectrum of compositions (Table 6.1, Table 6.2), with silica values ranging from 51% (Uncle Bay Tonalite) to 76% (French Creek Granite). A bimodal distribution is evident in the analyzed samples (Fig.6.1) with peaks at 64% and 74% $SiO_2$, corresponding to granodioritic and monzogranitic compositions. The plutons exhibit a typical calc-alkaline trend on an AFM plot (Fig.6.2) and (excluding French Creek Granite) are calc-alkaline on a modified Peacock Diagram (Fig.6.3). Peacock indices for the Hohonu Batholith granitoids spread between 56-61 on Fig.6.3, in marked contrast to the alkali-calcic Separation Point Batholith (Peacock Index of ≈54, Muir *et al* 1995). The French Creek Granite is alkalic with a Peacock index of ≈44-45 (Fig.6.4).

A wide variation in Aluminium Saturation Index (ASI) occurs (Fig.6.5, Table 6.2), with a poorly defined trend of increasing A/CNK and decreasing A/NK[4] apparent with increasing average $SiO_2$ content. The relatively mafic plutons (Turiwhate Granodiorite, Uncle Bay Tonalite and Deutgam Granite) are metaluminous with high values of A/NK. Evolved members of these plutons, Jays Creek Granite, and Pah Point Granite are weakly peraluminous with A/CNK < 1.1. The higher $SiO_2$ plutons (Arahura Granite, Te Kinga Monzogranite, Summit Granite and Mount Graham Granite) are more strongly peraluminous with A/CNK = 1.0 to 1.2 and low A/NK. French Creek Granite has A/CNK and A/NK close to unity, resulting in weakly peraluminous to weakly metaluminous compositions. Several samples of hypersolvus French Creek Granite are peralkaline with both A/CNK and A/NK < 1.

### 6.1.1: Summary characteristics of Hohonu Batholith granitoid suites.

Geochemistry, in association with field and petrographic characteristics, has enabled subdivision of the Hohonu Batholith into four suites. The Deutgam Suite (Jays

---

4: A/CNK = ASI = molar($Al_2O_3$/CaO+$Na_2O$+$K_2O$).
A/NK = molar($Al_2O_3$/$Na_2O$+$K_2O$).

Creek Granite, Pah Point Granite, Uncle Bay Tonalite, Deutgam Granite and Turiwhate Granodiorite) and the Te Kinga Suite (Te Kinga Monzogranite and Arahura Granite) together form the Hohonu Super-suite which dominates the batholith. French Creek Granite and Summit Granite are unique within the Batholith and form two discrete suites; the French Creek Suite and the Summit Granite Suite. The criteria used to identify each suite are briefly summarized below and various geochemical plots used to distinguish the proposed suites of the Hohonu Batholith are presented in Fig.6.6, 6.7 and 6.8[5].

**The Hohonu Super-suite.**

The majority of plutons of the Hohonu Batholith are included within the Hohonu Super-suite, characterized by similar Sr and Nd isotopic characteristics ($Sr_{(110)}$ = 0.7062-0.7085, $\epsilon Nd_{(110)}$ = -4.4 to -6.1), similar patterns on mantle normalized spider-diagrams and, with a few exceptions, parallel trends on Harker diagrams (see Fig.6.8). The Hohonu Super-suite consists of two suites intruded between 113.5 to 109 Ma (Ch.5); the Deutgam Suite and the Te Kinga Suite. Both suites show similar enrichment of LREE, but contrast sharply in their abundances of HREE. The Hohonu Super-suite is compared with the Rahu Suite of Tulloch (1988a) in Ch.6.2.5.

**The Deutgam Suite:**

Jays Creek Granite, Pah Point Granite, Uncle Bay Tonalite, Deutgam Granite and Turiwhate Granodiorite are somewhat heterogeneous biotite ($\pm$ titanite $\pm$ allanite $\pm$ amphibole) tonalites to granodiorites. More evolved monzogranitic compositions also occur. The plutons are typical I- and evolved I-type granitoids in terms of the granitoid nomenclature of Chappell and White (1992). The Deutgam Suite is metaluminous to weakly peraluminous (A/CNK = 0.66-1.10) (Fig.6.5), has a wide range in silica (56-75% $SiO_2$), and is more mafic than the Te Kinga Suite.

The Deutgam Suite exhibits a flat trend of $Na_2O$ with increasing $K_2O$ (Fig.6.6) and relatively constant $K_2O/Na_2O$ with decreasing CaO (Fig.6.7), trends distinct from the Te Kinga Suite. The Deutgam Suite is also distinguished by lower levels of Sr and

---

5: Data Presentation. All data used in plots in this chapter are recalculated to an anhydrous total of 100%.

$Al_2O_3$ at similar $SiO_2$ contents to the Te Kinga Suite (Fig.6.8). The Deutgam Suite is LREE enriched with flat HREE and relatively large negative Eu anomalies (see Fig.6.12). Preliminary stable isotope studies indicate the Deutgam Suite has relatively low $\delta^{18}O$ values compared to the Te Kinga Suite with $\delta^{18}O \approx +8‰$ (see Table 6.5).

**The Te Kinga Suite:**

The Te Kinga Monzogranite and Arahura Granite are evolved muscovite-biotite monzogranites which do not fit comfortably into the I- or S-type classification scheme of Chappell and White (1992). Both are relatively large homogeneous plutons displaying porphyritic textures towards higher levels of exposure, indicative of relatively shallow depths of emplacement. The Te Kinga Suite has restricted high $SiO_2$ contents (70-75 wt%) and is moderately peraluminous with A/CNK between 1.0-1.16 (Fig.6.5). Along with the Deutgam Suite, the Te Kinga Suite falls within the I-type field on a plot of $K_2O$ versus $Na_2O$ (Fig.6.6), but displays distinct trends: $Na_2O$ decreasing with increasing $K_2O$ (Fig.6.6), and decreasing $Na_2O/K_2O$ with increasing CaO (Fig.6.7). Higher contents of Sr and $Al_2O_3$ at similar levels of $SiO_2$ are distinctive in the Te Kinga Suite and lower Rb and $K_2O$ are somewhat less effective at distinguishing it from the Deutgam Suite (Fig.6.8). The Te Kinga Suite is LREE enriched with depleted HREE and small negative Eu anomalies (Fig.6.12). Preliminary data indicate the Te Kinga Suite has $\delta^{18}O \approx +10‰$, significantly greater than the Deutgam Suite (see Table 6.5).

**The French Creek Suite.**

Field evidence and geochronological data (Ch.5), indicate French Creek Granite is considerably younger (81.7 $\pm$ 1.8 Ma) than the other plutons of the batholith. French Creek Granite is a composite body comprising a number of granitoids displaying textures consistent with a hypersolvus history and rapid crystallization at shallow levels. The pluton is also mineralogically distinct, containing Fe-rich biotite and sodic-calcic amphiboles (Ch.4). The granitoid is alkalic (Fig.6.4), and has high $K_2O/Na_2O$ and low CaO (Fig.6.6, Fig.6.7). It is also distinctly depleted in Sr and Ba, enriched in $Fe_2O_3$ and the high field strength elements, and has very high Rb/Sr (Fig.6.8). French Creek Granite has high $\Sigma$REE and is LREE enriched with flat HREE and large negative Eu anomalies (see Fig.6.71). French Creek Granite is isotopically

primitive, exhibiting characteristics consistent with a high degree of mantle involvement. Chemically and mineralogically, the French Creek Granite is a typical A-type granitoid (*sensu* Eby 1990).

**The Summit Granite suite:**

Field evidence, isotopic data, and a SHRIMP age of 381.2 ± 7.3 Ma (Ch.5), indicate Summit Granite is distinctly older than the remaining plutons of the batholith. Summit Granite is most likely related to the Palaeozoic Karamea Suite of Tulloch (1988a), the SHRIMP age being within error of the restricted range of ages collected from the Karamea Suite by Muir *et al* (1994c). Consequently Summit Granite suite is an informal name used only in this thesis. The granitoid contains rare garnet, has muscovite dominant over biotite, is typically leucocratic, foliated and contains abundant metasedimentary material, suggesting an S-type classification (*sensu* Chappell and White 1992). Summit Granite is strongly peraluminous (A/CNK 1.05-1.22) (Fig.6.5) and has relatively high $K_2O/Na_2O$ (Fig.6.6, Fig.6.7). The pluton can also be distinguished by high $P_2O_5$, Pb, Rb and Rb/Sr (typically 2-3), and low $Na_2O$ and Sr (Fig.6.8). The suite is LREE enriched with flat HREE, large negative Eu anomalies and distinctively low ΣREE (see Fig.6.80).

The petrographic dominance of muscovite, coupled with the strongly peraluminous chemistry of Mount Graham Granite, suggests affinities with the Summit Granite suite, although a single Sr isotopic analysis is much less radiogenic than the Summit Granite and may discount this. In the absence of geochronological data and with the limited chemical data available it is difficult to ascribe the Mount Graham Granite to any of the suites identified here and it may represent a fifth discrete unit. The chemistry of the Mount Graham Granite is discussed briefly in Ch.6.7.6.

The geochemistry of each suite is now discussed.

## 6.2: Geochemistry of the Hohonu Super-suite.

### 6.2.1: Major and trace elements.

Trends of decreasing $TiO_2$, $Al_2O_3$, CaO, $Fe_2O_3$, MgO and $P_2O_5$ are observed with increasing $SiO_2$ in both the Te Kinga and Deutgam Suites (Fig.6.9). $Na_2O$ remains

relatively constant, whereas $K_2O$ shows a crude increase with increasing $SiO_2$ (Fig.6.9), although both elements show different relative behaviours in each suite as discussed previously (Fig.6.6, Fig.6.7). Higher MgO contents distinguish the Turiwhate Granodiorite from the remaining plutons. The Hohonu Super-suite lies within the High-K calc-alkaline series of Peccerillo and Taylor (1976) (Fig.6.9).

Considerably greater scatter is observed within the trace elements of the Hohonu Super-suite (Fig.6.10). Sr, Ni, Zn, V, Cr, Zr, Ba and Ce decrease with increasing $SiO_2$ whereas Pb shows a crude increase. Th is scattered but generally increases in the Deutgam Suite then decreases at the higher $SiO_2$ contents of the Te Kinga Suite. Rb is also highly scattered, but generally increases in the Deutgam Suite, Rb contents are significantly lower in the Te Kinga Suite and show little variation with $SiO_2$. Most plutons have Rb/Sr values significantly less than one (Fig.6.10) and as noted above, Rb and Sr contents are particularly effective at distinguishing the two suites. Higher contents of the transition elements Cr, V, Ni and to a lesser extent Zn are evident in the Turiwhate Granodiorite (Fig.6.10).

Despite restricted $SiO_2$ contents, major and trace element variations within the Te Kinga Suite generally parallel those of the Deutgam Suite. Within the Te Kinga Suite itself, the Te Kinga Monzogranite has somewhat lower $TiO_2$, MgO, V and Rb, whereas the Arahura Granite has lower $Al_2O_3$, $Na_2O$, Ba and Sr.

### 6.2.2: Mantle normalized multi-element diagrams (Spider-diagrams).

The geochemistry of igneous rocks can be illustrated using mantle normalized multi-element diagrams or "spider-diagrams". Spider-diagrams of representative samples from each pluton are presented in Fig.6.11. Variation and scatter at the more mobile end of the spectrum (i.e. K, Rb, Ba, Th, U) partially reflects the solubility of these elements in aqueous fluids during alteration. Less importantly, lower analytical accuracies may also be reflected in the scattering of some elements, particularly Th, Pb and Nd.

The Hohonu Super-suite displays similarly inclined spider-diagrams, with negative anomalies at Ba, Nb-Ta, P and Ti (Fig.6.11). With increasing differentiation these anomalies increase as the appropriate minerals (feldspar, apatite and Fe-Ti oxides) are fractionated. In contrast, relatively incompatible elements, such as Zr, REE and Y may increase with evolution as they become preferentially concentrated in residual liquids. Comparison of the Te Kinga and Deutgam Suite at similar $SiO_2$ contents (e.g. Pah Point Granite *cf* Te Kinga Monzogranite) illustrates fundamental differences. Most importantly the Te Kinga Suite lacks distinct Sr and Ba anomalies and is relatively depleted in Y when compared with Deutgam Suite plutons with similar $SiO_2$ contents (Fig.6.11).

#### 6.2.2.1: Nb-Ta anomalies: a brief discussion.

Negative Nb-Ta anomalies are typical of many igneous rocks and the Hohonu Super-suite is no exception (Fig.6.11). Nb and Ta, along with Ti and P, are preferentially retained during dehydration of subducted eclogitic oceanic crust as a consequence of their relatively immobile behaviour during fluid alteration (Saunders *et al* 1980). The large ion lithophile element (LILE) enriched mantle wedge is consequently relatively depleted in these elements. In addition, Hofmann *et al* (1986) suggest that Nb and Ta are also preferentially retained in Ti-oxide minerals during extraction of continental material from the mantle during subduction. Consequently, Nb-Ta depletions are generally considered to indicate a subduction-related environmental signature. As pointed out by Saunders *et al* (1980) (and also implied by Hofmann *et al* 1986) Ti and P are also likely to be retained in the mantle or subducting slab. Therefore, although the P and Ti depletions common in many granitoids (e.g. Chappell and White 1992, Jones *et al* 1992) may reflect fractional crystallization of apatite and Fe-Ti oxides, they may also reflect a subduction signature inherited from the granitoids ultimate mantle source. As many granitoid sources have been through multi-stage processes since their ultimate derivation from the mantle, such subduction signatures simply reflect the source chemistry, not the actual tectonic environment at the time of magma generation (Arculus 1987, Weaver *et al* 1992).

### 6.2.3: Rare Earth Elements.

REE data for individual plutons are summarized in Table 6.3 and chondrite-normalized REE diagrams for individual plutons of the Hohonu Super-suite are presented in Fig.6.12. Additional data published by Mason and Taylor (1987) has been added, and correlate well with data of this study.

Although both suites display similar levels of LREE enrichment, the two suites display distinctly different Eu anomalies and HREE abundances. The Deutgam Suite is characterised by LREE enriched plots ($La/Yb_N \approx 6$-17) with flat HREE ($Gd/Yb_N \approx 1.5$-2.0) and relatively large negative Eu anomalies ($Eu/Eu^* \approx 0.70$ to 0.50). The Turiwhate Granodiorite has slightly lower abundances of HREE than the other members of this group, resulting in slightly higher $La/Yb_N$ values. In contrast, the Te Kinga Suite is immediately distinguishable with relatively steep LREE enriched ($La/Yb_N \approx 19$-43) and HREE depleted ($Gd/Yb_N \approx 2.26$-4.36) plots displaying small to negligible negative Eu anomalies ($Eu/Eu^* \approx 0.70$-1.00).

### 6.2.4: Isotopes.

#### 6.2.4.1: Radiogenic isotopes.

Sr and Nd isotopes for the Hohonu Super-suite are presented in Table 6.4, with detailed analytical methods discussed in Appendix B. Based on geochronological data discussed in Ch.5, initial strontium ratios ($Sr_{(t)}$) and Epsilon Nd ($\epsilon Nd_{(t)}$) values for the Hohonu Super-suite are age corrected to 110 Ma.

$Sr_{(110)}$ and $\epsilon Nd_{(110)}$ for the Hohonu Super-suite, Greenland Group, and depleted mantle (after Taylor and McClennan 1985) are plotted in Fig.6.13a. Buckland Granite, the only Rahu Suite pluton with available Sr and Nd isotope data, is also added for comparison, as is the Early Cretaceous Separation Point Suite (data recalculated from Muir *et al* 1995). On a broad scale the Hohonu Super-suite is well constrained, with $Sr_{(110)}$ between 0.7062 and 0.7085 and $\epsilon Nd_{(110)}$ between -4.4 and -6.1. Buckland Granite has similar isotopic compositions to the Hohonu Super-suite, whereas the Separation Point Suite is immediately distinguishable with much less radiogenic isotopic compositions. Isotopic compositions of the Separation Point Suite are consistent with derivation from partial melting of young mafic lithosphere (Muir *et al* 1995) whereas

initial isotopic compositions of the Hohonu Super-suite and Buckland Granite indicate involvement of a more mature and radiogenic crustal source.

Figure 6.13b is an enlargement of the $Sr_{(110)}$ and $\epsilon Nd_{(110)}$ plot and at this scale both inter-pluton and intra-pluton variation is evident within the Hohonu Super-suite. Buckland Granite has isotopic characteristics similar to Te Kinga Monzogranite, the least radiogenic pluton of the Hohonu Super-suite. Deutgam Granite, Pah Point Granite and Uncle Bay Tonalite are more radiogenic and isotopically identical. The remaining three plutons (Jays Creek Granite, Arahura Granite, Turiwhate Granodiorite) have isotopic compositions intermediate between Deutgam Granite and Te Kinga Monzogranite. The Te Kinga and Deutgam Suites identified in Ch.6.1.1 are isotopically indistinguishable, and although the Te Kinga Suite is slightly less radiogenic than the Deutgam Suite, the two suites display considerable overlap in isotopic compositions.

Individual plutons within the Hohonu Super-suite show internal variation greater than that expected from analytical error. This may be due to correction to inappropriate ages, varying degrees of contamination within individual samples, variable initial ratios within plutons, or isotopic adjustment by some post-crystallization process. Given the relatively low Rb-Sr ratios and the tightly constrained cluster of ages presented in Ch.5, incorrect age correction is considered an unlikely source of variation. Variable $Sr_{(110)}$ ratios in Turiwhate Granodiorite and Jays Creek Granite are consistent with contamination by small amounts of Greenland Group, and small inclusions of metasediments were noted at both outcrops where the two outlying samples (GSR4 and TH3) were collected. Arahura Granite, despite little variation in $Sr_{(110)}$, shows a wide range of $\epsilon Nd_{(110)}$ from -4.8 to -6.1. $\epsilon Nd_{(110)}$ values increase from the NW end of the pluton towards the Alpine Fault, although on the basis of only four samples this may not be significant. Nd isotope characteristics of Arahura Granite are inconsistent with contamination by highly radiogenic Greenland Group metasediments, instead a low $Sr_{(110)}$ and low $\epsilon Nd_{(110)}$ contaminant such as typical depleted Archaean gneiss is implied. No other evidence for such a contaminant is known in the Western Province and as such this is not considered a likely origin for the Nd scatter in the Arahura Granite.

Graham and White (1990) attributed alteration and some $Sr_{(i)}$ diversity in the Paparoa Batholith to low temperature alteration associated with lamprophyre dike intrusion. Nd and Sr isotopic analyses of limited members of the Hohonu Dike Swarm indicate a strong mantle signature (Table 7.2) and isotopic alteration would be expected to move the granitoids towards less radiogenic compositions. Isotopic contamination by the Hohonu Dike Swarm should be most evident in the Te Kinga Monzogranite, Uncle Bay Tonalite and Deutgam Granite, where the swarm is most intense. These three plutons are well constrained isotopically, and show no evidence for a shift towards more mantle-like compositions. Of note are samples KST4, KUC1, KFR7, HRS12, and HRS17, all collected within several metres of exposed dikes and in areas of dike concentration. These samples show no evidence for isotopic modification consistent with alteration by the isotopically primitive Hohonu Dike Swarm. The only evidence of mafic dike intrusion chemically or mineralogically altering granitoid country rock is minor fenitization adjacent to rare phonolitic dikes (Ch.7). This is in contrast to alteration in Blackwater Granite ascribed to dike intrusion by Graham and White (1990). White (1994) later considered alteration of the Blackwater Granite to be due to migration of hydrothermal fluids along the Ohika Detachment Fault. All other scatter in Fig.6.13 is attributed to variable initial ratios in the plutons.

Depleted mantle model ages ($T_{DM}$) are considered to be more appropriate than model ages calculated relative to the Chondritic Uniform reservoir (CHUR, $T_{CH}$) due to evidence for the widespread existence of LREE depleted reservoirs contributing to the generation of continental crust (Goldstein *et al* 1984, Liew and M$^c$Culloch 1985, Pickett and Wasserburg 1989). This is confirmed by several samples giving unrealistically small or even negative $T_{CH}$ values (Table 6.4b). $T_{DM}$ ages in this study are calculated based on mantle depletion beginning at 4.5 Ga (e.g. Maas and McCulloch 1991 *cf* Liew and M$^c$Culloch 1985) and are presented in Table 6.4b. This method of calculation results in $T_{DM}$ ages about 0.2 Ga older than those calculated using the method of DePaolo (1981b)[6] (Goldstein *et al* 1984). Consequently, all data from other sources have been recalculated to be consistent with the new data presented here. $T_{DM}$ for the Hohonu Super-suite range between 0.9 to 1.5 Ga and cluster around

---

6: For example, $T_{DM}$ ages for the Separation Point Suite (Muir *et al* 1995) calculated using the method of DePaolo (1981b) are $\approx$500 Ma, yet shift to $\approx$700 Ma using the method of calculation of this study.

1.2 Ga. Te Kinga Monzogranite has somewhat lower $T_{DM}$ at about 1.0 Ga, and the Deutgam Granite is more variable with $T_{DM}$ ranging from 0.9 Ga to 1.5 Ga, the megacrystic samples giving consistently older model ages. $T_{DM}$ increases with increasing Sm/Nd, reflecting the strong dependence on calculated $^{147}Sm/^{144}Nd$.

$T_{DM}$ ages are difficult to interpret (Arndt and Goldstein 1987). If the granitoids are considered to be entirely crustal derived then the $T_{DM}$ ages represent the time since the source was originally derived from the mantle. However, if granitoids represent mixing between crustal and mantle components then the model ages can only give a minimum age for the ultimate mantle derivation of the crustal source, and represent an intermediate age between that of the mantle and crustal end members.

**6.2.4.2: Radiogenic outliers.**

Discussion is now made of several analyzed samples which have radiogenic isotope compositions distinct from other samples of the same unit.

A single sample (32RO) of Pickett and Wasserburg (1989) was described as belonging to Te Kinga Monzogranite and collected from a location very similar to RRS8 of this study. 32RO is distinctly more radiogenic than other analyzed samples of Te Kinga Monzogranite, and also the Hohonu Super-suite in general (Fig.6.13b). Analyses of Te Kinga Monzogranite in this study are well constrained, therefore this sample is not considered to represent major isotopic heterogeneity in Te Kinga Monzogranite, especially as RRS8 was collected from the same locality. Other data of Pickett and Wasserburg (1989) compare well with analyses of this and other studies, therefore this discrepancy is also unlikely to be result from inter-laboratory variation. 32RO is consequently not considered representative of the Te Kinga Monzogranite and may represent a labelling error by Pickett and Wasserburg, as it has compositions similar to those of the Granite Hill Complex (see Table 8.1). This sample is not regarded further.

IQ1 (Inchbonnie Quarry) was only tentatively included within the Deutgam Granite in Ch.3.6.2.8, and may represent a discrete magmatic event. $Sr_{(110)}$ values are similar to those of other Deutgam Granite samples, and IQ1 falls on the whole rock

Rb/Sr errorchron for this pluton (Fig.5.2). This sample has somewhat higher $\epsilon Nd_{(110)}$ than other Deutgam Granite samples, although it is within error of most samples, and can be confidently correlated with the Deutgam Granite on isotopic grounds.

UCC8 (Turiwhate Granodiorite) was collected within 20 metres of an intrusive contact with Greenland Group and the higher $Sr_{(110)}$ and similar $\epsilon Nd_{(110)}$ of this sample are consistent with contamination by the highly radiogenic Greenland Group. A similar situation exists for KST4 (Uncle Bay Tonalite). This sample is much more radiogenic than other Uncle Bay Tonalite samples, and was collected from outcrops containing numerous metasedimentary enclaves and large metasedimentary sheets, and is likely to be contaminated.

TFQ10 is a sample from large, sillimanite-bearing, metasedimentary sheet within Deutgam Granite on State Highway 73. Its isotopic composition is similar to analyses of Greenland Group (Fig.6.13a, see also Ch.2.2.4) and is very similar to 33RO of Pickett and Wasserburg (1989). This sheet is interpreted as a large raft of Greenland Group included within Deutgam Granite. The incorporation and assimilation of blocks of metasediment, such as TFQ10, is abundant in many plutons of this study, indicating isotopic contamination by Greenland Group may be a likely control on isotopic compositions.

**6.2.4.3: Oxygen isotopes.**

Several whole rock samples of the Hohonu Super-suite were analyzed for oxygen isotopes as part of a reconnaissance study (Table 6.5). Deutgam Suite has generally low $\delta^{18}O$ values ($\approx +8‰$) compared to the Te Kinga Suite, with $\delta^{18}O$ $\approx +10‰$, although scatter occurs in the limited data available. Four samples of Deutgam Granite from two locations vary from +7.7 to +10.5‰. The higher values are from Fitzgerald's Quarry (TFQ1, RNZ67) and may reflect the incorporation of metasediment into these rocks as indicated by field evidence, although this is not reflected in the radiogenic isotope data. The lower values of HRS12 and HRS13 are considered more representative of Deutgam Granite. A similar situation exists for sample TTC1, collected within 1500 m of the other Turiwhate Granodiorite sample, TGC1. No evidence for metasedimentary contamination occurs in the field or in the

radiogenic isotope data of TTC1 and a sample labelling error may have occurred, as discussed below. The remaining Deutgam Suite samples have $\delta^{18}O$ close to +8‰, typical of granitoids which have had minor involvement with crustal material (Taylor 1988). Oxygen isotope compositions of the Deutgam Suite are also typical of I-type granitoids in the Lachlan Fold Belt ($\delta^{18}O$ < +10‰ O'Neil and Chappell 1977, O'Neil *et al* 1977, Chappell and White 1992).

The Te Kinga Suite has $\delta^{18}O$ close to the +10‰ value considered to distinguish I- and S-type granitoids in the Lachlan Fold Belt (O'Neil and Chappell 1977, O'Neil *et al* 1977, Chappell and White 1992). A single sample of the Te Kinga Suite (IKD1) has $\delta^{18}O$ more typical of the Deutgam Suite, much lower than the otherwise well constrained Te Kinga Suite. This may be the result of interaction with meteoric water in a hydrothermal system (there are quartz veins exposed near to the sampling location). However, swapping the $\delta^{18}O$ data of IKD1 and TTC1, greatly improves the data set and suggests a sample labelling error may have occurred. Both samples are being re-analyzed at the time of writing. Oxygen isotopes are discussed further in Ch.6.5.3.3.

## 6.2.5: Regional correlation: a comparison of the Hohonu Super-suite, Rahu Suite, and Separation Point Suite.

Tulloch (1988a) subdivided Cretaceous granitoids of Westland into the Separation Point Suite and the Rahu Suite (Fig.1.3), the characteristics of which are summarized in Table 6.6. The granitoids of the Hohonu Batholith were included within the intermediate I/S-type Rahu Suite by Tulloch (1988a). Selected geochemical plots comparing the Hohonu Super-suite with the Separation Point Suite (data from Muir *et al* 1995) and the Rahu Suite[7] are presented in Fig.6.14. The distinctive chemistry of the Separation Point Suite is immediately obvious, notably elevated Sr, $Al_2O_3$, $Na_2O$ and $Na_2O/K_2O$ and low $Fe_2O_3$, Ni and Cr, although all 3 suites tend to overlap at high $SiO_2$ contents. The Rahu Suite and Hohonu Super-suite exhibit generally similar trends, suggesting similar sources and mechanisms of formation, and affiliation of the two suites. The Hohonu Super-suite extends to lower $SiO_2$ contents than the generally

7: Data for the Rahu Suite compiled from White (1987) (the Paparoa Batholith) with additional data for the Buckland Granite from Muir (unpublished data 1994), and Tulloch (1979a) (the Victoria Range).

highly evolved Rahu Suite plutons, a consequence of the more mafic compositions of the Deutgam Suite. The Hohonu Super-suite has $Sr_{(110)}$ overlapping and extending beyond the 0.706 to 0.707 range defined for the Rahu Suite by Tulloch (1988a). However, measured ratios of this study are encompassed within the somewhat wider range for the Rahu Suite of 0.705 to 0.7085 defined by Tulloch and Brathwaite (1986). $\epsilon Nd_{(110)}$ data for the Rahu Suite are only available for the Buckland Granite (Muir unpublished data 1994) which has isotopic compositions identical to the Te Kinga Monzogranite (see Table 6.4 and Fig.6.13). Limited geochronological data also suggest a similar age range for the Rahu Suite and the Hohonu Super-suite (Ch.5).

The recognition of more mafic compositions and distinctly I-type granitoids within the Deutgam Suite, as compared to the I/S-type classification of the Rahu Suite (Tulloch 1988a), and the more comprehensive geochemical and isotopic data base for the Hohonu Super-suite indicate retention of the term Hohonu Super-suite is appropriate for the Hohonu Batholith plutons, in preference to inclusion within the Rahu Suite. The term Rahu Suite is retained for the Paparoa Batholith and Victoria Range plutons, and is here considered to represent a third suite within the Hohonu Super-suite. By inference the Rahu Suite plutons of the Buller Gorge and Victoria Range are considered to represent similar petrogenetic processes, affecting similar sources in similar tectonic environments, to those which formed the Hohonu Super-suite.

## 6.3: The Deutgam Suite: geochemical discussion.

### 6.3.1: Major and trace elements.

Petrographic studies indicate that the Deutgam Suite is characterized by decreasing modal plagioclase, biotite, amphibole, opaques, and titanite with increasing $SiO_2$, and these phases could be important in controlling geochemical compositions via crystal fractionation processes. Removal of accessory minerals such as apatite, zircon and allanite may also play important roles in constraining trace element compositions (e.g. Fourcade and Allegre 1981, Noyles *et al* 1983, Gromet and Silver 1983).

Major and trace element geochemistry suggest an evolutionary sequence through the Deutgam Suite, from the more mafic Uncle Bay Tonalite and Deutgam Granite to

THE LIBRARY
UNIVERSITY OF CANTERBURY
CHRISTCHURCH N.Z.

the more evolved Pah Point Granite, controlled largely by amphibole and plagioclase, with alkali feldspar playing a role at more evolved compositions.

Troughs on spider-diagrams at Ti, P, Nb-Ta, Sr, Ba and Rb increase with $SiO_2$ content (Fig.6.11) suggesting fractionation of Fe-Ti oxides, apatite, feldspar and a Rb-bearing phase (alkali feldspar, biotite and/or amphibole). Depletions of Nb-Ta and Ti are present at even the most mafic compositions, suggesting these depletions are inherited from source (as discussed in Ch.6.2.2). Only minor depletions of P, Rb, Ba and Sr remain at low silica compositions, suggesting they are largely the result of fractionation or source retention of apatite (P), plagioclase (Ba, Sr) and biotite or hornblende (Rb, Ba). The large Ba trough of Turiwhate Granodiorite, even at lower $SiO_2$ contents, distinguishes it from the other plutons of the Deutgam Suite.

Plots of Na/K, Rb/Sr, Ca/Sr and K/Sr against $SiO_2$ (Fig.6.15, 6.16, 6.17, 6.18) are suggestive of plagioclase removal during evolution of the Deutgam Suite. Ca/Sr, K/Sr and Rb/Sr show inflections at around 70% $SiO_2$ (Pah Point Granite and evolved Deutgam Granite) and reflect the onset of fractionation of alkali feldspar and consequent removal of additional Sr in these phases.

K/Ba increases from intermediate to felsic compositions (Fig.6.19) and probably signifies combined removal of amphibole and alkali feldspar. Lower Ba contents in the Turiwhate Granodiorite, as exhibited in spider-diagrams, are also reflected in higher K/Ba ratios.

$Fe_2O_3$/MgO increases with $SiO_2$ content, particularly above 70% $SiO_2$ (Fig.6.20), indicating removal of a Mg-bearing phase such as amphibole or biotite. Higher MgO contents in the Turiwhate Granodiorite are reflected in lower $Fe_2O_3$/MgO ratios.

### 6.3.2: Fractionation modelling using trace and REE elements.

Log-log trace element diagrams have been used to establish which phases have dominated crystal fractionation processes in igneous systems (e.g. Brown *et al* 1981b, Atherton and Sanderson 1985, Ayusho and Arth 1992). Trace element diagrams, with

fractionation trends for various minerals assuming Rayleigh fractional crystallization and batch melting (as described by Hanson 1978), are presented in Fig.6.22 to Fig.6.35. Given the inherent generalizations generated by the need to choose from widely variable partition coefficients, the fractionation vectors calculated are purely qualitative and little emphasis is placed upon the absolute values depicted. The overall similarity of vectors produced by Rayleigh fractionation and batch melting indicate both processes could potentially produce the geochemical variation of the Deutgam Suite. The large amount of data ($\approx$ 50 analyses) from the Deutgam Granite exhibit trends identical to those displayed throughout the entire Deutgam Suite, suggesting processes within single plutons reflect those within the suite as a whole.

Increasingly negative Rb, Ba and Sr depletions on spider-diagrams (Fig.6.11) and decreasing Ca/Sr with increasing $SiO_2$ (Fig.6.17) are indicative of plagioclase and alkali feldspar fractionation during evolution of the Hohonu Super-suite. In addition, plots involving Ca, Sr and Ba (Fig.6.21, Fig.6.22) also indicate plagioclase and alkali feldspar fractionation. However, other evidence indicates additional phases must be involved. Eu anomalies do not increase systematically with decreasing Sr, Ba and Eu, as would be expected if plagioclase and/or alkali feldspar were the only fractionating phases (Fig.6.23, Fig.6.24, Fig.6.25). Partition coefficients of $\approx$2 for Eu in plagioclase and alkali feldspar (Rollinson 1993) indicate feldspar fractionation will lead to Eu depletion and larger Eu anomalies. In contrast, Eu remains relatively constant with increasing Eu anomalies (Fig.6.25). Increasingly negative Eu anomalies are coupled with increasing middle REE (MREE e.g. Sm, Fig.6.26) indicating that a MREE-bearing phase is controlling Eu anomalies.

Fractionation trends on log-log plots of Sr and Ba against Eu (Fig.6.27, Fig.6.28) are also inconsistent with plagioclase being the sole fractionating phase and instead indicate dual control by plagioclase and amphibole. Plots of Ti, Y and Rb against Zr (Fig.6.29, Fig.6.30, Fig.6.31) and Sr versus Rb (Fig.6.32) also indicate both plagioclase and amphibole were involved during evolution of the Deutgam Suite, as do plots of MREE (Gd) and HREE (Y) against Eu (Fig.6.33, Fig.6.34). The quantitative importance of each phase is unknown, although the log-log plots suggest that amphibole is more important than plagioclase, and most plots indicate

approximately 20% combined fractionation of plagioclase and amphibole. Several plots (e.g Fig.6.28, Fig.6.30, Fig.6.32) suggest alkali feldspar and biotite were also minor fractionating phases, particularly at higher $SiO_2$ contents. Given the similarity in calculated fractionation vectors for Rayleigh fractionation and batch melting either process could explain the trace element variations observed in the Deutgam Suite.

Accessory phases such as apatite, zircon, allanite and titanite are important reservoirs for REE and some trace elements in granitoid rocks (e.g. Mittlefehldt and Miller 1983, Gromet and Silver 1983, Evans and Hanson 1993), and fractionation of accessory phases may play a large role in constraining REE patterns (for example see the low totals for allanite analyses discussed in Ch.4.4). The relatively tightly constrained cluster of Ce and Y for the majority of samples of the Deutgam Suite is consistent with the observed similarity in REE patterns, and shows little evidence for major fractionation of accessory phases (Fig.6.35). Observed scatter in REE plots is likely to be the result of sample variations in the abundance of accessory minerals, probably largely a consequence of sample size, rather than any fractionation processes.

### 6.3.3: Rare Earth Elements.

REE plots of the Deutgam Suite are typically LREE enriched, slightly concave down with flat HREE (Fig.6.12). The presence of negative Eu anomalies indicate the involvement of plagioclase as a fractionating or residual phase, although trace element data presented above indicate that increasing negative Eu anomalies are controlled more by a MREE-bearing mineral. Flat HREE contents indicate that garnet was not stable in the source region of the Deutgam Suite, in contrast to the Te Kinga Suite.

Trace element diagrams (e.g. Fig.6.29, Fig.6.30, Fig.6.32) suggest approximately 20% combined removal of amphibole and plagioclase can explain much of the trace element variation within the Deutgam Suite. However, virtually identical REE patterns throughout the Deutgam Suite are inconsistent with such degrees of fractionation. In particular there is no obvious reduction in MREE and HREE generally considered typical of amphibole removal. Melting or fractionation of the amounts of plagioclase implied by trace element data result in only small changes in REE content (Fig.6.36), consistent with the minor REE variations observed in the Deutgam Suite.

However, even small degrees of amphibole removal results in reductions in M+HREE (Fig.6.36) greater than those observed in the Deutgam Suite, a consequence of high partition coefficients for MREE and HREE in amphibole at dacitic to rhyolitic compositions[8]. The variation in REE is less extreme using the batch melting model (Fig.6.36), but reductions in MREE and HREE remain irreconcilable with the amounts of fractionation implied by trace element data.

REE partition coefficients for amphibole vary widely as a function of composition, reducing to near 1 in basaltic-andesite to andesitic compositions, compared with 3-6 and higher in dacitic to rhyolitic compositions (Rollinson 1993). Reducing REE partition coefficients in amphibole to values more appropriate for basaltic-andesite to andesite compositions would improve the correlation between calculated REE contents and observed patterns in the Deutgam Suite. Considering that the parent magmas of the Deutgam Suite may well have been more mafic than the rocks currently exposed, such partition coefficients may be more appropriate. Varying $SiO_2$ content does not appear to have a large affect on partition coefficients for plagioclase.

#### 6.3.3.1: REE of the Deutgam Granite.

Analyses of several samples of Deutgam Granite were made to clarify the processes controlling the evolution of this large and complex pluton (Fig.6.37). Deutgam Granite exhibits decreasing REE contents with increasing $SiO_2$, the dominant megacrystic biotite Deutgam Granite (RNZ67, TFQ1, HRS12) being well constrained and exhibiting typical Deutgam Suite REE plots (see Fig.6.12). Scatter among LREE in these samples may represent the influence of varying quantities of titanite and/or allanite as discussed above. Interestingly, HWC4, a relatively high $SiO_2$ sample, has REE plots virtually identical to typical more mafic Deutgam, possibly a consequence of REE concentration in the abundant allanite (1 modal percent) present in this sample.

---

8: Amphibole is generally considered to preferentially take up the middle and heavy REE (Hanson 1978, 1980, Gromet and Silver 1983). However, partition coefficients for amphibole are highly variable, for example Sawka (1988) describes amphibole which prefers all REE, but prefers LREE over the MREE and HREE.

The most mafic sample of Deutgam Granite analyzed (IQ1, Inchbonnie Tonalite, 58% $SiO_2$) is relatively enriched in MREE, and to a lesser degree HREE. Inchbonnie Tonalite is characterized petrographically by relatively abundant titanite (1 modal percent). As titanite has a preference for all REE but preferentially retains MREE over HREE over LREE (Gromet and Silver 1983, Green and Pearson 1983), accumulation of this mineral could explain the observed REE patterns of the Inchbonnie Tonalite.

A sample of evolved equigranular Deutgam Granite (HMF7, $SiO_2$ = 73.4%) exhibits an overall depletion of REE, consistent with removal of ≈20% sub-equal quantities of amphibole and plagioclase (Fig.6.38). Such amounts of fractionation are also consistent with trace element fractionation diagrams. As indicated in Fig.6.38, fractionation of more amphibole than plagioclase results in too great a depletion of HREE, and removal of larger quantities of plagioclase than amphibole results in an increasing Eu anomaly, not observed in this sample. Removal of a LREE-enriched phase, such as allanite or apatite, is also required to produce LREE depletion displayed by HMF7. The high $SiO_2$ content of this sample indicates that dacitic to rhyolitic partition coefficients (Table 6.7) are appropriate, and the removal of amphibole and plagioclase represents a high level crystal fractionation process rather than a source level melting event. Although HMF7 and evolved Deutgam Suite plutons such as Pah Point Granite have similar $SiO_2$ contents their REE patterns are markedly different (Fig.6.12). This suggests that the basic REE patterns of the Deutgam Suite are controlled by lower partition coefficients during melting events at source, whereas consequent higher level crystal fractionation at higher $SiO_2$ (and partition coefficients more appropriate to these compositions) creates most of the intra-pluton variations.

Two aplite dikes from Deutgam Granite were also analyzed: HRS17 (76.6% $SiO_2$) and TFQ5 (74.8% $SiO_2$). Both display low ΣREE and a distinct depletion of MREE (Fig.6.37), consistent with fractionation of amphibole and plagioclase. Aplites may be derived from either highly fractionated $SiO_2$-rich melts or from residual aqueous fluids, and each process should supposedly be easily distinguishable using REE (Hanson 1980). Aqueous fluids are characterized by low REE abundances, due to low water-melt partition coefficients for REE, and resulting aplites should also have low ΣREE. In contrast, Hanson (1980) suggests feldspar fractionation should result in

aplites with high ΣREE. As ΣREE decreases with fractionation in Deutgam Granite, derivation of these aplites from either residual aqueous fluids or as the end product of extreme fractionation is feasible. The positive Eu anomaly of TFQ5 indicates some feldspar accumulation has occurred in this sample.

REE plots of the Uncle Bay Tonalite also show some scatter, with similarly decreasing ΣREE with increasing $SiO_2$ (Fig.6.39). An exception to this trend is KNB8, which shows enrichment of all REE, particularly LREE compared with other samples with similar $SiO_2$ contents. This may be related to the presence of modal tourmaline and abundant allanite.

### 6.3.4: Special Case: Turiwhate Granodiorite.

Turiwhate Granodiorite is distinguished from other Deutgam Suite plutons by higher contents of MgO, Cr, Ni and V, lower Ba and HREE (see Fig.6.9 and 6.10), and petrographically abundant amphibole and titanite. These features suggest that the Turiwhate Granodiorite has a petrogenetic history distinct from the remainder of the Hohonu Super-suite. The overall isotopic composition, I-type characteristics and similar REE contents of this pluton suggest close affinities with the Deutgam Suite, and it may represent a separate suite or sub-suite within the Hohonu Super-suite. Explanation of the geochemical differences exhibited by the Turiwhate Granodiorite is difficult. Although accumulation of amphibole, or less retention of amphibole at source, is consistent with the observed elevated MgO, Cr, Ni and V contents and the petrographic abundance of this mineral, it is inconsistent with the observed lower HREE contents. Increased activity of amphibole should result in an increase in MREE and HREE contents, at odds with the lower HREE of Turiwhate Granodiorite. Slightly less radiogenic compositions of the Turiwhate Granodiorite suggest a chemically and isotopically distinct source is likely, although this source is broadly similar to that for other Deutgam Suite granitoids. Lower HREE contents could reflect differing source compositions, or lower partition coefficients for REE at the differing compositions.

### 6.3.5: Mafic rocks associated with the Deutgam Suite.

The Eastern Hohonu River Gabbro (Ch.3.12.1) and the Rose Creek Diorite (Ch.3.12.3) are poorly exposed mafic rocks which occur in association with the

Deutgam Granite and Turiwhate Granodiorite respectively. Spider-diagrams of the Eastern Hohonu River Gabbro are compared with mafic enclaves from the Deutgam Granite and representative low-$SiO_2$ compositions of the Deutgam Granite in Fig.6.40. The two gabbroic samples have variable chemistry, a consequence of their cumulative nature, as indicated by field evidence (see Ch.3.12.1). Low LREE, $P_2O_5$, Y and Zr distinguish EHR8 from EHR29 and may indicate fractionation/cumulation of accessory phases such as apatite and zircon. Relatively high LREE and $P_2O_5$ in EHR29 are consistent with the presence of abundant modal apatite (Fig.6.40, see also Fig.3.47), apatite was not observed in EHR8. High Sr, and a positive Eu anomaly (Fig.6.41), in EHR8 suggest plagioclase accumulation. Elevated $TiO_2$ in EHR8 may also indicate accumulation of Fe-Ti oxides, consistent with their modal abundance in this sample (11.2 modal percent). Field evidence indicates the Eastern Hohonu River Gabbro was incorporated into the Deutgam Granite as cool brittle blocks, and therefore there is no suggestion of a genetic relationship between the two units. Limited geochemical data also give no definitive evidence for any petrogenetic relationship between the Eastern Hohonu River Gabbro and the Deutgam Granite or its mafic enclaves. In contrast, the Rose Creek Diorite displays geochemical evidence for affinities with the Turiwhate Granodiorite. Although no contacts were observed between Rose Creek Diorite and Turiwhate Granodiorite, the diorite occurs as a limited body between Turiwhate Granodiorite and Greenland Group. Rose Creek Diorite has a mantle-normalized chemistry similar to the neighbouring Turiwhate Granodiorite and mafic enclaves common within Turiwhate Granodiorite (Fig.6.42). The Rose Creek Diorite may therefore represent a mafic phase of Turiwhate Granodiorite, portions of which have been incorporated within the main granodiorite phase as mafic enclaves. In the absence of quantitative age and isotopic data it is impossible to establish any definite petrogenetic relationships between the Eastern Hohonu River Gabbro, Rose Creek Diorite and the Deutgam Suite.

### 6.3.6: Summary: Deutgam Suite.

Agreement between observed trace element and REE variations in the Deutgam Suite is most easily accomplished via the batch melting model and partition coefficients typical of intermediate to mafic compositions. Several factors, including the decreasing modal abundance of amphibole and plagioclase with increasing $SiO_2$, trace element

evidence for fractionation of alkali feldspar at higher $SiO_2$ contents, and evidence for control of REE compositions both at source and during later fractionation (Ch.6.3.3.1), indicate that processes during source melting and crystal fractionation have combined to produce the geochemical variation of the Deutgam Suite.

## 6.4: The Te Kinga Suite: Geochemical discussion.

### 6.4.1: Introduction.

The restricted petrographic and geochemical variation, and the elevated $SiO_2$ contents, of the Te Kinga Suite make elucidation of a fractionation history difficult. Petrographic studies indicate that biotite, muscovite and feldspar are most likely to be the major phases involved in any crystal fractionation process. However, little modal variation is observed and given the evolved compositions of the suite it is impossible to observe phases which have been removed during fractionation. Apatite and zircon may also act as important accessory phase. The presence of titanite in a single specimen of Arahura Granite and rare allanite in both the Te Kinga Monzogranite and Arahura Granite may be important in controlling some of the original REE patterns, but will have had little effect on evolution of major element compositions within the suite. No major geochemical differences are observed between the textural varieties of either the Te Kinga Monzogranite or the Arahura Granite.

### 6.4.2: Major and trace elements.

Higher Sr, Ba, $Al_2O_3$ and $Na_2O$ and lower $K_2O$ contents distinguish Te Kinga Suite from similarly evolved Deutgam Suite granitoids and preclude derivation by simple feldspar fractionation from the Deutgam Suite. Despite the high $SiO_2$ contents of the Te Kinga Suite granitoids, the absence of large negative Sr, Ba and Rb anomalies on spider-diagrams (Fig.6.11) and the lack of substantial negative Eu anomalies (Fig.6.12) also discount major feldspar fractionation. Relatively low Y contents in the Te Kinga Suite correlate with low HREE concentrations and are considered to be a consequence of retention of residual garnet during partial melting.

As noted above (Ch.6.1.1.), the Te Kinga Monzogranite and Arahura Granite do not display identical trends for several elements. Te Kinga Monzogranite has relatively low $TiO_2$, MgO, V and Rb and relatively high $Al_2O_3$, $Na_2O$, Ba and Sr

compared with Arahura Granite. These differences suggest the retention or removal of more plagioclase and less amphibole in the Te Kinga Monzogranite. Distinct isotopic compositions (Fig.6.13), although still within the general range of the Hohonu Super-suite, indicate that the Arahura Granite and Te Kinga Monzogranite can also not be related by fractionation of a single magma. Nevertheless, the overall similarity of the two plutons, particularly compared to the Deutgam Suite, indicate similar processes operated during their genesis, and discussion as a distinct suite is still considered justifiable.

Although spider-diagrams preclude large amounts of feldspar fractionation within the Te Kinga Suite, several plots indicate that minor feldspar fractionation did occur. $Na_2O$-$K_2O$ ratios decrease with increasing $SiO_2$ (Fig.6.43) and indicate minor feldspar fractionation. $Na_2O/K_2O$ values are generally higher and more variable than the Deutgam Suite, reflecting higher $Na_2O$ and lower $K_2O$ contents in the Te Kinga Suite (Fig.6.43). Increasing Rb/Sr with increasing $SiO_2$ is also consistent with feldspar removal (Fig.6.44). Rb/Sr ratios are lower than the Deutgam Suite and reflect higher Sr contents in the Te Kinga Suite (Fig.6.44 and Fig.6.10), for similar reasons Rb-Sr ratios are also distinct between the two plutons of the Te Kinga Suite. Increasing CaO with increasing Sr (Fig.6.45), and trends of Ca/Sr against increasing $SiO_2$ (Fig.6.46), also suggest feldspar fractionation. Ca/Sr increases slightly in the Te Kinga Monzogranite, possibly a consequence of minor alkali feldspar fractionation whereas Ca/Sr decreases initially in the Arahura Granite then flattens with increasing $SiO_2$, suggesting plagioclase fractionation following by combined alkali feldspar and plagioclase fractionation (Fig.6.46).

$Fe_2O_3$-MgO ratios increase with $SiO_2$, and are somewhat higher and more scattered in Te Kinga Monzogranite than Arahura Granite (Fig.6.47). Biotite is the only modal mineral able to fractionate MgO, although increasing amounts of amphibole retention at source could also increase $Fe_2O_3$-MgO ratios. K/Ba increases with $SiO_2$ (Fig.6.48), also suggesting small amounts of biotite fractionation, or retention of amphibole at source. K/Ba values are distinctly different in the two plutons of the Te Kinga Suite and are lower than the Deutgam Suite, reflecting lower $K_2O$ and higher Ba contents in the Te Kinga Suite.

Log-log trace element plots for the Te Kinga Suite are presented in Fig.6.49 to Fig.6.53 with Rayleigh fractionation and batch melting vectors calculated as described in Ch.6.3.2. For most trace elements (except Y) garnet produces fractionation trends similar to, but less extreme than amphibole. The slightly different chemical characteristics of the Te Kinga Monzogranite and Arahura Granite are indicated in many of the trace element plots. Decreasing Ti with decreasing Zr (Fig.6.49) is suggestive of feldspar fractionation and/or amphibole retention. Zr and $TiO_2$ decrease with increasing $SiO_2$ in both the Te Kinga Monzogranite and Arahura Granite (Fig.6.9 & 6.10), indicating amphibole retention is a more likely cause, as feldspar fractionation alone will result in an increase in the concentrations of these elements. No evidence for major biotite fractionation is present.

Sr generally decreases with increasing Rb, consistent with plagioclase fractionation (Fig.6.50). Amphibole retention is also indicated by a smaller decrease in Sr than would be expected by plagioclase fractionation alone. The trends of decreasing Sr and increasing Rb with increasing $SiO_2$ are incompatible with variation of Rb and Sr caused by biotite fractionation (Fig.6.10). Alkali feldspar fractionation may have occurred in a few Te Kinga Monzogranite samples but otherwise appears minor. Log-log plots of Rb against Zr (Fig.6.51) and Y against Zr (Fig.6.52) are also consistent with geochemical control by both hornblende and plagioclase.

A plot of Ce versus Y illustrates a relatively tightly constrained cluster for the Te Kinga Suite, although values are somewhat lower in the Te Kinga Monzogranite (Fig.6.53). The lack of variation indicates little if any fractionation of accessory phases. Increasing the amount of garnet retained at source would cause significant reductions in Y contents, with only small changes in Zr and Ce. Relatively consistent Y contents therefore suggest constant amounts of residual garnet at source.

### 6.4.3: Rare earth elements.

One of the most important distinctions between the Te Kinga Suite and the Deutgam Suite are the HREE-depleted chondrite normalized plots of the Te Kinga Suite (Fig.6.12). The absence of large negative Eu anomalies also contrasts with the Deutgam Suite and invalidates major feldspar retention at source or later feldspar

fractionation. Garnet has high partition coefficients for HREE (Hanson 1978, 1980, Wilson 1989, Rollinson 1993) and retention of garnet as a residual phase during partial melting is commonly attributed to the formation of HREE depletions such as those observed in the Te Kinga Suite (e.g. Gromet and Silver 1987, Norman *et al* 1992, Muir *et al* 1995). Trace element diagrams presented above are also consistent with retention of amphibole at source during generation of the Te Kinga Suite. Low partition coefficients for Sr and Ba in garnet may also contribute to the high abundances of these elements in the Te Kinga Suite.

### 6.4.4: Summary: Te Kinga Suite.

Calculated fractionation vectors on log-log trace element plots for the Te Kinga Suite are less informative than for the Deutgam Suite, largely a consequence of restricted, high $SiO_2$ contents. Some minor feldspar fractionation is indicated by increasing Rb/Sr and decreasing $Na_2O/K_2O$, however, as stated above, the lack of negative Sr, Ba and Eu anomalies indicate the Te Kinga Suite cannot be derived from the Deutgam Suite by feldspar fractionation. Evidence for retention of varying degrees of amphibole at source is also indicated by increasing $Fe_2O_3/MgO$ and plots of $TiO_2$, Rb and Y against Zr. Garnet retention at source is necessary to produce the observed REE patterns of the Te Kinga Suite. Although varying amounts of residual amphibole are implied by trace element diagrams, no evidence is present for varying amounts of residual garnet.

## 6.5: The Hohonu Super-suite: Petrogenesis and discussion.

### 6.5.1: Introduction.

Petrogenetic interpretation of the Hohonu Super-suite must explain the fundamental differences between the Te Kinga and Deutgam Suites, including;

- differing HREE contents,
- contrasting $Al_2O_3$, $Na_2O$, Sr, Ba and Eu contents,
- the felsic, non-fractionated, peraluminous nature of the Te Kinga Suite compared with the more mafic, yet more fractionated and metaluminous compositions of the Deutgam Suite.

Petrogenetic interpretation must also explain these differences within the constraints of similar radiogenic isotope signatures and comparable general geochemistry of the two suites.

**6.5.2: Source compositions.**

*"Granitoids image their sources, but these sources are ill-defined and do not correspond to simple, easily-recognized materials"*

Miller *et al* (1988) p135.

Granitoid chemistry is controlled by two main factors; source characteristics, and processes which affect this source and the resulting melts. The relatively restricted radiogenic isotopic compositions, similar slopes and troughs on spider diagrams and largely parallel trends on Harker diagrams prohibit radically different source rocks for the constituent plutons of the Hohonu Super-suite. Radiogenic isotopic data constrain the source for both the Te Kinga Suite and the Deutgam Suite to having $Sr_{(110)}$ = 0.7062-0.7085, $\epsilon Nd_{(110)}$ = -4.4 to -6.1 and $T_{DM} \approx 1.2$ Ga (Table 6.4). Inter-pluton isotopic variation within the Hohonu Super-suite suggests the source may be heterogeneous on a small scale, with different plutons having tapped slightly different compositions. Similarly, somewhat variable $T_{DM}$ ages are suggestive of heterogeneous source characteristics. Trace element data indicating the presence of residual plagioclase, amphibole and garnet, and the overall I-type character of the super-suite, suggest a metaluminous source of broadly meta-basaltic composition. An attempt to identify the source characteristics of the Hohonu Super-suite is now made.

Metaluminous to weakly peraluminous compositions, coupled with much less radiogenic compositions, of the Hohonu Super-suite are incompatible with derivation directly from the peraluminous, highly radiogenic Ordovician Greenland Group. Isotopic ratios are also inconsistent with derivation of the Hohonu Super-suite directly from typical depleted mantle-derived magmas, and instead indicate the involvement of relatively mature continental crust.

**6.5.2.1: What constitutes the Buller terrane mid-lower crustal?**

Geochemical evidence indicates that the Hohonu Super-suite was generated near the lower limits of plagioclase stability (i.e. $\approx$10 kb) equating to approximately 35 km depth and conditions generally considered to represent the base of typical continental crust. Accordingly, a lower crustal source component is required. In the absence of exposures of lower crustal rocks in the Buller terrane, extrapolation of upper crustal rocks from the Buller terrane and elsewhere is required to identify these possible lower crustal components. Given the complex igneous and tectonic history of the Western Province, and the Gondwana margin as a whole, the lower continental crust is unlikely to be a single, simple, easily characterized entity.

An important constraint in establishing lower crustal compositions of the Buller terrane is the use of $\epsilon$Nd values and depleted-mantle model ages ($T_{DM}$). Care must be taken in the interpretation of $T_{DM}$ ages (Arndt and Goldstein 1987) and in the case of granitoids formed from an unknown mixture of mantle and complex crustal materials, only a minimum average age of the crustal component is given. $T_{DM}$ ages for the Hohonu Super-suite cluster at $\approx$1.2 Ga, yet range from 0.9 to 1.5 Ga, and suggest a heterogeneous, yet not particularly old, crustal component. Additionally, $\epsilon Nd_{(110)}$ values with a maximum of $\approx$-6 give no indication of the involvement of a Rb-depleted, Archaean crustal component in the Hohonu Super-suite, as such a component would shift isotopic compositions towards low $Sr_{(t)}$ and much more negative $\epsilon Nd_{(t)}$ values (DePaolo and Wasserburg 1979).

Average Greenland Group was used as a crustal end-member in the mixing models of Pickett and Wasserburg (1989) (see Fig.6.56, also Fig.6.57 and 6.59) and as stated previously, Greenland Group alone is too radiogenic to represent an appropriate single source. However, assumptions that the entire crustal thickness of the Western Province is composed of Greenland Group compositions are probably much too simplistic. The turbiditic nature of the Greenland Group suggests it overlies pre-Ordovician oceanic crust, yet even this is probably too simplistic a model for Western Province crust.

Inheritance studies indicate a predominance of Cambrian (500-600 Ma) zircons in many Western Province granitoids, coupled with a smaller inherited peak at ≈1000 Ma (Muir *et al* 1994a+c). Devono-Carboniferous granitoids in south-eastern Australia have similar inheritance patterns (Williams *et al* 1992) and all reflect zircon age peaks in the Greenland Group and metamorphic equivalents (Ireland 1992), and equivalent sediments in Australia (Williams *et al* 1992). These inheritance peaks may simply reflect incorporation of upper crustal sediments, such as the Greenland Group, into the granitoids. Alternatively, these zircon inheritance patterns may be derived from lower crustal source rocks. The distinct Cambrian zircon population is unlikely to have been derived from oceanic crust which may underlie Greenland Group. These zircons may be inherited from lower crustal equivalents of Cambrian volcanic arcs, remnants of which are widespread throughout the Gondwana margin. Cambrian volcanics are preserved in the Takaka terrane as the Devil River Volcanics (Cooper and Tulloch 1992, Maclean 1994), with probable metamorphosed equivalents present in Western Fiordland (Gibson 1992). Probable correlatives also occur in south-eastern Australia as the Heathcote Greenstone Belt (Crawford and Cameron 1985), in Tasmania as the Mount Read Volcanics (Crawford *et al* 1992) and in Northern Victoria Land as the Glasgow Formation of the Bowers Supergroup (Weaver *et al* 1984). Nd and Sr isotopic data for some of the Victorian Cambrian volcanics are presented by Nelson *et al* (1984). Age correction of this data to 110 Ma result in a wide range of compositions with $\epsilon Nd_{(110)}$ between +4.8 to -13.0 and $Sr_{(110)}$ = 0.7055 to 0.7107. Although one sample of Nelson *et al* (1984), an andesite from Mount Dryden, has isotopic compositions similar to the Hohonu Super-suite, the majority of the Cambrian volcanics are too primitive to represent unique sources for the Hohonu Super-suite (Fig.6.54). The remaining samples are much more radiogenic than the Hohonu Super-suite. Although extrapolation of these rocks to beneath the Buller terrane is purely conjectural, isotopic data suggest the Cambrian volcanics could represent appropriate crustal sources for the Hohonu Super-suite if they are mixed with more radiogenic material such as the Greenland Group.

The Charleston Metamorphic Group, considered to be of mid-crustal origin, has been interpreted to represent metamorphosed equivalents of the Greenland Group and intrusive granitoids (Tulloch and Kimbrough 1989, Kimbrough and Tulloch 1989) and,

as such, is compositionally unsuitable as a source for the Hohonu Super-suite. Amphibolite-grade metamorphic rocks in the Fraser and Granite Hill Complexes (Ch.8) may also represent mid-crustal lithologies and indicate the likely complexity of the Western Province mid-lower crust. The Granite Hill and Fraser Complex gneisses appear to be distinct from the Charleston Metamorphic Group and may represent a slightly younger, more volcanogenic protolith, or may be related to similar rocks in Western Fiordland (Ch.8). Lower crustal equivalents of the garnet-plagioclase-amphibole gneisses of the Granite Hill and Fraser Complexes may offer appropriate source compositions for metaluminous I-type melts such as the Deutgam Suite. In support of this, migmatitic rocks within the Fraser and Granite Hill Complex indicate metamorphic gradients peaked above solidus conditions, with one such migmatite yielding a single 115 $\pm$ 6 Ma metamorphic zircon (Ireland 1992). This age overlaps with those of both the Separation Point Suite and the Hohonu Super-suite and may be related to regional melting events during genesis of these suites. No isotopic data are available for these metabasites so their potential as crustal sources for any Western Province granitoid suite remains unresolved. Even if the metabasites are isotopically primitive, large amounts of melting of the Granite Hill Complex would be unlikely to produce isotopic or chemical compositions similar to those of the Hohonu Super-suite as metabasites are subordinate to highly radiogenic and peraluminous paragneisses and orthogneisses at the current levels of exposure. Relatively large areas of metabasite are exposed in the Mount Misery area in the Fraser Complex (Rattenbury 1987a) and, if greater quantities of metabasite occur at deeper crustal levels, these could potentially provide crustal sources for the Hohonu Super-suite.

Similar lower crustal end-members may also be represented by the amphibolite facies gneisses of Western Fiordland. Rocks of the western Fiordland block are generally considered to represent mid-crustal metamorphosed equivalents of the Western Province, particularly the Takaka terrane (e.g. Gibson 1992). These rocks have been exposed during Cretaceous crustal extension (Gibson *et al* 1988) and are now offset by the Alpine Fault. These rocks provide an important window to deeper crustal levels than those currently exposed in northwest Nelson. Further links to the Takaka terrane have been made by recent correlation of the granulite facies Western Fiordland Orthogneiss (WFO) (J.Y.Bradshaw 1989, Mattinson *et al* 1986) and the Separation

Point Batholith (Muir *et al* 1995). Predominantly mid-Palaeozoic (or older) WFO country rocks represent probable equivalents of the volcanic and sedimentary successions of the Takaka terrane (e.g. Cooper and Tulloch 1992) and include a complex variety of amphibolite-grade metabasites, metapelites, metapsammites, quartzites, quartzofeldspathic gneisses and marbles intruded by a series of granitoids and more mafic orthogneisses (see Bradshaw 1990 and Gibson 1982a+b for a more comprehensive review). Such rocks could potentially produce an extremely complex, heterogeneous crustal source for the Hohonu Super-suite, providing their presence beneath the Buller terrane can be established. Stitching of the Takaka and Buller terranes by 111 Ma with emplacement of the Mount Olympus Granite (Muir *et al* 1994a) indicates that the two terranes were adjacent during Hohonu Super-suite magma generation. Additionally, amphibolite-facies gneisses in the Fraser and Granite Hill Complexes bear some resemblance to Fiordland Gneisses (Ch.8) and may indicate the presence of Fiordland equivalents beneath the Buller terrane. Unfortunately, geochemical studies have concentrated on the WFO and few geochemical and isotopic data are available for the country rocks, or their equivalents in northwest Nelson. The WFO itself, and other mafic igneous rocks in Fiordland such as the Darren Complex, can be discounted as Hohonu Super-suite sources as they are isotopically much too primitive (McCulloch *et al* 1987). However, mixing between melts of these rocks and more radiogenic metasediments[9] cannot be discounted. Much more appealing are a series of mid-Palaeozoic granitoids intruding country rock and occurring as enclaves incorporated within the WFO (Bradshaw and Kimbrough 1991). Only limited Sr isotope data are available for these granitoids, but at 110 Ma, four such enclaves have $Sr_{(110)}$ of 0.7043-0.7084[10] (Bradshaw and Kimbrough 1991), overlapping the $Sr_{(110)}$ range observed in the Hohonu Super-suite. These granitoids, or their sources, may also represent potential sources for the Hohonu Super-suite, but given the current lack of data on WFO country rocks, it is difficult to clarify such suggestions.

---

**9:** For example, a migmatitic paragneiss sample which yields decay corrected initial ratios at 110 Ma of $^{87}Sr/^{86}Sr$ = 0.7132 and $\epsilon Nd$ = -9.3 (sample RPK2.26 of McCulloch *et al* 1987).

**10:** The two remaining samples are considerably more radiogenic, with $Sr_{(110)}$ = 0.7171 and 0.743, the latter ratio attributed to included xenoliths of migmatitic metasediment (Bradshaw and Kimbrough 1991).

Whatever its' make up, the lower continental crust of the Western Province has been affected by several mid-Palaeozoic and Mesozoic magmatic events prior to emplacement of the Hohonu Super-suite. These igneous events, and any mafic underplating associated with them, will have added material to, and changed the composition of, the lower crust of the Buller terrane and potentially produced crustal sources or end-members suitable for the genesis of the Hohonu Super-suite.

Irrefutable evidence that the Devonian Karamea Suite contributed to Buller terrane crust beneath the Hohonu Super-suite is represented by the Palaeozoic Summit Granite (Ch.6.7). Devono-Carboniferous equivalents to the Karamea Suite event are also widespread throughout the Gondwana margin, such as the Lachlan Fold Belt granitoids of Australia (e.g. Chappell and White 1992), the Ford Granodiorite of Marie Byrd Land (Weaver *et al* 1991) and the Admiralty intrusives of Northern Victoria Land (Borg *et al* 1987). Lower crustal Karamea Suite granitoids and their equivalents, their sources (either melt-depleted or pristine), and any mafic underplate developed during granitoid generation, will have contributed to the Hohonu Super-suite crustal source component, and also may have acted as higher level contaminants following magma generation. Age correction of Devono-Carboniferous granitoid isotopic data (Fig.6.55) indicate that the Karamea Suite and contemporaries are too radiogenic at 110 Ma to represent unique, primary sources for the Hohonu Super-suite, although some Australian I-type granitoids do approach Hohonu compositions. However, the presence of Devonian granitoids as a contaminant, or as a lower crustal component in any mantle-crustal mixing event, is highly probable.

Only recently recognized in the Western Province is a small area of poorly exposed Ferrar Supergroup equivalents near Reefton (Mortimer *et al* 1995). Age correction of the Kirwans Dolerite isotope ratios to 110 Ma (Fig.6.55) indicates it is also too radiogenic to represent a simple, unique source for the Hohonu Super-suite. Although widespread throughout continental Gondwana, this unit is of very limited occurrence in the Western Province (1 $km^2$) and is unlikely to be an important component in any granitoid source.

The Cretaceous in New Zealand (and along the Gondwana margin) was an extremely active period in terms of magmatic and tectonic activity, as discussed in more detail in the next section. Subduction, with associated accretion of exotic terranes (the Eastern Province) occurred from the Permian to the mid-Cretaceous (J.D.Bradshaw 1989). A series of Early Triassic to Early Cretaceous volcanic arcs associated with this subduction are now preserved as the highly dismembered Median Tectonic Zone (MTZ) (Bradshaw 1993, Kimbrough *et al* 1993). Although the Hohonu Super-suite appears to bear no direct relationship to this subduction zone (Ch.6.5.3), it is feasible that subduction-related fluids affected and contributed to the lower crust, and underlying mantle, of the inboard Buller terrane.

Late stage Separation Point Suite activity, contemporaneous with emplacement of the Hohonu Super-suite, is indicated by the 111.4 $\pm$ 2.0 Ma emplacement of the Olympus Granite (Muir *et al* 1994a). This pluton has a distinctive Separation Point Suite chemical signature (Muir *et al* 1995) and is intrusive into Buller terrane rocks (Fig.1.2). Muir *et al* (1995) have proposed a model involving thickening of the MTZ, following collision with the Western Province, and melting of an Early Palaeozoic mafic underplate to the MTZ, to generate the characteristic "adakite" compositions of the Separation Point Suite. Isotopic data indicate the Separation Point Batholith and the MTZ are inappropriate unique source rocks for the Hohonu Super-suite, being distinctly more primitive (McCulloch *et al* 1987, Muir *et al* 1995, Fig.6.55). In a similar manner to the MTZ magmas, Separation Point Suite magmas may have contributed to the lower crustal component of the Hohonu Super-suite. However, the partially contemporaneous nature of the Hohonu Super-suite and Separation Point Suite suggests a more direct petrogenetic link between the two suites.

Excluding those components which are currently isotopically unconstrained, the above discussion of possible and probable lower crustal components of the Buller terrane has failed to identify a unique crustal source with isotopic compositions appropriate for generation of the Hohonu Super-suite. Apart from the relatively primitive Separation Point Suite, rocks of the Median Tectonic Zone, and poorly defined Cambrian volcanic sequences, all recognized lower crustal components for which isotopic data are available are considerably more radiogenic than the Hohonu

Super-suite. This suggests involvement of a mantle-derived component and/or more direct involvement of the Separation Point Suite rocks.

**6.5.2.2: Is there a mantle component?**

It is now generally accepted that many granitoids consist of at least two isotopically and chemically distinct components; a depleted mantle melt and relatively radiogenic continental crust (e.g. Allègre and Ben Othman 1980, DePaolo 1981b+c, McCulloch and Chappell 1982, Pickett and Wasserburg 1989). The relatively radiogenic isotope ratios of the Hohonu Super-suite are typical of crustal-derived I-type granitoids (e.g. McCulloch and Chappell 1982, Chappell and White 1992) and indicate the involvement of an important crustal component as discussed above. However, the Hohonu Super-suite also plots close to the more radiogenic end of the present day mantle array of DePaolo and Wasserburg (1979) (see Fig.6.55) and has compositions overlapping the widespread compositions of modern day subduction-related basalts (Wilson 1989), also suggesting the involvement of an important mantle-derived component. Additional support for a mantle influence is given by the adherence of the Hohonu Super-suite to calculated mixing curves between mantle and crustal components such as the Greenland Group (e.g. Pickett and Wasserburg 1989, Fig.6.56, 6.57, 6.59). Variations within the Super-suite are too great to allow for derivation from a single, isotopically mature mantle source and the general trend towards higher $Sr_{(110)}$ and more negative $\epsilon Nd_{(110)}$ within the Super-suite (Fig.6.13) supports the involvement of more radiogenic crustal component. Intra- and inter-pluton variation indicates this crustal component is somewhat heterogeneous, as is likely given the discussion of probable lower crustal components given above (Ch.6.5.2.1). Incorporation of a complex crustal component also manifests itself in variable $T_{DM}$, which cluster at $\approx 1.2$ Ga, yet actually vary considerably from 0.9-1.5 Ga (see Table 6.4). The fact that most possible lower crustal components of the Buller terrane are considerably more radiogenic than the Hohonu Super-suite (Fig.6.55) also strongly suggests an important mantle component in the genesis of these granitoids. A model for generation of the Hohonu Super-suite involving mixing of a mantle end-member and complex lower continental crust component therefore seems likely. The question then arises: Is this mantle component identifiable?

Pickett and Wasserburg (1989) postulated that a depleted mantle component, based on the depleted-mantle evolution model of DePaolo (1981b), underlies the Western Province and could be involved in granitoid genesis. Mixing between this depleted mantle component and Greenland Group was attempted by Pickett and Wasserburg (1989) (see Fig.6.56) yet considered an unlikely mechanism for generation of Western Province granitoids. For similar reasons, such models are considered unsuitable for generation of the Hohonu Super-suite. The large amounts of mixing required ($\approx$50%) (Fig.6.56) are too high to retain the metaluminous I-type characteristics of the Deutgam Suite and although this problem is reduced somewhat by assimilation-fractional crystallization modelling (AFC of DePaolo 1981a, Fig.6.57), high assimilation rates are still required ($r \geq 0.5$). Additionally, similar partition coefficients are required for Sr and Nd in such models (Fig.6.57), indicating either incompatible behaviour of Sr, or compatible behaviour of Nd, neither of which is likely in a typical, feldspar dominated granitoid system. Muir *et al* (1995) also reject mixing between the depleted mantle used by Pickett and Wasserburg (1989) and Greenland Group to generate the Separation Point Suite, as such a model requires $\approx$20% involvement of continental crust. The absence of an inherited zircon component in the Separation Point Suite indicates little or no crustal involvement during petrogenesis (Muir *et al* 1995). This suggests that the depleted-mantle and/or the Greenland Group components are inappropriate as end-members in any mantle-crust mixing scheme.

Recent work has suggested that the mantle beneath the Western Province is considerably less depleted than that postulated by Pickett and Wasserburg (1989). The Separation Point Batholith is considered to have formed by melting of a mantle-derived, young basaltic underplate and to have undergone no interaction with radiogenic crust (Muir *et al* 1995). Isotopic and U-Pb zircon studies (McCulloch *et al* 1987, Mattinson *et al* 1986) on the mid-lower crustal equivalent of the Separation Point Batholith in Fiordland (Western Fiordland Orthogneiss) are also compatible with a similar derivation involving little or no crustal interaction. As the Separation Point Batholith and equivalents directly reflect their mantle source, the composition of this source can be accurately determined. This mantle source is here termed the Separation Point-type Depleted Mantle (SPDM) and its isotopic composition is taken as an average of the uncontaminated Separation Point Batholith analyses presented by Muir *et al* (1995)

($Sr_{(110)}$ = 0.7042, $\epsilon Nd_{(110)}$ = 1.4). Mid-Cretaceous mantle-derived A-type granitoids and mafic intrusives in Marie Byrd Land (Weaver *et al* 1994) and have very similar isotopic signatures to the Separation Point Batholith and indicate that SPDM can be inferred to have underlain large regions of the Western Province and equivalents during the mid-Cretaceous. Thus, SPDM can be modelled as a potential depleted mantle component involved in the petrogenesis of the Hohonu Super-suite.

Contemporaneous activity in the Separation Point Suite and the Hohonu Super-suite suggests a direct petrogenetic link between the two suites. Although the Hohonu Super-suite comprises typical calc-alkaline granitoids, chemically distinct from the alkali-calcic Separation Point Suite (see Ch.6.2.5), the relatively high Sr contents of the Te Kinga Suite (up to 800 ppm) overlap with compositions of the Separation Point Suite and support a genetic link between the two suites. Also distinctive of the Separation Point Suite are elevated Sr-Y ratios (Muir *et al* 1995). The Hohonu Super-suite has Sr/Y more typical of island arc compositions (Fig.6.58) but overlaps with the Separation Point Suite at the higher $SiO_2$ contents of the Te Kinga Suite. The overlap of the Hohonu Super-suite with some of the distinctive compositions of the Separation Point Suite suggest that there may be a genetic link between the two suites. Contemporaneous activity in both suites also suggests a genetic link, implying the involvement of the SPDM component in both the Hohonu Super-suite and the Separation Point Suite. SPDM may be involved as contemporaneous SPDM mantle-derived magmas, or via melting of the same Early Palaeozoic mafic underplate source inferred for the Separation Point Batholith (Muir *et al* 1995). Whatever their method of generation, the SPDM-derived magmas must have interacted with a radiogenic lower continental crustal component to produce the isotopic compositions of the Hohonu Super-suite. The relatively primitive, mantle-like isotope ratios of the Separation Point Suite are attributed to emplacement at the margin of thin continental crust, and a consequent lack of involvement of mature crust (Muir *et al* 1995). This contrasts markedly with the Hohonu Super-suite which was emplaced inboard of the Separation Point Suite and into relatively thick continental crust. Radiogenic isotopic compositions and the presence of inherited zircons (T.R.Ireland *pers.comm.* 1994) in the Hohonu Super-suite reflect this increased interaction with crust. This suggests that the fundamental distinctions between the Separation Point Suite and the Hohonu Super-suite

may be a consequence of increased interaction of SPDM-derived magmas with a mature and complex continental crust.

AFC modelling (Fig.6.59) indicates that the isotopic compositions of the Hohonu Super-suite are achievable by mixing of a SPDM-derived melt and average Greenland Group compositions. Smaller degrees of Greenland Group contamination are required (20-30%) than models using a more depleted mantle component (see Fig.6.56 and Fig.6.57). Moreover, the amount of Greenland Group contamination required can be further reduced (to around 10%) by increasing the amount of assimilation compared to the amount of crystallization so that the system approaches simple mixing. Furthermore, in contrast to the depleted mantle model used by Pickett and Wasserburg (1989), partition coefficients required for Sr and Nd are more realistic for granitic systems. Mixing between Greenland Group with $T_{DM} \approx 1.8$ Ga and SPDM with $T_{DM} \approx 0.6$ Ga is also compatible with the 1.2 Ga model ages calculated for the Hohonu Super-suite. Therefore, AFC between SPDM and Greenland Group provides a feasible mechanism for generating the Hohonu Super-suite, at least in terms of isotopic compositions.

Although the above paragraph suggests that the Hohonu Super-suite may simply represent SPDM-derived melts mixed with Greenland Group, in reality the situation cannot be this simple. As mentioned previously, use of the Greenland Group as a crustal end-member is highly simplistic. The lower continental crust of the Buller terrane is more likely to be an extremely complex and heterogeneous mixture of unknown lower crustal and other Palaeozoic-Mesozoic igneous components, presently impossible to constrain chemically or isotopically (Ch.6.5.2.1). The adakite compositions of the Separation Point Suite are distinct from the more typically calc-alkaline compositions of the Hohonu Super-suite, and whether mixing of SPDM magmas with lower crustal components is capable of masking the distinctive chemistry of the Separation Point Suite is also unknown. It is pertinent, however, to note that despite evidence for significant continental crust involvement in the Olympus Granite (abundant inherited zircon, Rennison 1992, Muir *et al* 1994a) and Canaan Granodiorite (atypically radiogenic isotopes, Muir *et al* 1995), both plutons retain the distinctive Separation Point Suite chemical signature. There are, however, some similarities

between the two suites. In particular the Separation Point Suite and the Te Kinga Suite are both characterized by relatively elevated Sr, $Na_2O$ and $Al_2O_3$ (Fig 6.14) (and to a lesser extent elevated Sr/Y (Fig.6.58)) and depleted HREE and Y (see Ch.6.2.5, Muir *et al* 1995). These chemical characteristics in both the Separation Point Suite and Te Kinga Suite are attributed to melting in equilibrium with a plagioclase-free, eclogitic residue (Ch.6.5.3, Muir *et al* 1995). In contrast, it is argued that the Deutgam Suite is derived by melting of the same source, but at drier and somewhat shallower conditions, resulting in an amphibolitic (amphibole + plagioclase) residue (Ch.6.5.3). Therefore, melting at different crustal levels and with distinct residues, interaction with a complex lower crustal component, and a distinctly different tectonic environment (see Ch.6.5.4), have all combined to produce the characteristic compositions of the Hohonu Super-suite, these compositions being distinct from those of the Separation Point Suite.

#### 6.5.2.3: Conclusion.

Several lines of evidence have lead to a model for generation of the Hohonu Super-suite as a complex mixture of a depleted mantle-derived component and a lower continental crustal component. The depleted mantle end-member can be relatively well constrained as the Separation Point-type Depleted Mantle (SPDM), derived either directly from partial melting of the underlying mantle, or from melting of the Palaeozoic underplate inferred as the source for the Separation Point Suite. The lower crustal component is less well-defined, yet is likely to be a complex, heterogeneous mixture of unknown components, mafic underplating events and other Palaeozoic to Mesozoic magmatic events which have affected the Western Province crust. The current inability to more accurately define this crustal end-member precludes more detailed modelling of mantle and crustal components.

### 6.5.3: Processes.

Recognition of a similar source for both the Deutgam and Te Kinga Suites implies that the fundamental geochemical differences between the two suites must be a consequence of differing processes affecting this source. Primarily, a method must be envisaged that enables derivation of both relatively mafic, metaluminous, flat HREE melts and relatively felsic, peraluminous, HREE depleted melts from the same source.

**6.5.3.1: Control by residual assemblages.**

The Deutgam and Te Kinga Suites are characterized by differing contents of Sr, Ba, $Al_2O_3$, $Na_2O$ and Eu, strongly indicative of compositional control by plagioclase feldspar. Plagioclase has low partition coefficients for all REE except Eu, for which it shows a large positive anomaly (Hanson 1978 + 1980) and partition coefficients of 2-5 (Henderson 1982, Rollinson 1993). Consequently, source retention or subsequent fractionation of plagioclase will create negative Eu anomalies in the resulting melts. Retention, or fractionation, of plagioclase will also result in a melt relatively depleted in $Al_2O_3$, $Na_2O$, $K_2O$, Sr and Ba. Relatively low concentrations of these elements in the Deutgam Suite, coupled with relatively large negative Eu anomalies, indicate significant removal of plagioclase. In contrast, relatively high concentrations of these elements and small negative Eu anomalies, coupled with small to absent Sr and Ba troughs on spider-diagrams, preclude either major source retention or fractionation of plagioclase during generation of the Te Kinga Suite. Importantly, the lack of chemical evidence for major feldspar fractionation in the Te Kinga Suite indicate differing amounts of fractionation of a single melt cannot explain the geochemical differences between the Te Kinga Suite and the Deutgam Suite.

The HREE depleted nature of the Te Kinga Suite contrasts strongly with the flat HREE patterns of the Deutgam Suite (Fig.6.12). As garnet has high partition coefficients for HREE (Henderson 1982, Rollinson 1993), depleted HREE contents such as those present in the Te Kinga Suite are generally attributed to the presence of residual garnet in the source. The incoming of garnet, although somewhat dependent upon bulk composition, is largely considered to occur at about 10 kb ($\approx$35-40 km) (e.g. Rudnick 1992, Wyllie and Wolf 1993). Therefore, REE and major and trace element data indicate that the Te Kinga Suite is derived from melts generated at deeper levels of the crust ($>$10 kb) in equilibrium with garnet. In contrast Deutgam Suite melts are derived from shallower levels ($<$10 kb) and were in equilibrium with plagioclase, not garnet. Trace element data indicate both suites were in equilibrium with amphibole.

Geochemical contrasts similar to those which distinguish the Te Kinga and Deutgam Suites (i.e. varying HREE, Eu and Sr contents) have also been identified in the Peninsular Ranges Batholith of California (Gromet and Silver 1987). These authors invoke a relatively shallow (30-45 km) plagioclase-bearing gabbroic source in the western portion of the batholith to produce granitoids with relatively high, flat HREE contents, negative Eu anomalies and low Sr. In contrast a garnet-bearing, plagioclase-poor eclogitic or garnet amphibolitic source at "greater than 45 km and most probably greater than 60 km" (Gromet and Silver 1987, p 110) is required to produce the HREE depleted, high Sr and Eu plutons of the eastern batholith. In a similar fashion, Sr-depleted, Y-undepleted and Sr-undepleted, Y-depleted Proterozoic granitoids in Australia require sources that contain "either plagioclase or garnet, but rarely both" (Wyborn *et al* 1992, p 202). A similar change in depth and modal mineralogy of source may explain the geochemical differences between the Deutgam and Te Kinga Suites.

Varying residual assemblages can also be produced by melting of meta-basaltic to meta-andesitic compositions at differing water contents. Experimental data have shown that dehydration melting of metabasaltic compositions, where all water is supplied by the breakdown of hydrous phases such as amphibole, results in a wide plagioclase stability field. Plagioclase is the dominant liquidus phase between 0-10 kb, and may persist to 20-25 kb. Dehydration melting also reduces the stability field of garnet to greater than 14 kb (Green 1982) (Fig.6.60). Addition of 5% $H_2O$ to produce water under saturated conditions results in an expansion of the partial melting field to a wider, generally lower, range of temperatures. Moreover, the stability field of plagioclase is greatly reduced and garnet appears on the liquidus between 7-10 kb, becoming prominent above 15 kb (Green 1982) (Fig.6.60). Experimental data (Green 1982, Rapp *et al* 1991, Rushmer 1991), recently summarized by Peacock *et al* (1994), indicate that water undersaturated melting of tholeiitic basalt at 8-12 kb will produce a melt in equilibrium with an eclogitic residue (hbl + cpyx + gar but no plag) equivalent to the Te Kinga Suite. In contrast, dehydration melting of amphibolite at the same conditions produces tonalitic melts in equilibrium with an amphibolitic residue (hbl + cpyx + plag $\pm$ opyx), analogous to the Deutgam Suite (see Table 2 of Peacock *et al* 1994). Therefore the differing chemistries of the Deutgam and Te Kinga Suites may also be attributed to melting at differing water contents.

**6.5.3.2: Te Kinga Suite: generation of high $SiO_2$, peraluminous melts.**

The high $SiO_2$, yet unfractionated, and peraluminous nature of the Te Kinga Suite, as compared with the more mafic, metaluminous Deutgam Suite, has yet to be explained. Although peraluminous melts can be generated by prolonged crystal fractionation (Zen 1986, Champion and Chappell 1992) this cannot be the case for the Te Kinga Suite as relatively high Sr and Ba contents, and a lack of significant negative Eu anomalies, are inconsistent with extensive crystal fractionation. Small degree I-type minimum melts may also produce high $SiO_2$, peraluminous compositions like the Te Kinga Suite (Ellis and Thompson 1986) but the problem arises of efficiently separating and accumulating such small degree partial melts prior to migration and intrusion to upper crustal levels. Melting of a distinct, felsic peraluminous protolith seems unlikely given the similar radiogenic isotope and broad geochemical characteristics of the Te Kinga Suite and Deutgam Suite.

The high $SiO_2$ and peraluminous compositions of the Te Kinga Suite are also attainable by melting at high $H_2O$ contents. Experimental studies indicate varying water fugacity strongly effects the compositions of partial melts of metabasalts at mid-lower crustal conditions (see Peacock *et al* (1994) for a recent summary). Helz (1976) showed that 20-40% melting of tholeiitic basalts at 5 kb $P_{H2O}$ produces peraluminous melts with $\approx$70% $SiO_2$ and little residual feldspar. Similar peraluminous compositions have been produced by wet melting of basalt by Holloway and Burnham (1972), Beard and Lofgren (1991) and Green and Ringwood (1968). Ellis and Thompson (1986), in a detailed study on the CaO + MgO + $Al_2O_3$ + $SiO_2$ + $H_2O$ system, describe peritectic melting of basaltic rocks under excess $H_2O$ conditions to produce peraluminous-corundum normative liquids. In summary, all such experiments produce peraluminous, $SiO_2$-rich granitoid melts at realistically high degrees of partial melting. In contrast, during dehydration melting of identical or similar basaltic compositions (where all water is produced by the breakdown of amphibole and/or biotite) intermediate, tonalitic-granodioritic, metaluminous melts more typical of the Deutgam Suite are produced (Ellis and Thompson 1986, Beard and Lofgren 1991). Therefore, the contrast in ASI and $SiO_2$ content between the two suites is also consistent with partial melting of a metabasaltic source at conditions of different water activity; $H_2O$ undersaturated to saturated conditions producing the silica rich, peraluminous unfractionated compositions

of the Te Kinga Suite, whereas dehydration melting produces metaluminous intermediate melts typical of the Deutgam Suite.

Similarly contrasting granitoid compositions in the Chilliwack Batholith of Washington have also been attributed to melting of a homogeneous source at varying $H_2O$ contents (Tepper *et al* 1993). Leucocratic and intermediate plutons with restricted isotopic compositions dominate the batholith. The absence of negative Eu anomalies and depleted MREE elements in the leucocratic plutons preclude derivation by fractional crystallization of plagioclase and amphibole from the intermediate plutons. Tepper *et al* (1993) therefore propose that the intermediate plutons of the Chilliwack Batholith (equivalent to the Deutgam Suite) form by dehydration melting of an amphibolitic source rock as a result of underplating of dry basaltic magmas. In contrast, the leucocratic plutons (analogous to the Te Kinga Suite) are formed by melting of the same source rocks at higher water fugacity associated with water released during the crystallization of underplated hydrous basalts. A major difference between the Chilliwack Batholith and the Hohonu Super-suite is a lack of evidence for residual garnet in either suite of the Chilliwack Batholith. It would thus appear that as well as varying water contents, an increase in depth to source of the Te Kinga Suite is required to ensure the presence of residual garnet.

**6.5.3.3: Oxygen isotopes: a brief discussion.**

The Te Kinga Suite has $\delta^{18}O$ values $\approx 10‰$ (Table 6.5), often considered to represent interaction of granitoid magmas with high $\delta^{18}O$ sediments or altered volcanics (Taylor 1988), hence the use of oxygen isotopes to identify S-type granitoids (O'Neil and Chappell 1977, O'Neil *et al* 1977, Chappell and White 1992). However, such a high $\delta^{18}O$ sedimentary component will also have elevated radiogenic isotopes. Consequently, its involvement in granitoid genesis should also be reflected in elevated Sr and Nd isotopes, as observed in the Peninsular Ranges Batholith by Taylor (1986). Higher $\delta^{18}O$ values in the Te Kinga Suite cannot be explained by involvement of a high $\delta^{18}O$ sedimentary rock as they are not associated with more radiogenic Sr and Nd isotope compositions. Modelling has indicated that closed system crystal fractionation will result in only a 0.4‰ enrichment in $\delta^{18}O$ per 10 wt% increase in $SiO_2$ (Sheppard and Harris 1985, Hoefs 1987), as oxygen isotope fractionation between silicate liquids

and minerals is so small at magmatic temperatures (Taylor 1977, Taylor and Sheppard 1986). The $\delta^{18}O$ differences between the Te Kinga Suite and Deutgam Suite thus cannot be a simple consequence of differing $SiO_2$ contents and amounts of fractionation. Enrichment of $^{18}O$ is commonly attributed to equilibration with low $\delta^{18}O$ meteoric water ($\delta^{18}O$ = 0 to -6‰) at low temperatures (< 100-250°C) (Faure 1986). As $\delta^{18}O$ values are variable within individual plutons, and show no correlation with radiogenic isotopes, elevated $\delta^{18}O$ values in the Te Kinga Suite most likely reflect a late stage, shallow subsolidus interaction with meteoric water. Interaction with meteoric waters may be a reflection of the higher levels of emplacement of the Te Kinga Suite implied by petrographic and field evidence (Ch.3.5.1, Ch.3.10.1).

### 6.5.4: Tectonic environment of emplacement.

In the following section the term Hohonu Super-suite is considered to also include the Rahu Suite plutons of the Buller Gorge and Victoria Range (see Ch.6.2.5).

Previous studies have assumed that the granitoids of the Hohonu Batholith represent typical calc-alkaline granitoid melts generated above a westward-dipping subduction zone (Tulloch 1983, 1988a, Muir *et al* 1995). Association of the Hohonu Super-suite with subduction could be inferred from the typical subduction signature indicated by geochemical data. The tectonic discrimination diagrams of Pearce *et al* (1984) (Fig.6.61) classify the Hohonu Super-suite as Volcanic Arc Granite, analogous to the I-type granitoids of Chappell and White (1992), and generally considered to be directly related to the subduction process. Negative Nb-Ta anomalies (Fig.6.11) are also generally considered to indicate a subduction-related signature (Saunders *et al* 1980). Although subduction (with associated terrane accretion) of the proto-Pacific plate occurred along the Pacific margin of the New Zealand portion of Gondwana from the Permian to the Early Cretaceous (J.D.Bradshaw 1989) it seems unlikely that the Hohonu Super-suite is related directly to melting above this subduction zone. Tectonic reconstructions at 110 Ma (Fig.6.62) indicate that the Mesozoic Gondwana margin was at least 700 km outboard of the Hohonu Batholith. Consequently, unless extremely shallow subduction is invoked[11], subduction of the proto-Pacific plate beneath the

11: Less than 10° if the depth of magma generation above the down-going slab is assumed to be around 100 km.

Gondwana margin is considered too distant to be involved directly in the genesis of the Hohonu Super-suite. Similarly, although the Median Tectonic Zone (MTZ) is considered to represent a dismembered long-lived volcanic arc system (Bradshaw 1993, Kimbrough *et al* 1993) it is also too far inboard to be related to subduction along the Pacific margin trench. Muir *et al* (1995) consequently argue that another subduction zone must have existed west of the Torlesse accretionary prism, possibly along the Livingstone Fault and the Dun Mountain Ophiolite belt or the eastern edge of the MTZ. U-Pb zircon dating indicates that volcanic arc components of the MTZ have ages in the range 247-131 Ma (Kimbrough *et al* 1994b, Muir *et al* 1994d) and significantly predate the Hohonu Super-suite. This suggests that the Hohonu Super-suite is unlikely to be related to melting above the subduction zone which produce the MTZ arc. Consequently, the Hohonu Super-suite cannot be directly related to melting above a recognized subduction zone, and other methods of melt generation must be investigated. As discussed in Ch.6.2.2.1, the subduction signature in the Hohonu Super-suite is likely to have been inherited from source chemistry, rather than to reflect the actual tectonic environment at the time of magma generation.

An important factor to consider when discussing the origin of the Hohonu Super-suite is that despite voluminous igneous activity east of the Buller terrane during the Mesozoic (e.g. MTZ, WFO, Separation Point Batholith), Early Cretaceous granitoid magmatism in the Buller Terrane itself is restricted to a short pulse between 113-109 Ma. This suggests that Early Cretaceous activity in the Buller Terrane was triggered by a discrete event rather than being related to continuous subduction along the Gondwana margin.

Muir *et al* (1995) attribute generation of the Separation Point Batholith at $\approx$118 Ma to crustal thickening during juxtaposition of the MTZ volcanic arc complex and the Western Province. Emplacement of the Mount Olympus Granite into the Western Province at 111 Ma (Muir *et al* 1994a) is contemporaneous with intrusion of the Hohonu Super-suite and suggests that crustal thickening may have also contributed to genesis of the Hohonu Super-suite. Both the Te Kinga Suite and the Separation Point Suite have geochemistries compatible with magma generation by melting of relatively deep regions of thickened crust. However, basalt melting experiments have shown that

compositions similar to the Te Kinga Suite can also be generated by water-undersaturated melting at relatively low pressures (Ch.6.5.3.2) and greater than normal crustal thicknesses need not be invoked. Furthermore, the requirement for residual plagioclase, yet no residual garnet, indicate the Deutgam Suite was generated at relatively shallow crustal depths ($\approx$10 kb $\approx$35 km) (Ch.6.5.3.1). Consequently, generation of the Hohonu Super-suite at the base of an overthickened crustal pile is precluded and another mechanism must be sought.

Mathematical modelling by England and Thompson (1986) indicates that fluid-absent melting of amphibolitic crust (and the generation of I-type calc-alkaline melts in equilibrium with residual plagioclase but no garnet, analogous to the Deutgam Suite) is feasible at crustal depths of $\approx$35-40 km, given a number of specific conditions (Fig.6.63). In this model, the thickness of continental crust is doubled over a period of 30 Ma, left for 30 Ma, then thinned to its original thickness over the remaining 30 Ma (Fig.6.63). England and Thompson (1986) note that a higher than average geotherm, typical of Mesozoic-Cenozoic tectonic regions, is required for melting to occur. Such a geotherm is probably appropriate given the relatively young and tectonically active nature of the New Zealand region during the Mesozoic. Most importantly, in these calculations, dehydration melting of amphibolite occurs 50-90 Ma after the initiation of thickening, with the bulk of melting occurring during the extensional phase and the return to normal crustal thicknesses.

Several other recent studies have proposed a link between crustal extension and granitoid genesis[12]. Models for the generation of granitoids in extensional environments generally invoke rapid uplift and isothermal melting of hot crustal roots generated during previous crustal thickening in a similar manner to the mathematical models of England and Thompson (1986) (e.g. Brown *et al* 1981a, Leake 1987, 1990). Intrusion of basaltic melts, generated by adiabatic melting of the underlying mantle, into the lower crust further increases ambient temperatures and facilitates lower crustal

---

**12:** An important consequence of the link between granitoid genesis and extension is solution of the long debated "granitoid space problem". Although most recent workers have concentrated on granitoid emplacement into transtensional and dilational jogs on strike-slip fault systems (e.g. Leake 1990, Hutton and Reavy 1992, D'Lemos *et al* 1992, Grocott *et al* 1994), studies have also been made on emplacement into extensional listric fault systems (e.g. Hutton *et al* 1990).

melting to produce abundant granitoid magmas (Leake 1990). More recently other authors (Harry *et al* 1993, Hervé *et al* 1993) have proposed similar mechanisms whereby overthickened crust collapses following the cessation of compression. Widespread ductile flow in the lower crust leads to the formation of metamorphic core complexes and rapid thinning of the lithosphere. This results in near adiabatic decompression of the lithospheric mantle and consequent melting. These mantle melts underplate the lower crust, which already has an elevated geotherm due to uplift, and cause voluminous partial melting of the lower crust, as modelled by Huppert and Sparks (1988). Similar crustal extension and development of metamorphic core complexes with associated magmatism is inferred to have followed crustal thickening in regions such as the Basin and Range region of North America (Wernicke *et al* 1982, 1987, Coney 1987). In the models of England and Thompson (1986) uplift and exhumation occurs by erosion only, however, they note that if low-angle normal faulting leads to rapid exhumation, then significantly greater quantities of magma will be produced than by exhumation by erosion alone.

A variation on the simple lithospheric thinning theme as described above, initially proposed by Bird (1979) and Houseman *et al* (1981), involves large scale delamination at the base of overthickened crust. Delamination has been proposed as a mechanism of producing large quantities of granitoid magma that otherwise cannot be easily explained by plate tectonic theory, such as the voluminous Lachlan Fold Belt granitoids (Cox *et al* 1991, Collins 1994) (see also Kay and Kay 1991, 1993, Looseveld and Etheridge 1990, Nelson 1992, Davis *et al* 1994). Although the processes which lead to magmatism are similar to the thinning models above (i.e. adiabatic uplift and melting), the precursory events are strikingly different. Following collision and crustal overthickening, the relatively cool and dense overthickened root becomes unstable, detaches, and sinks into the asthenosphere (Houseman *et al* 1981, Kay and Kay 1993). The actual zone along which delamination occurs is a subject of speculation. Houseman *et al* (1981) consider only the lower part of the lithospheric mantle to delaminate, although they suggest that removal of the entire mantle is feasible, as proposed by Nelson (1992). Kay and Kay (1993) extend the argument and consider that the base of the lower crust may also delaminate. Although it is impossible to prove a delamination event during generation of the Hohonu Super-suite, if such an

event did occur then retention of the lower crust is necessary to retain appropriate source rocks. Whichever zone of delamination is considered, the net result is the same, delaminated crust and/or mantle material is replaced rapidly by hot asthenospheric mantle which creates a substantial thermal anomaly, heating the overlying lithosphere and causing uplift and extension. Juxtaposition of hot asthenosphere against relatively cool lithosphere, associated with concomitant adiabatic melting of the asthenosphere and mafic underplating of the lower crust, results in voluminous melting of the lower crust and the production of granitoid magmas (Kay and Kay 1993). In the models of England and Thompson (1986) heat input from the mantle is kept constant (Fig.6.63). However, they note that if delamination occurs, as proposed by Houseman *et al* (1981), then the mantle energy inputs they propose are probably significantly underestimated and greater amounts of granitoid melt production are likely. In a similar fashion, mafic underplating during adiabatic melting of the underlying mantle, as proposed by Leake (1990), must also lead to an increase in heat input from the mantle and the amount of crustal melting.

Many of the key ingredients indicating generation of the Hohonu Super-suite during a period of crustal extension immediately following a crustal thickening event are present in the geohistory of the Western Province. An initial crustal overthickening event is provided by collision of the MTZ with the Western Province, as invoked by Muir *et al* (1995) during generation of the Separation Point Batholith. Granulite facies metamorphism in Fiordland has also been attributed to a major crustal thickening event in the early Cretaceous (Mattinson *et al* 1986, J.Y.Bradshaw 1989). These thickening events are presumably ultimately related to accretion and subduction along the New Zealand/Gondwana margin and thus provide an, albeit indirect, link to the subduction process. Crustal thickening in the Western Province may have occurred over a long time period during the long-lived activity of the MTZ arc (247-131 Ma, Kimbrough *et al* 1994b, Muir *et al* 1994d). However, the main thickening event is well constrained as it must postdate the youngest MTZ arc rocks (131 Ma, Kimbrough *et al* 1994b) and predate emplacement of the relatively undeformed Western Fiordland Orthogneiss at 125.4 $\pm$ 1.7 Ma (Muir *et al* 1994d). Collision of the Pacific-Phoenix spreading ridge with the Eastern Province at 105 $\pm$ 5 Ma is believed to have halted subduction and terrane accretion (J.D.Bradshaw 1989), with consequent reorganization of plate

boundary forces allowing the onset of crustal relaxation, thinning and uplift. A time period of $\approx$15-30 Ma between the peak of thickening and the onset of extension is indicated, and is compatible with the models of England and Thompson (1986) who note that most amphibolite melting will occur 20 to 60 Ma after the peak of thickening.

Several geological features indicate the onset of uplift and extension in the Western Province occurred at $\approx$110 Ma and was contemporaneous with intrusion of the Hohonu Super-suite. Of particular importance is the Buckland Granite (109.6 $\pm$ 1.7 Ma, Muir *et al* 1994a), which is chemically, temporally and petrographically very similar to the Te Kinga Monzogranite and part of the Rahu Suite (see Ch.6.2.4.1). Buckland Granite occurs within the core of the Paparoa Metamorphic Core Complex (Tulloch and Kimbrough 1989) which represent extension between 114 $\pm$ 18 Ma and 108 Ma (Tulloch and Kimbrough 1989) contemporaneous with emplacement of the Hohonu Super-suite. Mylonitic fabrics in the Buckland Granite have been previously interpreted as providing a maximum age for initiation of the core complex (Tulloch and Kimbrough 1989, Muir *et al* 1994b), however there may be a more direct genetic link between the Buckland Granite and the Paparoa Metamorphic Core Complex. Mylonitic fabrics in the Buckland Granite may be interpreted as representing the final stages of cooling, through the conditions of quartz ductility, of a pluton emplaced along a crustal scale detachment fault, as proposed by Hutton *et al* (1990). The Buckland Granite may therefore be intimately related to the crustal extension and uplift of the Paparoa Core Complex, and represent intrusion into an active detachment fault, not simply uplift of a completely crystalline portion of the basement core. If so, the 109.6 $\pm$ 1.7 Ma age of the Buckland Granite dates actual extension in the Paparoa Metamorphic Core Complex, rather than providing a maximum age of extension and indicates emplacement of the Buckland Granite, Rahu Suite and Hohonu Super-suite occurred contemporaneous with major crustal extension in the Paparoa Metamorphic Core Complex[13].

---

**13:** The intimate relationship between Buckland Granite, the Paparoa Batholith, and the Paparoa Metamorphic Core Complex suggests other Rahu Suite/Hohonu Super-suite plutons may also be related to detachment faults (Tulloch 1988b). No evidence for detachment faults have been observed in the Hohonu Batholith (see also Ch.8.7.2), although the presence of a major crustal detachment zone at depth which acted as a conduit for migration of the Hohonu Super-suite magmas cannot be discounted.

Recently, Gibson and Ireland (1994) have recognized 107 Ma anorthositic veins and dikes cutting the Western Fiordland Orthogneiss which they interpret as representing partial melting initiated by decompression at the early stages of uplift. Metamorphic assemblages also indicate rapid, near-isothermal uplift consistent with exhumation during continental extension (Gibson and Ireland 1994). The Western Fiordland area is considered to have underlain much of the north Westland-Nelson region during the Cretaceous, and the decompressional partial melting event recognized by Gibson and Ireland (1994) may also represent the same extensional event recognized here during generation of the Hohonu Super-suite. Sharp, discordant high level intrusive contacts between Hohonu Super-suite plutons and country rock, and the generally undeformed nature of the plutons, are also compatible with passive emplacement into an extensional post-tectonic environment.

Sedimentological evidence for extension as early as 110 Ma and contemporaneous with the Hohonu Super-suite is tantalizing. The WNW-ESE oriented basins of the Pororari Group (Laird 1988) are believed to have initiated in the mid-late Albian (105-100 Ma) (Laird 1993). However, a recent SHRIMP age of 101 Ma (Muir unpublished data 1994) for the Stitts Tuff at the base of the Pororari Group in the Lower Buller Gorge suggests extension is considerably younger than the Hohonu Super-suite. The appearance of deformed Buckland Granite clasts in the Pororari Group breccias indicating surface exposure and erosion by $\approx$105 Ma (Tulloch and Palmer 1990), and removal of the overlying Greenland Group must have occurred during the preceding few million years. Extension directions indicated by the orientations of the Pororari Group basins, the offshore Takutai and Challenger basins (Bishop 1992, Wood 1991), and stretching lineations in the Paparoa Metamorphic Core Complex (Tulloch and Kimbrough 1989) are indicative of parallel NNE-SSW oriented extension. Importantly, these extension directions are also perpendicular to the inferred Cretaceous convergent margin of New Zealand and are consistent with collapse of a tectonically overthickened belt developed parallel to this margin.

Several extensional events in the Western Province occurred at 105 $\pm$ 5 Ma; formation of the Paparoa Metamorphic Core Complex, opening of the Pororari Group sedimentary basins and the cessation of a compressive subduction regime along the

Gondwana margin. These events postdate the crustal thickening event which generated the Separation Point Batholith and create a scenario identical to those considered to be conducive to generation of granitoids melts in extensional environments (e.g. Brown *et al* 1981b, England and Thompson 1986, Leake 1987, 1990). Thus, generation of the Hohonu Super-suite is considered to be the result of adiabatic melting during uplift and thinning following thermal collapse of overthickened crust produced during collision of the MTZ with the Western Province. This results in a major re-interpretation of the causes of mid-Late Cretaceous crustal extension in the Western Province. The parallel nature of many Early to mid-Cretaceous structures on the West Coast (e.g. Paparoa Metamorphic Core Complex, Pororari Group basins, Takutai half graben, Hohonu Dike Swarm etc) has generally been attributed to a single prolonged period of extension prior to the opening of the Tasman Sea (e.g. Tulloch and Kimbrough 1989, Bishop 1992, see also Ch.7). More recently Laird (1993, 1994) has indicated that such a scenario is probably too simplistic and he has recognized several extensional events prior to actual separation of Australia and New Zealand. Although mid-Cretaceous extensional structures parallel late Cretaceous features directly related to Tasman opening (e.g the Hohonu Dike Swarm Ch.7) the arguments presented above indicate mid-Cretaceous extension is instead a consequence of crustal collapse and thinning of overthickened crust following cessation of subduction.

### 6.5.5: Synthesis: a model for the petrogenesis of the Hohonu Super-suite.

Generation of the Hohonu Super-suite granitoids is believed to be intimately related to crustal extension in the Western Province. This is indicated by:

A: The strong temporal and geochemical similarities of the Hohonu Super-suite and the Buckland Granite, and the intimate relationship between Buckland Granite, crustal scale extension in the Paparoa Metamorphic Core Complex, and the extensional basins of the Pororari Group.

B: The virtually contemporaneous emplacement of the Hohonu Super-suite with the cessation of subduction along the Gondwana margin, removing the compressive forces causing thickening of Western Province crust.

A possible model is proposed whereby generation of the Hohonu Super-suite magmas occurred during thermal relaxation, rapid uplift and thinning of continental crust (perhaps associated with mantle delamination) previously thickened by collision of the MTZ and the Western Province. Mafic underplating associated with adiabatic melting of the underlying mantle, and isothermal heating of the lower crust during rapid uplift, resulted in crustal melting and the generation of granitoid magmas. A schematic model of events leading to the generation of the Hohonu Super-suite is presented in Fig.6.64.

Geochemical and isotopic data indicate the source for the Hohonu Super-suite was a mixture of Separation Point-type depleted mantle melts and a complex lower crustal component (Ch.6.5.2). The mantle-derived melts may have been generated during adiabatic melting of the underlying mantle as illustrated in Fig.6.64, or alternatively represent crustal melts generated from the same mafic underplate which generated the Separation Point Batholith. These components have combined to produce a source with relatively tightly constrained compositions ($Sr_{(110)}$ = 0.7062 to 0.7085, $\epsilon Nd_{(110)}$ = -4.4 to -6.1 and $T_{DM} \approx$ 1.2 Ga).

The geochemical contrasts between the two constituent suites of the Hohonu Super-suite are a consequence of melting of this source at differing water fugacities and with differing residual assemblages. The Deutgam Suite represents tonalitic to granodioritic I-type metaluminous melts generated in equilibrium with an amphibolitic residue during dehydration melting of a meta-basaltic source at relatively shallow regions of the crust ($<$10 kb $\approx$35 km). Residual plagioclase retains Sr, Ba, $Al_2O_3$, $Na_2O$ and Eu and results in relatively low contents of these elements in the Deutgam Suite. The Te Kinga Suite represents $SiO_2$-rich, weakly peraluminous melts formed in equilibrium with an eclogitic residue (garnet + amphibole) during melting of the same source at greater depths ($>$10 kb) and greater water fugacities. The lack of residual plagioclase in the Te Kinga Suite enriches the melt in Sr, Ba, $Al_2O_3$, $Na_2O$ and Eu, and residual garnet retains HREE, resulting in the distinguishing compositions of the Te Kinga Suite. A schematic portrayal of the generation of the two constituent suites of the Hohonu Super-suite is presented in Fig.6.65.

Following melting, the tonalitic-granodioritic I-type metaluminous melts of the Deutgam Suite segregate from source and migrate to upper crustal levels ($\approx$4 kb), fractionating amphibole, plagioclase and alkali feldspar *en route*. Te Kinga Suite melts are emplaced to slightly higher crustal levels and undergo only minor feldspar fractionation in the process. Slightly lower $Na_2O$, $Al_2O_3$, Ba and Sr in the Arahura Granite, as compared to the Te Kinga Monzogranite, are suggestive of varying degrees of minor plagioclase retention in source or minor high level plagioclase fractionation.

## 6.6: Geochemistry of the French Creek Suite

### 6.6.1: Introduction.

The French Creek Granite is a composite body comprising several intrusive bodies with physical and petrological features typical of A-type granitoids, emplaced along the northwestern margin of the Hohonu Ranges. Field geology and petrography of French Creek Granite are discussed in detail in Ch.3.7 and indicate emplacement as a wholly molten, relatively anhydrous magma at shallow, sub-volcanic levels. Several variants of the French Creek Granite are identified; the dominant subsolvus biotite syenogranite (subsolvus-FCG) and volumetrically minor hypersolvus amphibole monzogranite (hypersolvus-FCG) and quartz alkali feldspar syenite (QAF-syenite). A single sample of aegirine arfvedsonite alkali feldspar syenite (LHR10) was also collected from float but not found *in situ*. These rocks, composite dikes cutting the French Creek Granite, and rhyolitic dikes intruding the Deutgam Granite are here included within the French Creek Suite.

French Creek Suite is alkalic with a Peacock Index of $\approx$44-45 (Fig.6.4), and is peraluminous to weakly metaluminous to peralkaline (Fig.6.5) with A/CNK and A/NK close to 1. As indicated previously, French Creek Suite is distinguishable chemically from the Hohonu Super-suite by enrichment of the high field strength elements (HFSE) (Zr, Nb, LREE), high $Fe_2O_3$, and low Ba, Sr and CaO contents (see Fig.6.8).

### 6.6.2: Major elements.

The subsolvus-FCG and hypersolvus-FCG have overlapping, high $SiO_2$ contents (71-76%) and both display reasonable trends of decreasing $TiO_2$, $Al_2O_3$, $Fe_2O_3$, CaO and $P_2O_5$ with increasing $SiO_2$ (Fig.6.66). $Na_2O$ and $K_2O$ scatter but also decrease

broadly with $SiO_2$. This scatter, and the peraluminous compositions, may be a consequence of deuteric alteration and exchange and loss of alkalies. French Creek Suite is characterized by very low contents of CaO (0.2-1.1 wt%) and MgO ($\approx$0.3 to below XRF detection limits (0.05 wt%)) (Fig.6.66). Predominantly weakly peraluminous compositions of subsolvus-FCG contrast with weakly metaluminous to weakly peralkaline compositions of hypersolvus-FCG, a consequence of lower $Al_2O_3$ and higher $Na_2O$ contents in the latter.

The QAF-syenite is distinctly more mafic than typical subsolvus-FCG and hypersolvus-FCG ($SiO_2$ = 62-63 wt%) and is weakly metaluminous to peraluminous (A/CNK = 0.99-1.17). QAF-syenite has lower $TiO_2$, $Fe_2O_3$, MgO, CaO, $K_2O$ and $P_2O_5$ and higher $Na_2O$ and $Al_2O_3$ than would be expected by continuing linear trends observed in the remainder of French Creek Suite (Fig.6.66). Low totals in EHR3 were found to be a consequence of $\approx$1.41 weight percent $SO_3$.

**6.6.3: Trace elements.**

French Creek Suite is characterized by low contents of Cr (<7 ppm), Ni (<6 ppm), V (<13 ppm) and Sr (10-80 ppm) and distinctly high Zr (240-750 ppm), Nb (45-105 ppm), Ga (18-32 ppm) and Y (35-60 ppm), features typical of many A-type granitoids (Whalen *et al* 1987, Eby 1990 and 1992) (see Fig.6.8). Ba and Sr decrease consistently with increasing $SiO_2$, whereas Rb shows a crude increase (Fig.6.67), resulting in Rb-Sr ratios increasing to high values (up to 30) with increasing $SiO_2$ (Fig.6.68). Because $SiO_2$ cannot increase much above minimum melt compositions (76% $SiO_2$) most incompatible elements increase with little change in $SiO_2$.

The hypersolvus-FCG has generally lower Ba, Rb and Sr contents and higher Nb and REE (Ce+Y) contents than the subsolvus-FCG. Particularly distinct are elevated Zn and Zr contents in hypersolvus-FCG (Fig.6.67). This feature has also been observed in peralkaline, hypersolvus A-type granitoids, as compared with metaluminous or peraluminous subsolvus A-types, in Australia (Collins *et al* 1982). These authors attribute higher Zr contents to the presence of excess alkalis and high F

contents[14] in peralkaline melts. Excess alkalis over aluminium increases the solubility of Zr and prevents zircon crystallization, thereby concentrating Zr in the liquid phase. Prior to the final stages of crystallization, when biotite and amphibole remove F, most Zr probably exists as Na-Zr-F complexes. In a similar manner Zn forms complexes with F at high temperatures and high Zn concentrations can also be explained by these processes (for a more detailed discussion see Collins *et al* 1982 and Taylor *et al* 1981).

Compared with the remainder of the French Creek Suite the QAF-syenite has similar HFSE, and relatively low REE and Cr and high Sr and Ba (Fig.6.67).

**6.6.4: Spider-diagrams.**

Mantle-normalized multi-element diagrams of French Creek Suite (Fig.6.69) indicate highly fractionated compositions. Large negative troughs at Ba, Sr, $P_2O_5$ and Ti are consistent with removal of feldspar, apatite and a Ti-bearing phase such as Fe-Ti oxide, biotite or amphibole. Negative Nb-Ta anomalies are absent, immediately distinguishing these rocks from others of the batholith, and reflect the high Nb contents of the French Creek Suite. Negative Nb-Ta anomalies are commonly related to subduction processes (as discussed in Ch.6.2.2.1) and their absence is typical of many anorogenic, intraplate rocks such as the French Creek Suite. Compared with Hohonu Super-suite (Fig.6.11), French Creek Suite plots are slightly convex up reflecting higher HFSE contents and greater depletion of the compatible elements, illustrative of the highly fractionated nature of the samples. The subsolvus-FCG and hypersolvus-FCG display virtually identical spider-diagrams, although the higher Zr and LREE and lower Ba and Sr of the hypersolvus-FCG are evident.

Compared with typical subsolvus-FCG the QAF-syenite is similar but less evolved with smaller negative Ba, Sr, $P_2O_5$ and $TiO_2$ troughs, lower LREE and Y and higher $Na_2O$ (Fig.6.70). Such plots suggest that the QAF-syenite may represent a primitive, less evolved variant of the dominant French Creek Granite.

---

14: A sample of subsolvus French Creek Granite (P45456 (K32 751385) Tulloch and Robertson 1987) has high fluorine contents (838 ppm F at 73.37% $SiO_2$) typical of many A-type granitoids. Despite high fluorine contents, fluorite has not been identified optically. Several microprobe analyses of biotite indicate a maximum of $\approx$1 wt% fluorine (Ch.4.2) suggesting most fluorine could be residing in biotite and possibly also fluorapatite.

**6.6.5: Rare Earth Elements.**

Five samples of subsolvus-FCG display REE plots typical of many A-type granitoids (Whalen *et al* 1987, Eby 1992). The subsolvus-FCG has LREE enriched ($La/Yb_N$ = 7.59-13.99), convex down plots with flat HREE ($Gd/Yb_N$ = 1.18-1.91) (Fig.6.71) and large negative Eu anomalies (Eu/Eu* = 0.16-0.36), indicative of significant feldspar fractionation. Decreasing Sr and Ba coupled with increasing Eu/Eu* are also indicative of feldspar fractionation. The samples are enriched in total REE (ΣREE = 283-437 ppm), also typical of A-type granitoids. Flat HREE contents and relatively abundant Y suggest a source containing stable plagioclase. No samples of hypersolvus-FCG or QAF-syenite were analyzed for REE in this study.

**6.6.6: Nd and Sr isotopes.**

Radiogenic isotope data for the French Creek Suite and associated rocks are presented in Table 6.8 (see also Fig.6.81). Although $\epsilon Nd_{(83)}$ values are relatively restricted (+0.5 to +2.5) and primitive, $Sr_{(83)}$ is much more scattered, ranging from 0.7055 to 0.7098[15], and does not show consistent variation with increasing $\epsilon Nd_{(83)}$. Positive $\epsilon Nd_{(83)}$ values suggest a strong mantle component during petrogenesis, whereas the wide range in $Sr_{(83)}$ (larger than that observed in the Hohonu Super-suite) also suggests the involvement of radiogenic continental crust. The spread in $Sr_{(83)}$ is largely produced by two samples (EHR17 and EHR14), the clustering of the remaining samples and the crude whole rock Rb-Sr isochron for French Creek Granite suggest an initial Sr ratio of $\approx$0.7065 (see Fig.5.3). The only sample of hypersolvus-FCG analyzed (EHR14) has $\epsilon Nd_{(83)}$ more primitive than the subsolvus-FCG (+2.49), but also has more radiogenic $Sr_{(83)}$ (0.70929). Calculated $T_{DM}$ ages are mostly between 600 to 700 Ma, except for EHR17 with a $T_{DM}$ of $\approx$1100 Ma.

The wide scatter of $Sr_{(83)}$ in French Creek Granite is incompatible with mixing with any exposed country rock as $Sr_{(83)}$ and $\epsilon Nd_{(83)}$ do not exhibit trends typical of mixing between a low $Sr_{(83)}$, high $\epsilon Nd_{(83)}$ magma and a high $Sr_{(83)}$, low $\epsilon Nd_{(83)}$ country rock (see Fig.6.81). Low Sr contents (10-80 ppm), and high Rb-Sr ratios indicate small variations in Sr concentration (either due to contamination or analytical error) will result in large variations in calculated $^{87}Rb/^{86}Sr$ and decay corrected initial $^{87}Sr/^{86}Sr$.

---

15: Tulloch *et al* (1994) report a $Sr_{(83)}$ value of 0.707, within the range observed here.

Low Sr contents also indicate small amounts of contamination by the higher Sr country rocks will result in large changes in measured $^{87}Sr/^{86}Sr$. Scatter in the Sr isotope data is therefore interpreted as varying degrees of contamination by high $^{87}Sr/^{86}Sr$ country rock.

### 6.6.7: Dikes associated with French Creek Suite.

Trachyte to rhyolite dikes restricted to the Hohonu Ranges are considered to be petrogenetically related to the French Creek Granite. Most of these dikes have chemistries similar to varieties of the French Creek Granite and also plot within the A-type or Within-Plate Granitoid fields of various tectonic discrimination diagrams.

#### 6.6.7.1: Composite dikes.

Several relatively wide (up to 12 m) porphyritic trachyte to rhyolite dikes are observed intruding both subsolvus-FCG and hypersolvus-FCG. The dikes are consistently dark brown to orange, suggestive of highly oxidized compositions. The dikes are typically composite, being strongly zoned from margin to core and classify chemically as trachyte (LHR5), trachydacite (EHR27) to rhyolite (EHR11, EHR26, EHR18, LHR6) (Fig.6.72). One dike in the Eastern Hohonu River ($\approx$K32 755380) grades smoothly from orange rhyolite in the core (EHR26) to brown trachydacite (EHR27) to thin rim of grey-black trachybasalt (EHR28) similar to many Hohonu Dike Swarm compositions at its margin (see Fig.7.5). Petrographically, the composite dikes consist of varying proportions of alkali feldspar, plagioclase (deuterically altered to albite) and occasional euhedral, embayed quartz phenocrysts set in a felsitic to spherulitic groundmass. All mafic phases have been altered to blue-green chlorite. These dikes are similar in description to "trachyandesite" dikes cutting the Deutgam Granite described by Hamill (1972).

Composite dikes have $SiO_2$ contents mostly between 64-67%, although a single dike is more felsic with 72% $SiO_2$. The dikes are oversaturated and weakly peraluminous (A/CNK = 1.01-1.05) and generally lie at the mafic end of most Harker plots of French Creek Suite (see Fig.6.66, Fig.6.67). The peraluminous nature of these dikes may be attributable to Na loss during crystallization as described for similarly peralkaline silicic lavas on Mayor Island (Weaver *et al* 1990). Mantle normalized

spider-diagrams of the composite dikes (Fig.6.73) display negative troughs at Ba, Sr, $P_2O_5$ and $TiO_2$, somewhat smaller and less evolved than typical French Creek Granite. Composite dikes are geochemically intermediate between typical French Creek Suite and average Hohonu Dike Swarm, suggesting a genetic link between the two. Their oversaturated nature indicates they may be related to the subordinate saturated to oversaturated trend observed in the Hohonu Dike Swarm proper (see Fig.7.10). In addition, the composite dike which grades into mafic material at its margins also suggests affinities with the Hohonu Dike Swarm. The mafic material (EHR28) is a clinopyroxene porphyritic basaltic trachyandesite, and apart from somewhat more enriched LILE contents, consistent with its slightly higher $SiO_2$ contents, is similar to average Hohonu Dike Swarm compositions (Fig.6.73).

**6.6.7.2: Trachyte dikes.**

Two blue trachyte dikes (EHR6 and EHR21) intruding Deutgam Granite have $SiO_2$ contents of $\approx$63.5%, and are distinct from other composite trachyte dikes in that they are thinner, much less altered, are not compositionally zoned and they are not restricted to French Creek Granite. These dikes may be equivalent to the quartz trachytes described by Hamill (1972). The trachyte dikes are weakly metaluminous and have very similar chemistry to the QAF-syenite (Fig.6.74). Both dikes may represent hypabyssal dikes derived from the QAF-syenite, in particular EHR21 was collected in a small tributary immediately upstream of the contact between QAF-syenite and Deutgam Granite. Further links between the trachytes and the QAF-syenite are given by high $SO_3$ ($\approx$2.80 wt%) in EHR21, a similar high $SO_3$ content was also obtained for a sample of QAF-syenite (EHR3).

**6.6.7.3: Rhyolite Dikes cutting Deutgam Granite.**

Cream to blue rhyolitic dikes containing abundant alkali amphiboles (see Ch.3.12.2), intrude Deutgam Granite on the Hohonu Ranges. These dikes have been previously interpreted as highly evolved end-members of the Hohonu Dike Swarm (Soda rhyolites of Hamill 1972), or as hypabyssal equivalents of the French Creek Granite (Tulloch *et al* 1994). Although rhyolites are observed to rarely cut the mafic dikes of the Hohonu Dike Swarm, the opposite is also true and no consistent age relationship between the two sets of dikes can be established. No rhyolite dikes were

observed to intrude French Creek Suite granitoids, suggesting that they may predate intrusion of French Creek Granite.

The rhyolites are typically very highly evolved with $SiO_2$ values between 74.2 to 77.1% (average = 76.0%), and have ASI values identical to typical French Creek Suite, being weakly peraluminous to metaluminous to peralkaline (A/CNK = 0.92-1.04, A/NK = 0.94-1.09). High Rb/Sr (3-55, see Fig.6.68) reflects generally low Sr concentrations. The rhyolites are comenditic (*sensu* Le Maitre *et al* 1990) and generally plot at the high $SiO_2$ end of geochemical trends within French Creek Suite (see Fig.6.66 and Fig.6.67).

Spider-diagrams (Fig.6.75) illustrate that, compared with typical subsolvus-FCG, the rhyolite dikes are more evolved with larger depletions of Ba, Sr, P and $TiO_2$, consistent with fractionation of feldspar, apatite and Fe-Ti-oxides. Additionally, the rhyolites have higher contents of Rb and Nb, suggesting these elements continued to behave incompatibly during fractionation (Fig.6.75). Distinctly lower contents of La, Ce, Nd and Y suggests removal of both LREE and HREE bearing phases such as apatite, zircon and/or allanite, or loss of REE associated with the loss of volatiles on crystallization and devitrification of peralkaline magmas (Weaver *et al* 1990).

A single isotope analysis of a rhyolitic dike (HDP8, Table 6.8) has $\epsilon Nd_{(83)}$ within the range observed in the French Creek Granite, suggesting the rhyolites are hypabyssal equivalent of the granitoids, as previously indicated by Tulloch *et al* (1994). HDP8 has $\epsilon Nd_{(83)}$ most similar to the hypersolvus-FCG, suggesting a greater affinity to this unit, however, it is likely that further analyses of rhyolite dikes would encompass the entire spectrum of compositions observed within both the subsolvus-FCG and hypersolvus-FCG. $Sr_{(83)}$ for this rhyolite is unrealistically low (Table 6.8), probably a consequence of very low Sr contents ($\approx$3 ppm) and high Rb/Sr ($\approx$122). Small variations in Sr will radically change Rb/Sr and thus the decay-corrected initial ratio. Such variations may be a consequence of Sr loss during alteration, analytical error or

small amounts of contamination by country rocks[16]. The large variability in calculated initial Sr ratios means that little significance can be placed on this analysis.

**6.6.8: Petrogenesis of the French Creek Suite.**

Numerous geochemical tectonic discrimination diagrams have been published to distinguish the highly characteristic chemistries of A-type granitoids from more typical I- and S-type granitoids, generally utilizing the distinctly high contents of HFSE. All varieties of French Creek Granite, and associated rhyolite and composite dikes, plot consistently within the fields of A-type or Within-Plate granitoids in these diagrams (Fig.6.76). In addition, mineralogical, geochemical and field characteristics of French Creek Suite indicate designation as a typical A-type granitoid.

Literature concerning A-type granitoids has been reviewed by Whalen *et al* (1987), and more recently by Eby (1990 and 1992). Several models have consequently been proposed for the origin of A-types granitoids, including:

1: Melting of a residual granulite source, previously depleted by removal of an I-type melt (Collins *et al* 1982, Clemens *et al* 1986, Whalen *et al* 1987).
2: Melting of I-type tonalite or granodiorite (Sylvester 1989, Creaser *et al* 1991, Weaver *et al* 1992).
3: Fractionation of a mantle derived melt, undergoing varying degrees of interaction with continental crust (Loiselle and Wones 1979, Eby 1990 and 1992, Eby *et al* 1992, Turner *et al* 1992).

The relatively primitive radiogenic isotopic compositions of the French Creek Suite immediately preclude an origin involving melting or fractionation of the much more radiogenic Hohonu Super-suite I-type granitoids. Melting of depleted residual sources remaining after generation of the Hohonu Super-suite is also precluded by the radically different isotopic compositions of the Hohonu Super-suite and the French Creek Suite. Y-Nb ratios for both the Hohonu Super-suite and Greenland Group ($\approx 2$)

---

**16:** For example, data presented in Table 6.8 uses isotope dilution Rb-Sr ratios, if XRF Rb/Sr (=164) is used, an increase in $Sr_{(83)}$ to 0.82971 results.

are significantly higher than the low values observed in French Creek Suite ($\approx$0.6-1.0) and also preclude derivation from exposed country rocks.

Relatively primitive radiogenic isotope compositions of French Creek Suite are consistent with involvement of a major mantle component during petrogenesis. Derivation by fractionation of a mantle-derived melt is also indicated by French Creek Suite plotting consistently in the $A_1$ sub-type granitoid fields of the discrimination diagrams of Eby (1992) (Fig.6.77). $A_1$ sub-type granitoids have trace element compositions similar to ocean island basalts (Fig.6.77) and are interpreted to be extreme crystal fractionates of mantle-derived melts, generally occurring in regions of continental rifting, or related to hotspots or mantle plumes[17] (Eby 1992). Such an origin is consistent with the relatively primitive radiogenic isotopes and the 81.7 Ma age (Ch.5) for the French Creek Granite. This age is coincident with separation of Australia and New Zealand, the appearance of the first oceanic crust in the Tasman Sea and thus an unequivocal continental rifting environment (see Ch.6.6.10).

Geochemical data indicate that French Creek Suite has undergone large amounts of fractionation, consistent with derivation via prolonged fractionation of a mafic mantle melt. High Rb/Sr, low contents of CaO, $Al_2O_3$, and large depletions of Sr and Ba and Eu are diagnostic of major plagioclase ($\pm$ alkali feldspar) fractionation. Low MgO contents, relatively high $Fe_2O_3$/MgO and low transition elements (Cr, Ni, V) are also indicative of prolonged fractionation of mafic phases (clinopyroxene and/or amphibole) within French Creek Suite, or its mafic precursors, prior to emplacement. Petrographic evidence suggests that biotite crystallized late in the subsolvus-FCG as $H_2O$ became concentrated at the final stages of crystallization, therefore it is unlikely to have acted during crystal fractionation processes, and removal of alternative mafic phases must have occurred at more primitive compositions. Although sodic amphiboles in the hypersolvus-FCG are euhedral to subhedral and could potentially be fractionating phases, there is little evidence for this chemically (see Fig.6.80). Large depletions of $P_2O_5$ and $TiO_2$ suggest removal of apatite and Fe-Ti oxides or some other Ti-bearing mineral.

---

17: $A_2$ sub-type granitoids have element ratios intermediate between continental crust and island arc basalts, and are interpreted as being derived from continental crust, or crust that has been through a cycle of continent collision or island arc magmatism (Eby 1992).

The high LREE and HFSE of A-type granitoids indicate that they cannot be derived from a typical chondritic or depleted mantle, or by crustal contamination and fractionation, therefore a relatively enriched mantle source is required (e.g. Martin *et al* 1994). A potential enriched mantle source has also been tapped by the closely associated and partially contemporaneous Hohonu Dike Swarm (Ch.7). Thus the French Creek Suite may represent differentiation products of either the Hohonu Dike Swarm itself, or basic magmas derived from the same source.

**6.6.9: Generation of the French Creek Suite by fractionation of the Hohonu Dike Swarm.**

Radiogenic isotopes and trace element data are consistent with derivation of French Creek Suite by extreme fractionation of an enriched mantle-derived basic melt. The hypothesis that these parent magmas are represented by the Hohonu Dike Swarm is now tested.

Field studies indicate an intimate relationship between the Hohonu Dike Swarm and the French Creek Suite (Ch.7). Although the bulk of the Hohonu Dike Swarm pre-dates French Creek Granite, occasional cross-cutting dikes, and the composite dike grading into Hohonu Dike Swarm-like compositions described above, indicates that mafic activity continued during and after intrusion of French Creek Granite. Although the majority of the Hohonu Dike Swarm is undersaturated and evolves towards strongly Ne-normative phonolitic compositions, several dikes are saturated and evolve towards weakly oversaturated compositions (Fig.7.10) and may represent parental compositions to the French Creek Suite. The composite and rhyolite dikes described above may represent an extension of this trend. A consequence of this is that the hypotheses that rhyolitic dikes on the Hohonu Ranges represent extreme differentiates of the Hohonu Dike Swarm (Hamill 1972) or hypabyssal equivalents of the French Creek Suite (Tulloch *et al* 1994) are not necessarily mutually exclusive. No field evidence is present for magma mingling or mixing between French Creek Granite and the Hohonu Dike Swarm.

Harker diagrams, using data from French Creek Suite, saturated and oversaturated members of the Hohonu Dike Swarm, composite dikes and rhyolite dikes,

form consistent trends for most major and trace elements (Fig.6.78). The composite dikes act as intermediate "links" between the Hohonu Dike Swarm and French Creek Suite on most Harker plots, although as these dikes obviously post-date the French Creek Granite they cannot represent actual intermediate compositions. $TiO_2$, $Fe_2O_3$, MnO, MgO, $P_2O_5$ and CaO all decrease systematically from the mafic dikes through to the French Creek Suite (Fig.6.78). $Na_2O$ increases slightly in the Hohonu Dike Swarm and decreases slightly in the French Creek Suite and $K_2O$ increases consistently with increasing $SiO_2$. $Al_2O_3$ increases in the dikes and then decreases in the French Creek Suite. Cr, Ni and Sr decrease with increasing $SiO_2$ to very low levels in the French Creek Suite, whereas Rb, Th and the LREE increase from the dikes through to the granitoids. Ba, Zr, and Zn increase initially in the saturated dikes then decrease in the French Creek Suite. The QAF-syenite often plots off trends between typical French Creek Suite and the Hohonu Dike Swarm, indicating a separate origin. Major chemical modification by metasomatism is likely given the highly altered nature of the QAF-syenite, therefore the chemistry of these rocks is treated with caution. Some feldspar accumulation may be indicated by the much higher $Na_2O$ and $Al_2O_3$ contents of the QAF-syenite.

Trends on Harker diagrams are consistent with an origin of the French Creek Suite by extreme fractionation of feldspar (predominantly plagioclase, although decreasing Ba and $Na_2O$ suggest some albite/alkali feldspar fractionation also occurred at later stages in the French Creek Granite) and various mafic phases from the Hohonu Dike Swarm. Low MgO and transition element contents, and relatively consistent chemical compositions, in French Creek Granite suggest most fractionation, particularly of mafic phases, had occurred prior to its emplacement.

A major silica gap exists between the most felsic member of the Hohonu Dike Swarm ($\approx$ 51% $SiO_2$) and the most mafic of the granitoids and composite dikes ($\approx$ 61% $SiO_2$). Such "Daly gaps" have been often raised as objections to a fractionation origin for A-types (e.g. Bailey 1987, Sylvester 1989) yet are relatively common (e.g Ascension Island, Emuruangogolak (Weaver 1977)) and by themselves do not disprove a fractionation model (Turner *et al* 1992). Daly gaps have been attributed to density contrasts during magma differentiation (Baker 1987).

If the Hohonu Dike Swarm and French Creek Suite are cogenetic, a simple test would be preservation of incompatible trace element ratios, as is generally accepted during evolution via fractional crystallization. A plot of Ce - Y (Fig.6.79) indicates that the French Creek Suite and Hohonu Dike Swarm have similar ratios and that evolution has occurred without significant preferential removal of either the HREE or LREE in accessory phases. However, disparate and generally lower values in the rhyolitic dikes indicate REE removal via fractionation of accessory phases such as zircon, apatite and allanite, or REE loss in volatile phases during crystallization. In addition, Y-Nb, Ga-Nb, Y-Zr and La-Zr ratios are relatively similar in both the French Creek Suite, Hohonu Dike Swarm and intermediate dikes, suggesting a common source and origin via crystal fractionation (Fig.6.79). Again, lack of preservation of incompatible element ratios in the rhyolitic dikes reflects removal of accessory phases or chemical modification during crystallization and devitrification (Weaver *et al* 1990). Isotopic data indicate the French Creek Suite did not act as a simple closed system, and some scatter in trace element ratios may also be a consequence of crustal contamination. It is valuable to note that the consistency of trace element ratios means the Hohonu Dike Swarm also plots in the OIB region typical of $A_1$ sub-type granitoids in the discrimination plots of Eby (1992) (Fig.6.77).

Log-log plots using Sr, Rb and Ba (Fig.6.80) indicate a two stage evolutionary history. Fractionation trends for the saturated members of the Hohonu Dike Swarm are consistent with those for the swarm as a whole (Ch.7), indicating removal of a combination of plagioclase, amphibole, olivine and clinopyroxene during evolution. The trends of the Hohonu Dike Swarm intersect with those of the mafic end of the composite dike and French Creek Suite spectrum. Fractionation vectors indicate much of the variation in the French Creek Suite can be produced by fractionation of alkali feldspar with lesser amounts of plagioclase. These trends are consistent with the petrographic presence of either a single mesoperthitic feldspar, or abundant alkali feldspar and minor albite to sodic oligoclase. Fractionation of a single, ternary feldspar has important consequences for the geochemical evolution of a pluton, yet probably only occurs at very shallow levels, and has been discussed by Fuhrman *et al* (1988). No evidence for major amphibole or biotite fractionation in the French Creek Suite is

evident in Fig.6.80, suggesting depletion in the ferromagnesium and transition elements occurred prior to emplacement of French Creek Granite.

Isotopic data (Table 6.8, Table 7.2, Fig.6.81) indicate that French Creek Suite is more radiogenic than the Hohonu Dike Swarm and the two cannot be related by direct, closed system crystal fractionation. Minor crustal contamination could easily produce the observed isotopic compositions and such contamination is also indicated by the variable $Sr_{(83)}$ isotopic data. Simple mixing, using the equations of Langmuir *et al* (1978), indicates that French Creek Suite isotopic compositions can be achieved by $\approx$25% mixing between a typical saturated mafic dike (IQ5) and Greenland Group, although given the wide range of $Sr_{(83)}$ ratios this can only be considered as a crude estimate (Fig.6.81). Mixing between Hohonu Dike Swarm and typical Hohonu Super-suite granitoid (HRS12) requires larger amounts of mixing and fails to produce isotopic compositions similar to French Creek Granite (Fig.6.81). More isotopic data are needed to further constrain the mixing history of the French Creek Suite. Uniform geochemical compositions and a lack of enclaves suggests that interaction with continental crust occurred at depth and was homogenized by later convection, suggesting contamination by small degrees of lower continental crust (see Ch.6.5.2.1) seems more likely. Higher level interaction of low-Sr French Creek magmas with continental crust probably caused the wide range of observed initial Sr values. $T_{DM}$ model ages for the French Creek Suite are mostly $\approx$600-700 Ma, distinctly older than $\approx$350-450 Ma for the Hohonu Dike Swarm, consistent with mixing between the Hohonu Dike Swarm and the older $T_{DM}$ of the Greenland Group.

A MASH type model (as proposed by Hildreth and Moorbath 1988, and applied by Eby *et al* 1992) is envisaged. Mantle-derived magmas, derived from an isotopically-depleted (relative to Bulk Earth) yet trace element-enriched source with OIB-like characteristics, pond at the base of the crust. Given the extensional tectonic environment (Ch.6.6.10), the base of the crust was most likely at relatively shallow levels ($<$10 kb) allowing for the presence of stable plagioclase. The magmas evolve via crystal fractionation of plagioclase, clinopyroxene, hornblende and olivine to evolved, oversaturated A-type compositions. Other magmas derived from the same mantle source are emplaced directly to higher crustal levels and form the alkali basalt

to phonolite trend of the Hohonu Dike Swarm (see Ch.7.7.2). Minor crustal contamination occurs within the magma chamber, and then the homogeneous magmas are emplaced to high crustal levels, slightly predated by emplacement of the rhyolitic dikes. Further fractionation of predominantly alkali feldspar, with minor plagioclase, possibly coupled with crustal interaction and contamination also occurs. Continued mantle-derived activity in the magma chamber results in the intrusion of composite dikes.

This model, and geochemical data, indicate large amounts of fractionation have occurred to produce the French Creek Suite. The question then arises, where are the cumulates? No cumulate rocks are exposed, however, they may be tentatively be indicated at relatively shallow levels in the crust (due to thinning associated with crustal breakup) by a large (220+ nanotesla) aeromagnetic anomaly (DSIR geophysics division unpublished data, Robinson and Davey 1981) and a positive Bouguer anomaly (Bennie and Ferry 1977) centred on the central Hohonu Ranges. Alternatively, cumulates may have returned to the mantle due to their high density contrast compared with continental crust, as recently proposed by Glazner (1994).

### 6.6.10: Tectonic environment of emplacement.

French Creek Suite compositions plot consistently within the A-type fields of published geochemical discrimination diagrams (Fig.6.76, Fig.6.77). A-type granitoids are generally considered to indicate anorogenic environments, or more specifically in the case of $A_1$ sub-types (such as the French Creek Suite), environments of continental rifting, hotspot or mantle plume activity (Eby 1992). As discussed further in Ch.7, the age of 81.7 $\pm$ 1.8 Ma for French Creek Granite, and the contemporaneous Hohonu Dike Swarm, is consistent with emplacement into an anorogenic, rifting environment. The late Cretaceous was an unambiguous period of continental extension in the Western Province, as indicated by abundant erosion, the formation of sedimentary basins and the intrusion of alkaline mantle-derived magmas (Nathan *et al* 1986, Tulloch *et al* 1994). The Late Cretaceous age of the French Creek Granite also coincides remarkably well with the appearance of the first oceanic crust in the Tasman Sea (Chron 33 at $\approx$82 Ma, Weissel and Hayes 1977, Stock and Molnar 1987, Tulloch *et al* 1994). The emplacement of the Hohonu Dike Swarm is closely related to extension associated with

Australia-New Zealand continental breakup, as indicated by a strong preferred NNE-SSW orientation of the swarm parallel to the line of eventual continental breakup (Ch.7). Therefore, genetic links between the French Creek Granite and Hohonu Dike Swarm are also indicative of an anorogenic, extensional continental rifting environment of emplacement, associated with the separation of Australia from New Zealand.

Laird (1993, 1994) recognized at least two extensional periods in the Cretaceous history of the Western Province, one in the mid-Albian, associated with generation of the Hohonu Super-suite (Chap.6.5.4), and a second at around 80-84 Ma (mid-Campanian) associated with Tasman Sea opening. The late Cretaceous rifting event is marked by the onset of a major transgression and the deposition of glauconitic sandstones and limestones. Extension paralleled the line of opening of the Tasman Sea and deposition of late Cretaceous coal measures occurred, often in basins developed in the earlier mid-Albian extensional phase (Laird 1993). The occurrence of relatively abundant alkaline magmatism at $\approx$82 Ma, closely associated with a strong extensional event, is suggestive of decompressional melting of mantle material as a result of stretching and thinning of the lithosphere during rifting, as modelled by M$^c$Kenzie and Bickle (1988) and Keen *et al* (1994). In contrast to the petrogenesis of the Hohonu Super-suite, where similar processes are believed to have occurred (Ch.6.5.4), this thinning and melting occurred in crust already thinned by the mid-Albian event, allowing high level intrusion of mafic melts as represented by the Hohonu Dike Swarm. Some ponding of material at the base of the already thinned crust lead to generation of the French Creek Suite. It is interesting to note that the sites of previous Hohonu Super-suite/Rahu Suite magmatism and associated extension, were again the sites of renewed late Cretaceous extension and magmatism, as indicated by the presence of the Hohonu and Buller Gorge Dike Swarms (Adams and Nathan 1978).

The extensional environment operating at the time of French Creek magmatism allowed rapid intrusion to shallow crustal depths ($\approx$1 kb) and the consequent generation of miariolitic cavities and hypersolvus textures. Despite the strong WNW-ESE trend of the Hohonu Dike Swarm parallel to the regional extension (Ch.7), French Creek Granite is oriented NE-SW. Intrusion was most likely controlled by a

pre-existing crustal anisotropy created by the contact between Deutgam Granite and Greenland Group.

**6.6.11: Regional discussion.**

Magmatism associated with Gondwana breakup is widespread in New Zealand, particularly in the Eastern Province. A distinct burst of alkaline, anorogenic magmatism in the Eastern Province of New Zealand occurs around 100-80 Ma, (i.e. Blue Mountains (Grapes 1975), Mount Somers Volcanic Group including Banks Peninsula rhyolites (Barley *et al* 1988), Mandamus Igneous Complex (Weaver and Pankhurst 1991), Tapuaenuku Igneous Complex and nearby volcanics (Baker *et al* 1994)). Many of these ages are in the range 97-90 Ma and are presumably related to Antarctica-New Zealand break up. A slightly younger age of 80.9 $\pm$ 1.9 Ma from Banks Peninsula (Barley *et al* 1988) and a range of 85-98 Ma for the Mount Somers Group (Oliver and Keene 1989) may reflect the Tasman extensional event in the Eastern Province. A-type plutonism in Marie Byrd Land has also been linked to New Zealand-Antarctica separation (Weaver *et al* 1992, Weaver *et al* 1994). To date, intraplate magmatism in the Western Province related to Australia-New Zealand separation is restricted to the Hohonu Dike Swarm and French Creek Suite, the Buller Dike Swarm and possibly also the younger basalts at Kowhiterangi, Arahura-1 drillhole and Pike River (see Ch.7). The slightly earlier New Zealand-Antarctica event is not well represented magmatically in the Western Province, although the recent $\approx$ 101 Ma age for the Stitts Tuff (Muir *et al*, unpublished data 1994) begs the question of its tectonic significance. It therefore appears that during the late Cretaceous the entire New Zealand continent was undergoing major extension, allowing generation of numerous centres of mantle-derived alkaline magmatism.

As a final note, it is interesting to recognize that a similar sequence of events as those observed in the Hohonu Batholith is recorded in the Cretaceous of Marie Byrd Land (Weaver *et al* 1994). In Marie Byrd Land, I-type granitoids (believed to be subduction-related) are followed by mafic activity and partially contemporaneous, but mainly younger A-type plutonism related to New Zealand-Antarctica continental rifting. Similarly, in the Hohonu Batholith, I-type granitoids of the Hohonu Super-suite are

followed by mafic activity and the penecontemporaneous A-type activity of the French Creek Suite, associated with New Zealand-Australia breakup.

### 6.6.12: Conclusions: French Creek Suite.

The French Creek Suite is a typical A-type granitoid intruded into an anorogenic, extensional environment associated with continental break-up and the opening of the Tasman Sea. Field relationships indicate a penecontemporaneous relationship between the French Creek Granite and the Hohonu Dike Swarm, this is corroborated by geochemical data which suggests the French Creek Suite could be derived by prolonged fractionation of feldspar and mafic phases from a typical Hohonu Dike Swarm magma. Limited isotopic data indicate some contamination by more radiogenic continental crust may have occurred.

## 6.7: The Summit Granite suite: Geochemical discussion.

### 6.7.1: Major and trace elements.

The only Palaeozoic pluton in the Hohonu Batholith, the Summit Granite, is a highly evolved, two-mica monzogranite with $SiO_2$ contents of 72 to 75%. The pluton is weakly to strongly peraluminous with A/CNK of 1.05 to 1.22 and A/NK of 1.21 to 1.42 (see Fig.6.5). Summit Granite is chemically distinguishable from the other plutons of the Hohonu Batholith by relative enrichment in Pb and Rb (Fig.6.8), resulting in Rb-Sr ratios of about 2. Summit Granite is also relatively potassic with $Na_2O/K_2O$ less than one (see Fig.6.6).

High silica contents and limited geochemical variation in Summit Granite permits for only limited elucidation of fractionation history. Within the major elements reasonable trends of decreasing $TiO_2$, $Fe_2O_3$, MgO, CaO and $P_2O_5$, and increasing $Na_2O$ are observed with increasing $SiO_2$. Most trace elements have no consistent trend with $SiO_2$, although Zr decreases crudely with increasing $SiO_2$.

### 6.7.2: Mantle-normalized spider-diagrams.

Spider-diagrams of the Summit Granite (Fig.6.82) exhibit typical calc-alkaline granitoid patterns, similar to those of the Hohonu Super-suite, with troughs at Ba, Sr and Ti, symptomatic of feldspar and Fe-Ti oxide removal, and a marked Nb-(Ta)

depletion (see Ch.6.2.2.1 for discussion). Importantly, no major trough at P is evident, indicating apatite fractionation has not been an important process. High Y contents are consistent with relatively flat HREE pattern (see Ch.6.7.3). The REE (La, Ce, Nd) show crude decreases with increasing $SiO_2$, suggesting removal in a fractionating accessory phase. The aplitic sample, MT16, has distinctly low REE, Zr and to a lesser degree P, also suggesting further removal of the REE in accessory apatite and zircon at a late stage in the crystallization history of the pluton. The distinctively high Pb and Rb contents of the pluton are also evident.

**6.7.3: REE elements.**

Typical Summit Granite displays slightly convex down ($La/Yb_N$ = 1.5-8.5), LREE enriched chondrite-normalized REE plots with relatively flat HREE and negative Eu anomalies (Eu/Eu* = 0.36-0.62) (Fig.6.83). Flat HREE preclude the presence of garnet at source and the negative Eu anomaly is indicative of feldspar removal, consistent with the Sr and Ba troughs apparent in the multi-element plots (Fig.6.82). Summit Granite has overall low abundances of REE (ΣREE = 66 to 84 ppm), distinguishing it from other Hohonu Batholith granitoids (see Table 6.3). Low ΣREE may be a reflection of an original source with low total REE, or, more likely, removal of REE during fractionation of accessory phases such as apatite, monazite or zircon. The lack of a distinct negative P trough in Fig.6.82 appears to preclude major apatite fractionation. Monazite was not positively identified in the Summit Granite, but may also be important in controlling REE contents (Wark and Miller 1993, Zhao and Cooper 1993). A lack of available REE data precludes comparison with other Palaeozoic granitoids to establish if low ΣREE are characteristic of Palaeozoic magmatism. Analyses have been presented from Mt M$^c$Lean (Pickett and Wasserburg 1989), an undated pluton of the Tarn Summit Suite of Tulloch (1979a) and a sample from the Kakapotahi River (5AX of Mason and Taylor 1987). Mt M$^c$Lean is isotopically atypical of Palaeozoic plutonism and may represent melted Greenland Group (see Ch.6.7.4) and therefore is not comparable to the Summit Granite. The Tarn Summit sample (45089) shows a similar REE pattern to the Summit Granite, but has somewhat higher ΣREE with $La_N \approx 100$ and $Yb_N \approx 11$, possibly a consequence of its lower silica contents (66.29%). The Kakapotahi sample of Mason and Taylor (1987)

exhibits an unusually flat REE plot ($La/Yb_N$ = 1.26, $La_N \approx 30$) with a large Eu anomaly and is distinctly dissimilar to any Summit Granite analyses.

A single sample of Summit Granite (MT16) displays a distinct REE pattern with low LREE, depleted MREE and elevated HREE ($La/Yb_N$ = 1.52). The sample is aplitic, contains relatively abundant garnet and is atypical of the pluton as a whole. The accumulation of garnet and fractionation of apatite may explain the observed REE pattern and lower P in MT16 is consistent with a depletion of LREE by apatite removal. Concentration of garnet will enhance HREE contents. Similar "V"-shaped patterns are relatively common in leucogranitic systems and are commonly attributed to fractionation of REE-rich accessory minerals (e.g Zhao and Cooper 1993).

**6.7.4: Radiogenic isotopes.**

Three samples of Summit Granite were analyzed for Sr and Nd isotopes and results are presented in Table 6.9 and Fig.6.84. Isotopic compositions of the Granite Hill and Fraser Complexes, Greenland Group and several other Palaeozoic plutons are also included for comparison and discussion. All isotope data are decay-corrected to 381 Ma following the SHRIMP age on the Summit Granite (Ch.5), although recalculation to 375 Ma may be more appropriate, as indicated by the work of Muir *et al* (1994c).

The three samples of Summit Granite have highly variable isotopic compositions with $Sr_{(381)}$ ranging from 0.7038 to 0.7143 and $\epsilon Nd_{(381)}$ from -3.3 to -7.0. Depleted mantle model ages ($T_{DM}$) are also variable, ranging from 2.1 to 1.5 Ga. $Sr_{(381)}$ for sample MT8 is less than Bulk Earth and may represent alteration and/or resetting during Cretaceous plutonism, as may much of the variability within the pluton. Geochronological data (Ch.5) indicate that mica systems were disturbed during intrusion of the Deutgam and Turiwhate plutons, and this is likely to have disturbed radiogenic isotopes systems, particularly Sr. The presence of abundant, partially digested sheets of metasediment within Summit Granite, and a large component of inherited zircon (T.Ireland *pers.comm.* 1994), is indicative of significant interaction with continental crust. A sample from one such biotite paragneiss sheet (MT19) has a chemistry virtually indistinguishable from other Greenland Group analyses of this

study. Some of the variability of isotopic compositions of Summit Granite may therefore be attributable to country rock contamination, although the samples do define a typical mixing trend between a more primitive source magma and Greenland Group. Importantly, neither the Summit Granite or other Palaeozoic granitoids can represent partial melts of Greenland Group metasediments and another source must be envisaged. An exception to this is WL17, from Mt M$^{c}$Lean, which has an isotopic composition and a distinctly older $T_{DM}$ consistent with an origin via melting of Greenland Group sediments (Pickett and Wasserburg 1989).

Summit Granite isotopic compositions overlap with the somewhat more constrained compositions of other Palaeozoic granitoids from the Buller terrane, suggesting similar source rocks and correlation with the Karamea Suite of Tulloch (1983, 1988). Palaeozoic plutonism in the Takaka terrane is represented by the Riwaka Gabbro, which is contemporaneous with the Buller terrane Karamea Batholith (Muir *et al* 1994c). Radiogenic isotope data for the Riwaka Gabbro indicate a much stronger mantle-signature than is observed in the Karamea Suite, which has isotopic compositions consistent with derivation from a mature continental source.

Decay correction of the Granite Hill and Fraser Complex rocks (see Ch.8) to 381 Ma indicate that these gneisses, particularly the paragneisses, have isotopic compositions overlapping those of the Summit Granite and other Palaeozoic granitoids. Two scenarios could therefore be suggested: A: The Fraser and Granite Hill Complex paragneisses, orthogneisses and metabasites represent the source rocks for Palaeozoic Western Province plutonism. B: The paragneisses and metabasites of the Fraser and Granite Hill Complexes represent source rocks for Palaeozoic plutonism, and the included orthogneiss bodies are metamorphosed equivalents of the Summit Granite and other Palaeozoic granitoids. Less radiogenic compositions of the two orthogneiss samples (GRH1, UMB1) indicates the latter suggestion may be more feasible. $T_{DM}$ for Buller Terrane Palaeozoic plutons are around 1.7 Ga, very similar to those calculated for the paragneissic units of the Granite Hill and Fraser Complexes and also suggesting a genetic relationship between the granitoids and the paragneisses, additionally the "S-type" characteristics of the Summit Granite and Karamea Suite are also consistent with derivation from a paragneissic source such as the Fraser and Granite Hill Complexes.

At present the Fraser and Granite Hill Complex orthogneisses are undated and further geochronological work is required to clarify any genetic relationship with Palaeozoic plutonism.

**6.7.5: Regional correlations: The Karamea Suite.**

In Tulloch's 1983 and 1988a subdivisions of Western Province granitoids all Palaeozoic plutons are included within the Karamea Suite, a group of relatively potassic S-type granitoids. More recently the identification of Palaeozoic A-type (Toropuihi Suite) and I-type (Paringa Suite) plutons (Cooper and Tulloch 1992) and the recognition of two distinct Palaeozoic events at $\approx$375 Ma and $\approx$320 Ma (Muir *et al* 1994a, 1994c) suggests that our understanding of Palaeozoic magmatic events in the Western Province is far from complete. A geochemical study of the Karamea Batholith is currently in progress by Muir and co-workers.

The Karamea Suite is described as comprising commonly foliated, calc-alkali to alkali, mica- and quartz-rich biotite granodiorites and tonalites and biotite muscovite granites (Tulloch 1983). Relatively radiogenic isotopes ($Sr_{(i)}$ = 0.709-0.710) and potassic peraluminous compositions lead Tulloch (1983) to classify the Karamea Suite as S-type (*sensu* Chappell and White 1974), although the Karamea Suite is dissimilar to Lachlan Fold Belt S-types in that it does not contain strongly peraluminous mineral assemblages such as common garnet and aluminosilicates. For want of a better description the Summit Granite can also be considered to be S-type, based on its two-mica, garnet-bearing, peraluminous and radiogenic nature, although at high levels of $SiO_2$, such as in the Summit Granite, the distinction between I- and S-types becomes ambiguous (Chappell and White 1992).

The geochemistry of the Summit Granite is also in accordance with inclusion in the Karamea Suite. The Summit Granite consistently plots at the high $SiO_2$ end of Harker diagrams utilizing data from the Karamea Batholith (Muir unpublished data 1994). Furthermore, the relatively potassic chemistry, Rb enrichment, and similar radiogenic isotopic compositions of the Summit Granite are similar to the initial description of the Karamea Suite by Tulloch (1983). As discussed in Chapter 5, the

SHRIMP age of 381 Ma for the Summit Granite is also within error of a relatively well constrained data set of SHRIMP ages from the Karamea Suite of Muir *et al* (1994c).

Geochemistry and geochronology of the Summit Granite therefore indicate correlation with the Karamea Suite, and as such the term Summit Granite suite is an informal one used only in this thesis. The nearest Karamea Suite plutons to the Summit Granite are the geochemically largely unstudied Rangitoto and Kakapotahi Granites of the Rangitoto Batholith (Jury 1981), although as discussed below the Mount Graham Granite may also be related to the Karamea Suite.

It is now recognized that the Karamea Suite of New Zealand is part of the widespread granitoid magmatic event that can be traced along the Gondwana margin from northeast Australia (Richards 1980) to the Lachlan Fold Belt of southeast Australia (White and Chappell 1983), Tasmania (Cocker 1982), the Ford Granodiorite of Marie Byrd Land (Weaver *et al* 1991) and the Admiralty Intrusives of North Victoria Land (Borg *et al* 1986). Although this Devonian belt of granitoids is commonly attributed to subduction and accretion of exotic terranes along the Gondwana margin (Weaver *et al* 1991, Borg *et al* 1987), other studies have invoked a post-tectonic environment with uplift and adiabatic melting creating at least some of the Devonian plutons (Vetter and Tessensohn 1987). This concept has been further advanced recently by Collins (1994) who proposes a major crustal delamination event to generate the voluminous plutonism of the Lachlan Fold Belt.

### 6.7.6: The Mount Graham Monzogranite.

Petrographically, the two-mica Mount Graham Monzogranite is very similar to the Summit Granite, suggesting affinities between the two plutons. Four geochemical analyses of the Mount Graham Monzogranite indicate a relatively evolved chemistry with $SiO_2$ contents ranging between 72.87 to 74.11%. The granite is peraluminous, with A/CNK between 1.10 and 1.20 and A/NK between 1.30 to 1.40 (Fig.6.5), and relatively potassic with $Na_2O/K_2O$ averaging 0.88 (Fig.6.6). Mantle-normalized spider-diagrams of the Mount Graham Granite (Fig.6.85) are similar to the Summit Granite and exhibit negative anomalies at Ba, Nb, Sr and Ti. However, the Mount Graham

Granite is relatively more enriched in Sr and depleted in Pb compared to Summit Granite.

The age of the Mount Graham Monzogranite is unknown and unconstrained by field relationships. A Nd isotope analysis of one Mount Graham Granite sample yielded a $\epsilon Nd_{(381)}$ similar to the Summit Granite and Karamea Suite, suggesting correlation. However, decay-corrected Sr isotopes for the Mount Graham Monzogranite at 381 Ma are unrealistically low at 0.702, less than Bulk Earth (Fig.6.84). Alternatively, decay correction of the isotopic data to 110 Ma, the age of the Hohonu Super-suite, gives a more geologically reasonable value, although much more radiogenic than the Hohonu Super-suite (see Fig.6.13). The Mount Graham Monzogranite may thus represent an isolated Cretaceous pluton distinct from, and more radiogenic than, the Hohonu Super-suite. Alternatively, it may be equivalent to the Palaeozoic Summit Granite, but its Sr isotopic systematics have been disrupted by alteration or later Cretaceous activity, as also indicated by the variable Sr data from the Summit Granite. Geochronological data are required to further establish the affinities of the Mount Graham Granite, and assignment to any of the suites identified in this study is currently difficult.

# Chapter 7

# The Hohonu Dike Swarm.

## 7.1: Introduction.

The Hohonu Dike Swarm comprises numerous, alkalic mafic dikes intruding Buller Terrane basement in the vicinity of Lake Brunner, North Westland. The dikes of the Hohonu-Turiwhate region were first described by Bell and Fraser (1906), the only other detailed study to date being Hamill (1972). Mafic dike swarms also occur in the Buller gorge region (Hunt and Nathan 1976, Nathan 1978, White 1987) and concentrations of mafic dikes are also reported in the Victoria Range (Tulloch 1979a, Pirajno 1982), and at Reefton and Mount Radiant (Hunt and Nathan 1976). Lamprophyre dikes in the Haast Region, known as the Alpine Dike Swarm (A.Cooper 1971, 1979, 1986) were once considered to be correlatives of the Hohonu Dike Swarm and were used by Suggate (1963) as evidence for pre-Cretaceous strike-slip movement on the Alpine Fault. This view was later discredited by Cooper *et al* (1987) due to differing geochemical properties and evidence for a Late Oligocene to Early Miocene age for the Alpine swarm, as compared with a probable Late Cretaceous age for the Hohonu swarm.

Rhyolitic dikes (Ch.3.12.2) cutting the Deutgam Granite were considered to be evolved end-members of the Hohonu Dike Swarm by Hamill (1972) but are now considered to be represent hypabyssal variants of the French Creek Granite (Ch.6.6.7.3, Tulloch *et al* 1994).

## 7.2: Regional Geology.

The Hohonu Dike Swarm intrudes the predominantly I-type Cretaceous granitoids of the Hohonu Batholith and regional basement, the Ordovician Greenland Group. Mafic dikes also intrude the gneisses of the Granite Hill Complex (Ch.8, Mason and Taylor 1987, Mason 1990) yet are unaffected by the amphibolite facies metamorphism which the gneisses have experienced. Dikes with many similarities to the Hohonu Dike Swarm also intrude the gneisses of the Fraser Complex, where they have been deformed by the pervasive mylonitization affecting this region (Rattenbury 1987a, 1991).

## 7.3: Field characteristics.

The Hohonu Dike Swarm is concentrated on the Hohonu Ranges and western side of Mount Te Kinga (Fig.7.1). Although in some instances dikes may represent up to 40% of outcrop or stream float (e.g. Carew Creek, Fig.7.2) several stream traverses indicate approximately 7% crustal dilation occurred during dike emplacement. Dike abundances decrease dramatically to the south and north of the Hohonu Ranges and Mount Te Kinga, with about 30 dikes observed on Mount Turiwhate, and only 2 dikes seen on Mount Tuhua.

In outcrop, the dikes are black, dark green or dark grey, fine grained, equigranular to porphyritic rocks showing no evidence of deformation apart from minor offset along joint planes (Fig.7.3). Dikes are commonly preferentially eroded with respect to their host granitoids and many creeks flow along channels left by eroded dikes, the only dike remnants being thin chilled margins left attached to country rock. Dikes vary in width from 0.1-15 m, although the majority are about 1 metre wide. Internal flow-alignment of feldspars, and flow segregation of feldspar phenocrysts towards the centre of larger dikes is common (Fig.7.3a). Dikes are straight over the distance of outcrops and appear to have been intruded along pre-existing joints in crystalline, cooled host rocks, occasionally being offset along intersecting joint planes. No evidence for magma mingling was observed. Chilled margins are generally thin, rarely exceeding 2 mm, and consist of fine grained to glassy material containing flow oriented finely crystalline plagioclase laths and occasional clinopyroxene phenocrysts. Dike intrusion has had little affect upon the host granitoids apart from minor fenitization adjacent to phonolitic varieties (see Tulloch and Brathwaite 1986). Incorporation of granitic xenoliths is common on both outcrop and microscopic scales.

## 7.4: Orientation data.

Approximately 650 strike and dip measurements of the Hohonu Dike Swarm were collected during this study and are presented in Fig.7.4. Most of these data (585 measurements) were collected from Mount Te Kinga and the Hohonu Ranges, reflecting the strong concentration of mafic dikes in this area. A very strong WNW-ESE trend for the dike swarm is indicated,with most dikes having a near-vertical attitude. Similar trends have previously been recognized on the northwestern Hohonu

Ranges (Hamill 1972) in the Buller Gorge Swarm (White 1987, Grindley and Oliver 1979). A NE-SW trend reported from the Fraser Complex to the south (Rattenbury 1987a) may be a consequence of rotation associated with deformation adjacent to the Alpine Fault.

**7.5: Age and correlatives.**

Published K/Ar whole rock and mineral ages for several dikes of the Hohonu Dike Swarm range between 140 to 77 Ma (Wellman and Cooper 1971), with additional unpublished K-Ar data on Hohonu dikes also giving a wide range of ages, mostly Late Cretaceous or older (80 to 190 Ma) (Adams 1980, Adams and Cooper *pers.comm.*). As almost all dikes dated intrude the 110.4 $\pm$ 2.2 Ma Deutgam Granite (Ch.5), any K-Ar ages older than 110 Ma are geologically unreasonable. Anomalously old ages were attributed to accumulation of excess argon from the host granitoids by Wellman and Cooper (1971), an interpretation strengthened by the presence of granitoid xenoliths in many dikes. Similarly, anomalously old K-Ar ages in the Alpine Dike Swarm were also attributed to excess argon accumulation (Cooper *et al* 1987). Given the volatile-rich nature of these dikes, interaction and exchange between deuteric fluids and country rock is likely. Of the two remaining geologically reasonable ages of Wellman and Cooper (1971), one is 77 $\pm$ 2 Ma, the other 93 $\pm$ 5 Ma. The remaining geologically acceptable ages of Adams and Cooper (*pers.comm.*) are $\approx$81 Ma. Similar dikes of the Buller Gorge Swarm, give K-Ar ages between 90-78 Ma (Adams and Nathan 1978), similar to age patterns identified in the Hohonu Dike Swarm.

An upper age limit for the Hohonu Dike Swarm is indicated by the presence of basaltic clasts in Oligocene limestone conglomerates exposed along the northwestern margin of the Hohonu Ranges (Ch.9). Geological evidence, including intrusion along joint planes and chilled margins, indicates Hohonu Dike Swarm activity postdates cooling of the Hohonu Super-suite plutons. Emplacement of these plutons between 113.5 $\pm$ 1.9 and 108.7 $\pm$ 3.0 Ma (Table 5.1) indicates the Hohonu Dike Swarm can be no older than 109 Ma. Similar lower limit age constraints are given by unmetamorphosed and undeformed members of the Hohonu Dike Swarm which must pre-date metamorphism of host Granite Hill gneisses which underwent a high-grade metamorphic event at 115 $\pm$ 6 Ma (Ireland 1992).

Very few members of the Hohonu Dike Swarm intrude the A-type French Creek Granite, in stark contrast to the abundance of dikes intruding the neighbouring Deutgam Granite. Consequently, it can be inferred that the bulk of Hohonu Dike Swarm activity preceded intrusion of French Creek Granite. Additionally, aplite dikes of French Creek Granite cross-cut dikes of the Hohonu Dike Swarm (see Fig.3.25) and indicate French Creek Granite activity, in part, postdates emplacement of the Hohonu Dike Swarm. However, rare mafic dikes intruding French Creek Granite also indicate that minor mafic dike activity continued after emplacement of the French Creek Granite (see Fig.3.24). Relationships between the Hohonu Dike Swarm and rhyolitic dikes associated with French Creek Granite (Ch.3.12.2) show variable cross cutting relationships and suggesting a complex temporal relationship between the French Creek Granite and Hohonu Dike Swarm. A large composite dike intruding French Creek Granite in the Eastern Hohonu River ($\approx$K32 755379) comprises a central core of porphyritic, quartz-normative rhyolite (EHR26) with geochemical affinities to the French Creek Granite. This rhyolite grades rapidly through trachydacite (EHR27) into a 1 m rim of mafic material (EHR28) typical of the Hohonu Dike Swarm (Fig.7.5). This dike, and similar composite dikes in the Little Hohonu and Greenstone Rivers, indicate that French Creek Granite and the Hohonu Dike Swarm are, at least in part, contemporaneous. Although no field evidence was observed for magma mixing or mingling, geochemical and isotopic data indicate that French Creek Granite may represent an extreme differentiate of the Hohonu Dike Swarm contaminated by small amounts of crustal material (see Ch.6.6.9 for a more complete discussion), strengthening the hypothesis that both units are contemporaneous. Combining field evidence, geochemical and geochronological data, it is concluded that the Hohonu Dike Swarm represents a (possibly) relatively prolonged period of activity, predominantly preceding but also partially contemporaneous with the intrusion of French Creek Granite. Given the 81.7 $\pm$ 1.8 Ma SHRIMP age for the French Creek Granite (Ch.5), a similar age is inferred for the Hohonu Dike Swarm, although activity immediately postdating emplacement of the Hohonu Super-suite plutons at $\approx$110 Ma cannot be discounted. These age constraints are in agreement with the K-Ar data of Wellman and Cooper (1971) and also agree with K-Ar data from the Buller Gorge Swarm (Adams and Nathan 1978).

**7.6: Petrographic description.**

Dolerite, lamprophyre and phonolite dikes are recognized in the Hohonu Dike Swarm on the basis of textural and mineralogical criteria summarized in Table 7.1. These groupings are not entirely distinct and some gradational varieties are observed. No obvious differences in field occurrence were noted between the differing varieties, and no consistent cross cutting relationships were observed.

Light to dark-grey, fine to medium-grained dolerites dominate the swarm, and are composed primarily of subhedral to euhedral clinopyroxene (augite) and plagioclase (andesine-labradorite) (Fig.7.6). Texturally, most doleritic dikes are equigranular to clinopyroxene-phyric with an interstitial doleritic texture, although occasional plagioclase-phyric variants also occur. Flow differentiation, alignment and concentration of plagioclase towards the centre of dikes is common in the plagioclase-phyric dikes (see Fig.7.3a), as is the development of strong, commonly oscillatory, zoning and sieve textures in plagioclase phenocrysts.

Dark-green to dark-grey lamprophyres are subordinate to the dolerites and petrographically consist primarily of zoned euhedral kaersutite and plagioclase (calcic-oligoclase to andesine) with accessory biotite and abundant apatite (Fig.7.7). The lamprophyres are camptonites according to the classification scheme of Rock (1991) and display equigranular to panidiomorphic textures.

Phonolite dikes are rare within the swarm and only three dikes were found to outcrop, a fourth sample (HPC1) was collected from abundant float in Petrel Creek (K32 806383). Petrographically, the phonolites comprise phenocrysts of subhedral, turbid alkali feldspar, euhedral nepheline, occasional Ti-rich amphibole and rare yellow-brown to near black pleochroic biotite in a trachytoid groundmass of fine grained alkali feldspar and nepheline and abundant prismatic aegirine-augite (Fig.7.8). Interstitial sodalite and possibly analcime also occur. Granitoid country rock adjacent to two phonolites (KNB6, HRS15) has a weak blue colouration indicative of fenitization as mentioned by Tulloch and Brathwaite (1986). The phonolite dikes may be related to the enigmatic sodalite syenite collected by Mason and Taylor (1986) from New River, and yet to be found *in situ*.

The source of lamprophyric float boulders containing kaersutite megacrysts and spinel harzburgite xenoliths (Tulloch and Nathan 1990) was located in a small tributary of an unnamed creek draining into Lake Brunner (K32 844387). The dike is ≈2 metres wide and composite, comprising an outer margin of phonolite containing sparse kaersutite megacrysts (KST8), grading over about 10 mm into a typical, panidiomorphic lamprophyre (KST2). The lamprophyric core of the dike contains abundant large (up to 50 mm) subhedral, kaersutite megacrysts and spinel harzburgite xenoliths exhibiting varying degrees of alteration to talc and serpentine. The xenoliths comprise olivine, orthopyroxene and chrome spinel, and were interpreted as either accidental xenoliths or the refractory residue of a mantle previously depleted by generation of their host dikes (Tulloch and Nathan 1990). The composite nature of this dike is important as it indicates that the phonolites and lamprophyres were contemporaneous and do not represent temporally distinct events. Similar megacrystic and xenolith-bearing float was observed rarely in Carew Creek (K32 788390) and the Eastern Hohonu River (K32 750386) (e.g.EHR12).

### 7.6.1: Alteration mineralogy

Despite often appearing fresh in outcrop all dikes examined reveal abundant petrographic evidence of greenschist facies deuteric alteration, a consequence of their volatile-rich nature. Alteration effects decrease through the mafic dike spectrum from the lamprophyric dikes (most altered), through the doleritic dikes to the plagioclase-phyric varieties (least altered), suggesting a decrease in volatile activity. The most common alteration product is secondary amphibole (uralite), occurring as prisms or fibrous masses of green ferro-actinolite or colourless tremolite after amphibole and pyroxene. In more extreme examples uralite in turn has altered to chlorite. Titanium, which cannot be contained within the crystal structure of secondary amphiboles, resides in numerous small anhedral blebs of ilmenite and/or titanite within uralite, indicating the Ti-rich nature of many of the primary ferromagnesium minerals. Olivine, rarely present in some dikes, is ubiquitously altered to talc and serpentine, with associated fine grained iron oxides. Sericitization and sausseritization of feldspar is also common and those dikes containing nepheline display ubiquitous alteration of nepheline to cancrinite and calcite.

Xenocrysts of granitoid are relatively common in some dikes, displaying reaction rims of fine grained clinopyroxene and/or secondary amphibole. Additionally, several members of the Hohonu Dike Swarm contain conspicuous ocelli up to 7 mm across. Ocelli are generally filled with epidote/clinozoisite, calcite and quartz and are considered to be the result of late stage water-rich solutions present at the final stages of crystallization rather than representing liquid immiscibility (see A.Cooper 1979). Epidote crystals are commonly euhedral, up to 2 mm long, and display increasing birefringence towards the centre of the vugs, indicative of increasing Fe and/or Mn content. Many vugs also consist entirely of calcite with a few small anhedral crystals of quartz at the core. Vugs are less abundant in the dolerite dikes and were not observed in any of the phonolites.

## 7.7: Geochemistry.

### 7.7.1: Introduction.

The $SiO_2$ content of analyzed mafic dikes ranges between 39-52 wt% and 54-56 wt% in the phonolites (Appendix C). Variable and occasionally high loss on ignition values decrease generally with increasing $SiO_2$ and reflect the high volatile contents and deuteric alteration typical of dikes of lamprophyric affinities, all analyses are therefore recalculated volatile-free prior to plotting. Chemical distinctions between the lamprophyric and doleritic dikes are subtle with lamprophyres generally having lower $SiO_2$ and Ni, and higher Cr, $TiO_2$, Zr, Ba, $P_2O_5$, Rb, Nb, La, and Ce contents. Cr and Ni contents ($\approx$500 and $\approx$350 ppm respectively) and Mg numbers of $\approx$65 in the most primitive dikes are consistent with primary melts in equilibrium with typical mantle compositions. Hohonu Dike Swarm compositions scatter considerably on a total alkali-silica diagram (Fig.7.9), many are alkali basalts, with some dispersion into the basanite and hawaiite fields. The felsic dikes are mostly phonolites, except for KNB6 which chemically is a trachyandesite. Much of the scatter in Fig.7.9 may reflect the mobility of alkalis during alteration, and possibly some alkali exchange with country rock granitoids.

The majority of dikes in the Hohonu Dike Swarm are undersaturated, containing up to 13% normative nepheline (Fig.7.10). Despite these high normative nepheline contents, modal nepheline is only identified in the highly undersaturated phonolites. A

weak trend towards oversaturated compositions is also observed, typical of many intra-plate basalt suites (e.g. Weaver and Smith 1989). The migration from dominantly undersaturated to oversaturated compositions may represent polybaric fractionation at relatively high pressures (4+ kb) and migration of the thermal divide into the nepheline field. At such conditions the thermal divide lies within the undersaturated field and an originally ne-normative melt will evolve towards more saturated and eventually oversaturated compositions. A relatively deep magma reservoir where such fractionation may occur is indicated by the petrogenetic and temporal affinities of the French Creek Granite and Hohonu Dike Swarm. The saturated to oversaturated compositions of the Hohonu Dike Swarm may represent the primitive members of a lineage fractionating towards French Creek Granite compositions as discussed in more detail in Ch.6.6.9. At shallower levels (<4 kb) the thermal divide coincides with the critical plane of undersaturation and ne-normative melts will evolve towards more undersaturated alkaline compositions such as the phonolites. Care must be taken in applying CIPW norms for the Hohonu Dike Swarm to petrogenetic interpretations, given the sensitivity of the normative mineral calculation to small variations in $Na_2O$ likely in altered rocks such as the Hohonu Dike Swarm (Rollinson 1993).

### 7.7.2: Major and trace elements

Considerable scatter occurs within the major and trace elements of the Hohonu Dike Swarm, a consequence of varying degrees of deuteric alteration. Zr is used as an index of fractionation in the following diagrams due to its immobility during alteration, variable abundances (100-700 ppm) and most importantly because Zr has acted incompatibly throughout the swarm. Rb, $K_2O$, Ti, Na, P, Y, Nb and REE increase relatively consistently with increasing Zr whereas more compatible elements such as Cr, MgO and $Fe_2O_3$ decrease with increasing Zr, reaching very low concentrations in the phonolitic dikes (Fig.7.11). In addition CaO, $TiO_2$, Ni, and Cr decrease, and $Na_2O$ and $K_2O$ increase, with decreasing MgO (not shown). Such trends are compatible with combined fractionation of plagioclase and the common petrographic mafic phases amphibole and clinopyroxene.

Calculated Rayleigh fractionation vectors for selected elements (Ba, Rb, Ni, Zr, Ti) are also consistent with evolution of the Hohonu Dike Swarm by combined fractionation of plagioclase, amphibole and clinopyroxene (Fig.7.12 to Fig.7.15). Although Sr would be expected to decrease consistently with increasing Zr in a system undergoing plagioclase fractionation it instead shows abundant scatter (Fig.7.16). This is likely to reflect combined fractionation of mafic phases with low partition coefficients for Sr, offsetting the affects of plagioclase fractionation, and mobility of Sr during feldspar alteration. Although the observed trends are also consistent with olivine fractionation, the petrographic rarity of this phase indicate it is unlikely to have played a major role in the evolution of the Hohonu Dike Swarm.

Phonolite dikes are characterized by considerably lower $TiO_2$ contents than the mafic members of the dike swarm (Fig.7.11). This trend is unlikely to be a consequence of major fractionation of Fe-Ti oxides as this would result in much greater increases in $SiO_2$ than observed, and is attributed to increased removal of Ti-rich amphibole and augite. Although the LREE La and Ce, and the HREE equivalent Y, are generally incompatible in basaltic compositions, the phonolites are distinctly depleted in these elements, indicating compatible behaviour and removal in a fractionating phase. Low La, Ce and $P_2O_5$ in the phonolites are consistent with fractionation of apatite (Fig.7.11), a consequence of large partition coefficients for LREE in apatite. However, low contents of Y in the phonolites cannot be attributed to apatite fractionation, nor can they result from zircon fractionation as the phonolites do display a concomitant decrease in Zr. Low Y contents in the phonolites probably reflect the increase of amphibole fractionation as indicated by low $TiO_2$ contents, coupled with an increase in the partition coefficients for MREE and HREE in amphibole with increasing whole rock $SiO_2$ content (Rollinson 1993). Alternatively, low Y may reflect retention of Y and HREE by garnet during melting of a relatively deep mantle source.

The high field strength elements (HFSE) (Ti, Zr, Y, Nb, P and REE) are immobile during metamorphism and alteration (Winchester and Floyd 1977, Pearce and Norry 1979) and relative contents should therefore be unaffected by fractionation processes. In addition, immobile element ratios should be preserved and retain the characteristic ratios of the parent magmas and their sources. In general, incompatible

element ratios (e.g. Nb/Zr, Rb/Zr, La/Nb) are retained throughout the Hohonu Dike Swarm (Fig.7.11 and 7.17), consistent with all members of the Hohonu Dike Swarm belonging to a co-genetic suite related by crystal fractionation. As noted previously, $P_2O_5$ and the REE La, Ce and Y have acted compatibly at phonolitic compositions and consequently incompatible element ratios are not preserved at these compositions.

A single trachyte dike, containing abundant small magnesio-riebeckite crystals, collected from an unnamed peak above Lake Ruby (HMS5), may represent a continuation of the weak trend towards saturated and oversaturated compositions in the dike swarm and an intermediate stage between the Hohonu Dike Swarm and the French Creek Granite. The dike is atypically fresh, has high $SiO_2$ (67.50%), is oversaturated and peralkaline and was consequently originally considered related to the rhyolitic dikes emanating from the French Creek Granite. Isotopic ratios for this dike suggest greater affinities to the Hohonu Dike Swarm (Ch.7.7.4). The trachyte dike displays evolved REE patterns with $La/Yb_N$ = 14.73, very high total REE ($\Sigma$REE = 781 ppm), elevated LREE ($Ce_N$ = 450) and a large negative Eu anomaly (Eu/Eu* = 0.05) (Fig.7.18). If this dike is related to the Hohonu Dike Swarm, REE patterns suggests large amounts of fractionation have occurred, particularly of feldspar to generate the Eu anomaly.

Inclusion of country rock xenoliths is relatively common in the Hohonu Dike Swarm on both outcrop and microscopic scales, indicating that crustal assimilation may have affected dike chemistry. Crustal contamination will result in relative enrichment of the mobile elements (e.g. K, Rb, Ba and Sr) concentrated in continental crust. In contrast, relatively immobile elements such as Nb, La, and Zr will not be affected by crustal contamination (Mohr 1987). Mobile-immobile element ratios (Fig.7.19) remain relatively constant through the dike swarm, even at phonolitic compositions, indicating crustal contamination has been generally unimportant. The few analyses which did show elevated mobile-immobile element ratios, indicative of crustal contamination, were removed from the data set. Similar mobile-immobile element and incompatible-incompatible element ratios for both the phonolitic and more mafic dikes preclude genesis of the felsic members by assimilation of crustal material by the mafic dikes.

**7.7.2.1: Spider-diagrams.**

Multi-element mantle normalized spider-diagrams for selected samples of the Hohonu Dike Swarm (Fig.7.20) indicate progressive enrichment of most elements with increasing Zr content, with minor depletion of Sr and P at higher Zr contents symptomatic of plagioclase and apatite fractionation. The negative K anomaly present in many other South Island intraplate rocks (Weaver and Smith 1989) is absent in the Hohonu Swarm. Low Y contents in the spider-diagrams may indicate derivation from a source containing stable garnet although detailed REE data is needed to extrapolate on this observation. Spider-diagrams of the phonolites reflect their highly evolved nature with distinct troughs at Ba and Sr, reflecting feldspar fractionation, and at $P_2O_5$ and $TiO_2$ reflecting removal of apatite and Ti-rich mafic phases.

**7.7.3: Tectonic discrimination.**

Spider-diagrams for the Hohonu Dike Swarm (Fig.7.20) display LILE enriched, "humped" plots typical of alkaline basalts (Thompson *et al* 1983) and lack the Nb (Ta) anomalies typical of alkaline rocks and indicating a tectonic environment unrelated to subduction (Gill 1981). Furthermore, the Hohonu Dike Swarm plots consistently in the Within Plate Basalt fields of various published tectonic discrimination diagrams (e.g. Fig.7.21). A strong trend of increasing Nb/Y with consistent low $Zr/P_2O_5$ is also typical of continental alkali basalts (Floyd and Winchester 1975) (Fig.7.22). As such, chemical parameters are strongly indicative of a Within-Plate, anorogenic setting for the Hohonu Dike Swarm. Alkaline within-plate basalts are typical of non-orogenic rifting environments such as seen today in the East-African rift system and a similar extensional setting has been inferred for the Buller Terrane in the Late Cretaceous (Laird 1993, 1994). The A-type chemistry of the contemporaneous French Creek Granite is also indicative of emplacement and generation in an anorogenic, intraplate, extensional environment (Ch.6.6.10, Tulloch *et al* 1994).

**7.7.4: Radiogenic isotopes.**

Four dikes, a dolerite, a lamprophyre, a phonolite, and the trachyte (HMS5) were analyzed for Nd and Sr isotopic ratios as part of a broader study on the granitoids of the Hohonu Batholith (Table 7.2). At 82 Ma the dikes show some scatter (see

Fig.6.81), but are generally indicative of derivation from a time integrated depleted mantle source, although not as extreme as MORB mantle. Initial Sr ratios at 82 Ma are variable, ranging from 0.7027 to 0.7045. The lower value, for the phonolite dike (HRS15), is unrealistically low and may reflect Sr loss, whereas the $Sr_{(82)}$ value for the lamprophyric dike (KRC7) may indicate interaction with continental crust. $Sr_{(82)}$ for the trachytic dike (HMS5) is also unrealistically low, a consequence of very low Sr contents ($\approx$4 ppm) and high Rb/Sr. Small variations in Sr will radically change Rb/Sr and thus result in substantial variations in the decay-corrected initial ratio. Such variations may be a consequence of Sr loss during alteration, analytical error or small amounts of country rock contamination. The large variability in calculated initial Sr ratios for this sample means that little significance can be placed on the analysis. $\epsilon Nd_{(82)}$ values are somewhat better constrained, reflecting the greater stability of Sm and Nd. $\epsilon Nd_{(82)}$ ranges from +5.3 to +7.0, with the trachytic dike giving a value of +4.74. Although this value is lower than the other Hohonu Dike Swarm analyses it is considerably higher than those of the French Creek Granite and associated rhyolite dikes ($\epsilon Nd_{(82)}$ = +0.5 to +2.5), hence its inclusion within the Hohonu Dike Swarm. Lower $\epsilon Nd_{(82)}$ in the trachytic dike suggest it may represent an intermediate stage between the Hohonu Dike Swarm and the even lower $\epsilon Nd_{(82)}$ values of the co-genetic French Creek Granite, attributed to interaction with continental crust (Ch.6.6.9). More comprehensive isotopic data is needed to more fully constrain the mantle source characteristics of the Hohonu Dike Swarm.

## 7.8: Discussion.

Sparse K-Ar data (Wellman and Cooper 1971) combined with the close genetic and temporal links between the Hohonu Dike Swarm and the French Creek Granite, indicate emplacement of the Hohonu Dike Swarm immediately prior to, and contemporaneous with, the French Creek Granite at 81.7 $\pm$ 1.8 Ma. Additionally, both the Hohonu Dike Swarm and French Creek Granite have geochemistries typical of magmas generated in intraplate, extensional environments, and detailed orientation data indicates the crust was undergoing strong NNE-SSW extension during emplacement of the Hohonu Dike Swarm. The age of the Hohonu Dike Swarm and the French Creek Granite coincide almost perfectly with the first appearance of oceanic crust in the Tasman Sea around 82 Ma (Chron. 33, Weissel and Hayes 1977). Similarly, extension

directions in the Hohonu Dike Swarm parallel the line of Australia-New Zealand breakup and are almost certainly related to extension during the formation of the Tasman Sea. Similar extension directions, alkaline chemistries and K-Ar ages (90-78 Ma, Adams and Nathan 1978) in the Lower Buller Gorge dike swarm (Grindley and Oliver 1979, White 1987, Tulloch and Kimbrough 1989) suggest close genetic links to the Hohonu Dike Swarm.

Many Cretaceous structures on the West Coast display a preferred WNW-ESE orientation and are generally considered to reflect NNE-SSW extension during the continental separation of New Zealand and Australia and the opening of the Tasman Sea (e.g. Bishop 1992, Tulloch and Kimbrough 1989). However, a single, prolonged extensional event prior to opening of the Tasman Sea may be a too simplistic scenario and up to four distinct extensional events may be involved (Laird 1993, 1994). The first of these extensional events occurred in the mid-Cretaceous (Albian) and is reflected in the NNE-SSW oriented mid-Cretaceous sedimentary basins of the Pororari Group (Nathan *et al* 1986), the offshore Takutai half-graben (Bishop 1992) and the Paparoa Metamorphic Core Complex (Tulloch and Kimbrough 1989). These structures predate emplacement of the Hohonu Dike Swarm by $\approx$30 Ma and may be unrelated to Gondwana breakup. Instead, it is argued in Ch.6.5.4 that the Albian extensional event is related to the thermal collapse and thinning of overthickened crust associated with generation of the Separation Point Suite (Muir *et al* 1995). This extensional event is also attributed to the generation of the Hohonu Super-suite granitoids, as discussed in detail in Chapter 6.5.4.

On a broader scale NNE-SSW extension is also indicated by the Bounty Trough, the New Caledonia Basin and the Challenger Basin (Wood 1991, Bishop 1992, Laird 1994), although there are few constraints on the age of these extensional events. A second extensional event is predominantly expressed in the Eastern Province and reflects the onset of New Zealand-Antarctica break-up. This event may be represented on the West Coast by peaks in K-Ar and fission track uplift and cooling ages at 95-100 Ma (Laird 1994, see also Ch.5).

Emplacement of the Hohonu Dike Swarm and the French Creek Granite is correlated with a third period of extension in the Early Campanian (Laird 1994), contemporaneous with, and directly attributable to, opening of the Tasman Sea. Parallel extension directions in the Albian and Late Cretaceous extensional phases may reflect Late Cretaceous reactivation of structures developed during the earlier extensional event. In contrast to the Albian extensional event described above, which resulted in spatially limited but relatively thick sedimentary deposits, there is a major hiatus in sedimentation during the Late Cretaceous, indicating this was a time of uplift and erosion. Campanian age strata (NZ Piripauan stage) are poorly represented on the West Coast, the only recognized deposits being non-marine sediments at Paringa (Laird 1994).

Sea-floor spreading in the Tasman Sea continued from break-up until $\approx$60 Ma (Weissel and Hayes 1977), and related extension resulted in near continuous sedimentation until the Palaeocene (Laird 1994). A fourth period of increased extension and associated volcanism may be indicated by basalts at Mt Kowhiterangi (Gage and Wellman 1944) and in the Arahura-1 drill hole (Nathan *et al* 1986), dated at 68.0 $\pm$ 1.4 Ma and 68.4 $\pm$ 2.6 Ma respectively (Sewell *et al* 1988), the Arnott Basalts of South Westland (Sewell and Nathan 1987), basalt flows in the Greymouth Coalfield (Gage 1952) and the equivalent Morgan Volcanics in the lower Paparoa Ranges (McDougall 1993). All these basalts have geochemistries typical of within-plate extensional environments (Sewell and Nathan 1987, Sewell *et al* 1988, McDougall 1993).

Isotopic data indicate the Hohonu Dike Swarm was derived by partial melting of a depleted mantle source, probably during adiabatic uplift of the mantle in response to unloading during lithospheric attenuation. In contrast to the relatively depleted mantle source indicated by isotopic data, trace element data (e.g. spider-diagrams) indicate the dikes are relatively enriched in most trace elements relative to primordial mantle (Fig.7.20) and a comparably recent mantle enrichment event is indicated. A similar situation has been identified in the Tertiary Alpine Dike Swarm of the Haast region (Barreiro and Cooper 1987). Depleted mantle model ages for the Alpine Dike Swarm range from 269 Ma to 509 Ma (recalculated for this study) and overlap with those from

the Hohonu Dike Swarm (339 Ma to 516 Ma) (Table 7.2). Barreiro (1983) and Barreiro and Cooper (1987) interpreted these model ages to represent a mid-Palaeozoic mantle enrichment event which they attribute to interaction of a carbonated hyperalkaline magma with normal "depleted" peridotite. Coombs *et al* (1986) have suggested that this enrichment event is widespread and can be recognized in Eastern Australia, Antarctica and Otago. Preliminary isotope data, coupled with trace element data, suggests this mantle province may also have existed beneath the Western Province in the Late Cretaceous. Notably, this mantle source is distinct from that which generated the source for the Separation Point Suite and was involved in generation of the Hohonu Super-suite.

As a final note, the occurrence of Cretaceous I-type plutonism in the Hohonu Batholith, followed by mafic dike activity and partly contemporaneous, mostly younger A-type plutonism (French Creek Granite) is very similar to the sequence of events observed in Marie Byrd Land by Weaver *et al* (1994) which were associated with the rifting of the Campbell Plateau from Marie Byrd Land and the opening of the Southern Ocean.

# Chapter 8

# The Granite Hill and Fraser Complexes.

## 8.1: Introduction.

Two blocks of high-grade metamorphic rocks, the Granite Hill Complex to the north and the Fraser Complex to the south, lie between the Hohonu Batholith and the Alpine Fault. In this chapter the field geology, petrography and chemistry of both units are briefly described and compared, and possible correlatives in the Western Province are discussed. Only limited field work and sampling were carried out on the Granite Hill and Fraser Complexes and the following chapter is considered as a reconnaissance study only.

## 8.2: The Granite Hill Complex.

### 8.2.1: Introduction and field relationships.

The Granite Hill Complex was initially recognized by Mason (1990) and comprises the crystalline rocks of Granite Hill and "Rotomanu Hill", the low inlier dissected by Thirsty Creek (K32 915373). Mason (1990) also includes the Thirsty Creek Norite of Tulloch and Brathwaite (1986) in the Granite Hill Complex, and this unit is discussed briefly at the end of this chapter (Ch.8.8).

A major fault, considered to be a northerly extension of the Fraser Fault, was inferred by Mason (1990) and Young (1968) to separate metamorphic rocks of the Granite Hill Complex from the granitoids of Mount Te Kinga and the Greenland Group of Bell Hill. The fault, here termed the Granite Hill Fault, is a poorly exposed reverse fault, striking approximately north-south and dipping moderately (64°) to the east, separating brittly deformed Greenland Group from Granite Hill paragneiss on the western side of Granite Hill (≈K32 969437). Young (1968) postulated that this fault may extend further north to a crushed zone separating granite from gneiss on Mount Elliot in the southern Victoria Ranges. The eastern boundary of the Granite Hill Complex is the Alpine Fault.

Members of the Hohonu Dike Swarm intrude all metamorphic rocks of the Granite Hill Complex (*cf* Mason 1990, p65), although dikes are considerably less

abundant than on the nearby Mount Te Kinga. Dikes are unmetamorphosed and cross-cut foliations within the Granite Hill Complex, indicating that metamorphism and foliation development in the gneisses pre-dates mafic dike activity at ≈ 82 Ma (see Fig.7.3b) and cannot be related to Alpine Fault movement.

### 8.2.2: Description of the Granite Hill Complex.

Three major metamorphic rock types are identified within the Granite Hill Complex: biotite (± garnet ± sillimanite) paragneiss, hornblende (± garnet) metabasite and biotite granodioritic orthogneiss. Many of the gneisses are protomylonitic, although no well developed mylonites or ultramylonites were observed within the Granite Hill Complex during this study, in marked contrast to the Fraser Complex (Rattenbury 1991). Foliations within the Granite Hill Complex are somewhat variable but mostly trend NNE, approximately parallel to the Alpine Fault, and dip steeply to the east (Fig.8.1).

#### 8.2.2.1: Biotite paragneisses.

Paragneisses of the Granite Hill Complex are generally biotite rich, finely banded gneisses (Fig.8.2), occasionally migmatitic in appearance. More felsic, equigranular biotite (± muscovite) gneisses occur and are also considered to have had sedimentary precursors, although the distinction between paragneiss and orthogneiss was at times problematic. Paragneisses occur over most of Granite Hill and Rotomanu Hill, but are particularly dominant along the Evans River and on the Granite Hill summit.

Petrographically, the paragneisses comprise quartz + plagioclase + biotite ± garnet ± sillimanite ± alkali feldspar with accessory apatite, zircon, opaques and minor secondary muscovite (Fig.8.3).

Quartz is abundant and occurs as anhedral crystals up to 4 mm across, sometimes as mosaics of quartz, and with common undulatory extinction. Plagioclase is mainly calcic oligoclase to labradorite (An 53-36%), with a single crystal of bytownite (An 74%) analyzed in GRT1. It occurs as anhedral, albite twinned crystals up to 7 mm long. Biotite is ubiquitous, making up to 20 modal percent as platy to anhedral crystals

up to 1.5 mm long and displaying yellow-brown to dark brown or bright red-brown pleochroism. Microprobe analyses[18] of biotite from the Granite Hill Complex indicate variable Ti (0.17-0.46 cations), Fe/(Fe+Mg) between 46 and 61 and relatively high Al(tot) (3.06-3.36) compared with Hohonu Batholith granitoids (see Ch.4). Garnet is occasionally abundant and generally occurs as subhedral to euhedral crystals up to 5 mm across. Microprobe data indicate that garnets are iron-rich (almandine 65-69%, pyrope 16-24%, grossular 3-11%, spessartine 2-5%, andradite 0-5%) being richer in Mg and poorer in Mn component than garnets of the Pecksniff Metasedimentary Gneiss (Charleston Metamorphic Group) in the Paparoa Ranges (almandine 52-69%, pyrope 7-15%, grossular 3-18%, spessartine 11-26%, andradite 0-2%, White 1987). Sillimanite occurs in a single specimen (GH3) as abundant aggregates of prismatic crystals up to 0.2 mm across. Mason (1990) reports sillimanite with a similar habit from the Thirsty Creek area. Apatite is an abundant accessory phase present as relatively large (0.2 mm) crystals and occasional brown metamict zircons also occur.

The paragneisses are considered to represent a predominantly pelitic sequence, possible precursors and correlatives are discussed in Ch.8.7.1.

**8.2.2.2: Metabasites.**

Hornblende-bearing gneisses outcrop sporadically on Granite Hill as weakly foliated, melanocratic, equigranular hornblende-rich rocks with occasional mesocratic variants. Mafic and felsic-rich layers are common on a centimetre to metre scale, with garnet occurring preferentially in the felsic bands (Fig.8.4). The gneisses are equigranular and generally fine to medium grained, although a large (5 $m^3$+) block of coarse grained (average crystal size $\approx$ 2 cm) gabbroic rock was found in float in a tributary of the Evans River (K32 987407). Outcrops of metabasite occur in the Crooked River, several creeks draining the western slopes of Granite Hill, a tributary of Evans River and in Boatmans Creek.

Petrographically, the metabasites are dominated by amphibole and plagioclase with varying proportions of quartz + biotite $\pm$ garnet $\pm$ epidote/allanite and accessory apatite, zircon and magnetite (Fig.8.5). Amphibole occurs as subhedral to anhedral

18: Microprobe analyses are presented in Appendix D.

crystals up to 5 mm across, commonly exhibiting both lattice and shape preferred orientations. Amphibole typically displays yellow-brown to green-brown or brown pleochroism and may comprise up to 75 modal percent of the gneiss. Plagioclase occurs as subhedral to euhedral crystals (≈An 40-30%) up to 5 mm long, often occurring in the interstices between amphibole crystals. Quartz is generally a minor constituent in the metabasites, occurring as anhedral crystals up to 7 mm across with minor undulatory extinction. Biotite is a variable component, occasionally making up to 20 modal percent of the metabasites as anhedral crystals up to 1 mm long and displaying yellow-brown to orange-brown or brown pleochroism. Garnet occurs as euhedral to subhedral crystals up to 7 mm across, although large (up to 10 cm), euhedral garnets were observed within felsic segregations in metabasite exposed in an unnamed creek draining into the Evans River (K32 972399) (Fig.8.6).

Similar metabasites in the Fraser Complex are interpreted by Rattenbury (1987a, 1991) as meta-volcanic or meta-tuffaceous beds interbedded within the sedimentary precursors of the paragneisses, and an analogous interpretation is probable for the Granite Hill metabasites. Alternatively, the metabasites may represent basaltic dikes intruded into a sedimentary sequence prior to metamorphism. A single sample (CR5) from the Crooked River contains zoned andesine (An45%) crystals, elongate parallel to (010) and twinned on the Carlsbad law, indicating an igneous origin. These observations, coupled with plutonic igneous textures, indicate this specimen represents a metamorphosed mafic plutonic dioritic rock. A similar dioritic sample (IMC2) was collected from MacPherson Creek in the Fraser Complex.

#### 8.2.2.3: Granodioritic orthogneiss.

Orthogneiss occurs intermittently on Granite Hill, particularly along the western margin and in Boatman's Creek. Although contacts are poorly exposed, the orthogneisses are considered to be the metamorphic equivalents of granitoids intruded into the other metamorphic units recognized. A typical outcrop of strongly foliated, protomylonitic, megacrystic granodioritic orthogneiss, cut by a prominent vertical fault plane, occurs in a quarry on Rotomanu Hill (K32 925381) (Fig.8.7). Shear sense indicators signify dextral deformation, consistent with movement on the nearby Alpine Fault. However, the presence of several undeformed members of the Hohonu Dike

Swarm (Ch.7) sharply cutting the foliation in the granodiorite indicate foliation development must pre-date Late Cretaceous mafic dike activity and cannot be related to current Alpine Fault movement.

Petrographically, the orthogneisses consist of quartz + plagioclase + alkali feldspar + biotite ± muscovite ± allanite and accessory apatite, zircon and opaques (Fig.8.8). Quartz is present as anhedral crystals up to 1 mm long, occasionally forming a symplectite with feldspar. Quartz displays ubiquitous undulatory extinction and often occurs as dynamically recrystallizing aggregates or quartz ribbons up to 10 mm long in more deformed examples. Plagioclase occurs as augen and fractured anhedral to subhedral, crystals (An 47-35%) up to 7 mm long. Alkali feldspar occurs as zoned and Carlsbad twinned phenocrysts up to 40 mm long, commonly as augen and defining a strong foliation. Biotite is the dominant mafic phase, present as yellow-brown to green-brown or brown pleochroic platy crystals up to 2 mm long, generally sheared parallel to the foliation. In more deformed examples biotite is commonly bent and sheared around resistant feldspar augen. Allanite is abundant in two samples (GBC1 and RQ3) as subhedral to euhedral zoned crystals up to 2 mm long. Epidote also occurs intermittently throughout the orthogneiss, often as a late stage mineral associated with brittle shear zones. Accessory phases include minor muscovite, abundant, distinctive, euhedral crystals of apatite up to 0.4 mm across and abundant euhedral brown and metamict crystals of zircon up to 0.2 mm across. Opaque phases are rare.

A single sample of equigranular, medium grained tonalitic orthogneiss (GRH1) containing abundant subhedral garnet, red-brown biotite and calcic andesine (An 47-43%) was collected from the southeast margin of Granite Hill.

### 8.2.3: Conditions of metamorphism of the Granite Hill Complex.

The metamorphic assemblages of andesine-almandine-biotite ± sillimanite in the paragneisses and amphibole-garnet-andesine in the metabasites are typical of amphibolite facies metamorphic conditions. The presence of occasional migmatitic rocks also suggests partial melting occurred. Application of the garnet-biotite geothermometer of Ferry and Spear (1978) to mineral pairs in samples GRH1 and GRT1 produced temperatures inconsistent with the observed metamorphic assemblages.

Average temperatures of 356 ± 20°C (1 s.d.) and 436 ± 46°C (1 s.d.) were obtained for GRH1 and GRT1 respectively, assuming a pressure of 4 kb. Low calculated temperatures may be a consequence of late stage retrograde alteration. A detailed geothermobarometric study of the Granite Hill and Fraser Complexes similar to that of White (1994) on the metamorphic rocks of the Charleston Metamorphic Complex was considered beyond the scope of this study.

## 8.3: The Fraser Complex.

### 8.3.1: Introduction and field relationships.

The Fraser Complex is a diverse group of metamorphic rocks, first identified by Morgan (1908) and named the Fraser Formation by Young (1968). The unit extends from the Waitaha River in the south to MacPherson Creek in the north as a thin belt, bounded by the Alpine and Fraser Faults. More recent mapping, and the identification of "distinct and mappable lithologic variations", led Rattenbury (1987a, 1991) to revise the name to the Fraser Complex. Most of the previous geological accounts of the Fraser Complex have concentrated on the better exposures to the south around Mount Misery and Fraser Peak (e.g. Rattenbury 1986, 1987a & b, 1991) and only the northernmost portion of the Fraser Complex from the Styx River to MacPherson Creek was examined in this study.

The Fraser Complex consists of epidote-amphibolite to upper amphibolite facies metapelitic, quartzo-feldspathic and hornblende gneisses, intruded by several granitoids, in turn intruded by mafic dikes similar to those of the Hohonu Dike Swarm. These rocks have consequently been tectonically disrupted and enveloped by numerous anastomosing mylonite zones (Rattenbury 1991). Dextral strike-slip shear indicators and a general parallelism of foliations suggests mylonitization is related to movement upon the Alpine Fault (Rattenbury 1987a, 1987b, 1991).

The Fraser Complex is bounded to the east by the Alpine Fault and to the west by the Fraser Fault and more recent thrusts associated with the Alpine Fault, including the Bald Hill Range Thrust (Rattenbury 1986). Rattenbury (1987a) describes the trace of the Fraser Fault as "a crushed and jointed zone of green chloritized cataclasite 50 to 200 m thick". The Fraser Fault is exposed in several locations in the northern sector of

the Fraser Complex. The trace of the Fraser Fault runs through a low valley and along the steep northwestern face of Mount Upright, separating brittly deformed and highly epidotized Turiwhate Granodiorite and hornblende-rich mylonites of the Fraser Complex in the Styx River (J33 575121). Cataclased and chloritized Arahura Granite at the junction of Lebel, Wainihinihi and MacPherson Creeks (J33 665202) also occurs close to the inferred trace of the Fraser Fault. The Fraser Fault is also exposed in a tributary of Geologist's Creek (J33 613149). Here Arahura Granite becomes increasingly brecciated and chloritized towards the fault, and is then juxtaposed against garnet paragneisses, migmatites and mylonites of the Fraser Complex. Further up this creek the Alpine Fault is well exposed as a sheet of chloritized cataclasite thrust over recent gravels. The Fraser Fault is also reported to be exposed in the headwaters of Geologist's Creek (Rattenbury 1987a).

Most rocks in the northern section of the Fraser Complex exhibit a strong foliation and are variably mylonitized. Foliation orientations are somewhat scattered but mostly strike ENE and dip steeply to the southeast (Fig.8.9), sub-parallel to the Alpine Fault and the foliation orientations noted by Rattenbury (1987a) further south.

The Fraser Complex was interpreted by Rattenbury (1987a, 1991) as a deep crustal, high grade metamorphic basement to the Greenland Group, mylonitized by dextral strike-slip movement upon the Alpine Fault and uplifted along the Fraser Fault since the Late Miocene (about 9 Ma) (Rattenbury 1987a, 1991). More recently Kimbrough *et al* (1994a) have proposed that the Fraser Fault represents a low angle detachment fault, similar to those bounding the Paparoa Metamorphic Core Complex, subsequently steepened during Cenozoic compression across the Alpine Fault. This is discussed further in Ch.8.7.2.

### 8.3.2: Description of Fraser Complex.

Three gneiss units were identified in the Fraser Complex by Rattenbury (1991): sillimanite gneisses comprise quartz + plagioclase + garnet + orange-brown biotite ± alkali feldspar ± sillimanite ± kyanite interpreted as upper amphibolite facies metapelites; hornblende gneisses range from hornblendite to more felsic compositions and contain yellow to dark green hornblende + plagioclase ± quartz ± dark brown to

orange-brown biotite ± garnet ± epidote ± magnetite and are interpreted to represent volcanogenic sediments and tuffaceous horizons interbedded with the metapelites; migmatitic gneisses are restricted to east of Mount Misery and the Hokitika Gorge and consist of quartz + plagioclase + alkali feldspar + biotite ± garnet ± hornblende ± muscovite ± epidote and accessory apatite and zircon. The migmatitic gneiss is crudely layered and interpreted as partially melted quartzo-feldspathic sediments distinct from the pelitic precursors of the sillimanite gneisses (Rattenbury 1991).

Rattenbury (1987a) also identified 2 granitoid plutons intruding the Fraser Complex gneisses; The Fraser Peak Granite, a porphyritic green-brown biotite + muscovite (± hornblende) granite to granodiorite and the Doughboy Tonalite which contains yellow to green-brown biotite, minor muscovite, titanite and epidote. Rattenbury (1987a, 1991) also notes a number of mafic and trachytic dikes cutting all above units. A cursory examination of the dikes of the Fraser Complex held in the University of Otago collection indicates strong petrographic similarities to the dikes of the Hohonu Dike Swarm, although most are deformed to varying degrees by the mylonitization affecting the Fraser Complex.

Field observations in the northern portion of the Fraser Complex are in agreement with the studies of Rattenbury (1987a+b, 1991). Medium grained, equigranular, banded hornblende gneisses exposed on the eastern side of Mount Upright on the Lawyers Delight track (GMU7, GMU8), and fine grained, garnet-bearing, amphibole-rich mylonites in the Styx River (GSR2) are considered equivalent to the Hornblende Gneisses of Rattenbury (1991). A hornblende and clinozoisite rich gneiss exposed at the base of a narrow gorge in MacPherson Creek (J33 674197), previously described as a granite-derived mylonite by Reed (1964) (his sample 5153), is probably also analogous to the Hornblende Gneisses. Mica-rich, highly banded and folded mylonites (GMU5, GMU6) exposed on the western side of Mount Upright are considered to be correlative with the Sillimanite Paragneisses of Rattenbury (1991). Biotite-rich paragneisses and mylonites exposed in a tributary of Geologist's Creek (J33 613149), biotite paragneiss (IMC6) and occasional garnet-bearing paragneisses (IMC1) in MacPherson Creek are also correlated with the Sillimanite Gneisses of Rattenbury (1991).

Well exposed in Mount Brown Creek and also present in a small, unnamed creek near Stoney Creek (J33 650180) is a strongly foliated, porphyritic biotite granodiorite. The rock (UMB1, TW47) exhibits a protomylonitic fabric and comprises undulatory quartz showing a weak crystallographic preferred orientation, anhedral to subhedral cataclased crystals of sodic oligoclase ($\approx$An37%), augen of alkali feldspar up to 40 mm long, and sheared green-brown biotite. The presence of relatively abundant, large (up to 0.4 mm) euhedral crystals of apatite, and minor muscovite appears characteristic of this unit. Accessory phases include minor zircon and opaques. Epidote is common and mostly secondary, resulting from alteration of feldspars and growth in late stage brittle shear zones. Green, strongly foliated and broadly banded, chloritized and epidotized, medium grained mylonite (AR1) outcropping in the Arahura River (J33 659177), Upper MacPherson Creek (IMC4) and in the Styx River probably represent more highly cataclased variants of the Mount Brown Creek body. The Mount Brown Creek granodiorite is texturally similar to biotite-rich, porphyritic protomylonites exposed at the eastern base of the Doughboy, termed the Doughboy Tonalite by Rattenbury (1987a).

Mafic-rich, medium to coarsely crystalline granitoid mylonite (IMC2) poorly exposed in the upper parts of MacPherson Creek is distinct from the Mount Brown Creek granodiorite and is distinguished by the abundance of euhedral light-brown to green amphibole crystals up to 2 mm long and minor titanite. A distinct, more mafic dioritic plutonic phase is indicated, similar to sample CR5 from the Crooked River, Granite Hill.

Several thin (5-30 cm) mafic dikes occur in close proximity in MacPherson Creek. One of these dikes (IMC3) cuts foliation at a moderate angle and is mylonitized. Rattenbury (1987a, b) reports a single, undeformed, altered basaltic dike crosscutting mylonitization from this same location. Rattenbury (1987b) suggests this dike may be related to Late Miocene (5-10 Ma) basaltic activity in South Westland, and thus gives a minimum age for mylonitization in the Fraser Complex. The occurrence of a mylonitized dike at what appears to be the same location as Rattenbury's undeformed sample is perplexing, and may put his interpretation of a minimum age in question. No other dikes were observed in MacPherson Creek or the northernmost portion of the

Fraser Complex. The presence of mafic dikes deformed by mylonitization within the Fraser Complex gives a maximum age on this deformation (Rattenbury 1987b) of ≈82 Ma, presuming the dikes are contemporaneous with the Hohonu Dike Swarm.

Green, broken schist, identical to exposures near the Alpine Fault in a tributary of Geologist's Creek (J33 618148), directly overlies Arahura Granite in Geologist's Creek (J33 607150), approximately 1000 m from the current trace of the Alpine Fault. Similar rocks are also exposed in a small unnamed tributary on southeast Mount Tuhua (J33 645180), and garnet-muscovite schist is exposed west of the Alpine Fault immediately north of the Styx River Bridge (J33 594123). Rattenbury (1987a) identified similar rocks to the south in Surveyors Creek near Mount Misery, and on the Doughboy, and interpreted them as stranded schist nappes representing inactive surface traces of the Alpine Fault.

## 8.4: Comparison of Granite Hill and Fraser Complexes.

The recognition of a similar amphibolite facies assemblage of paragneisses, metabasites and orthogneisses in both the Granite Hill Complex (this study) and the Fraser Complex (Rattenbury 1991) strongly suggests that the Granite Hill Complex represents a northerly continuation of the Fraser Complex. Similar inferences have previously been made by Young (1968) and Mason (1990). In particular, the megacrystic granodioritic orthogneisses of the Granite Hill Complex are strikingly similar to the Mount Brown Creek Granodiorite which in turn strongly resembles the Doughboy Tonalite of Rattenbury (1987a), further indicating a link between the Granite Hill and Fraser Complexes. Similar orthogneisses also occur to the north in Haupiri Quarry (S52 300765) and possible northern correlatives of the Granite Hill and Fraser Complexes may also occur in the largely unstudied southern Victoria Range. Mason and Taylor (1987) describe Mount Elliot in the Victoria Range as consisting primarily of biotite + almandine ± hornblende ± sillimanite gneisses, with minor biotite-rich granodioritic orthogneiss. Hornblende gneisses similar to those of the Fraser and Granite Hill Complexes are also described from the Ahaura region by Mason and Taylor (1987).

Despite the lithological similarities between the Granite Hill Complex and Fraser Complex, the tectonic histories of the two differ, as indicated by the paucity of true mylonites and lack of deformed mafic dikes in the Granite Hill Complex. This suggests that the Fraser Complex has been more strongly affected by recent movement on the Alpine Fault. Scant apatite fission track data from the Granite Hill Complex range in age between 6-10 Ma, somewhat older than the 2 Ma ages obtained in the Fraser Complex (Kamp *et al* 1992, Ch.5), suggesting an increase in uplift age from south to north. The consequent lack of pervasive mylonitization in the Granite Hill Complex may be a consequence of uplift above conditions of ductile deformation of quartz prior to major strike slip motion on the Alpine Fault.

## 8.5: Geochemistry of the Fraser Complex and Granite Hill Complex.

Geochemical analyses of various rock types from the Fraser and Granite Hill Complexes are presented in Appendix C and E. Analyses of Fraser Complex lithologies from Rattenbury (1987a) and several Granite Hill Complex analyses published by Mason and Taylor (1987) were also included within the data set for comparison.

### 8.5.1: Biotite (+ sillimanite) paragneisses.

Five analyses of paragneisses from both the Fraser and Granite Hill Complex have silica contents ranging between 59-77% $SiO_2$, reflecting a progression from pelitic to psammitic compositions. Reasonable trends of decreasing $TiO_2$, $Al_2O_3$, $Fe_2O_3$, MgO, CaO, $K_2O$, $P_2O_5$, Sr Ba and Rb are observed with increasing $SiO_2$, similar to trends in the data set of Rattenbury (1987a).

Chondrite-normalized REE patterns for several paragneiss samples, including data from Mason and Taylor (1987), are presented in Fig.8.10. All show similar straight, LREE enriched ($La/Yb_N \approx 10$-12) plots with only one sample displaying an appreciable negative Eu anomaly. REE plots of the paragneisses are broadly similar to those of the Greenland Group and the post-Archaean average shale (see Fig.2.4).

### 8.5.2: Metabasites.

Three analyzed metabasite samples have silica contents ranging between 51-59% $SiO_2$ and are somewhat variable in terms of major and trace element chemistry. Two

hornblende-garnet gneiss samples from the Crooked River (6CR and 4CR of Mason and Taylor 1987) display relatively flat to slightly HREE depleted REE abundances with $La/Yb_N$ = 3.6 and 1.5 and Eu/Eu* = 1.03 and 0.80 respectively (Fig.8.11).

**8.5.3: Granodioritic orthogneiss.**

Several samples of the megacrystic orthogneisses of Mount Brown Creek and the Granite Hill Complex have relatively similar chemistries with silica contents ranging between 62-67% $SiO_2$. The orthogneisses are weakly peraluminous with A/CNK between 1.02-1.06 and are very similar in composition to analyses of the Doughboy Tonalite (Rattenbury 1987a), and the orthogneiss exposed in the Haupiri Quarry (6HP of Mason and Taylor 1987). A data set combining all these analyses shows good trends of decreasing $TiO_2$, $Al_2O_3$, $Fe_2O_3$, MgO, CaO and $P_2O_5$ with increasing $SiO_2$ (Fig.8.12). The Doughboy Tonalite and equivalent megacrystic orthogneisses contrast with the Fraser Peak Granite (Rattenbury 1987a) in having lower $SiO_2$ and $K_2O$ and higher $Na_2O$ (Fig.8.12).

REE patterns of orthogneiss from the Granite Hill Complex (5RO and 5CR of Mason and Taylor 1987) and the Haupiri Quarry (6HP of Mason and Taylor 1987) (Fig.8.13) display similar, straight LREE enriched plots with $La/Yb_N \approx$ 19-25 and minor negative Eu anomalies (Eu/Eu* = 0.76-1.08). The REE patterns are similar to those of the Te Kinga Suite and relatively low HREE contents suggest a source containing residual garnet.

**8.5.4: Radiogenic isotopes.**

Radiogenic isotope data for several paragneiss and orthogneiss samples from the Fraser and Granite Hill Complex are presented in Table 8.1.

**8.5.4.1: Orthogneisses.**

An absence of age control for the orthogneisses precludes accurate decay correction and calculation of initial isotopic ratios. The two orthogneiss samples analyzed (GRH1 and UMB1) are distinctly more radiogenic than the Hohonu Super-Suite plutons at 110 Ma (see Fig.6.13) yet are less radiogenic than published Karamea Suite granitoid data at 381 Ma (see Fig.6.84) and thus cannot also be confidently

related to this Palaeozoic magmatic event. $T_{DM}$ for these two orthogneiss samples range from 1.1 to 1.3 Ga, overlapping the range observed in the Hohonu Super-suite (see Table 6.4).

**8.5.4.2: Paragneisses.**

Decay correction of the paragneisses of the Fraser and Granite Hill Complexes to both 110 Ma (Fig.6.13) and 381 Ma (Fig.6.84) produces initial compositions distinctly less radiogenic than available analyses of the Greenland Group. Additionally, even when recalculated to 500 Ma, the approximate age of deposition of the Greenland Group, these paragneisses remain less radiogenic than available Greenland Group data (Fig.8.14). Thus, isotopic data suggests that the Fraser and Granite Hill Complex paragneisses are unlikely to represent highly metamorphosed equivalents of the Greenland Group. As noted previously (Ch.6.7.4) recalculation of the paragneissic samples to 381 Ma results in a broad overlap with the Summit Granite and other available Karamea Suite granitoid data, suggesting a genetic link between the paragneisses and Palaeozoic plutonism. Further isotopic data are required to fully interpret these observations. $T_{DM}$ ages for Fraser and Granite Hill Complex paragneiss are $\approx$ 1.7 Ga, slightly younger than those calculated for the Greenland Group (see Table 6.4).

**8.6: Age constraints.**

As noted in the previous section, the age of the Granite Hill and Fraser Complex gneiss precursors remains largely unconstrained. Ireland (1992) published SHRIMP data on 9 zircons from a Granite Hill Complex garnet-sillimanite gneiss (10RO) collected from Thirsty Creek. A single zircon crystal from this sample was dated at 115 $\pm$ 6 Ma and interpreted to represent a high grade metamorphic-anatexis event, based on the low Th/U and small size of the crystal, typical of metamorphic zircons. This age is within error of Hohonu Super-Suite and Separation Point Suite ages and may be associated with either intrusive event. Of the remaining zircons, five are dated at 399 $\pm$ 9 to 524 $\pm$ 12 Ma and (assuming none reflect anatectic events) indicate a Silurian ($\approx$ 400 Ma) precursor for the Thirsty Creek paragneiss. Such a parent rock is $\approx$100 Ma younger than the protolith of the Victoria Paragneiss, generally considered to be the Ordovician Greenland Group (Ireland 1992). A Silurian precursor is also

indicated for a similar sillimanite-garnet gneiss collected in Troulands Creek, Mount Elliot (sample 12AA, Ireland 1992).

Kimbrough *et al* (1994a) present a conventional U-Pb zircon age of 157 $\pm$ 21 Ma for a migmatitic leucosome in the Hokitika Gorge. They interpret this age to represent the crystallization age of the leucosome and a period of peak metamorphism and migmatization in the Fraser Complex.

K-Ar age data from the Fraser Complex are widely variable with hornblende ages of 228-298 Ma, biotite ages of 44-61 Ma and whole rock ages of 45-91 Ma, the latter controlled by the relative modal abundances of biotite and hornblende (Rattenbury 1987a, 1991). The clustering of biotite ages around 44 Ma gives a maximum age for mylonitization, considerably older than the 25 Ma generally considered as the age of inception of the Alpine Fault (Kamp 1986, Cooper *et al* 1987). The anomalously old ages were ascribed to excess argon contamination by Rattenbury (1987b).

Fission track data (Fig.5.4) indicate recent rapid uplift of the Fraser Complex and Granite Hill Complex over the past 8 Ma associated with uplift along the Alpine Fault.

## 8.7: Discussion.

### 8.7.1: Regional correlatives

Previous comparisons have been made between the Granite Hill and Fraser Complex gneisses, the Charleston Metamorphic Group of Nathan (1975) and the Victoria Paragneiss of the northern Victoria Range (Tulloch 1979a) (Young 1968, Mason and Taylor 1987, Kimbrough and Tulloch 1989, Mason 1990). Such high-grade metamorphic rocks in the Buller Terrane were considered to represent pre-Cambrian crystalline basement (e.g. Adams 1975, Mason and Taylor 1987) or metamorphosed Greenland Group (Shelley 1970). Recent geochronological work (Kimbrough and Tulloch 1989, Ireland 1992) has challenged the presence of a regional pre-Cambrian basement to the Western Province and much of the metamorphic terrain is now considered to represent metamorphosed equivalents of the Greenland Group and intrusive granitoids uplifted in a series of Cretaceous metamorphic core complexes

(Tulloch 1988b, Tulloch and Kimbrough 1989). The inference is that the Granite Hill/Fraser Complex gneisses also represent metamorphosed Greenland Group and intrusive granitoids (Tulloch 1988b, Tulloch and Kimbrough 1989, Kimbrough *et al* 1994b). The findings of this study are inconsistent with such an interpretation for the Fraser and Granite Hill Complexes. Of particular note are the relative abundance of hornblende-bearing gneisses, interpreted as meta-volcanic or meta-tuffaceous beds (Rattenbury 1987a, 1991). Hornblende gneisses are unknown in the Charleston Metamorphic Group (Nathan 1975, White 1987, Laird 1988) and rare in the Victoria Paragneiss (Tulloch 1979a). Additionally, interbedded volcanic beds, representing appropriate precursors for the hornblende gneisses, are unknown in the Greenland Group. However, tuffs are reported from the Martins Bay Formation in South Westland, which is considered to be a metamorphosed equivalent of the Greenland Group (Mutch and McKellar 1964). As discussed previously the Granite Hill and Fraser Complex paragneisses are also isotopically distinct from the Greenland Group (Ch.8.5.4.2). Furthermore, preliminary SHRIMP dating (Ireland 1992) indicates discrepancies in the age of the Granite Hill paragneiss precursor and the Victoria Paragneiss which has a zircon inheritance pattern similar to Greenland Group. Thus the metabasite-paragneiss association of the Granite Hill and Fraser Complexes does not appear to represent a metamorphosed equivalent of currently exposed Greenland Group. Granite Hill and Fraser Complex granitoids are isotopically distinct from other Western Province intrusives (Ch.8.5.4.1) and do not display clear affinities with other Western Province granitoid suites. Correlation of the Granite Hill Complex and Fraser Complex within the Charleston Metamorphic Group thus seems unlikely and designation as a distinct metamorphic basement terrain seems more appropriate.

An alternative to suppositions that the Fraser and Granite Hill Complex are Buller terrane rocks is that they may represent fragments of Takaka terrane and Fiordland equivalents left behind during strike-slip motion on the Alpine Fault. Apparently similar amphibolite-grade gneisses to those of the Granite Hill/Fraser Complexes make up regional basement in the western Fiordland region. Descriptions of rocks in the Franklin Mountains region, given by Bradshaw (1990), include sequences of pelitic-semi-pelitic schist and gneiss (the George Sound Paragneiss) with locally associated gneissic granitoids (Rafted Granitoid Gneiss) also found as enclaves within

WFO (Bradshaw and Kimbrough 1991). Also present are a series of layered amphibolitic gneisses occasionally containing garnet (Jagged Gneiss and Arthur River Complex of Bradshaw 1990). Sequences of similar hornblende + biotite gneisses (Deep Cove Gneiss and Mount Barber Gneiss) and plagioclase-biotite ± hornblende gneiss with minor quartzite, metapsammite, metapelite and quartzofeldspathic gneiss intruded by orthogneiss (Western Manapouri Province) also occur in the Doubtful Sound Region (Gibson 1982a). Potential protoliths for these gneisses are represented in the Takaka terrane by the Cambrian Devil River Volcanics and sediments of the Tasman and Anatoki Formations (Cooper and Tulloch 1992). The occurrence of amphibolitic paragneisses and metabasites with associated orthogneisses in Fiordland is similar to observations in the Granite Hill and Fraser Complexes (this study and Rattenbury 1991), and may suggest correlation between the two areas. The Fiordland rocks are generally considered to represent metamorphic equivalents of Takaka terrane rocks (e.g. Ward 1984, Gibson 1992) and are intruded by the Early Cretaceous Western Fiordland Orthogneiss (WFO) (J.Y.Bradshaw 1989, 1991). Such observations are strengthened by the intrusive relationships between the chemical equivalent of the WFO, the Separation Point Batholith (Muir *et al* 1995), and Takaka terrane country rocks in west-Nelson. The proposition that the Fraser and Granite Hill Complex gneisses are equivalent to the Fiordland Gneisses, and in turn represent metamorphosed equivalents of the Takaka terrane, leads to the question of how they obtained their present position. Two explanations are feasible: either the metamorphic rocks were sheared from the Fiordland block during strike-slip movement on the Alpine Fault; or Takaka terrane equivalents currently conformably or tectonically underlie the Buller terrane and have been uplifted as a result of compression across the Alpine Fault.

Migmatites within the Deep Cove Gneiss yielding a Rb-Sr age of 388 ± 23 Ma (Gibson 1982a), and the Seaforth orthogneiss and Mount George Gabbro (360-345 Ma (syn-metamorphic intrusions into the Doubtful Sound Gneisses (Gibson 1982b))), indicate a Devono-Carboniferous age of metamorphism in Fiordland. Orthogneiss enclaves within WFO, considered to represent included country rock, have also yielded U-Pb zircon ages of 341 ± 34 Ma and a Rb-Sr isochron of 391 ± 48 Ma (Bradshaw and Kimbrough 1991) and suggest a pre-Devonian metasedimentary basement intruded by Devonian granitoids. If correlation of the Fiordland gneisses with the Fraser

Complex and Granite Hill Complexes is appropriate then the age constraints from Fiordland may then be applied to the Granite Hill and Fraser Complexes.

Despite overall similarities between the gneisses of the Fiordland and Fraser/Granite Hill Complex, there are difficulties in correlating these rocks. Firstly, although marbles and limestones are reasonably common in both the Takaka terrane and Western Fiordland, none are observed in the Fraser or Granite Hill Complexes. Secondly, initial Sr ratios in granitoid enclaves are considerably more primitive than those for the orthogneisses of this study (Bradshaw and Kimbrough 1991). The Fraser Complex and Granite Hill Orthogneisses instead display isotopic similarities to the Karamea Suite (Ch.8.5.4.1) which is restricted to the Buller terrane. Considerably more detailed work is required to establish any links between the western Fiordland region and the Fraser and Granite Hill Complexes.

**8.7.2: Structural interpretation.**

High-grade metamorphic rocks of the Paparoa and northern Victoria Ranges have been interpreted as lower-plate assemblages of metamorphic core complexes (Tulloch 1988b, Tulloch and Kimbrough 1989). Similar interpretations have been made for the Granite Hill and Fraser Complexes (Tulloch 1988b, Kimbrough *et al* 1994a). However, major rotation of a previously shallowly dipping detachment surface is required to explain the current steeply dipping reverse nature of the Fraser Fault, and no evidence for such rotation is observed west of the Fraser/Granite Hill Faults. Additionally, the current trend of the Fraser and Granite Hill Complexes and the Fraser Fault is perpendicular to supposedly analogous structures in the Paparoa Metamorphic Core Complex of Tulloch and Kimbrough (1989). A simpler interpretation of the Fraser and Granite Hill Complex as a mid-crustal block, uplifted as a wedge during compressional movement on the Alpine Fault, was proposed by Kamp *et al* (1992) on the basis of fission track data (see Fig.5.6), and is considered to be a more appropriate interpretation. This interpretation is unaffected by correlation of the Fraser/Granite Hill Complexes with western Fiordland gneisses, or their interpretation as a distinct mid-crustal region of the Buller terrane.

## 8.8: The Thirsty Creek Norite.

### 8.8.1: Introduction and field relationships.

The Thirsty Creek Norite is a melanocratic, equigranular, medium to coarse grained rock first described by Tulloch and Brathwaite (1986) and later in more detail by Mason and Taylor (1987) and Mason (1990) who included it within the Granite Hill Complex. Although distinct from the metamorphic rocks of the Granite Hill Complex it is discussed in this chapter as no equivalent rocks are observed to the west of the Granite Hill Fault. Outcrops occur in Thirsty Creek (K32 911374) and in the foundations of the Evans River Bridge (K32 949410). Similar rocks also outcrop in the middle reaches of Rough and Tumble Creek (K32 965425), the probable source of boulders of norite and pyroxenite described by Mason (1990). Possible correlatives of Thirsty Creek Norite occur to the north, Mason (1990) describes similar rocks from Lake Ahaura, and Mason and Taylor (1987) also note rare pebbles of pyroxenite from Troulands Creek in the Southern Victoria Range. The Tobins Diorite (Tulloch 1983, Tulloch and Brathwaite 1986) in the Victoria Range may also be correlatable to the Thirsty Creek Norite.

The age of the Thirsty Creek Norite is unknown. Thirsty Creek Norite intrudes the Granite Hill Complex gneiss and is unaffected by the metamorphism and deformation that has affected the host rock gneisses, and it must therefore postdate the metamorphic events in the Granite Hill Complex. Numerous inclusions of Granite Hill Gneiss are also apparent within Thirsty Creek Norite. Recognition of an anatectic event in the Granite Hill Complex at 115 $\pm$ 6 Ma (Ireland 1992), suggest the Thirsty Creek Norite is Cretaceous or younger.

### 8.8.2: Petrographic description.

The rocks outcropping in Thirsty Creek (RTC1 and RTC2) and in Evans River (CR2) classify as pyroxene hornblende norites. These rocks exhibit a sub-ophitic texture and consist mainly of subhedral crystals of plagioclase (An 55-80%[19]) up to 2 mm long and highly twinned, subhedral green pleochroic hornblende (2 mm). Also present are subhedral to anhedral crystals of hypersthene (Fs34) up to 3 mm long, occasional euhedral olivine altered to serpentinite, anhedral crystals of yellow-brown to

19: Microprobe data from Mason (1990).

orange-brown to red-brown biotite, anhedral magnetite up to 1 mm, apatite and minor anhedral quartz.

Sample GRT5, a pyroxene hornblende norite from Rough and Tumble Creek, differs from the previously described samples by being finer grained, and in having a much higher proportion of orthopyroxene, approximately sub-equal in amount to amphibole. The orthopyroxene occurs in a sub-ophitic groundmass of green hornblende and highly twinned anhedral labradorite ($\approx$An60%).

**8.8.3: Geochemistry.**

Samples of the Thirsty Creek Norite from Thirsty Creek itself have $\approx$48% $SiO_2$ (Mg# $\approx$60), whereas samples from Evans River and Rough and Tumble Creek are more evolved with $\approx$52% $SiO_2$ (Mg# $\approx$74). Chondrite-normalized REE plots for two samples from Thirsty Creek are relatively flat, LREE enriched ($La/Yb_N \approx 7$) with no appreciable Eu anomaly (Fig.8.15). REE plots are also similar to a hornblende diorite (20AA) from the southern end of the Mount Elliot Massif (Mason and Taylor 1987). Radiogenic isotopes for two samples from Thirsty Creek (Table 8.1) are distinctly more radiogenic than the Hohonu Dike Swarm and preclude correlation of the two units. At 110 Ma, the Thirsty Creek Norite has radiogenic isotope compositions similar to the Hohonu Super-suite, suggesting a possible petrogenetic relationship to Cretaceous plutonism in the Buller terrane. Low Rb-Sr and Sm-Nd ratios result in only minor variations in calculated initial ratios for the Thirsty Creek Norite at various assumed ages.

# Chapter 9

# Late Cretaceous and Tertiary sediments.

## 9.1. Introduction.

Late Cretaceous and Tertiary sediments have only limited outcrop within the study area, the most significant of these being along the northwestern margin of the Hohonu Ranges. Sedimentary rocks are also poorly exposed near the Gentle Annie region of Mount Graham. Tertiary and Cretaceous sediments are considerably more widespread to the north and west of the study area, and have also been identified in numerous oil-related exploratory drillholes to the west of the Hohonu Fault (see Wellman 1950a, Nathan *et al* 1986, Spanninga 1993). Tertiary sediments form part of the infill of the Grey-Inangahua depression, a tectonic trough between by the Paparoa and Hohonu Ranges filled with up to 4000 m of Miocene to Quaternary sediments. Sediments of the Grey Valley trough grade from predominantly marine in the Greymouth Region to largely non-marine north of Ahaura (Nathan *et al* 1986).

### 9.2.1. The Pororari Group.

The only outcrops of Pororari Group in this study are found in Blue Bottle Creek, Mount Graham (≈J33 541191). Exposures comprise red to mauve, clast-supported conglomerates consisting primarily of rounded clasts of Greenland Group and subordinate granitoid up to 50 cm across, and large boulders (up to 1 m) of red, medium grained, well sorted, indurated, micaceous sandstone in a red medium sand matrix (Fig.9.1). The conglomerate is interbedded with red sandstone similar in appearance to the large red sandstone clasts. Conglomerate and sandstone are exposed for ≈100 m in Blue Bottle Creek and apparently overlie altered red-brown Greenland Group sandstones, although no contacts are exposed. The occurrence of maroon stained Greenland Group is common below outcrops of Hawks Crag Breccia (Nathan *pers.comm.*) and is inferred to be a consequence of deep leaching of basement rocks by the overlying terrestrial sediments. More typical Greenland Group metasediments occur further downstream and upstream of the Pororari Group sediments. Red-maroon conglomerate is also common in float in a tributary stream entering Blue Bottle Creek (J33 535201) although no outcrops were located. The coarse conglomeratic nature of this unit, and its deep maroon-red-brown colour, indicate it belongs within the Hawks

Crag Breccia Formation of the Pororari Group (Nathan *et al* 1986, Laird 1988). The Pororari Group is interpreted as a non-marine sequence series of valley-fill alluvial sediments dominated by coarse clastic debris. The sediments are inferred to have been deposited in fault-bounded basins initiated during mid-Cretaceous crustal extension (Laird 1988, 1993, 1994). The Hawks Crag Breccia is the most widespread of Pororari Group formations and is generally interpreted as debris-flow deposits on alluvial fans formed by rapid erosion of exposed fault scarps (Nathan *et al* 1986, Laird 1988). Microfloral studies indicate that the Pororari Group is largely Motuan to possibly Ngaterian ($\approx$100-105 Ma) in age (Raine 1984). Recent SHRIMP dating of the Stitts Tuff from the basal Pororari Group in the Lower Buller Gorge has yielded an age of 101 Ma (Muir *pers.comm.* 1994), giving a maximum age of deposition of the Pororari Group in the Buller Gorge.

Hawks Crag Breccia outcrops to the south at Mount Kowhiterangi (J33 450115) and has also been identified in several drillholes to the west of the study area. A detailed description of Mount Kowhiterangi is given by Gage and Wellman (1944) who describe a basal, well indurated, brown to brick-red, sub-angular to sub-rounded greywacke breccia/conglomerate with occasional beds of red sandstone and grit (unit K2). This unit is overlain by two, finer grained, red greywacke conglomerates (units K3 and K5) correlated with the Hawks Crag Breccia by Nathan (1974). A basalt flow or sill between units K3 and K5 dated at 68.4 $\pm$ 1.4 Ma by Sewell *et al* (1988) has been correlated with the similar Morgan Volcanics within the Late Cretaceous to Palaeocene Paparoa Coal Measures. Paparoa Coal Measures do not outcrop in the study area, although they have been identified in a number of drillholes (see Nathan *et al* 1986).

### 9.2.2. Brunner Coal Measures.

Brunner Coal Measures are poorly exposed at Gentle Annie, Mount Graham ($\approx$J33 539212) where an old coal mine operated sometime before 1906. A description given by Bell and Fraser (1906) describes a stratigraphic sequence consisting of rusty pebble conglomerate, ferruginous micaceous sandstone and grits, fine grained dark green argillaceous shales and sandstones, containing 4 foot and 5½ foot coal seams, overlain by arenaceous shale and sandstone. Investigations during this study located

only some old, rather dangerous looking, mine workings. The Brunner Coal Measures are Eocene and are considered to represent fluvial to marginal marine sediments deposited in meandering streams and peat swamps developed on a surface of low relief during a period of relative tectonic quiescence (Nathan *et al* 1986, Laird 1988). Brunner Coal Measures are identified in several drillholes to the west of the Hohonu Fault and also outcrop at Mount Kowhiterangi (Nathan *et al* 1986).

### 9.2.3. Nile Group.

Pink to light brown-grey fine grained sandy and muddy limestone outcrops in Deep and Clear Creeks and on Knoll Point on the shores of Lake Brunner (K32 797397). The Nile Group has been subdivided into a number of different formations (see Nathan 1974, Nathan *et al* 1986, Laird 1988) and Hamill (1972) correlated these limestones with the Cobden Limestone. Given the limited outcrops in the study region these limestones are here not attributed to any formation and are considered as an undifferentiated unit within the Nile Group.

Exposed in Deep Creek are several distinctive limestone conglomerates, comprising well rounded clasts of granitoid and Greenland Group with subordinate mudstone, limestone, basalt and rare coal in a brown sandy limestone matrix (Fig.9.2). Granitoid clasts include the nearby megacrystic Deutgam Granite but are dominated by a medium grained, equigranular two mica granite similar to Te Kinga Monzogranite and Summit Granite. Some mylonite clasts were also noted. Following a major flood, Wellman (1950b) was able to observe a gradation from limestone into greywacke-quartz limestone conglomerate lying in direct sedimentary contact with Greenland Group. No contact was observed between the limestone and the overlying Blue Bottom Formation, yet it is presumably an unconformity as is seen in other areas (Nathan 1974).

Knoll Point (K32 798398) consists of pink, well indurated limestone. The limestone is mostly detritus-free but contains a few sandy bands and may contain some fragments of Greenland Group (Morgan 1919). These outcrops were sampled for foraminifera by Morgan (1919) but none were found. Nile Group Limestone also occurs at Mount Kowhiterangi and in numerous drillholes around the area.

The Nile Group has age limits ranging from Whaingaroan to early Otaian (Oligocene to Early Miocene) (Nathan 1974) and is considered to represent deposition at the peak of a marine transgression (Nathan *et al* 1986).

### 9.2.4. Blue Bottom Group.

Mudstones and sandstones outcropping in Deep and Clear Creeks, the Little Hohonu River and the Greenstone River are correlated with the Waitakian to Waipipian (Late Oligocene to Mid-Pliocene) Blue Bottom Group (Nathan 1974). Abundant Blue Bottom is exposed to the west of the study area (see Warren 1967) and is also found in most oil exploration drillholes. In this study Blue Bottom Group sediments consist of mainly brown to blue-grey, fine to medium grained, indurated, well sorted, bioturbated, micaceous, massive sandstones with rare shellbeds (Fig.9.3). Thin conglomerate beds containing pebble to cobble sized, well-rounded granitoid and Greenland Group pebbles are common and are often the only indication of bedding (Fig.9.3). No sedimentary contacts between the Blue Bottom and any underlying units were observed in the field area, but it is generally considered to unconformably overly older units (Nathan 1974). Although the Blue Bottom has been differentiated into a number of formations (Nathan 1974, Laird 1988) no such subdivision is attempted here.

Outcropping in the Eastern Hohonu River, approximately 300 m upstream of the Mitchell's Road, is an exposure of conglomerate comprising well rounded granitoid, sandstone, Greenland Group, quartz and minor coal clasts, in erosive contact with a micaceous, medium sandstone. Kaiatan and Waitakian (Late Eocene and Oligocene respectively) foraminiferal faunas from pebbles in this conglomerate (Wellman 1950b) suggest correlation with either the Blue Bottom or Nile Group. This exposure is correlated with the Blue Bottom Group due to its non-calcareous terrigenous nature. Well-bedded, moderately dipping sandstones and conglomerates exposed west of Ruru (K32 862465) may also belong within the Blue Bottom Group (Wellman 1950a).

The Blue Bottom is generally considered to represent outer shelf or deeper open water conditions and an influx of terrigenous clastic sediments reflecting the onset of Alpine Fault movement and the initiation of a marine regression (Nathan *et al* 1986).

The presence of numerous thin conglomerate bands within the sandstone is indicative of a shallow water deposit reasonably close to source. Shallow water microfauna from granitic breccia and breccia conglomerate from the Deep/Clear creek region (N.de B.Hornibrook *pers.comm.* in Nathan *et al* 1986) also indicates the proximity of land in Oligocene times and it is likely that most Tertiary sediments in the Hohonu region represent near shore, relatively high energy environments.

## 9.3: Discussion.

Late Cretaceous and Tertiary sediments are poorly exposed in this study area and are consequently only a minor proportion of this study. The sections exposed in Deep and Clear Creeks are complex and have been discussed in some detail by Wellman (1950b), Wellman and Suggate (1950) and Hamill (1972). Several days field work added little to the observations of these workers, largely due to a deterioration in the amount of exposure, with many described outcrops no longer being exposed. Outcrops are also generally small and sparsely distributed making interpretation problematic. The only major change to earlier observations being recognition of the infaulted block of granitoid in Deep Creek as Deutgam Granite, rather than Brunner Granite (French Creek Granite) as identified by Hamill (1972). The section exposed along the front of the Hohonu Ranges is considered to represent a dismembered assemblage of the more complete Tertiary sequence recorded to the west of the Hohonu Fault in numerous drillholes. These sediments are incorporated as part of the Hohonu Fault in a complex series of reverse fault bounded slices uplifted in response to the recent uplift of the Hohonu Ranges (see cross section B-B', map pocket).

# Chapter 10

## Synopsis and future work.

This chapter summarises the major observations and conclusions of this study, and also incorporates those aspects which could be extended and improved by further research.

Ten lithologically distinct granitoid plutons have been mapped intruding typical Greenland Group metasediments, which are metamorphosed to biotite hornfels facies near intrusive contacts. Field relationships of the granitoids and adjacent rocks are summarised in a 1:50 000 scale geological map (see map pocket).

From north to south the plutons are:

→ Jays Creek Granite - a white, massive, mesocratic, medium grained biotite granodiorite;

→ Pah Point Granite - an orange, massive, mesocratic, coarse grained megacrystic biotite monzogranite;

→ Uncle Bay Tonalite - a grey, massive, mesocratic, medium to coarse grained biotite (± hornblende) tonalite;

→ Te Kinga Monzogranite - a white, equigranular, leucocratic, fine or coarse grained biotite muscovite monzogranite which exhibits porphyritic textures on the summit of Mount Te Kinga and is mylonitized along the shores of Lake Poerua;

→ Deutgam Granite - a complex pluton dominated by white to grey, massive, mesocratic, coarse grained megacrystic biotite (± hornblende) granodiorite. In the centre of the pluton, gabbroic blocks termed the Eastern Hohonu River Gabbro are incorporated within Deutgam Granite. The relationship of this, and other isolated mafic bodies associated with the batholith (e.g. Rose Creek Diorite, Thirsty Creek Norite), with the Hohonu Batholith granitoids is unclear and requires more detailed isotopic and geochronological study;

→ French Creek Granite - a pluton with distinct A-type characteristics, dominated by a red, subsolvus, massive, medium to coarse grained, equigranular biotite syenogranite with characteristic granophyric textures and distinctive biotite compositions. Subordinate hypersolvus alkali amphibole-bearing monzogranite and

quartz alkali feldspar syenite varieties are also recognized. Rhyolitic dikes cutting Deutgam Granite have geochemical affinities with French Creek Granite and are considered to represent hypabyssal equivalents of this pluton;

→ Turiwhate Granodiorite - a white to green, medium grained, equigranular titanite hornblende granodiorite with distinct I-type characteristics;

→ Summit Granite - a white, leucocratic, fine to medium grained, equigranular, biotite muscovite granodiorite to monzogranite containing abundant metasedimentary material and commonly displaying a moderate foliation. Summit Granite sits as a cap on top of Mount Turiwhate and has been intruded by Turiwhate Granodiorite and Deutgam Granite. The field relationships between the Summit Granite, Turiwhate Granodiorite, and Deutgam Granite remain unclear along the south-west margin of Mount Turiwhate, a consequence of difficult terrain and inaccessibility;

→ Arahura Granite - a large, homogeneous, white to pink, medium to coarse grained, mesocratic to leucocratic, megacrystic biotite monzogranite with accessory muscovite. This pluton displays porphyritic textures at higher levels of exposure;

→ Mount Graham Granite - a poorly exposed, white, leucocratic, equigranular, medium grained biotite muscovite monzogranite similar in appearance to the Summit Granite. The isolated nature of this pluton indicates it is not part of the Hohonu Batholith *sensu stricto.*

On the basis of textural, mineralogical, geochemical, isotopic and geochronological criteria, the granitoids of the Hohonu Batholith are sub-divided into four suites; the Summit Granite suite, Deutgam Suite, Te Kinga Suite and French Creek Suite. The Deutgam Suite and Te Kinga Suite comprise the Hohonu Super-suite.

The Devonian Summit Granite suite comprises the Summit Granite (381 Ma) and is the only definitive Palaeozoic pluton identified in the batholith. Summit Granite displays chemical, petrographic, chronological and isotopic affinities with the Karamea Suite, consequently the term Summit Granite suite is an informal one used only in this study. The suite is characterized chemically by peraluminous compositions, relatively high $P_2O_5$, Pb, Rb and Rb/Sr, low Na, Sr and ΣREE, and relatively radiogenic isotopic compositions. Intrusion of the Deutgam Granite and Turiwhate Granodiorite in the mid-Cretaceous has affected the Sr and Nd isotope systematics of the Summit Granite.

Limited geochemical and isotopic data for the Mount Graham Granite suggest affinities with the Summit Granite, although much more detailed studies are required to firmly establish any genetic links between Summit Granite, Mount Graham Granite, and also the Palaeozoic plutons of the Rangitoto Batholith to the south.

The Hohonu Batholith is dominated by the mid-Cretaceous (114-109 Ma) I-type Hohonu Super-suite. This group of plutons is characterized by relatively restricted radiogenic compositions ($Sr_{(i)}$ = 0.7062 to 0.7085, $\epsilon Nd_{(i)}$ = -4.4 to -6.1, $T_{DM} \approx 1.2$ Ga) and plutons display similar trends on Harker diagrams. The plutons of the Hohonu Batholith have previously been placed within the Rahu Suite of Tulloch (1988a). Similar isotopic compositions and similar age ranges to Rahu Suite plutons of the Paparoa Batholith and Southern Victoria Range are also suggestive of inclusion within the Rahu Suite. However, because of the recognition of two distinct suites within the Hohonu Super-suite of the Hohonu Batholith and the much more comprehensive and variable isotopic, geochemical and geochronological data set acquired in this study, the Hohonu Super-suite is given priority over the Rahu Suite. The Rahu Suite is considered to represent a third suite within the Hohonu Super-suite, generated from similar sources and by similar mechanisms.

Two suites are recognized within the Hohonu Super-suite in the Hohonu Batholith. The relatively mafic, metaluminous biotite ($\pm$ hornblende and titanite) tonalites and granodiorites of the Deutgam Suite (Jays Creek Granite, Pah Point Granite, Uncle Bay Tonalite, Deutgam Granite and Turiwhate Granodiorite) are characterized by relatively low contents of Sr, $Al_2O_3$, $Na_2O$, flat HREE contents and relatively large negative Eu anomalies. Fractionation modelling within the Deutgam Suite indicates plagioclase and amphibole were important phases during chemical evolution of these plutons. However, the amounts of fractionation indicated by trace element modelling are inconsistent with relatively invariable REE abundances throughout the suite. This suggests that REE compositions of the plutons were constrained during differing degrees of melting at conditions where partition coefficients for basaltic compositions (particularly for amphibole) are more appropriate. Variable REE patterns in evolved variants of Deutgam Granite suggest fractionation of amphibole and plagioclase also occurred at more evolved compositions. The large

variability in published partition coefficients for granitic compositions precludes quantitative determinations of amounts of fractionation which have occurred within the Deutgam Suite. Preliminary Al-in hornblende geobarometry indicates the Deutgam Suite plutons crystallized at pressures of $\approx$4 kb.

The biotite ($\pm$ muscovite) monzogranites of the Te Kinga Suite (Arahura Granite and Te Kinga Monzogranite) are characterized by high $SiO_2$ contents, peraluminous compositions and relatively high Sr, $Al_2O_3$ and $Na_2O$, coupled with depleted HREE contents and negligible negative Eu anomalies. Preliminary studies also indicate the Te Kinga Suite has relatively high $\delta^{18}O$, probably a consequence of late stage, subsolidus interaction with meteoric waters. Elevated and restricted $SiO_2$ contents in the Te Kinga Suite make a fractionation history difficult to elucidate, although trace element modelling indicates that amphibole and minor feldspar were involved in controlling chemical compositions. Low HREE contents are attributed to the presence of residual garnet in the source.

Overlapping isotopic compositions in the Te Kinga and Deutgam Suites indicate both were derived from a single source region. Geochemical and isotopic data are consistent with generation of the Hohonu Super-suite by partial melting of a source consisting of a complex lower continental crustal component and material derived from a relatively depleted mantle component. Magmatism in the Separation Point Suite contemporaneous with the Hohonu Super-suite (Mount Olympus Granite), isotopic compositions close to the radiogenic end of the mantle array and overlapping with those of modern day subduction-related basalts, and the adherence of Hohonu Super-suite compositions to mixing curves between mantle and crustal components, are indicative of the involvement of a mantle component in the Hohonu Super-suite. The recognition of a major depleted mantle component in the Early Cretaceous Separation Point Suite (Muir *et al* 1995), and also in Cretaceous mantle-derived rocks of Marie Byrd Land (Weaver *et al* 1994), indicate this mantle component was widespread beneath the Western Province and equivalents in the mid-Cretaceous. This mantle component is here termed the Separation Point-type depleted mantle (SPDM) and has isotopic compositions taken as the average of uncontaminated Separation Point Suite compositions presented by Muir *et al* (1995). SPDM is substantially less depleted than

mantle compositions proposed by Pickett and Wasserburg (1989) and is considered suitable as a mantle component in the genesis of the Hohonu Super-suite. SPDM may be involved in the petrogenesis of the Hohonu Super-suite as adiabatic melts of underlying mantle material, or as melts derived from a pre-existing mantle-derived mafic underplate, as is inferred for the Separation Point Batholith (Muir *et al* 1995).

A lower continental crustal source component for the Hohonu Super-suite remains largely unconstrained, yet is likely to be an extremely complex amalgamation of metasedimentary material such as the Greenland Group, granitoids such as the Karamea Suite, metabasaltic underplates associated with previous magmatic events, and other unknown components. Although assimilation-fractional crystallization modelling between SPDM-derived magmas and average Greenland Group compositions can produce isotopic compositions similar to those of the Hohonu Super-suite at geologically reasonable conditions, the complex nature of the Western Province continental crust makes this a too simplistic scenario. Potential lower crustal sources for Western Province granitoid magmatism may be represented by the metabasaltic rocks of the Fraser and Granite Hill Complexes, Takaka terrane and Fiordland. No isotopic data are available for these basalts and metabasalts and a detailed isotopic study of these rocks would be extremely useful in establishing their suitability as appropriate source rocks for granitoid plutonism in the Western Province, and also for comparison with similar rocks in Australia and West Antarctica.

Because isotopic data indicate the Hohonu Super-suite is derived from a single source, major and trace element differences between the two suites must be a consequence of differing processes affecting this source and the resultant melts. Despite the high $SiO_2$ contents of the Te Kinga Suite, derivation by simple feldspar fractionation from the Deutgam Suite is precluded by the high Sr, Ba, $Al_2O_3$ and Eu contents of the Te Kinga Suite. Instead, the contrasting compositions of the Deutgam and Te Kinga Suites are attributed to melting at differing crustal depths, with varying water fugacities and contrasting residual assemblages. Published experimental results have shown that relatively mafic metaluminous compositions, such as those of the Deutgam Suite, can be achieved by dehydration melting of metabasaltic compositions. In contrast, high $SiO_2$ peraluminous compositions, similar to the Te Kinga Suite, can be

generated by melting of the similar metabasaltic materials at water under-saturated to water-saturated conditions. Dehydration melting leaves an amphibolitic residual assemblage of plagioclase and amphibole, residual retaining Sr, $Al_2O_3$ and $Na_2O$ resulting in the low contents of these elements and negative Eu anomalies in the Deutgam Suite. Water-saturated to under-saturated melting of the same metabasaltic compositions, probably at slightly greater depths, leaves an eclogitic residual assemblage of garnet and amphibole to produce the Te Kinga Suite. Residual garnet in the Te Kinga Suite results in HREE-depleted compositions, whereas the absence of residual plagioclase produces the high Sr, $Al_2O_3$ and $Na_2O$ contents and the relative absence of negative Eu anomalies which characterize this suite.

The Hohonu Super-suite cannot be easily linked to melting above any recognized subduction zone. Recently, several studies have proposed that a close link exists between crustal extension and granitoid genesis, and a similar model is proposed for the Hohonu Super-suite. An initial crustal thickening event is indicated by generation of the Median Tectonic Zone volcanic arc and its subsequent juxtaposition with the Western Province. Cessation of subduction along the Gondwana margin is believed to have occurred at 105 $\pm$ 5 Ma (J.D.Bradshaw 1989), and removed the compressional forces maintaining the overthickened Western Province crust. Consequent thermal relaxation of the previously overthickened Western Province crust results in crustal extension, uplift and thinning, marked by development of the Paparoa Metamorphic Core Complex and the formation of the extensional sedimentary basins of the Pororari Group. The age of the Hohonu Super-suite (114-109 Ma) coincides with this extensional event and a model is proposed whereby granitoid melts are generated during isothermal uplift and adiabatic melting of the lower crust. Adiabatic melting of the underlying mantle and underplating of hot mantle melts may have also contributed to the generation of the Hohonu Super-suite.

Late Cretaceous alkaline granitoid magmatism in the Hohonu Batholith is represented by the French Creek Suite, a composite pluton with petrological and geochemical characteristics typical of A-type granitoids. Rhyolitic dikes once considered to be evolved members of the Hohonu Dike Swarm (Hamill 1972) are

shown to have strong geochemical affinities to the French Creek Granite and are considered to be early, hypabyssal phases of French Creek magmatism.

French Creek Granite is characterized geochemically by values of A/CNK and A/NK $\approx 1$, high concentrations of high field strength elements, fluorine and REE, and low Ba, Sr and CaO, features typical of A-type granitoids. French Creek Granite has trace element compositions typical of the $A_1$-type granitoids of Eby (1992), which are attributed to derivation via extreme fractionation of mantle-derived melts. A mantle derived origin is also indicated by the primitive isotopic compositions of the French Creek Granite, and field, geochemical and geochronological evidence for a penecontemporaneous relationship with the Hohonu Dike Swarm. Trace element fractionation diagrams indicate that fractionation of feldspar and apatite explains many of the geochemical variability in the French Creek Granite. Fractionation trends within the French Creek Granite also coincide with the evolved members of the Hohonu Dike Swarm and indicate a genetic relationship between the dikes and the French Creek Granite. Preliminary isotopic data indicate $\approx 20\%$ interaction with continental crust such as the Greenland Group is required to produce the isotopic compositions of the French Creek Granite, although more isotopic data are needed, particularly for the Hohonu Dike Swarm, to fully constrain such models.

All major units of the study area are cut by members of the Hohonu Dike Swarm, a swarm of alkaline dikes concentrated on the Hohonu Ranges and Mount Te Kinga. The swarm is dominated by doleritic (clinopyroxene + plagioclase) dikes with subordinate camptonites (kaersutite + plagioclase + biotite) and rare phonolites (nepheline + alkali feldspar + alkali amphibole + biotite), all dikes displaying varying degrees of greenschist facies deuteric alteration. The swarm has a very strong WNW-ESE preferred orientation perpendicular to separation of Australia and New Zealand during opening of the Tasman Sea. Complex field and geochemical relationships between the French Creek Granite and the Hohonu Dike Swarm indicate the swarm is penecontemporaneous with the French Creek Granite, indicating an age of $\approx$ 82 Ma for the Hohonu Dike Swarm. Consequently a strong link is established between the extensional environment generated during opening of the Tasman Sea at 82 Ma, and the alkaline compositions of the Hohonu Dike Swarm and French Creek

Granite which typify such tectonic environments. Additional geochronological work is required to further constrain the age, or range of ages, of the Hohonu Dike Swarm. The generally highly altered nature of many of the dikes, and isotopic evidence for mobilization, indicate that it will be difficult to accurately date these dikes by most geochronological methods, although U-Pb zircon work may be feasible on the evolved end-members of the swarm. Geochemical data indicate the majority of the dikes are ne-normative, although a weak trend towards oversaturated compositions is also present and may be related to a fractionation trend culminating in the French Creek Granite. Trace element data indicate the dike swarm evolved by the combined fractionation of plagioclase, amphibole and pyroxene, with no consistent evidence for crustal contamination. In addition, late stage fractionation of Ti-rich amphibole and apatite are required to produce the distinctive compositions of the phonolite dikes. Detailed mineral analysis studies would help considerably in more accurately modelling the fractionation history of the Hohonu Dike Swarm. Isotopic data are sparse and display scatter probably attributable to alteration and crustal contamination. More detailed isotopic work is required on the Hohonu Dike Swarm to clarify geochemical relationships between the French Creek Granite and the Hohonu Dike Swarm. In addition, detailed isotopic studies, especially Pb isotopes, are necessary to accurately establish the mantle source of the Hohonu Dike Swarm. Initial data indicate a depleted mantle source, although trace element data suggest this source has undergone a relatively recent large ion lithophile element enrichment event.

Rb-Sr mica ages, coupled with sparse K-Ar data and zircon fission track data, record rapid uplift and cooling of the batholith between the emplacement of the $\approx 110$ Ma plutons and the 82 Ma French Creek Granite. This uplift reflects extension and uplift of the Western Province during Gondwana breakup and is followed by a period of relative hiatus. Recent uplift, associated with compression across the Alpine Fault, is recorded in young apatite fission track ages throughout the Hohonu Batholith.

Due to limited time, and somewhat difficult terrain, the geology of the Granite Hill Massif was only briefly covered in this study and more detailed mapping and metamorphic petrology is necessary in this region. Published descriptions of rocks from the Mount Elliot region (Mason and Taylor 1987, Young 1968) indicate that similar

rock types and associated undeformed granitoids also occur to the north of Granite Hill. This region remains one of the few unmapped and unstudied regions of the West Coast, yet represents an important link between the Granite Hill Complex (and the Hohonu Batholith) and the rocks of the Victoria Range.

Reconnaissance mapping of the Granite Hill Complex indicates it comprises amphibolite-facies paragneisses, orthogneisses and metabasites and can be confidently correlated with the Fraser Complex to the south. A lack of true mylonites in the Granite Hill Complex indicates it has had a recent tectonic history distinct from the highly deformed Fraser Complex, perhaps a consequence of differing uplift histories with respect to major strike-slip movement on the Alpine Fault. Isotopic compositions, the dominance of metabasaltic compositions, and distinct zircon inheritance patterns in two paragneiss samples (Ireland 1992), preclude correlation of the Granite Hill and Fraser Complexes with rocks of the Charleston Metamorphic Group. Consequently, the Fraser and Granite Hill Complex gneisses cannot be considered as highly metamorphosed equivalents of the Greenland Group and intrusive granitoids. Many similarities occur between the gneisses of the Granite Hill and Fraser Complexes and metamorphic rocks of the Fiordland region. Consequently, the Granite Hill and Fraser Complex gneisses may be correlated with the gneisses of Fiordland and their probable unmetamorphosed equivalents in the Takaka terrane. If so, the gneisses of this study may represent slices of Fiordland material sheared off during strike-slip motion on the Alpine Fault, or mid-crustal material uplifted during Cenozoic compression across the Alpine Fault. A detailed isotopic-geochemical-geochronological study of the Granite Hill and Fraser Complex gneisses and their possible equivalents in Fiordland and the Takaka terrane is required to fully establish relationships between these rocks.

**Acknowledgements.**

First and foremost I would like to extend my gratitude to my supervisors, Associate Professor Steve Weaver and Associate Professor David Shelley, and unofficial supervisor Dr Roddie Muir, for their constructive (or should that be destructive) comments on various stages of the text and general support during my research. In particular I would especially like to thank Steve, as principal supervisor, for his support, not only scientifically and personally, but also for corection of gramir, access to pre-prints of the Separation Point paper and data set, and for helping to find the financial means to provide the geochemical and geochronological data which were invaluable to the completeness of this study. I would also like to thank Dr Andy Tulloch (Associate supervisor) for allowing the use of his U/Pb zircon ages and discussion on the field geology of the region. I wish to acknowledge the financial support of the New Zealand Vice Chancellors Committee, and the Mason Trust and a University of Canterbury Research Grant which helped with the financial logistics of field work.

Many thank yous (in no particular order) must also go to the many people who helped make this book possible, my apologies if I forget anyone. The entire technical and secretarial staff of the Geology Dept were invaluable, in particular I need to acknowledge the help of; Albert Downing and Kerry Swanson for help with photography, Rob Spiers (and part-time assistants Steve and Sacha) for the excellent job made of all my thin sections, Steve and Catherine Brown for producing all those geochemical numbers, Michael Finnemore for help with computer woes, Lee Leonard for draughting, Michele Wright for lending me lots of expensive equipment, and Arthur Nicholas for fixing it when it broke. Other members of staff in the Geology Department also did their bit; Jarg Pettinga helped with map production, Jane and Nigel Newman provided useful discussion on the Late Cretaceous - Tertiary history of the West Coast, and Jim Cole was a supportive H.O.D. during most of this work. Trevor Ireland of Australian National University, Canberra, is thanked for many hours slaving over a hot SHRIMP. Terry Spell should be thanked, but I can't really think why, and Lockwood Smith doesn't get thanked at all. The staff at the Institute of Geological and Nuclear Sciences were very supportive throughout this study, particularly Simon Nathan and Nick Mortimer. I would also like to thank Lloyd Homer for a chopper ride and for allowing the use of his superb photos, and Pat Suggate for assistance with the complex Tertiary exposures at Taramakau. Alan Cooper of Otago University provided several useful discussions on the Hohonu Dike Swarm and Yosaka Kawachi, also of Otago University, helped with the formidable task of taking on the microprobe. Ian Meighan of Queens University in Belfast and Tony Fallick of the Scottish Universities Research and Reactor Centre provided oxygen isotope data. I also greatly appreciate the assistance of Prof. Nelson Eby from the University of Lowell, Massachussetts for running my INAA samples and for a most enjoyable weekend spent

with John Tarney and Roddie Muir on "Le Grand Tour de la West Coast granites". I also thank the staff and students at La Trobe University, Melbourne, in particular Richard Price, Jorg Metz and especially Dr Roland Maas who ably assisted me towards isotope geology proficiency and also let me have a good time while doing it. Thanks to Rowena for providing distraction, support and friendship from too far away, a place to stay during visits to Aussie, and for Mr Kookaburra who kept a watchful beak on proceedings. The people of the West Coast must be thanked for their hospitality and for granting some crazy guy looking at rocks access to their land, as one farmer said "Rocks eh?....Plenty of them around". Especially I would like to thank; Pat Fitzgerald and family (Wainihinihi) for the occasional meal and bed, and refuge from the pouring rain; Gerry Paaps of the Moana Camping ground and staff at the Hokitika Camping ground; David Cook, Nicki Donovan and Bridget (Ruru), for good meals and good conversation and good whisky and for a day in the jetboat on Lake Brunner; Tony McDougall, Sally Couper and kids for a place to crash and last but not least, Michael Meates of Wainihinihi and Adam Trevor of Ruru for much appreciated helicopter assistance. Scott Waight, Ali Dean, Stu McRoberts, Vicki Addison, Kirsty Brown, Kay Cooper, Richard Smith, Ralf Gerstenburger and Sacha Baldwin are thanked for fortitude in the face of adversity as I dragged them all number of crazy places as field assistants. Fellow geologists and friends Stu Brown, Richard Smith, Richard Jongens, Barbara Hobden, Simon Ward, Sonya, Moosh, Coxie, Don, Rod and numerous flatmates are thanked for general distractions, geophilosophical discourse and good times, remember me when you are famous. Ali Dean must be thanked for providing a bed when I was homeless, a meal when I was hungry and for enabling me to become proficient at identifying epidote from 10 paces. Thanks to Sacha Baldwin, for making fusion beads and other things when I was incapacitated with a broken collar bone, being a fieldy and for being a Very Good Friend, but I don't know if turning up again two weeks before I handed in was such a good idea! I must also thank Lesley and Jean the happy Café ladies who kept me feed and supplied with coffee. I would like to thank my parents Sandra and Stuart, who helped keep my car running and made sure I never ran out of underwear. I thank you for being always quietly encouraging and confident, never once questioning why I was doing all this, and for allowing me the freedom to make my own decisions and mistakes. Finally, I feel utmost gratitude towards my faithful coffee plunger and mug which helped me get going in the morning, and kept me going at the end of the night.

"Whaia Te Kahurangi
Me Ka Tuoho Koe
He Maunga Tei Tei"
In one's search for the stars
If one has to bend
Let it be to a lofty mountain.

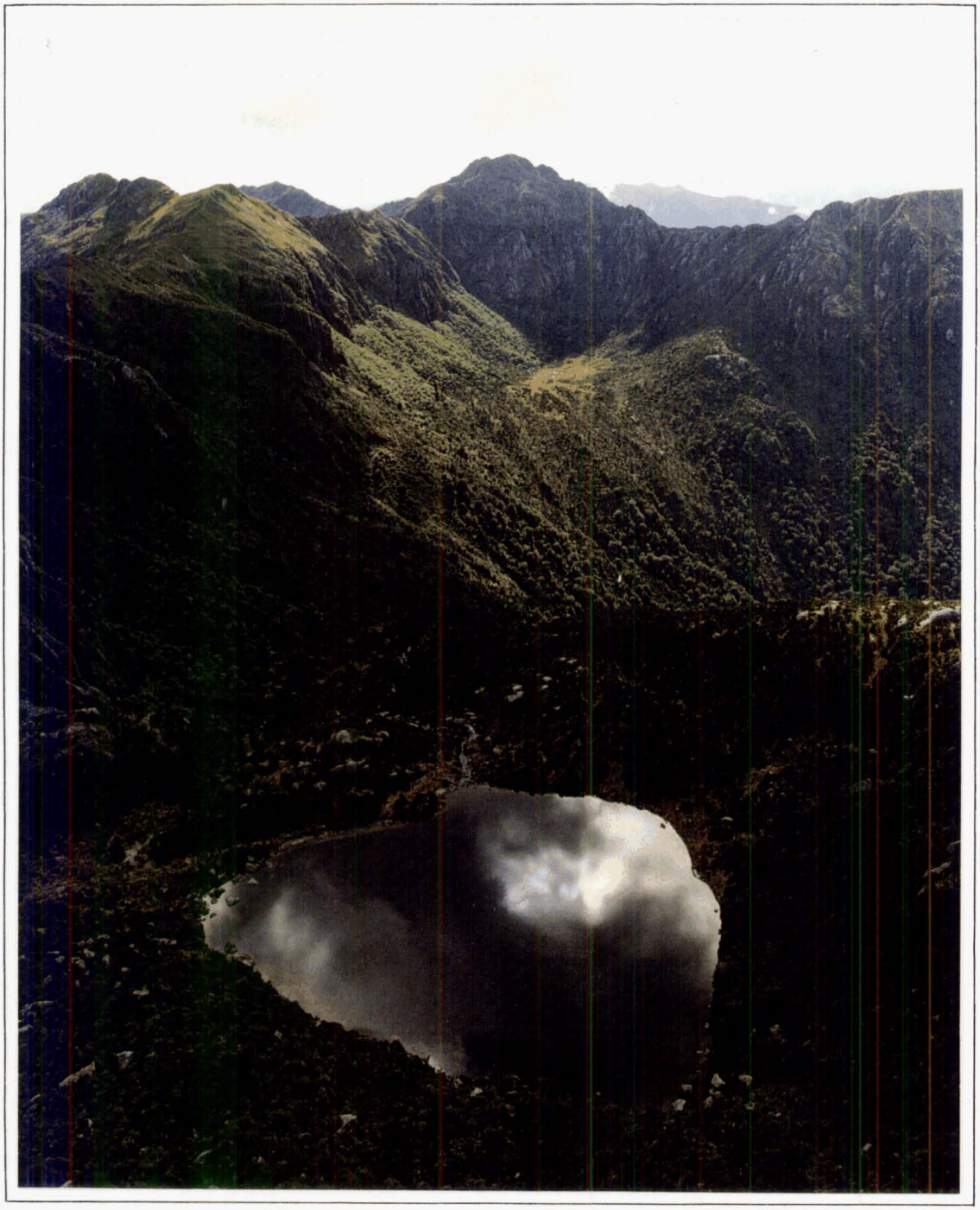

Lake Ruby, looking east towards Deutgam Peak and Taff Torr with Mount Te Kinga visible in the background.

Photo: Lloyd Homer, Institute of Geological and Nuclear Sciences.

## References cited.

Adams, C.J. (1975): Discovery of Precambrian rocks in New Zealand: age relations of the Greenland Group and Constant Gneiss, Westland. *Earth and Planetary Science Letters* 28: 98-104.

Adams, C.J. (1980): New K-Ar age data for South Island Lamprophyre Dyke swarms in the Buller - S.Westland and Haast - Wanaka areas. *Geological Society of New Zealand Conference, Christchurch*, Nov. 24-27, Programme and abstracts. p 14.

Adams, C.J., and Nathan, S. (1978): Cretaceous chronology of the Lower Buller Valley, South Island, New Zealand. *New Zealand Journal of Geology and Geophysics*, 18: 39-48.

Adams, C.J., Seward, D. and Weaver, S.D. (1995): Geochronology of Cretaceous granites and metasedimentary basement on Edward VII Peninsula (Ross Sea margin), Marie Byrd Land, West Antarctica: *Antarctic Science*, (in press).

Adams, C.J. and Weaver, S.D. (1990): Age and correlation of metamorphic basement in Edward VII Peninsula, Marie Byrd Land, West Antarctica, and correlation with Northern Victoria Land and Southern New Zealand. *Zbl.Geol.Palaont.*, 1: 75-86.

Allègre, C.J. and Ben Othman, D. (1980): Nd-Sr isotopic relationship in granitoid rocks and continental crust development: a chemical approach to orogenesis. *Nature*, 286: 335-342.

Allibone, A. (1993): Volcanogenic and granitoid rocks from the northwest Stewart Island. *New Zealand Journal of Geology and Geophysics*, 34: 35-50

Angus, P.V.M. (1984): The Geology of Inchbonnie, Westland. B.Sc.(Hons) project, University of Otago.

Arculus, R.J. (1987): The significance of source versus process in the tectonic controls on magma genesis. *Journal of Volcanology and Geothermal Research*, 32: 1-12.

Arndt, N.T. and Goldstein, S.L. (1987): Use and abuse of crust-formation ages. *Geology*, 15: 893-895

Aronson, J.L. (1968): Regional geochronology of New Zealand. *Geochemica et Cosmochimica Acta*, 32: 669-697.

Arth, J.G. (1976): Behaviour of trace elements during magmatic processes - a summary of theoretical models and their applications. *Journal of Research of the U.S. Geological Survey*, 4: 41-47.

Atherton, M.P. and Sanderson, L.M. (1985): The chemical variation and evolution of the super-units of the segmented Coastal Batholith. *In*: Pitcher, W.S., Atherton, M.P., Cobbing, E.J. and Beckinsale, R.D. (Eds.) Magmatism at a Plate edge: The Peruvian Andes. Blackie, Glasgow and London, pp 208-227.

Ayuso, R.A. and Arth, J.G. (1992): The Northeast Kingdom batholith, Vermont: magmatic evolution and geochemical constraints on the origin of Acadian granitic rocks. *Contributions to Mineralogy and Petrology*, 111: 1-23.

Bailey, D.K. (1987): Mantle metasomatism - perspective and prospect. *In*: Fitton, J.G. and Upton, B.G.J. (Eds.): Alkaline Igneous Rocks, *Geological Society Special Publication*, 30: 1-13.

Baker, B.H. (1987): Outline of the petrology of the Kenya rift alkaline province. *In*: Fitton, J.G. and Upton, B.G.J. (Eds.): Alkaline Igneous Rocks, *Geological Society Special Publication*, 30: 293-311.

Baker, J.A., Gamble, J.A. and Graham, I.J. (1994): The age, geology, and geochemistry of the Tapuaenuku Igneous Complex, Marlborough, New Zealand. *New Zealand Journal of Geology and Geophysics*, 37: 249-268.

Barker, D.S. (1970): Compositions of granophyre, myremekite, and graphic granite. *Geological Society of America Bulletin*, 81: 3339-3350.

Barley, M.E., Weaver, S.D. and de Laeter, J.R (1988): Strontium isotope composition and geochronology of intermediate-silicic volcanics, Mount Somers and Banks Peninsula, New Zealand. *New Zealand Journal of Geology and Geophysics*, 31: 197-206.

Barreiro, B.A. (1983): An isotopic study of Westland Dike Swarm, South Island, New Zealand. *Carnegie Institution of Washington Year Book*, 82: 471-475.

Barreiro, B.A. and Cooper, A.F. (1987): A Sr, Nd and Pb isotope study of alkaline lamprophyres and related rocks from Westland and Otago, South Island, New Zealand. *Geological Society of America Special Paper*, 215: 115-125.

Barth, T.F.W. (1969): Feldspars. John Wiley and Sons Inc. London. 261 pp.

Beard, J.S. and Lofgren, G.E. (1991): Dehydration melting and water-saturated melting of basaltic and andesitic greenstones and amphibolites at 1, 3 and 6.9 kb. *Journal of Petrology*, 32: 365-401.

Bell, J.M., and Fraser, C. (1906): The Geology of the Hokitika sheet, Northwest quadrangle. *New Zealand Geological Survey Bulletin* 1.

Bennie, S.L. and Ferry, L.M. (1977): Sheet 17, Hokitika (1st edition), "Gravity map of New Zealand, 1:250,000; Bouguer anomalies". DSIR, Wellington, New Zealand.

Bickle, M.J., Wickham, S.M., Chapman, H.J and Taylor, H.P.,Jr. (1988): A strontium, neodymium and oxygen isotope study of hydrothermal metamorphism and crustal anatexis in the Trois Seigneurs Massif, Pyrenees, France. *Contributions to Mineralogy and Petrology*, 100: 399-417.

Bird, P. (1979): Continental delamination and the Colorado Plateau. *Journal of Geophysical Research* 84: 7561-7571.

Bishop, D.J. (1992): Extensional tectonism and magmatism during the middle Cretaceous to Palaeocene, North Westland, New Zealand. *New Zealand Journal of Geology and Geophysics*, 35: 81-91.

Blundy, J.D. and Holland, T.J.B. (1990): Calcic amphibole equilibria and a new amphibole-plagioclase geothermometer. *Contributions to Mineralogy and Petrology*, 104: 208-224.

Blundy, J.D. and Holland, T.J.B. (1992a): "Calcic amphibole equilibria and a new amphibole-plagioclase geothermometer": Reply to the comments of Hammarstrom and Zen, and Rutherford and Johnson. *Contributions to Mineralogy and Petrology*, 111: 269-272.

Blundy, J.D. and Holland, T.J.B. (1992b): "Calcic amphibole equilibria and a new amphibole-plagioclase geothermometer"- reply to the comment of Poli and Schmidt. *Contributions to Mineralogy and Petrology*, 111: 278-282.

Borg, S.G., Stump, E., Chappell, B.W., McCulloch, M.T., Wyborn, D., Armstrong, R.L. and Holloway, J.R. (1987): Granitoids of Northern Victoria Land, Antarctica: Implications of chemical and isotopic variations to regional crustal structure and tectonics. *American Journal of Science*, 287: 127-169.

Borg, S.G., Stump. E. and Halloway, J.R. (1986): Granitoids of Northern Victoria Land, Antarctica: A reconnaissance study of field relations, petrography and geochemistry. *In*: Stump, E. (Ed.): Geological investigations in Northern Victoria Land. American Geophysical Union, Washington D.C., pp 115-189.

Bradshaw, J.D. (1989): Cretaceous geotectonic patterns in New Zealand. *Tectonics*, 8: 803-820.

Bradshaw, J.D. (1993): A review of the Median Tectonic Zone: terrane boundaries and terrane amalgamation near the Median Tectonic Line. *New Zealand Journal of Geology and Geophysics*, 36: 117-125.

Bradshaw, J.Y. (1989): Origin and metamorphic history of an early Cretaceous polybaric granulite terrain, Fiordland, southwest New Zealand. *Contributions to Mineralogy and Petrology*, 103: 346-360.

Bradshaw, J.Y. (1990): Geology of crystalline rocks of Northern Fiordland: details of the granulite facies Western Fiordland Orthogneiss and associated rock units. *New Zealand Journal of Geology and Geophysics*, 33: 465-484.

Bradshaw, J.Y. and Kimbrough, D.L. (1991): Mid-Palaeozoic age of granitoids in enclaves within Early Cretaceous granulites, Fiordland, southwest New Zealand. *New Zealand Journal of Geology and Geophysics*, 34: 455-469.

Brown, G.C. (1982): Calc-alkaline intrusive rocks; Their diversity, evolution and relation to volcanic arcs. *In*: Thorpe, R.S. (Ed.) Andesites. John Wiley, London, p 437-431.

Brown, G.C., Cassidy, J., Locke, C.A., Plant, J.A. and Simpson, P.R. (1981a): Caledonian plutonism in Britain: A summary. *Journal of Geophysical Research*, 86 B11: 10502-10514.

Brown, M., Friend, C.R.L., McGregor, V.R. and Perkins, W.T. (1981b): The late Archaean Qôrqut granite complex of southern west Greenland. *Journal of Geophysical Research*, 86, B11: 10617-10632.

Brown, W.L. and Parsons, I. (1989): Alkali feldspars: ordering rates, phase transformations and behaviour diagrams for igneous rocks. *Mineralogical Magazine*, 53: 25-42.

Champion, D.C. and Chappell, B.W. (1992): Petrogenesis of felsic I-type granites: an example from northern Queensland. *Transactions of the Royal Society of Edinburgh: Earth Sciences*, 83: 115-126.

Chappell, B.W., White, A.J.R. and Wyborn, D. (1987): The importance of residual source material (restite) in granite petrogenesis. *Journal of Petrology*, 28(6): 1111-1138.

Chappell, B.W. and White, A.J.R. (1974): Two contrasting Granite types. *Pacific Geology*, 8: 173-174.

1.

Clemens, J.D., Holloway, J.R. and White, A.J.R. (1986): Origin of an A-type granite: Experimental constraints. *American Mineralogist*, 71: 317-324.

Cocker, J.D. (1982): Rb-Sr geochronology and Sr isotope composition of Devonian granitoids, east Tasmania. *Journal of the Geological Society of Australia*, 29: 139-158.

Collins, W.J. (1994): Upper- and middle-crustal response to delamination: An example from the Lachlan fold belt, eastern Australia. *Geology*, 22: 143-146.

Collins, W.J., Beams, S.D., White, A.J.R. and Chappell, B.W. (1982): Nature and origin of A-type granites with particular reference to southeastern Australia. *Contributions to Mineralogy and Petrology*, 80: 189-200.

Coney, P.J. (1987): The regional tectonic setting and possible causes of Cenozoic extension in the North American Cordillera. *In*: Coward, M.P., Dewey, J.F. and Hancock, P.L. (Eds.): Continental extensional tectonics. *Geological Society Special Publication*, 28: 177-186.

Coombs, D.S., Cas, R. Kawachi, Y., Landis, C.A., McDonough, W.F. and Reay, A. (1986): Cenozoic volcanism in north and east Otago. *In*: Smith, I.E.M. (Ed.): Late Cenozoic volcanism in New Zealand. Publication of the Royal Society of New Zealand, pp 278-312.

Cooper, A.F. (1971): Carbonatites and fenitization associated with a lamprophyre dike swarm intrusive into the schists of the New Zealand Geosyncline. *Geological Society of America Bulletin* 82: 1327-1340.

*Addendum*

[1]Chappell, B.W. and White, A.J.R. (1992): I- and S-type granites in the Lachlan Fold Belt. *Transactions of the Royal Society of Edinburgh: Earth Sciences*, 83: 1-26.

Cooper, A.F. (1979): Petrology of ocellar lamprophyres from Western Otago, New Zealand. *Journal of Petrology*, 20: 139-164.

Cooper, A.F. (1986): A carbonatitic lamprophyre dyke swarm from the Southern Alps, Otago and Westland. *Royal Society of New Zealand Bulletin*, 18: 35-43.

Cooper, A.F., Barreiro, B.A., Kimbrough, D.L. and Mattinson, J.M. (1987); Lamprophyre dike intrusion and the age of the Alpine Fault, New Zealand. *Geology*, 15: 941-944.

Cooper, R.A. (1974): Age of the Greenland and Waiuta Groups, South Island, New Zealand. *New Zealand Journal of Geology and Geophysics*, 17: 955-962.

Cooper, R.A. (1979): Lower Palaeozoic rocks of New Zealand. *Journal of the Royal Society of New Zealand*, 9: 29-84.

Cooper, R.A. (1989): Early Palaeozoic terranes of New Zealand. *Journal of the Royal Society of New Zealand*, 19: 73-112.

Cooper, R.A. and Tulloch, A.J. (1992): Early Palaeozoic terranes in New Zealand and their relationship to the Lachlan Fold Belt. *Tectonophysics*, 214: 129-144.

Cox, S.F., Etheridge, M.A., Cas, R.A.F. and Clifford, B.A. (1991): Deformational style of the Castlemaine area, Bendigo-Ballarat Zone: Implications for evolution of crustal structure in central Victoria. *Journal of Australian Earth Sciences*, 38: 151-170.

Crawford, A.J. and Cameron, W.E. (1985): Petrology and geochemistry of Cambrian boninites and low-Ti andesites from Heathcote, Victoria. *Contributions to Mineralogy and Petrology*, 91: 93-104.

Crawford, A.J., Corbett, K.D. and Everard, J.J. (1992): Geochemistry of Cambrian volcanic-hosted massive sulphide-rich Mount Read Volcanics, Tasmania, and some tectonic implications. *Economic Geology*, 87: 597-619.

Creaser, R.A., Price, R.C. and Wormald, R.J. (1991): A-type granites revisited: Assessment of a residual-source model. *Geology*, 19: 163-166.

Davis, W.J., Fryer, B.J. and King, J.E. (1994): Geochemistry and evolution of Late Archean plutonism and its significance to the tectonic development of the Slave Craton. *Precambrian Research*, 67: 207-241.

Deer, W.A., Howie, R.A. and Zussman, J. (1966): An introduction to the rock forming minerals. *Longman Scientific and Technical, Essex*. 528 pp.

Defant, M.J. and Drummond, M.S. (1990): Subducted lithosphere-derived andesitic and dacitic rocks in young volcanic arc setting. *Nature*, 347: 662-665.

DePaolo, D.J. (1981a): Trace element and isotopic effects of combined wallrock assimilation and fractional crystallization. *Earth and Planetary Science Letters*, 53: 189-202.

DePaolo, D.J. (1981b): Neodymium isotopes in the Colorado Front Range and crust-mantle evolution in the Proterozoic. *Nature*, 291: 193-196.

DePaolo, D.J. (1981c): A neodymium and strontium isotopic study of the Mesozoic calc-alkaline granitic batholiths of the Sierra Nevada and Peninsular Ranges, California. *Journal of Geophysical Research*, 86: 10470-10488.

DePaolo, D.J. (1988): Neodymium isotope geochemistry: An introduction. Springer Verlag, New York.

DePaolo, D.J. and Wasserburg, G.J. (1979): Petrogenetic mixing models and Nd-Sr isotopic patterns. *Geochemica et Cosmochimica Acta*, 43: 615-627.

D'Lemos, R.S., Brown, M. and Strachon, R.A. (1992): Granite magma generation, ascent and emplacement within a transpressional orogen. *Journal of the Royal Society of London*, 149: 487-490.

Droop, G.T.R. (1987): A general equation for estimating $Fe^{3+}$ concentrations in ferromagnesian silicates and oxides from microprobe analyses, using stoichiometric criteria. *Mineralogical Magazine*, 51: 431-435.

Eby, G.N. (1990): The A-type granitoids: A review of their occurrence and chemical characteristics and speculations on their petrogenesis. *Lithos*, 26: 115-134.

Eby, G.N. (1992): Chemical subdivision of the A-type granitoids: Petrogenetic and tectonic implications. *Geology*, 20: 641-644.

Eby, G.N., Krueger, H.W. and Creasy, J.W. (1992): Geology, geochronology, and geochemistry of the White Mountain Batholith, New Hampshire. *In*: Puffer, J.H. and Ragland, P.C. (Eds.): Eastern North American Mesozoic magmatism: *Geological Society of America Special Paper*, 268: 379-397.

Ellis, D.J. and Thompson, A.B. (1986): Subsolidus and partial melting reactions in the quartz-excess $CaO + MgO + Al_2O_3 + SiO_2 + H_2O$ system under water-excess and water deficient conditions to 10 kb: Some implications for the origin of peraluminous melts from mafic rocks. *Journal of Petrology*, 27: 91-121.

England, P.C. and Thompson, A. (1986): Some thermal and tectonic models for crustal melting in continental collision zones. *In*: Coward, M.P. and Ries, A.C. (Eds.): Collision Tectonics. *Geological Society Special Publication*, 19: 83-94.

Evanelakakis, C., Kroll, H., Voll, G., Wenk, H-R., Meisherg, H. and Köpcke, J. (1993): Low-temperature coherent exsolution in alkali feldspars from high grade metamorphic rocks of Sri Lanka. *Contributions to Mineralogy and Petrology*, 114: 519-537.

Evans, O.C. and Hanson, G.N. (1993): Accessory-mineral fractionation of rare-earth (REE) abundances in granitoid rocks. *Chemical Geology*, 110: 69-93.

Faure, G. (1986): Principles of isotope geology. Second Edition, John Wiley and Sons, New York. 589 pp.

Ferry, J.M. and Spear, F.S. (1978): Experimental calibration of the partitioning of Fe between biotite and garnet. *Contributions to Mineralogy and Petrology*, 66: 113-117.

Floyd, P.A. and Winchester, J.A. (1975): Magma type and tectonic setting discrimination using immobile elements. *Earth and Planetary Science Letters*, 27: 211-218.

Fourcade, C.J. and Allegre, C.J. (1981): Trace element behaviour in granite genesis: A case study - the calc-alkaline plutonic association from the Querigut Complex (Pyrenees, France). *Contributions to Mineralogy and Petrology*, 76: 177-195.

Fuhrman, M.L., Frost, B.R. and Lindsley, D.H. (1988): Crystallizing conditions of the Sybille Monzosyenite, Laramie Anorthosite Complex, Wyoming. *Journal of Petrology*, 29: 699-729.

Fuhrman, M.L. and Lindsley, D.H. (1988): Ternary-feldspar modelling and thermometry. *American Mineralogist*, 73: 201-215.

Gage, M. (1948): The geology of the Reefton quartz lodes. *New Zealand Geological Survey Bulletin* 42.

Gage, M. (1952): Greymouth Coalfield. *New Zealand Geological Survey Bulletin* 45.

Gage, M. and Wellman, H. (1944): Geology of the Koiterangi Hill. *Transactions of the Royal Society of New Zealand*, 73(4): 531-364.

Gibson, G.M. (1982a): Stratigraphy and petrography of some metasediments and associated intrusive rocks from central Fiordland, New Zealand. *New Zealand Journal of Geology and Geophysics*, 25: 21-43.

Gibson, G.M. (1982b): Polyphase deformation and its relation to metamorphic crystalline rocks at Wilmot Pass, central Fiordland. *New Zealand Journal of Geology and Geophysics*, 25: 45-65.

Gibson, G.M. (1992): Medium - high-pressure metamorphic rocks of the Tuhua Orogen, western New Zealand, as lower crustal analogues of the Lachlan Fold Belt, SE Australia. *Tectonophysics*, 214: 145-157.

Gibson, G.M. and Ireland, T.R. (1994): Metamorphism and exhumation of the Western Fiordland orthogneiss, southwest New Zealand: Some thermobarometric and U-Pb age constraints. *Geological Society of New Zealand Miscellaneous Publication*, 80A: p 72.

Gibson, G.M., McDougall, I. and Ireland, T.R. (1988): Age constraints on metamorphism and development of a metamorphic core complex in Fiordland, southern New Zealand. *Geology*, 16: 405-408.

Gill, J.B. (1981): Orogenic andesites and plate tectonics. Springer, Berlin, Heidelberg, New York, 390 p.

Glazner, A.F. (1994): Foundering of mafic plutons and density stratification of continental crust. *Geology*, 22: 435-438.

Goldstein, S.L., O'Nions, R.K. and Hamilton, P.J. (1984): A Sm-Nd isotope study of atmospheric dusts and particulates from major river systems. *Earth and Planetary Science Letters*, 70: 221-236.

Graham, I.J. and White, P.J. (1990): Rb-Sr dating of Rahu Suite granitoids from the Paparoa Range, North Westland, New Zealand. *New Zealand Journal of Geology and Geophysics* 33:11-22.

Grapes, R.H. (1975): Petrology of the Blue Mountain Igneous Complex, Marlborough, New Zealand. *Journal of Petrology*, 16: 371-428.

Green, T.H. (1982): Anatexis of mafic crust and high pressure crystallization of andesite. *In*: Thorpe, R.S. (Ed.) Andesites: Orogenic andesites and related rocks. John Wiley and Sons, Chichester, pp 465-488.

Green, T.H. and Pearson, N.J. (1983): Effect of pressure on rare earth element partition coefficients in common magmas. *Nature*, 305: 414-416.

Green, T.H. and Ringwood, A.E, (1968): Genesis of the calc-alkaline igneous rock suite. *Contributions to Mineralogy and Petrology*, 18: 105-162.

Gregg, R. (1964): Sheet 18, Hurunui. Geological Map of New Zealand 1:250,000. Department of Scientific and Industrial Research, Wellington, New Zealand.

Grindley, G.W. (1961): Sheet S13, Golden Bay. Geological map of New Zealand 1:250,000. Department of Scientific and Industrial Research, Wellington, New Zealand.

Grindley, G.W. (1971): Sheet S8, Takaka. Geological map of New Zealand 1:250,000. Department of Scientific and Industrial Research, Wellington, New Zealand.

Grindley, G.W. and Oliver, P.J. (1979): Palaeomagnetism of Upper Cretaceous dikes, Buller Gorge, North Westland, in relation to the bending of the New Zealand orocline. *Bulletin of the Royal Society of New Zealand*, 18: 131-147.

Groccott, J., Brown, M., Dallmeyer, R.D., Taylor, G.K. and Treloar, P.J. (1994): Mechanisms of continental growth in extensional arcs: An example from the Andean plate-boundary zone. *Geology*, 22: 391-394.

Gromet, L.P. and Silver, L.T. (1983): Rare-earth distributions among minerals in a granodiorite and their petrogenetic implications. *Geochemica et Cosmochimica Acta*, 47: 925-939.

Gromet, L.P. and Silver, L.T. (1987): REE variations across the Peninsular Ranges Batholith: Implications for batholithic petrogenesis and crustal growth in magmatic arcs. *Journal of Petrology*, 28: 75-125.

Hamill, L.J. (1972): The Geology of the Western Hohonu Ranges, North Westland, New Zealand. Unpublished B.Sc(Hons) project, University of Otago.

Hammarstrom, J.M. and Zen, E-An. (1986): Aluminium in hornblende: An empirical igneous geobarometer. *American Mineralogist*, 71: 1297-1313.

Hammarstrom, J.M. and Zen, E-An. (1992): Discussion of Blundy and Holland's (1990) "Calcic amphibole equilibria and a new amphibole-plagioclase geothermometer". *Contributions to Mineralogy and Petrology*, 111: 264-266.

Hanson, G.N. (1978): The application of trace elements to the petrogenesis of igneous rocks of granitic composition. *Earth and Planetary Science Letters*, 38: 26-43.

Hanson, G.N. (1980): Rare earth elements in petrogenetic studies of igneous systems. *Annual Reviews of the Earth and Planetary Sciences*, 8: 371-406.

Harland, W.B., Armstrong, R.L., Cox, A.V., Craig, L.E., Smith, A.G. and Smith, D.G. (1990): A geologic time scale 1989. Press Syndicate, Cambridge, 263 pp.

Harry, D.L., Sawyer, D.S. and Leeman, W.P (1993): The mechanics of continental extension in western North America: Implications for the magmatic and structural evolution of the Great Basin. *Earth and Planetary Science Letters*, 117: 59-71.

Harvey, P.K., Taylor, D.M., Hendry, R.D. and Bancroft, F. (1973): An accurate fusion method for the analysis of rocks and chemically related materials by X-Ray Fluorescence spectrometry. *X-Ray Spect.* 2: 33-44.

Haselton, H.T., Hovis, G.L., Hemingway, B.S. and Robie, R.A. (1983): Calorimetric investigation of the excess entropy of mixing in analbite-sanidine solid solutions: lack of evidence for Na and K short range order and implications for two feldspar thermometry. *American Mineralogist*, 68: 398-413.

Haskin, L.A., Haskin, M.A., Fery, F.A. and Wilderman, T.R. (1968): Relative and absolute terrestrial abundances of the rare earths. *In*: Ahrens, L.H. (Ed.) *Origin and distribution of the elements, Volume 1*. Pergamnon, Oxford pp 889-911.

Helz, R. (1976): Phase relations of basalts in their melting ranges at $PH_2O$ = 5 kb. Part 2. Melt compositions. *Journal of Petrology*, 17: 139-193.

Henderson, P. (1982): Inorganic Geochemistry. Pergamon, Oxford. 353 pp.

Hervé, F., Pankhurst, R.J., Drake, R, Beck Jr, M.E. and Mpodoziz, C. (1993): Granite generation and rapid unroofing related to strike-slip faulting, Aysén, Chile. *Earth and Planetary Science Letters*, 120: 375-386.

Hewitt, D.A. and Wones, D.R. (1984): Experimental phase relations of the micas. *Reviews in Mineralogy*, 13: 201-256.

Hildreth, W. and Moorbath, S. (1988): Crustal contributions to arc magmatism in the Andes of Central Chile. *Contributions to Mineralogy and Petrology*, 98: 455-489.

Hoefs, J. (1987): Stable isotope geochemistry, 3rd edition. Springer-Verlag, New York, 241 pp.

Hofmann, A.W., Jochum, K.P., Serfert, M. and White, W.M. (1986): Nb and Pb in oceanic basalts: New constraints on mantle evolution. *Earth and Planetary Science Letters*, 79: 33-45.

Hollister, L.S., Grissom, G.C., Peters, E.K., Stowell, H.H. and Sisson, V.B. (1987): Confirmation of the empirical correlation of Al in hornblende with pressure of solidification of calc-alkaline plutons. *American Mineralogist*, 72: 231-239.

Holloway, J.R. and Burnham, C.W. (1972): Melting relations of basalt with equilibrium water pressure less than total pressure. *Journal of Petrology*, 13: 1-29.

Houseman, G., McKenzie, D., and Molnar, P. (1981): Convective instability of a thermal boundary layer and its relevance for the thermal evolution of continental convergent belts. *Journal of Geophysical Research*, 86: 6115-6132.

Hunt, T. and Nathan, S. (1976): Inangahua magnetic anomaly, New Zealand. *New Zealand Journal of Geology and Geophysics*, 19: 395-406.

Huppert, H.E. and Sparks, R.S.J. (1988): The generation of granitic magmas by intrusion of basalt into continental crust. *Journal of Petrology*, 29: 599-624.

Hurley, P.M., Hughes, H., Pinson, W.H., and Fairbairn, H.W. (1962): Radiogenic argon and strontium diffusion parameters in biotite at low temperatures obtained from Alpine Fault uplift in New Zealand. *Geochemica Cosmochimica Acta*, 26: 67-80.

Hutton, D.W.H., Dempster, T.J., Brown, P.E. and Becker, S.D. (1990): A new mechanism of granite emplacement: intrusion into active extensional shear zones. *Nature*, 343: 432-455.

Hutton, D.W.H. and Reavy, R.J. (1992): Strike-slip tectonics and granite petrogenesis. *Tectonics*, 11: 960-967.

Ireland, T.R. (1992): Crustal evolution of New Zealand: Evidence from age distributions of detrital zircons in Western Province paragneisses and Torlesse greywacke. *Geochemica et Cosmochimica Acta*, 56: 911-920.

Jacobsen, S.B. and Wasserburg, G.J. (1979): The mean age of Mantle and Crustal reservoirs. *Journal of Geophysical Research*, 84 B13: 7411-7429.

Johnson, M.C. and Rutherford, M.J. (1989): Experimental calibration of the aluminium-in-hornblende geobarometer with application to Long Valley caldera (California) volcanic rocks. *Geology*, 17: 837-841.

Jones, C.E., Tarney, J., Baker, J.H. and Gerouki, F. (1992): Tertiary granitoids of Rhodope, northern Greece: magmatism related to extensional collapse of the Hellenic Orogen? *Tectonophysics*, 210: 295-314.

Jury, A.P. (1981): Mineralisation at Mount Rangitoto and Mount Greenland, Westland. Unpublished M.Sc. thesis, University of Canterbury.

Kamp, P.J.J. (1986): Late Cretaceous-Cenozoic tectonic development of the southwest Pacific region. *Tectonophysics*, 121: 225-251.

Kamp, P.J.J., Green, P.F. and Tippet, J.M. (1992): Tectonic architecture of the mountain front-foreland basin transition, South Island, New Zealand, assessed by fission track analysis. *Tectonics*, 11: 98-113.

Kamp, P.J.J., Green, P.F. and White, S.H. (1989): Fission track analysis reveals character of collisional tectonics in New Zealand. *Tectonics*, 8: 169-195.

Kay, R.W. and Kay, S. Mahlburg (1991): Creation and destruction of lower continental crust. *Geologische Rundschau*, 80: 259-278.

Kay, R.W. and Kay, S. Mahlburg (1993): Delamination and delamination magmatism. *Tectonophysics*, 219: 177-189.

Keen, C.E., Courtney, R.C., Dehler, S.A. and Williamson, M.-C. (1994): Decompression melting at rifted margins: comparison of model predictions with the distribution of igneous rocks on the eastern Canadian Margin. *Earth and Planetary Science Letters*, 121: 403-416.

Kimbrough, D.L. and Tulloch, A.J. (1989): Early Cretaceous age of orthogneiss from the Charleston Metamorphic Group, New Zealand. *Earth and Planetary Science Letters*, 95: 130-140.

Kimbrough, D.A., Tulloch, A.J., Geary, E., Coombs, D.S. and Landis, C.A. (1993): Isotopic ages from the Nelson region of the South Island, New Zealand: Crustal structure and definition of the Median Tectonic Zone. *Tectonophysics*, 225: 433-448

Kimbrough, D.L., Tulloch, A.J., Coombs, D.S., Landis, C.A., Johnston, M.R. and Mattinson, J.M. (1994b): Uranium-lead zircon ages from the Median Tectonic Zone, South Island, New Zealand. *New Zealand Journal of Geology and Geophysics*, 37: 393-419.

Kimbrough, D.L., Tulloch, A.J. and Rattenbury, M.S. (1994a): Late Jurassic-Early Cretaceous metamorphic age of Fraser Complex migmatite, Westland, New Zealand. *New Zealand Journal of Geology and Geophysics*, 37: 137-142.

Kolker, A. and Lindsley, D.H. (1989): Geochemical evolution of the Maloin Ranch Pluton, Laramie Anorthosite Complex, Wyoming: Petrology and mixing relations. *American Mineralogist*, 74: 707-724.

Koons, P.O. (1978): The Pounamu Ultramafics: a study of metasomatism. Unpublished M.Sc. Thesis, Otago University.

Laird, M.G. (1972): Sedimentology of the Greenland Group in the Paparoa Range, West Coast, South Island. *New Zealand Journal of Geology and Geophysics*, 15: 372-393.

Laird, M.G. (1988): Sheet S37 Punakaiki. Geological map of New Zealand 1:63,360. Department of Scientific and Industrial Research, Wellington.

Laird, M.G. (1993): Cretaceous continental rifts: New Zealand region. *In*: Ballance, P.F. South Pacific sedimentary basins. Sedimentary Basins of the World, 2. Elsevier, Amsterdam, pp 37-49.

Laird, M.G. (1994): Geological aspects of the opening of the Tasman Sea. *In*: van der Lingen, G.J., Swanson, K.M. and Muir, R.J. (Eds.): Evolution of the Tasman Sea Basin: Proceedings of the Tasman Sea Conference, Christchurch, New Zealand, 27-30 November 1992. A.A. Balkema, Rotterdam, pp 1-17.

Laird, M.G. and Shelley, D. (1974): Sedimentation and early tectonic history of the Greenland Group, Reefton, New Zealand. *New Zealand Journal of Geology and Geophysics*, 17: 839-854.

Landis, C.A. and Coombs, D.S. (1967): Metamorphic belts and orogenesis in southern New Zealand. *Tectonophysics*, 4: 501-518.

Langmuir, C.H., Vocke, R.D. Jr., and Hanson, G.N. (1978): A general mixing equation with application to Icelandic basalts. *Earth and Planetary Science Letters*, 37: 380-392.

Leake, B.E. (1978): Nomenclature of Amphiboles. *The Canadian Mineralogist*, 16(4): 501-520.

Leake, B.E. (1987): Granite emplacement: the granites of Ireland and their origin. *In*: Bowes, D.R. and Leake, B.E. Crustal evolution in northwestern Britain and adjacent regions. Seel House Press, Liverpool, pp 221-248.

Leake, B.E. (1990): Granite magmas: their sources, initiation and consequences of emplacement. *Journal of the Geological Society of London*, 147: 579-589.

Le Maitre, R.W., Bateman, P., Dudek, A., Keller, J., Lameyre, J., LeBas, M.J., Sabine, P.A., Schmid, R., Sorenson, H., Streckeisen, A., Woolley, A.R. and Zanettin, B. (Eds.) (1989): A Classification of igneous rocks and glossary of terms, recommendations of the IUGS subcommision on the systematics of igneous rocks. *Blackwell Scientific Publications*, Oxford. 193 pp.

Liew, T.C. and McCulloch, M.T. (1985): Genesis of granitoid batholiths of Peninsular Malaysia and implications for models of crustal evolution: Evidence from a Nd-Sr isotopic and U-Pb zircon study. *Geochemica et Cosmochimica Acta*, 49: 587-600.

Loiselle, M.C. and Wones, D.R. (1979): Characteristics of anorogenic granites. *Geological Society of America Abstracts with Programs*, 11: 468

Loosveld, R.J.H. and Etheridge, M.A. (1990): A model for low-pressure facies metamorphism during crustal thickening. *Journal of Metamorphic Geology*, 8: 257-267.

Maas, R and McCulloch, M.T. (1991): The provenance of Archean clastic metasediments in the Narryer Gneiss Complex, Western Australia: Trace element geochemistry, Nd isotopes, and U-Pb ages for detrital zircons. *Geochemica et Cosmochimica Acta*, 55: 1915-1932.

Maclean, D.R. (1994): The geology and geochemistry of the Cambrian Devil River Volcanics, Anatoki Range, northwest Nelson. Unpublished M.Sc. thesis, University of Canterbury.

Mahood, G. and Hildreth, W. (1983): Large partition coefficients for trace elements in high-silica rhyolites. *Geochemica et Cosmochimica Acta*, 47: 11-30.

Martin, H., Bonin, B., Capdevila, R., Jahn, B.M., Lameyre, J. and Wang, Y. (1994): The Kuiqi peralkaline granitic complex (South East China): Petrology and geochemistry. *Journal of Petrology*, 35: 983-1015.

Mason, B. (1977): Geochemistry of the Greenland Group (Comment). *New Zealand Journal of Geology and Geophysics*, 20: 811-812.

Mason, B. (1990): The Geology of the Rotomanu district, North Westland. *Records of the Canterbury Museum*, 10: 55-68.

Mason, B. and Taylor, S.R. (1987): High grade basement gneisses and granitoids in Westland, New Zealand. *Journal of the Royal Society of New Zealand*, 17(2): 115-138.

Mattinson, J.M., Kimbrough, D.L. and Bradshaw, J.Y. (1986): Western Fiordland Orthogneiss: Early Cretaceous arc magmatism and granulite facies metamorphism, New Zealand. *Contributions to Mineralogy and Petrology*, 92: 383-392.

McCulloch, M.T., Bradshaw, J.Y. and Taylor, S.R. (1987): Sm-Nd and Rb-Sr isotopic and geochemical systematics in Phanerozoic granulites from Fiordland, Southwest New Zealand. *Contributions to Mineralogy and Petrology*, 97: 183-195.

McCulloch, M.T. and Chappell, B.W. (1982): Nd isotopic characteristics of S- and I-type granites. *Earth and Planetary Science Letters*, 58: 51-64.

McDonough, W.F., Sun, S-s, Ringwood, A.E., Jagoutz, E. and Hofmann, A.W. (1992): K, Rb and Cs in the earth and moon and the evolution of the earths mantle. *Geochemica et Cosmochimica Acta*, 56: 1001-1012.

McDougall, A.J. (1993): Investigation of Geological Structure, Coal Optical Fabrics, and Basin Evolution at Pike River Coalfield, West Coast, South Island. Unpublished M.Sc. thesis, University of Canterbury, Christchurch.

McKenzie, D. and Bickle, M.J. (1988): The volume and composition of melt generated by extension of the lithosphere. *Journal of Petrology*, 29: 625-679.

Miller, C.F., Stoddard, E.F., Bradfish, L.J. and Dollase, W.A. (1981): Composition of plutonic muscovite: genetic implications. *The Canadian Mineralogist*, 19: 25-34.

Miller, C.F., Watson, E.B. and Harrison, T.M. (1988): Perspectives on the source, segregation and transport of granitoid magmas. *Transactions of the Royal Society of Edinburgh: Earth Sciences*, 79: 135-156.

Mittlefehldt, D.W. and Miller, C.F. (1983): Geochemistry of the Sweetwater Wash Pluton, California: implications for "anomalous" trace element behaviour during differentiation of felsic magmas. *Geochemica et Cosmochimica Acta*, 47: 109-124.

Mohr, P.A. (1987): Crustal contamination in Mafic Sheets: a summary. *In*: Halls, H.C. and Fahrig, W.F. (Eds.) Mafic Dyke Swarms, *Geological Society of Canada Special Paper*, 34: 75-80.

Morgan, P.G. (1908): The geology of the Mikonui subdivision, North Westland. *New Zealand Geological Survey Bulletin* 6.

Morgan, P.G. (1911): The geology of the Greymouth subdivision, North Westland. *New Zealand Geological Survey Bulletin* 13.

Morgan, P.G. (1919): The limestone and phosphate resources of New Zealand. Part 1: Limestone. *New Zealand Geological Survey Bulletin* 22.

Mortimer, N., Parkinson, D., Raine, J.I., Adams, C.J., Graham, I.J., Oliver, P.J. and Palmer, K. (1995): Ferrar Supergroup rocks in New Zealand: Kirwans Dolerite, near Reefton. *Geology*, (submitted).

Muir, R.J., Bradshaw, J.D., Weaver, S.D. and Ireland, T.R. (1994b): Crustal extension prior to the opening of the Tasman Sea Basin: Evidence from New Zealand granites. *In*: van der Lingen, G.J., Swanson, K.M. and Muir, R.J. (Eds.): Evolution of the Tasman Sea Basin: Proceedings of the Tasman Sea Conference, Christchurch, New Zealand, 27-30 November 1992. A.A. Balkema, Rotterdam, pp 55-64.

Muir, R.J., Ireland, T.R., Weaver, S.D. and Bradshaw, J.D. (1994a): Ion microprobe U-Pb zircon geochronology of granitic magmatism in the Western Province of the South Island, New Zealand. *Chemical Geology (Isotope Geoscience section)*, 113: 171-189.

Muir, R.J., Ireland, T.R., Weaver, S.D. and Bradshaw, J.D. (1994c): Geochronology of Paleozoic magmatism in the Western Province, South Island, New Zealand: Implications for correlations with S.E. Australia, Tasmania and Antarctica (Abstract). *Geological Society of New Zealand Miscellaneous publication*, 80A: p 139.

Muir, R.J., Ireland, T.R., Weaver, S.D., Bradshaw, J.D and Shelley, D. (1994d): Geochronology of Eastern Fiordland, South Island, New Zealand (Abstract). *Geological Society of New Zealand Miscellaneous publication*, 80A: p 140.

Muir, R.J., Weaver, S.D., Bradshaw, J.D., Eby, G.N. and Evans, J.A. (1995): Geochemistry of the Cretaceous Separation Point Batholith, New Zealand: granitoid magmas formed by melting of mafic lithosphere. *Journal of the Geological Society of London*, 152: (In Press).

Mutch, A.R. and McKellar, I.C. (1964): Sheet 19: Haast. Geological map of New Zealand 1:250,000. Department of Scientific and Industrial Research, Wellington, New Zealand.

Nakamura, N. (1974): Determination of REE, Ba, Fe, Mg, Na and K in carbonaceous and ordinary chondrites. *Geochemica et Cosmochimica Acta*, 38: 757-775.

Nash, W.P. and Crecraft, H.R. (1985): Partition coefficients for trace elements in silicic magmas. *Geochemica et Cosmochimica Acta*, 49: 2309-2322.

Nathan, S. (1974): Stratigraphic nomenclature for the Cretaceous - Lower Quaternary rocks of Buller and north Westland, West Coast, South Island New Zealand. *New Zealand Journal of Geology and Geophysics*, 17: 423-445.

Nathan, S. (1975): Sheets S23 and S30, Foulwind and Charleston (1st ed.) "Geological Map of New Zealand 1:63,360". New Zealand Department of Scientific and Industrial Research, Wellington.

Nathan, S. (1976): Geochemistry of the Greenland Group (early Ordovician), New Zealand. *New Zealand Journal of Geology and Geophysics*, 19: 683-706.

Nathan, S. (1978): Sheets S31 and part S32 Buller-Lyell (1st edition) "Geological Map of New Zealand 1:63,360". New Zealand Department of Scientific and Industrial Research, Wellington.

Nathan, S., Anderson, H.J., Cook, R.A., Herzer, R.H., Hoskins, R.H., Raine, J.I. and Smale, D. (1986): Cretaceous and Cenozoic sedimentary basins of the West Coast region, South Island, New Zealand. New Zealand Geological Survey Basin Studies 1. 90 pp. Published by Department of Scientific and Industrial Research Wellington, New Zealand.

Nelson, D.R., Crawford, A.J. and McCulloch, M.T. (1984): Nd-Sr isotopic and geochemical systematics in Cambrian boninites and tholeiites from Victoria, Australia. *Contributions to Mineralogy and Petrology*, 88: 164-172.

Nelson, K.D. (1992): Are crustal thickness variations in old mountain belts like the Appalachians a consequence of lithospheric delamination. *Geology*, 20: 498-502.

Norman, M.D., Leeman, W.P. and Mertzman, S.A. (1992): Granites and rhyolites from the northwestern U.S.A.: temporal variation in magmatic processes and relations to tectonic setting. *Transactions of the Royal Society of Edinburgh: Earth Sciences*, 83: 71-81.

Norrish, K. and Hutton, J.T. (1969): An accurate X-Ray spectrographic method for the analysis of a wide range of geological samples. *Geochemica et Cosmochimica Acta*, 33: 431-453.

Noyles, H.J., Frey, F.A. and Wones, D.R. (1983): A tale of two plutons: Geochemical evidence bearing on the origin and differentiation of the Red Lake and Eagle Peak Plutons, central Sierra Nevada, California. *Journal of Geology*, 91: 487-509.

N.Z.Met.Service (1980): Rainfall normals for New Zealand 1951-1980. *New Zealand Meteorological Service Miscellaneous Publication*, 185.

Oliver, P.J. and Keene, H.W. (1989): Sheet K36 AC and part sheet K35 - Mount Somers. Geological map of New Zealand 1:50000. Wellington, New Zealand. Department of Scientific and Industrial Research.

O'Neil, J.R. and Chappell, B.W. (1977): Oxygen and hydrogen isotope relations in the Berridale Batholith. *Journal of the Geological Society of London*, 133: 559-571.

O'Neil, J.R., Shaw, S.E. and Flood, R.H. (1977): Oxygen and hydrogen isotope compositions as indicators of granite genesis in the New England Batholith. *Contributions to Mineralogy and Petrology*, 62: 313-328.

Peacock, M.A. (1931): Classification of igneous rock series. *Journal of Geology*, 39: 54-67.

Peacock, S.M., Rushmer, T. and Thompson, A.B. (1994): Partial melting of subducting oceanic crust. *Earth and Planetary Science Letters*, 121: 227-244.

Pearce, J.A. (1983): Role of sub-continental lithosphere in magma genesis at active continental margins. *In*: Hawkesworth, C.J. and Norry, M.J. (Eds.) Continental Basalts and mantle xenoliths. Shiva, Nantwich, pp 230-249.

Pearce, J.A. and Cann, J.R. (1973): Tectonic setting of basic volcanic rocks determined using trace element analyses. *Earth and Planetary Science Letters*, 19: 290-300.

Pearce, J.A., Harris, N.B.W. and Tindle, A.G. (1984): Trace element discrimination diagrams for the tectonic interpretation of granitic rocks. *Journal of Petrology*, 25: 956-983.

Pearce, J.A. and Norry, M.J. (1979): Petrogenetic implications of Ti, Zr, Y and Nb variations in volcanic rocks. *Contributions to Mineralogy and Petrology*, 69: 33-47.

Peccerillo, A. and Taylor, S.R. (1976): Geochemistry of Eocene calc-alkaline volcanic rocks from Kastamonu area, Northern Turkey. *Contributions to Mineralogy and Petrology*, 58: 63-81.

Pickett, D.A. and Wasserburg, G.J. (1989): Neodymium and strontium isotope characteristics of New Zealand granitoids and related rocks. *Contributions to Mineralogy and Petrology*, 103: 131-142.

Pirajno, F. (1982): Lamprophyre dikes in the Victoria Range Sector of the Karamea Batholith, New Zealand (note). *New Zealand Journal of Geology and Geophysics*, 25: 499-502.

Poli, S. and Schmidt, M.W. (1992): A comment on "Calcic amphibole equilibria and a new amphibole-plagioclase geothermometer" by J.D. Blundy and T.J.B. Holland (Contrib Mineral Petrol (1990) 104: 208-224). *Contributions to Mineralogy and Petrology*, 111: 273-278.

Raine, J.I. (1984): Outline of palynogical zonation of Cretaceous to Paleogene terrestrial sediments in West Coast Region, South Island, New Zealand. *New Zealand Geological Survey report*, 109.

Rapp, R.P., Watson, E.B. and Miller, C.F. (1991): Partial melting of amphibolite/eclogite and the origin of Archaean trondjhemites and tonalites. *Precambrian Research*, 51: 1-25.

Rattenbury, M.S. (1986): Late low-angle thrusting and the Alpine Fault, central Westland, New Zealand. *New Zealand Journal of Geology and Geophysics*, 29: 437-446.

Rattenbury, M.S. (1987a): Fraser Complex and Alpine Fault tectonics, Central Westland, New Zealand. Unpublished PhD thesis, University of Otago.

Rattenbury, M.S. (1987b): Timing of mylonitization west of the Alpine Fault, central Westland, New Zealand. *New Zealand Journal of Geology and Geophysics*, 30: 123-169.

Rattenbury, M.S. (1991): The Fraser Complex: High grade metamorphic and igneous and mylonitic rocks in Central Westland, New Zealand. *New Zealand Journal of Geology and Geophysics*, 34: 23-34.

Reed, J.J. (1958): Granites and mineralisation in New Zealand. *New Zealand Journal of Geology and Geophysics*, 1: 47-64.

Reed, J.J. (1964): Mylonites, cataclasites and associated rocks along the Alpine Fault, South Island, New Zealand. *New Zealand Journal of Geology and Geophysics*, 11(2): 645-684.

Rennison, M.W. (1992): The petrology, structure and geochemistry of the eastern margin of the Mount Olympus pluton, northwest Nelson, New Zealand. Unpublished B.Sc.(Hons) thesis, University of Canterbury.

Richard, P., Shimiru, N. and Allegre, C.J. (1976): $^{143}Nd/^{146}Nd$, a natural tracer: An application to oceanic basalts. *Earth and Planetary Science Letters*, 31: 269-278.

Richards, D.N.G (1980): Palaeozoic granitoids of northeast Australia. *In*: Henderson, R.A. and Stephenson, P.J. (Eds.) The Geology and Geophysics of northeast Australia.

Rickwood, P.C. (1968): On recasting analyses of garnet into end-member molecules. *Contributions to Mineralogy and Petrology*, 18: 175-198.

Rickwood, P.C. (1989): Boundary lines within petrologic diagrams which use oxides of major and minor elements. *Lithos*, 22: 247-263.

Robinson, A.G. and Davey, F.J. (1981): Bounty (1st Ed.) "Magnetic total force anomaly map, oceanic series, 1:1,000,000". Department of Scientific and Industrial Research, Wellington, New Zealand.

Robinson, P., Schumacher, J.C., and Spear, F.S. (1982): Formulation of electron probe analyses. *In*: Veblen, D.R., and Ribbe, P.H. (Eds.) Amphiboles: Petrology and experimental phase relations. *Reviews in Mineralogy*, 9b: 6-9.

Rock, N.M.S. (1991): Lamprophyres. Blackie and Son Ltd, Glasgow. 285 pp.

Rollinson, H. (1993): Using geochemical data: Evaluation, presentation, interpretation. Longman Group, U.K. 352 pp.

Rudnick, R.L. (1992): Xenoliths - samples of the lower continental crust. *In*: Fountain, D.M., Arculus, R. and Kay, R.W. (Eds.): Continental lower crust. *Developments in Geotectonics*, 23: 269-316.

Rushmer, T. (1991): Partial melting of two amphibolites; contrasting experimental results under fluid-absent conditions. *Contributions to Mineralogy and Petrology*, 107: 41-59.

Rutherford, M.J. and Johnson, M.C. (1992): Discussion of Blundy and Holland's (1990) "Calcic amphibole equilibria and a new amphibole-plagioclase geothermometer". *Contributions to Mineralogy and Petrology*, 111: 266-268.

Saunders, A.D., Tarney, J. and Weaver, S.D. (1980): Transverse geochemical variations across the Antarctic Peninsula: Implications for the genesis of calc-alkaline magmas. *Earth and Planetary Science Letters*, 46: 344-360.

Sawka, W.N. (1988): REE and trace element variations in accessory minerals and hornblende from the strongly zoned McMurry Meadows Pluton, California. *Transactions of the Royal Society of Edinburgh: Earth Sciences*, 79: 157-168.

Schmidt, M.W. (1992): Amphibole composition in tonalite as a function of pressure: an experimental calibration of the Al-in-hornblende barometer. *Contributions to Mineralogy and Petrology*, 110: 304-310.

Schroeder, B., Thompson, G., Sulanowska, M. and Ludden, J.N. (1980): Analysis of geologic materials using and automated X-Ray fluorescence system. *X-Ray Spect.* 9: 198-205.

Seward, D. (1989): Cenozoic basin histories determined by fission-track dating of basement gneisses, South Island, New Zealand. *Chemical Geology*, 79: 31-48.

Sewell, R.J. and Nathan, S. (1987): Geochemistry of Late Cretaceous and Tertiary basalts from South Westland. *New Zealand Geological Survey Record*, 18: 87-94.

Sewell, R.J., Nathan, S. and Adams, C.J. (1988): Geochemistry of late Cretaceous basaltic rocks from North Westland. *New Zealand Geological Survey Record*, 35: 113-121.

Shelley, D. (1970): The structure and petrography of the Constant Gneiss near Charleston, south-west Nelson. *New Zealand Journal of Geology and Geophysics*, 13: 370-391.

Shelley, D. (1985): Optical Mineralogy (2nd Ed.). Elsevier Science Publishing Co., Inc. New York. 321 pp.

Shelley, D. (1993): Igneous and metamorphic rocks under the microscope: Classification, textures, microstructures and mineral preferred orientations. Chapman and Hall, London. 445 pp.

Sheppard, S.M.F. and Harris, C. (1985): Hydrogen and oxygen isotope geochemistry of Ascension Island lavas and granites: variation with crystal fractionation and interaction with sea water. *Contributions to Mineralogy and Petrology*, 91: 74-81.

Smith, J.V. and Brown, W.L. (1988) Feldspar Minerals, Volume 1. Crystal structures, Physical, Chemical and Microtextural properties. Springer-Verlag, Berlin, 828 pp.

Spanninga, G.A. (1993): Evolution of the Grey Valley Trough. Unpublished M.Sc. thesis, University of Waikato.

Steiger, R.H. and Jäger, E. (1977): Subcommission on geochronology: Convention on the use of decay constants in geo- and cosmochronology. *Earth and Planetary Science Letters*, 36: 359-362.

Stock, J. and Molnar, P. (1982): Uncertainties in the relative position of the Australia, Antarctica, Lord Howe and Pacific plates since the late Cretaceous. *Journal of Geophysical Research*, 87: 4697-4717.

Suggate, R.P. (1963): The Alpine Fault. *Royal Society of New Zealand Transactions*, 2: 105-129.

Suggate, R.P. (1985): The glacial/interglacial sequence of North Westland, New Zealand. *New Zealand Geological Survey Record*, 7: 22 pp.

Sweatman, T.R. and Long, J.V.P. (1969): Quantitative electron microprobe microanalysis of rock-forming minerals. *Journal of Petrology*, 10: 332-379.

Sylvester, P.J. (1989): Post-collisional alkaline granites. *Journal of Geology*, 97: 261-280.

Taylor, H.P., Jr. (1977): Water/rock interactions and the origin of $H_2O$ in granitic batholiths. *Journal of the Geological Society of London*, 133: 509-558.

Taylor, H.P., Jr. (1986): Igneous rocks: II. Isotopic case studies of circumpacific magmatism. *In*: Valley, J.W., Taylor, H.P. Jr. and O'Neil, J.R. (Eds.) Stable isotopes in high temperature geological processes. *Reviews in Mineralogy*, 16: 273-317.

Taylor, H.P., Jr. (1988): Oxygen, hydrogen and strontium isotope constraints on the origin of granites. *Transactions of the Royal Society of Edinburgh: Earth Sciences*, 79: 317-338.

Taylor, H.P. Jr., and Sheppard, S.M.F. (1986): Igneous rocks: I. Processes of isotopic fractionation and isotope systematics. *In*: Valley, J.W., Taylor, H.P. Jr. and O'Neil, J.R. (Eds.) Stable isotopes in high temperature geological processes. *Reviews in Mineralogy*, 16: 227-271.

Taylor, R.P., Strong, D.F. and Fryer, B.J. (1981): Volatile control of contrasting trace element distributions in peralkaline granitic and volcanic rocks. *Contributions to Mineralogy and Petrology*, 77: 267-271.

Taylor, S.R. and McClennan, S.M. (1985): The continental crust: Its composition an evolution. Blackwell, Oxford.

Tepper, J.H., Nelson, B.K., Bergantz, G.W. and Irving, A.J. (1993): Petrology of the Chilliwack batholith, North Cascades, Washington: generation of calc-alkaline granitoids by melting of mafic lower crust with variable water fugacity. *Contributions to Mineralogy and Petrology*, 113: 333-351.

Thomas, W.M. and Ernst, W.G. (1990): The aluminium content of hornblende in calc-alkaline granitic rocks: a mineralogic barometer calibrated experimentally to 12 kbars. *In*: Spencer, R.J. and Chou, I-Ning (Eds.): Fluid-mineral interactions: a tribute to H.P. Eugster. *Geochemical Society Special Publication*, 2: 59-63.

Thompson, R.N., Morrison, M.A., Dickin, A.P. and Hendry, J. (1983): Continental flood basalts ... Arachnids rule OK?. *In*: Hawkesworth, C.J. and Norry, M.J. (Eds.): Continental basalts and mantle xenoliths. Shiva Geology Series, pp 158-185.

Tulloch, A.J. (1979a): Plutonic and metamorphic rocks in the Victoria Range segment of the Karamea Batholith. Unpublished PhD thesis, Otago University.

Tulloch, A.J. (1979b): Secondary Ca-Al Silicates as Low-Grade Alteration Products of Granitoid Biotite. *Contributions to Mineralogy and Petrology*, 69: 105-117.

Tulloch, A.J. (1983): Granitoid rocks of New Zealand - A brief review. *Geological Society of America Memoir*, 159: 5-20.

Tulloch, A.J. (1986) Hydrothermal alteration and scheelite mineralisation associated with the Barrytown Pluton, north Westland, New Zealand. *Mineral Deposits*, 5: 65-92.

Tulloch, A.J. (1988a): Batholiths, plutons and suites: Nomenclature for the granitoid rocks of Westland-Nelson. *New Zealand Journal of Geology and Geophysics*, 31: 505-509.

Tulloch, A.J. (1988b): Metamorphic Core Complexes and detachment faults in Westland, New Zealand - Implications for precious metal mineralization. *New Zealand Geological Survey Report M172*, 44 pp.

Tulloch, A.J. (1989) Magnetic Susceptibilities of Westland-Nelson plutonic rocks: Discrimination of Palaeozoic and Mesozoic granitoid suites. *New Zealand Journal of Geology and Geophysics*, 32: 197-203.

Tulloch, A.J. (1992): Petrology of the Sams Creek peralkaline dike, Takaka, New Zealand. *New Zealand Journal of Geology and Geophysics*, 35: 193-200.

Tulloch, A.J. and Brathwaite, R.L. (1987): C7: Granitoid rocks and associated mineralization of Westland - West Nelson. *In*:
Houghton, B.F. and Weaver, S.D. (Eds.): South Island Igneous Rocks: Tour guides A3, C2 and C7. *New Zealand Geological Survey Record*, 13: 65-92.

Tulloch, A.J. and Kimbrough, D.L. (1989): The Paparoa metamorphic core complex: Cretaceous extension associated with fragmentation of the Pacific margin of Gondwana. *Tectonics*, 8(6): 1217-1234.

Tulloch, A.J., Kimbrough, D.L. and Waight, T.E. (1994): The French Creek Granite, North Westland, New Zealand - Late Cretaceous A-type plutonism on the Tasman passive margin (extended abstract). *In*: van der Lingen, G.J., Swanson, K.M. and Muir, R.J. (Eds.): Evolution of the Tasman Sea Basin: Proceedings of the Tasman Sea Conference, Christchurch, New Zealand, 27-30 November 1992. A.A. Balkema, Rotterdam, pp 65-67.

Tulloch, A.J. and Nathan, S. (1990) Spinel harzburgite xenoliths in alkali basalt and camptonite from North Westland and southeast Nelson, New Zealand. *New Zealand Journal of Geology and Geophysics*, 33: 529-534.

Tulloch, A.J. and Palmer, K. (1990): Tectonic implications of granite cobbles from the mid-Cretaceous Pororari Group, southwest Nelson, New Zealand. *New Zealand Journal of Geology and Geophysics*, 33: 205-217.

Tulloch, A.J and Robertson, S (1987): Fluorine contents of Westland-Nelson granitoids and associated metasedimentary country rocks. *New Zealand Geological Survey Record*, 20: 89-94.

Turner, S.P., Foden, J.D. and Morrison, R.S. (1992): Derivation of some A-type magmas by fractionation of basaltic magma: An example from the Padthaway Ridge, South Australia. *Lithos*, 28: 151-179.

Tuttle, O.F. and Bowen, N.L. (1958): Origin of granite in the light of experimental studies in the system $NaAlSi_3O_8$-$KAlSi_3O_8$-$SiO_2$-$H_2O$. *Geological Society of America Memoir*, 74.

Vetter, U. and Tessensohn, F. (1987): S- and I-type granitoids of north Victoria Land, Antarctica, and their inferred geotectonic setting. *Geologische Rundschau*, 76: 233-243.

von Blanckenburg, F. Früh-Green, G. Diethelm, K. and Stille, P. (1992): Nd-, Sr-, O-isotopic and chemical evidence for a two-stage contamination history of mantle magmas in the Central Alpine Bergell intrusion. *Contributions to Mineralogy and Petrology*, 110: 33-45.

von Quadt, A. (1992): U-Pb zircon and Sm-Nd geochronology of mafic and ultramafic rocks from the central part of the Tavern Window (eastern Alps). *Contributions to Mineralogy and Petrology*, 110: 57-67.

Waight, T.E. (1990): The Geology of Mount Turiwhate, Island Hill and Mount Tuhua, North Westland, New Zealand. Unpublished B.Sc(Hons) project, University of Canterbury, Christchurch.

Ward, C.M. (1984): Geology of the Dusky Sound area, Fiordland -with emphasis on the structural - metamorphic development of some porphyroblastic staurolite pelites. Unpublished PhD. thesis, University of Otago, Dunedin.

Wark, D.A. and Miller, C.F. (1993): Accessory mineral behaviour during differentiation of a granite suite: monazite, xenotime and zircon in the Sweetwater Wash pluton, southeastern California, U.S.A. *Chemical Geology*, 110: 49-67.

Warren, G. (1967): Sheet 17, Hokitika. Geological map of New Zealand 1:250,000. Department of Scientific and Industrial Research, Wellington, New Zealand.

Weaver, S.D. (1977): The Quaternary caldera volcano Emuruangogolak, Kenya Rift, and the petrology of a bimodal ferrobasalt-pantelleritic trachyte association. *Bulletin of Volcanology*, 40-44: 2-22.

Weaver, S.D., Adams, C.J., Pankhurst, R.J. and Gibson, I.L. (1992): Granites of Edward VII Peninsula, Marie Byrd Land: Magmatism related to Antarctic-New Zealand rifting. *Transactions of the Royal Society of Edinburgh*, 83: 281-290.

Weaver, S.D., Bradshaw, J.D. and Adams, C.J. (1991): Granitoids of the Ford Ranges, Marie Byrd Land, Antarctica. *In*: Thomson, M.R.A., Crame, J.A. and Thomson, J.W. (Eds.): Geological evolution of Antarctica, Cambridge University Press, Cambridge, pp 345-351.

Weaver, S.D., Bradshaw, J.D. and Laird, M.G. (1984): Geochemistry of Cambrian volcanics of the Bowers Supergroup and implications for the Early Palaeozoic tectonic evolution of Northern Victoria Land, Antarctica. *Earth and Planetary Science Letters*, 68: 128-140.

Weaver, S.D., Gibson, I.L., Houghton, B.F. and Wilson, C.J.N. (1990): Mobility of rare earth and other elements during crystallization of peralkaline silicic lavas. *Journal of Volcanology and Geothermal Research*, 43: 57-70.

Weaver, S.D. and Pankhurst, R.J. (1991): A precise Rb-Sr age for the Mandamus Igneous Complex, North Canterbury, and regional tectonic implications. *New Zealand Journal of Geology and Geophysics*, 34: 341-345.

Weaver, S.D. and Smith, I.E.M. (1989): New Zealand intraplate volcanism, *In*: Johnson, R.W., Knutson, J. and Taylor S.R. (Eds.) Intraplate volcanism in Eastern Australia and New Zealand, Cambridge University Press, Cambridge, pp 157-188.

Weaver, S.D., Storey, B.C., Pankhurst, R.J., Mukasa, S.B., DiVenere, V., Dalziel, I.W.D. and Bradshaw, J.D. (1994): Antarctica-New Zealand rifting and Marie Byrd Land lithospheric magmatism linked to ridge subduction and mantle plume activity. *Geology*, 22: 811-814.

Weissel, J.K. and Hayes, D.E. (1977): Evolution of the Tasman Sea reappraised. *Earth and Planetary Science Letters*, 36: 77-84.

Wellman, H.W. (1950a): Geology of the Kotuku Oilfield, Westland. New Zealand Geological Survey Report 48, 46 pp.

Wellman, H.W. (1950b): Tertiary geology of Sheet 51 (Kumara) with notes on the Cretaceous and Tertiary outliers to the south (S57, 58 and 64). Unpublished manuscript, New Zealand Geological Survey, Lower Hutt.

Wellman, P. and Cooper, A. (1971): Potassium-Argon ages of some New Zealand lamprophyre dikes near the Alpine Fault. *New Zealand Journal of Geology and Geophysics*, 14(2): 341-350.

Wellman, H.W. and Suggate, R.P. (1950): Infaulted Tertiary section at Taramakau Settlement, Sheet 57. Unpublished manuscript, New Zealand Geological Survey, Lower Hutt.

Wernicke, B.P., Spencer, J.E., Burchfiel, B.F. and Guth, P.L. (1982): Magnitude of crustal extension in the southern Great Basin. *Geology*, 10: 499-502.

Wernicke, B.P., Christiansen, R.L., England, P.C. and Sonder, L.J. (1987): Tectonomagmatic evolution of Cenozoic extension in the North American Cordillera. *In*: Coward, M.P., Dewey, J.F. and Hancock, P.L. (Eds.): Continental extensional tectonics. *Geological Society Special Publication*, 28: 203-221.

Whalen, J.B., Currie, K.L., and Chappell, B.W. (1987): A-type granites: Geochemical characteristics, discrimination and petrogenesis. *Contributions to Mineralogy and Petrology*, 95: 407-419.

White, A.J.R. and Chappell, B.W. (1983): Granitoid types and their distribution in the Lachlan Fold Belt, southeastern Australia. *In*: Roddick, J.A. (Ed.) Circum-Pacific plutonic terranes. *Geological Society of America Memoir*, 159: 21-34.

White, P.J. (1987): The petrology, geochemistry and petrogenesis of igneous and metamorphic rocks from the Paparoa Range, southwest Nelson. Unpublished PhD thesis, Victoria University, Wellington.

White, P.J. (1994): Thermobarometry of the Charleston Metamorphic Group and implications for the evolution of the Paparoa Metamorphic Core Complex, New Zealand. *New Zealand Journal of Geology and Geophysics*, 37: 201-209.

White, S.H. and Green, P.F. (1986): Tectonic development of the Alpine Fault zone, New Zealand: a fission-track study. *Geology*, 14: 124-127.

Winchester, J.A. and Floyd, P.A. (1977): Geochemical discrimination of different magma series and their differentiation products using immobile elements. *Chemical Geology*, 20: 325-343.

Williams, I.S., Chappell, B.W., Chen, Y.D. and Crook, K.A.W. (1992): Inherited and detrital zircons - vital clues to the granite protoliths and early igneous history of southeastern Australia. *Transactions of the Royal Society of Edinburgh (Earth Sciences)*, 83: 503.

Wilson, M. (1989): Igneous Petrogenesis. Unwin Hyman Ltd, London. 466 p.

Wood, R.J. (1991): Structure and stratigraphy of the western Challenger Plateau. *New Zealand Journal of Geology and Geophysics*, 34: 1-9.

Wyborn, L.A.I., Wyborn, D., Warren, R.G. and Drummond, B.J. (1992): Proterozoic granite types in Australia: implications for lower crust composition, structure and evolution. *Transactions of the Royal Society of Edinburgh: Earth Sciences*, 83: 201-209.

Wyllie, P.J. and Wolf, M.B. (1993): Amphibolite dehydration-melting: sorting out the solidus. *In*: Prichard, H.M., Alabaster, T., Harris, N.B.W. and Neary, C.R. (Eds.): Magmatic processes and plate tectonics, *Geological Society Special Publication*, 76: 405-416.

Young, D.J. (1968): The Fraser Fault in Central Westland, New Zealand, and its' associated rocks. *New Zealand Journal of Geology and Geophysics*, 11(2): 291-310.

Zen, E-An (1986): Aluminum enrichment in silicate melts by fractional crystallization: some mineralogic and petrographic constraints. *Journal of Petrology*, 27: 1095-1117.

Zhao, Jian-Xin and Cooper, J.A. (1993): Fractionation of monazite in the development of V-shaped REE patterns in leucogranite systems: Evidence from a muscovite leucogranite body in central Australia. *Lithos*, 30: 23-32.